uOttawa

L'Université canadienne
Canada's university

FACULTÉ DES ÉTUDES SUPÉRIEURES ET POSTOCTORALES

uOttawa

L'Université canadienne
Canada's university

FACULTY OF GRADUATE AND POSDOCTORAL STUDIES

Gabriela Fonseca-Zepeda
AUTEUR DE LA THÈSE / AUTHOR OF THESIS

Ph.D. (Chemical and Biological Engineering)
GRADE / DEGREE

Department of Chemical and Biological Engineering
FACULTÉ, ÉCOLE, DÉPARTEMENT / FACULTY, SCHOOL, DEPARTMENT

Design of Pressure-Sensitive Adhesives Using Miniemulsion Polymerization

TITRE DE LA THÈSE / TITLE OF THESIS

Marc Dubé
DIRECTEUR (DIRECTRICE) DE LA THÈSE / THESIS SUPERVISOR

CO-DIRECTEUR (CO-DIRECTRICE) DE LA THÈSE / THESIS CO-SUPERVISOR

Xudong Cao

Handra Tezel

Joseph Schork (University of Maryland)

André Trembaly

Gary W. Slater
Le Doyen de la Faculté des études supérieures et postdoctorales / Dean of the Faculty of Graduate and Postdoctoral Studies

UNIVERSITY OF OTTAWA
Department of Chemical and Biological Engineering

DESIGN OF PRESSURE-SENSITIVE ADHESIVES USING MINIEMULSION POLYMERIZATION

by

Gabriela E. Fonseca

A thesis submitted to the Faculty of Graduate and Postdoctoral Studies
In partial fulfillment of the requirements for the degree of

**Doctor of Philosophy in
Chemical Engineering**

© Gabriela E. Fonseca, Ottawa, Canada, 2010

Library and Archives Canada

Published Heritage Branch

395 Wellington Street
Ottawa ON K1A 0N4
Canada

Bibliothèque et Archives Canada

Direction du Patrimoine de l'édition

395, rue Wellington
Ottawa ON K1A 0N4
Canada

Your file Votre référence
ISBN: 978-0-494-65559-7
Our file Notre référence
ISBN: 978-0-494-65559-7

NOTICE:

The author has granted a non-exclusive license allowing Library and Archives Canada to reproduce, publish, archive, preserve, conserve, communicate to the public by telecommunication or on the Internet, loan, distribute and sell theses worldwide, for commercial or non-commercial purposes, in microform, paper, electronic and/or any other formats.

The author retains copyright ownership and moral rights in this thesis. Neither the thesis nor substantial extracts from it may be printed or otherwise reproduced without the author's permission.

AVIS:

L'auteur a accordé une licence non exclusive permettant à la Bibliothèque et Archives Canada de reproduire, publier, archiver, sauvegarder, conserver, transmettre au public par télécommunication ou par l'Internet, prêter, distribuer et vendre des thèses partout dans le monde, à des fins commerciales ou autres, sur support microforme, papier, électronique et/ou autres formats.

L'auteur conserve la propriété du droit d'auteur et des droits moraux qui protège cette thèse. Ni la thèse ni des extraits substantiels de celle-ci ne doivent être imprimés ou autrement reproduits sans son autorisation.

In compliance with the Canadian Privacy Act some supporting forms may have been removed from this thesis.

While these forms may be included in the document page count, their removal does not represent any loss of content from the thesis.

Conformément à la loi canadienne sur la protection de la vie privée, quelques formulaires secondaires ont été enlevés de cette thèse.

Bien que ces formulaires aient inclus dans la pagination, il n'y aura aucun contenu manquant.

Canada

Statements of Contributions of Collaborators

I hereby declare that I am the sole author of this thesis. I performed the polymerization experiments, polymer characterization including thermal, rheological, chromatographic and imaging analysis, pressure-sensitive adhesive characterization and all the associated data analysis. The ^{1}H-NMR data was contracted out to the Faculty of Science NMR Facility at the University of Ottawa. Particle size analyses were carried out by me in the Department of Chemical and Biological Engineering at the University of Ottawa, Ontario and in the Department of Chemical Engineering at Queen's University, Kingston, Ontario.

The scientific guidance throughout the project and editorial comments of the written work were provided by my thesis supervisor Dr. Marc A. Dubé of the Department of Chemical and Biological Engineering at the University of Ottawa and by our collaborator, Dr. Timothy F. L. McKenna of the Department of Chemical Engineering at Queen's University, Kingston, Ontario, who appears as second author in all the publications.

Gabriela E. Fonseca Date

ABSTRACT

This thesis serves to investigate how miniemulsion polymerization, as an alternative to the conventional emulsion polymerization, can be used to produce pressure-sensitive adhesives. The key advantage that miniemulsion polymerization offers is its droplet nucleation mechanism, where polymer particles are created in such a way that intra- and extra-particle diffusion resistance is maximized. This results in the in-situ production of populations of polymer particles with different properties. The main objective of this thesis was to create an adequately stabilized miniemulsion to create bimodal distributions of particle size or molecular weight for pressure-sensitive adhesives applications.

The performance of pressure-sensitive adhesives is characterized by the quantification of an adhesion as well as a cohesion component. On the one hand, pressure-sensitive adhesives must be able to wet the surface and be able to flow under low stresses and on the other hand, they must be able to be removed from the surface and be able to dissipate energy. This leads to a conflicting set of properties wherein a compromise must be made in the final properties. In order to tackle this conflict, miniemulsion polymerization can potentially be used to create latexes with compensating properties at the nanoscale through the preparation of particles with different particle sizes and/or microstructures such as different molecular weights and copolymer composition.

Our work started by investigating the influence of surfactant concentration, copolymer composition and chain transfer agent concentration on the resulting latex, polymer and adhesive properties of pressure-sensitive adhesives prepared with poly(2-ethyl hexyl acrylate/vinyl acetate/methacrylic acid). It was found that a combination of an anionic surfactant (sodium dodecyl sulfate) with an ethoxylated linear fatty alcohol non-ionic surfactant adequately stabilized this copolymer yielding latexes with 43 wt.-% solids content and with a maximum change in the number of particles (N_p) with respect to the number of

droplets (N_d) of ~6%. Nevertheless, this copolymer showed considerable homogeneous nucleation in the water phase due to its water solubility, which unavoidably led to inadequate pressure-sensitive adhesives properties.

The second part of the study employed methyl methacrylate as a substitute for vinyl acetate to produce a 2-ethyl hexyl acrylate/methyl methacrylate/acrylic acid terpolymer. It was found that the surfactant mixture, sodium dodecyl sulfate/Disponil A3065, was also able to stabilize this miniemulsion. The adhesive properties of films cast from this polymer system were systematically compared to those produced by conventional emulsion polymerization using a factorial design. Significant differences between the latexes (or films) produced by these two techniques were found due to their different particle nucleation mechanisms. The most significant difference between the films obtained was shown via a viscoelastic analysis. The analysis showed that miniemulsion-based films presented more entangled networks, i.e., larger values of M_w/M_e (which is a measure of the entanglement density) compared to emulsion-based ones even though the weight-average M_w was generally lower for the latexes produced by miniemulsion polymerization.

In subsequent work, a one-pot two-step miniemulsion polymerization approach was used to create poly (2-ethyl hexyl acrylate/methyl methacrylate/acrylic acid) pressure-sensitive adhesives with well-defined and predictable bimodal particle size distributions or bimodal molecular weight distributions. The "in-situ bimodal" latexes produced using this approach were compared to monomodal latexes as well as bimodal latexes produced via conventional post-polymerization blending on the basis of their viscoelastic and pressure-sensitive adhesives properties.

Finally, an exploratory study of the use of Atomic Force Microscopy to investigate pressure-sensitive adhesives performance was conducted. Atomic force microscopy was used to acquire adhesion-force curves to investigate the effect of monomodal and bimodal distributions of molecular weight and particle size on the adhesion force and energy at the nanoscale.

In conclusion, this is a first attempt to engineer bimodal distributions of molecular weights and particle sizes using miniemulsion polymerization specifically for the production of pressure-sensitive adhesives. Our conclusions are broadly applicable to a large class of

soft materials based on deformable polymeric networks such as adhesives, coating and paints. It is expected that in the future, production of latexes with concurrent multimodal distributions of molecular weights, particle sizes and compositions can be produced using this approach.

RÉSUMÉ

Cette thèse vise à étudier comment la polymérisation en miniemulsion, comme une alternative à la polymérisation en émulsion classique, peut être utilisé pour produire des adhésifs sensibles à la pression. L'avantage principal que la polymérisation en miniémulsion offre est son mécanisme de nucléation des gouttelettes, où les particules de polymère sont créés de manière telle que la résistance de diffusion intra- et extra- des particules est maximisé. Ceci résulte en la création en situ de populations de particules de polymère avec des propriétés différentes. L'objectif principal de cette thèse était de créer une miniémulsion suffisamment stabilisée pour créer des distributions bimodales de taille de particules ou de poids moléculaires pour les applications des adhésifs sensibles à la pression.

La performance des adhésifs sensibles à la pression est caractérisée par la quantification d'une composante d'adhérence ainsi qu'une composante de cohésion. D'une part, les adhésifs sensibles à la pression doivent être capables de mouiller la surface et être en mesure de circuler sous de faibles contraints et d'autre part, ils doivent pouvoir être enlevés de la surface et être en mesure de dissiper l'énergie. Cela conduit à un ensemble de propriétés contradictoires dans lesquelles un compromis doit être fait dans les propriétés finales. Pour faire face à ce conflit, la polymérisation en miniémulsion peut potentiellement être utilisée pour créer des latexes de propriétés compensatoires à l'échelle nanométrique grâce à la préparation de particules de différentes tailles et/ou des microstructures telles que les différents poids moléculaires et de la composition du copolymère.

Notre travail a commencé par une enquête sur l'influence de la concentration de surfactant, la composition de copolymère et de la concentration d'agent de transfert de chaîne sur le latex qui en résultait, de polymères et les propriétés adhésives des adhésifs sensibles à la pression préparées avec poly (acrylate de 2-éthyl hexyle/acétate de vinyle/acide méthacrylique). Il a été constaté que la combinaison d'un tensioactif anionique (sulfate de

sodium dodecyl) avec un tensioactif non-ionique linéaire d'alcool gras éthoxylé a suffisamment stabilisé ce copolymère cédant un latex avec 43% en matières solides et avec une variation maximale du nombre de particules (N_p) par rapport au nombre de gouttelettes (N_d) d'environ 6%. Toutefois, ce copolymère a démontré une nucléation homogène considérable dans la phase aqueuse, ce qui conduit inévitablement aux propriétés insuffisantes des adhésifs sensibles à la pression.

La deuxième partie de l'étude a utilisé le méthacrylate de méthyle comme un substitut à l'acétate de vinyle pour produire le terpolymère acrylate de 2-éthyl hexyle/acétate de vinyle/acide méthacrylique. Il a été constaté que le mélange de surfactant, sulfate de sodium dodecyl/Disponil, a également été en mesure de stabiliser cette miniémulsion. Les propriétés adhésives des films de ce système de polymères ont été systématiquement comparées à celles produites par polymérisation en émulsion classique en utilisant un plan factoriel. Des différences significatives entre les latexes (ou films) produites par ces deux techniques ont été trouvées en raison de leurs mécanismes de nucléation de particules différentes. La différence la plus significative entre les films obtenus a été démontrée par une analyse viscoélastique. L'analyse a démontré que les films obtenus par la polymérisation en miniémulsion ont présenté des réseaux plus embrouillés, c'est-à-dire des valeurs élevées de M_w/M_e qui est une mesure de la densité d'embrouillement. Comparativement aux films obtenus par la polymérisation en émulsion classique de ceux basés sur le même si le taux moléculaire moyen M_w, a été généralement plus bas pour les latexes produits par polymérisation en miniémulsion.

Dans le travail subséquent, une synthèse dans un vaisseau unique à deux étapes de polymérisation a été utilisée pour créer des polymères de 2-éthyl hexyle/acétate de vinyle/acide méthacrylique avec des distributions bimodales de particules ou distributions bimodales de taux moléculaire bien défini et prévisible. Les latexes "en-situ bimodales" produits par cette approche ont été comparés à un latex monomodal ainsi qu'un latex bimodal produit par un mélange classique après la polymérisation sur la base de leurs propriétés viscoélastiques et des adhésifs sensibles à la pression.

Enfin, une étude exploratoire de l'utilisation de la microscopie à force atomique pour enquêter sur la performance des adhésifs sensibles à la pression a été réalisée. La

microscopie à force atomique a été utilisée pour acquérir des courbes d'adhérence-force pour étudier l'effet des distributions monomodales et bimodales de taux moléculaire et de la taille des particules sur la force d'adhérence et l'énergie à l'échelle nanométrique.

En conclusion, il s'agit d'une première tentative de contrôler des distributions bimodales des taux moléculaires et des tailles de particules en utilisant la polymérisation en miniémulsion spécifiquement pour la production des adhésifs sensibles à la pression. Nos conclusions sont largement applicables à une large classe de matériaux souples basés sur des réseaux déformables polymériques telles que les adhésifs, les revêtements et peintures. Il est prévu qu'à l'avenir, la production de latexes avec des distributions multimodales concurrentes de taux moléculaires, la taille des particules et compositions peuvent être produite en utilisant cette approche.

TABLE OF CONTENTS

LIST OF FIGURES

Chapter 4

Chapter 5

LIST OF TABLES

NOMENCLATURE

A_d = surface area of the droplets, [nm^2]

A_{surf} = surface area covered by surfactant, [nm^2]

a_S = area per surfactant molecule, [$Å^2$]

C = concentration, [mol L^{-1}]

D_d = Droplet diameter, [nm]

I = Initiator concentration, [parts per hundred of monomer]

k_B = Boltzmann's constant, [m^2 kg s^{-2} K^{-1}]

k_i = Initiation rate coefficient, [s^{-1}]

k_p = Propagation rate coefficient, [L mol^{-1} s^{-1}]

M = Monomer concentration, [mol L^{-1}]

M_c = Molecular weight between crosslink points, [g mol^{-1}]

M_e = Molecular weight between entanglements, [g mol^{-1}]

M_w = Molecular weight, [g mol^{-1}]

$\bar{n}$ = average number of radicals per particle

N_A = Avogadro's number, [mol^{-1}]

N_d = Number of droplets

N_p = Number of particles

phm = parts per hundred parts of monomer

P_L= Laplace pressure, [bar]

P_O = Osmotic pressure, [bar]

R = Universal ideal gas constant, [cm^3 bar mol^{-1} K^{-1}]

r_i = Reactivity ratio

R_p = Rate of polymerization, [mol L^{-1}]

S = Surfactant concentration, [mol L^{-1}]

T = temperature, [K]

T_g = Glass transition temperature, [°C]

v_m = volume of a single molecule [cm^3]

Greek symbols

σ = interfacial tension, [mN/m]

μ_c = chemical potential of concentration C,

μ_{c0} = chemical potential reference value

μ_{bulk} = chemical potentials of the bulk phase

μ_{disp} = chemical potentials of the dispersed phase

$\gamma_{LL,naked}$ = interfacial tension between these two phases without surfactant, [mN/m]

$\gamma_{LL,surf}$ = interfacial tension between the organic and aqueous phase with surfactant coverage, [mN/m]

LIST OF ABBREVIATIONS

^{1}H-NMR = Proton Nuclear Magnetic Resonance

AA = Acrylic acid

APS = Ammonium persulfate

BA = Butyl acrylate

BMA = Butyl methacrylate

BPO = Benzoyl peroxide

CEP = Conventional emulsion polymerization

CTA = Chain transfer agent

DDM = 1-dodecanethiol

DLS = Dynamic Light Scattering

DSC = Differential Scanning Calorimetry

DSD = Droplet size distribution

EHA = 2-ethyl hexyl acrylate

EPA = Environmental Protection Agency

GPC = Gel Permeation Chromatography

HLB = Hydrophile/Lipophile Balance

HQ = Hydroquinone

KPS = Potassium persulfate

LPO = lauroyl peroxide

MAA = Methacrylic acid

MMA = Methyl methacrylate

MP = Miniemulsion polymerization

M-PI = Malvern polydispersity index

MWD = Molecular weight distribution

ODA = Octadecyl acrylate

PDI = Polydispersity index

PSA = Pressure sensitive adhesives

PSD = Particle size distribution

PVOH = Polyvinyl alcohol

SDS = Sodium dodecyl sulphate

STY = Styrene

THF = Tetrahydrofuran

VAc = Vinyl acetate

VOC = volatile organic compounds

LIST OF CHEMICAL STRUCTURES

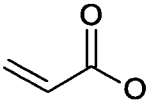	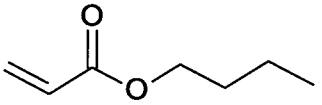
Acrylic Acid	Butyl acrylate
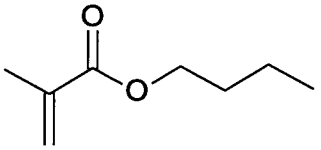	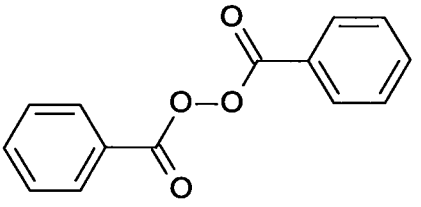
Butyl methacrylate	Benzoyl peroxide
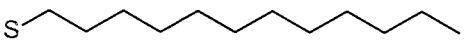	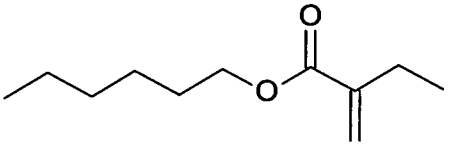
1-dodecanethiol	2-ethyl hexyl acrylate
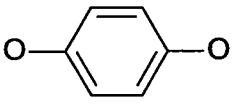	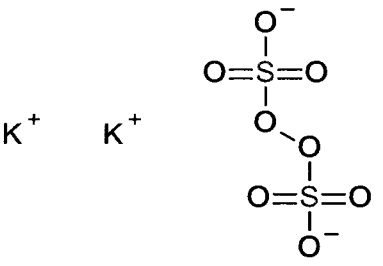
Hydroquinone	Potassium persulfate
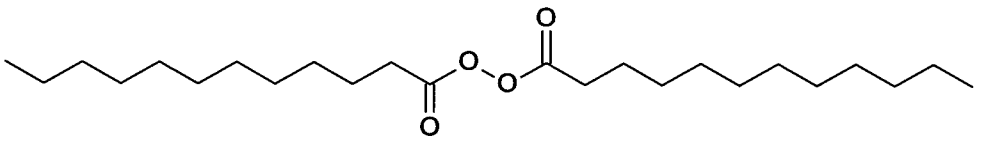	
Lauroyl peroxide	
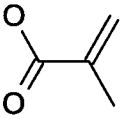	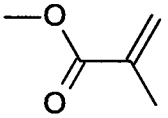
Methacrylic acid	Methyl methacrylate
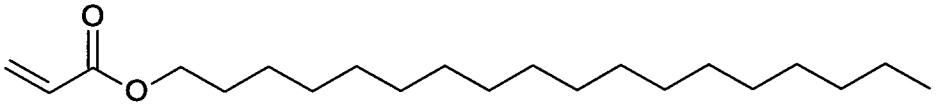	
Octadecyl acrylate	

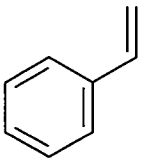	
Styrene	Tetrahydrofuran
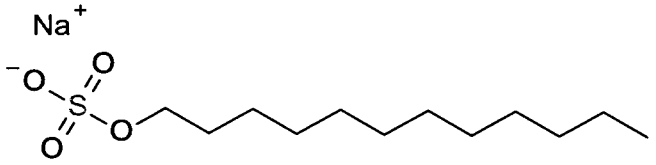	
Sodium dodecyl sulfate	
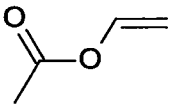	
Vinyl acetate	Vinyl alcohol

ACKNOWLEDGMENTS

I would like to thank all the people that have helped and inspired me in my doctoral studies.

First of all, I would like to express my most sincere gratitude to my advisor, Dr. Marc A. Dubé, for accepting me in his research group and for his continuing encouragement, patience and guidance over these years. I would not be here today without his support and the environment Dr. Dubé fosters. I want to thank him as well for allowing me to participate in various conferences (CSChE in Edmonton and Ottawa, Canada; The Adhesion Society Meeting in Austin, Texas, USA and the Polymer Reaction Engineering Conference in Niagara Falls, Canada) and in an international research program and visit Lyon, France. All combined has been an invaluable experience and I am truly indebted to him.

I also thank Dr. Timothy F. L. McKenna (Department of Chemical Engineering, Queen's University, Kingston, Canada) for his helpful discussions throughout this research project and for letting me learn from his research group in the LCPP-CNRS, in Lyon, France.

I would also like to thank Dr. Alexander Penlidis (Department of Chemical Engineering, University of Waterloo, Canada) for his help and collaboration in the writing of the review paper "Critical Overview of Sensors for Monitoring Polymerizations".

I thank my committee members, Dr. F. Joseph Schork (University of Maryland, USA), Dr. Xudong Cao, Dr. Handan Tezel and Dr. Andre Tremblay (University of Ottawa, Canada) for their criticism and inputs.

I am grateful to all the professors, office and technical staff of the Department of Chemical and Biological Engineering at the University of Ottawa. I particularly thank Louis Tremblay, Franco Ziroldo and Gérard Nina for their technical help.

To my colleagues and all the polymer reaction engineering group members (Renata Jovanovic, Hong Hua, Stéphane Roberge, Nicolas Brooks, Lili Qie, Somaieh Salehpour) for their valuable discussions and support. Specially, I would like to express my appreciation to

my friend and colleague, Lili Qie, for challenging my research ideas from start to finish, for her priceless friendship and for the Chinese food.

For the financial support of this project, I am grateful to the University of Ottawa International Research Initiative, the National Science and Engineering Research Council of Canada and to CONACYT Mexico for the doctoral scholarship.

I also want to acknowledge the support of all my friends. I specially want to thank my friend Nilesh Patel, who was there to help me academically and personally since the very first day.

I am indebted to my parents, Maria and Federico, and to my sister, Berenice, for all their sacrifices and support, without which I would have not been able to pursue my dreams.

Lastly, I want to thank my friend and husband Rodrigo Serna for his selfless patience and love. I am grateful to chance for letting me meet you.

Sit down before fact as a little child,

Be prepared to give up every preconceived notion,

Follow humbly wherever and to whatever abysses nature leads,

Or you shall learn nothing

Thomas Henry Huxley (1860)

A mis padres, Maria y Federico

A mi hermana, Berenice

CHAPTER 1

INTRODUCTION

Adhesives are a significant part of today's global economy, finding their way into the assembly of an almost endless list of products. They are used in many aspects of our lives and more likely than not, we are unaware of it. An important class of adhesives is called pressure-sensitive adhesives (PSA) (Petrie, 2000). PSAs are soft ductile materials that are inherently tacky. They can be applied to a large number of surfaces with only slight pressure. More importantly, they do not require a change of state or activation in order for them to be applied, as opposed to other types of adhesives, which obviously carries a number of benefits. PSAs are currently used in a wide number of applications that range from the ubiquitous Post-It® notes, tapes and labels for the packaging industry, to more specialized applications such as drug-delivery devices in the medical field.

Currently, solvent-based polymerization remains the main PSA production technology. However, increasingly stringent environmental regulations have led the PSA industry to shift to solvent-free technologies, such as hot-melt extrusion or technologies with environmentally-friendly solvents such as water-based polymerization and hot-melt extrusion. As a matter of fact, PSAs produced by water-based polymerization are gaining popularity for a number of reasons. The most prominent of these is the fact that switching from solvent-based to emulsion (latex)-based adhesives allows manufacturers to significantly reduce their emissions of volatile organic compounds. Thus, latex-based PSAs are less toxic and more environmentally friendly. Other benefits of using latex-based adhesives include the reduced risk of fire and minimization of the special precautions such as high ventilation, flameproof lighting and segregation from other factory operations required for the production of solvent-based adhesives. Water-based polymerization techniques such as emulsion polymerization can also yield products with higher solid contents at lower viscosities, which is desirable from a polymer processing standpoint.

Latex-based PSAs can be produced from natural or synthetic rubber, acrylics, silicones, polyvinyl ether, polyisobutylene and polybutadiene. Among these polymers,

acrylics are common commercial bases used to produce PSAs due to the inherent properties considered superior in comparison to other polymers. For example, their resistance to oxidation exceeds that of most polymers except for silicones; they are colorless and do not yellow with sunlight; they offer good shear strength and have the ability to form crosslinks; they are very versatile in the sense that their microstructure can be readily modified and polymerization can be carried out at atmospheric pressure (Satas, 1989). However, they also have various drawbacks: the properties of latex-based PSAs are inferior to those of solvent-based PSAs (Tobing and Klein, 2000), they display poor adhesion to low surface energy polymers, initial low tack and poor creep resistance compared to solvent-based adhesives (Petrie, 2000).

The performance of a PSA (solvent- or latex-based) will be reflected primarily on three properties that define whether the adhesive is effective or not. An effective adhesive must possess both liquid and solid properties: it must wet the surface when the bond is formed and must sustain a certain level of stress during debonding. These properties are tack, peel strength and shear strength and any technique used to produce PSAs must allow one to control them. Nevertheless, the optimum level of each one of these properties is often found at competing microstructural conditions, which represents a dilemma in PSA production and often leads to the addition of tackifiers and plasticizers (to improve tack or peel strength) or to post-polymerization blending of various polymers to achieve the desired properties (Geurts et al., 1996; Peters et al., 1996; Fabbroni et al., 2001). For instance, the three properties mentioned above usually increase with polymer molecular weight. However, the maxima of these properties appear at different values of molecular weight. The maximum of tack and peel strength is located at a relatively low molecular weight compared to the maximum for shear strength. The result is a set of conflicting properties where improvements to the adhesive component (usually represented by tack and peel strength) often result in a decrease in the cohesive component (usually represented by shear strength) and *vice versa* (Satas, 1989). Chemical composition and, in the case of latex-based polymerization, particle size distribution (PSD) also influence PSA performance (Jovanovic and Dubé, 2004).

A major limitation with post-polymerization blending and with the use of additives lies in the compatibility between the two polymers or between polymer and additive. They may not be completely compatible and the result would be a property-wise heterogeneous

material (Satas, 1989). Evidently, the more similar the chemical composition between the two polymers or between the polymer and tackifier, the more compatible they will be (Sung et al., 1998; Zhang et al., 2003; Sasaki et al., 2005). Since the change in properties when blending is additive (Satas, 1989), it is also possible that they can be tailored during polymerization as opposed to by blending. This idea triggered the present research project.

Emulsion polymerization is one of the water-based technologies that have been used in the production of PSAs (Jovanovic and Dubé, 2004). Several fundamental studies have increased our understanding of the performance of emulsion-based PSAs (Tobing and Klein, 2000; Tobing et al., 2001; Tobing and Klein, 2001a; Tobing and Klein, 2001b) and the microstructural differences with solvent-based PSAs that are responsible for their weaker performance. Miniemulsion polymerization is another water-based technique similar to conventional emulsion polymerization. Throughout this manuscript, this technique will be referred as "conventional emulsion polymerization" to better distinguish it from miniemulsion polymerization. The main difference between conventional emulsion and miniemulsion polymerization lies in how the particles are formed and its consequences in the polymerization mechanism (cf. Figure 1.1). In conventional emulsion polymerization, the polymer particles are formed during the reaction. Their size and number will depend on the concentration of the reactive species and surfactant. In contrast, miniemulsion polymerization uses mechanical energy to produce a dispersion of monomer droplets with a diameter range of 50 – 500 nm. These monomer droplets are stabilized against diffusional degradation and coalescence by the addition of surfactants and a highly hydrophobic compound. Miniemulsion polymerization is also characterized by the absence of surfactant micelles and smaller droplet sizes compared to conventional emulsion polymerization. All this combined leads to different particle growth mechanisms and thus, different final particle structures (cf. Figure 1.1).

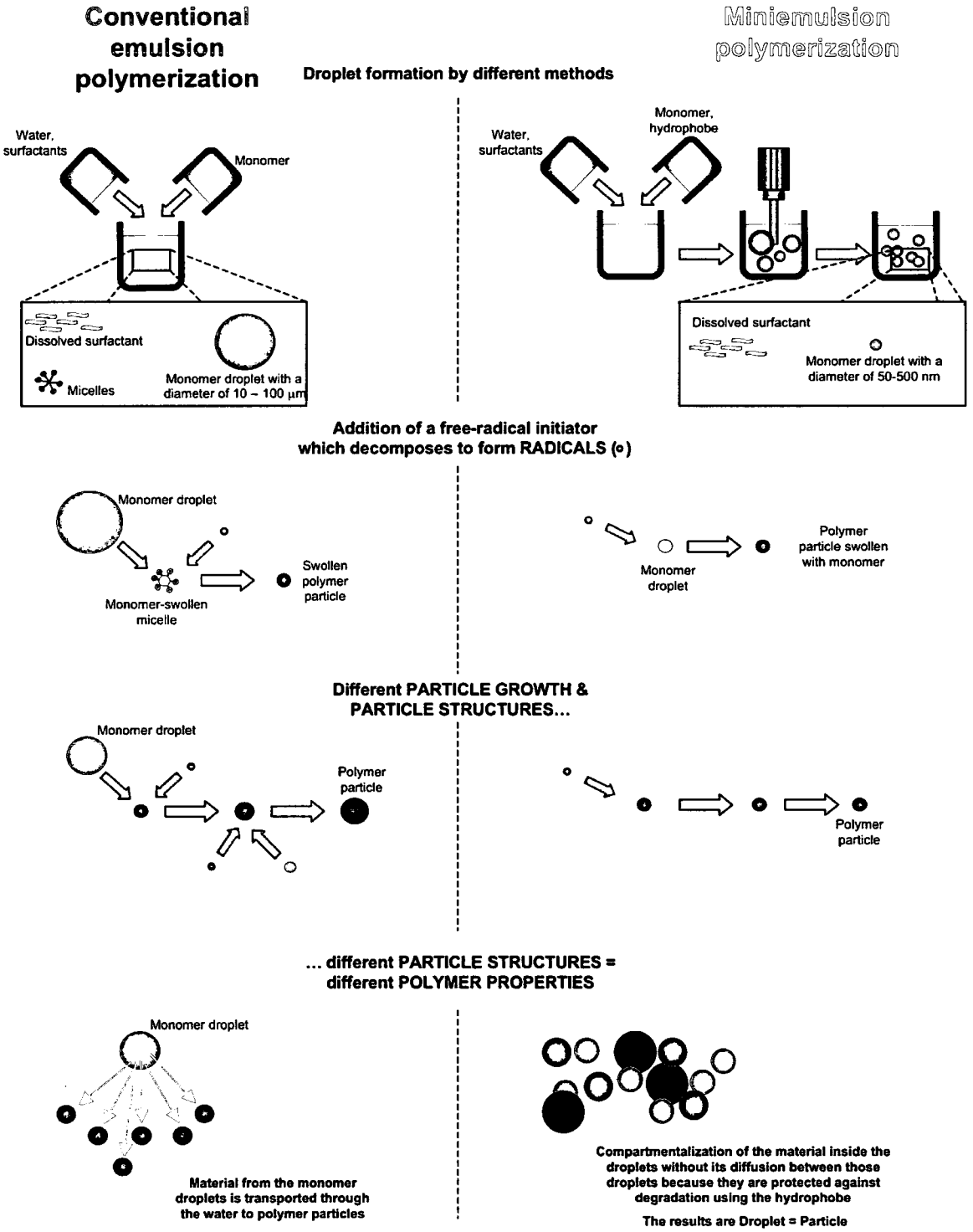

Figure 1.1. Conventional emulsion polymerization versus miniemulsion polymerization

The nucleation mechanism of miniemulsion polymerization offers a benefit to produce PSAs. The specific particle growth of miniemulsion polymerization is able to encapsulate any compound that can be regarded as hydrophobic, e.g., oligomers, monomers with low water solubility and inorganic particles (Asua, 2002). If the miniemulsion has been adequately stabilized, monomer transfer between droplets or between particles can be minimized, i.e., intra- and extra-particle monomer diffusion resistance can be maximized allowing the monomer droplets to keep their identity throughout the reaction without serious exchange kinetics involved. The latter has led to the name "nanoreactors" being given to the resulting polymer particles (Antonietti and Landfester, 2002). It is then possible to obtain different properties from unique systems at once by blending two or more miniemulsions prior to reaction since no matter is exchanged between the two polymer systems (Landfester et al., 1999; Ouzineb et al., 2004). This is the second idea that motivated this study.

If the intra- and extra-particle monomer diffusion resistance phenomena are exploited to produce various particle populations tailored to perform as PSAs with different adhesive properties that would counterbalance each other, miniemulsion polymerization could offer a unique advantage in the design of PSAs. Based on these considerations, a study of the production of PSAs using miniemulsion polymerization was conducted. The adhesive properties and microstructure of miniemulsion-based latexes were compared to those of latexes prepared using conventional emulsion polymerization. A one-pot two-step miniemulsion polymerization approach was developed to produce PSAs with bimodal distributions of molecular weight or particle size. Lastly, an exploratory study of the use of AFM in its force imaging mode was employed to evaluate adhesion forces of PSA surfaces and the influence of bimodal MWD or PSD on the resulting "nano-adhesive" properties.

1.1 OBJECTIVES OF THE RESEARCH

The principal aim of this research project was to exploit miniemulsion polymerization and to develop a process that generates multimodal molecular weight and/or particle size distributions for tailoring PSA properties. In order to achieve this, the following objectives were established:

(1) *Study the miniemulsion polymerization of two candidate polymer systems used commercially as PSAs.*

The stability and maximization of the intra- and extra-particle monomer diffusion resistance of the miniemulsion polymerization of 2-ethyl hexyl acrylate/vinyl acetate and 2-ethyl hexyl acrylate/methyl methacrylate were studied to identify a suitable candidate for the production of PSAs.

(2) *Compare the performance and microstructural differences of PSAs produced using conventional emulsion and miniemulsion polymerization.*

A factorial design was used to assess the influence of the copolymer composition, chain transfer agent concentration and surfactant concentration on the polymer properties (molecular weight, particle size), viscoelastic behaviour and PSA performance.

(3) *Develop a polymerization process using miniemulsion polymerization to create latexes with bimodal distributions of molecular weight and particle size.*

Latexes with bimodal distributions of molecular weight and particle size were produced and used to assess their influence on PSA performance. The knowledge obtained serves as a guide for PSA design. The PSA performance of the latexes with bimodal distributions was compared with that of blended latexes.

(4) *Study the use of Atomic Force Microscopy (AFM) as a tool to estimate adhesive force at the PSA film surface in view to relate them with macroscopic properties*

The surface morphology of PSA films with bimodal distributions of molecular weight or particle size was obtained using AFM in Tapping Mode. At the same time, force curves were collected to evaluate the attraction and adhesive forces using the jump-to-contact and jump-off-contact measurements. These measurements provided information about the chemical and adhesive heterogeneity of the resulting films.

1.2 STRUCTURE OF THESIS

The research project was accomplished following a research plan that contemplated the requirements needed to achieve the main goal of designing PSAs using bimodal distributions of molecular weight or particle size. As can be seen in the schematic shown in Figure 1.2, the research was divided into several sections. Each section was designed to fulfill one of the objectives outlined above.

The thesis is then subsequently divided into five chapters. With the exception of the chapter dedicated to the theoretical background, each one of the chapters is connected to a section in the research plan shown in the schematic as it is discussed below. Since this thesis is prepared in a journal article format, each one of these chapters corresponds to an independent publication that has been or will be submitted to a refereed scientific journal. With this in mind, the reader can expect to find similar information in the introductory and methodological sections of the various chapters.

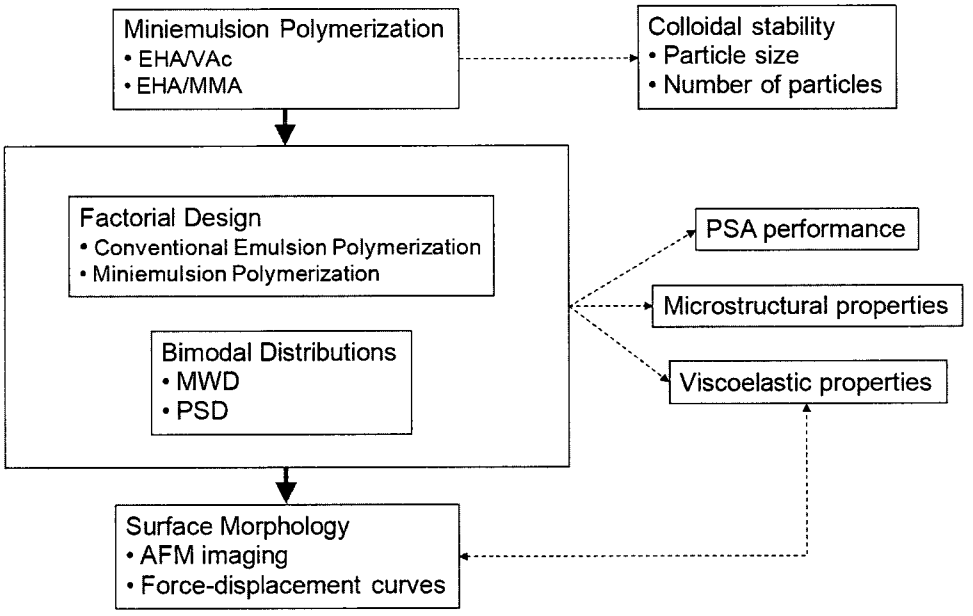

Figure 1.2. Schematic overview of research methodology

The chapters are arranged as follows:

Chapter 2. Theoretical background and research methodology

This chapter was designed to offer the reader concise background and fundamental information necessary to understand the following chapters. It covers the principles of emulsion and miniemulsion polymerization as well as information needed for an understanding of PSA performance. This chapter also includes a section devoted to the research methodology. The section contains detailed information on preparation, polymerization and characterization methods that, due to the concise nature of journal publications, were not given in the subsequent chapters. The information provided in this chapter does not intend to be a comprehensive review of the topic but rather an overview. Citations to thorough reviews in those areas are also given for those readers that wish to expand on their understanding of the various related subjects.

Chapter 3. Preparation of stable miniemulsions of poly (2-ethyl hexyl acrylate-co-vinyl acetate). Fonseca, G.E.; McKenna, T.F.L.; Dubé, M.A.; *Macromolecular Symposia*, in press.

This chapter presents the results of the preparation of miniemulsions as well as the subsequent copolymerizations of 2-ethyl hexyl acrylate and vinyl acetate. This copolymer was one of the candidates to be used as a PSA. A screening design was used to assess the stability of the miniemulsion. Next, a 2^3 factorial design was employed to assess the influence of the hydrophobe concentration, chain transfer agent concentration, copolymer composition and total surfactant concentration on the droplet size distributions and particle size distribution.

Chapter 4. Influence of particle nucleation in pressure sensitive adhesive properties: miniemulsion versus emulsion polymerization Fonseca, G.E.; McKenna, T.F.L.; Dubé, M.A.; *Macromolecular Symposia* 271, 83-93, 2008

This chapter presents a systematic comparison of the adhesives properties of latexes produced by miniemulsion and conventional emulsion polymerization. The results show that

under the conditions used in this work, it is possible to produce pressure sensitive adhesives using miniemulsion polymerization carried out mostly by droplet nucleation. The findings also served to refine the area of study and gave a better understanding of miniemulsion-based pressure-sensitive adhesives.

Chapter 5. Miniemulsion versus conventional emulsion polymerization for pressure-sensitive adhesives production. Fonseca, G.E.; McKenna, T.F.L.; Dubé, M.A.; *Chemical Engineering Science*, 65, 2797-2810, 2010

A systematic study of the production of poly (2-ethyl hexyl acrylate/methyl methacrylate/acrylic acid) PSAs via conventional emulsion and miniemulsion polymerization was carried out in order to discern and compare the influence of copolymer composition, chain transfer agent (CTA) and surfactant concentrations on the kinetics and microstructure of the resulting adhesive films as in the previous chapter.

Chapter 6. Bimodal particle size and molecular weight distributions using a one-pot two-step miniemulsion polymerization strategy. Fonseca, G.E.; McKenna, T.F.L.; Dubé, M.A.; *Industrial and Engineering Chemistry Research*, submitted.

In this chapter, a one-pot two-step miniemulsion polymerization approach is presented. The approach was successfully used to create poly (2-ethyl hexylacrylate/methyl methacrylate/acrylic acid) PSAs with well-defined and predictable bimodal particle size distributions (PSD) or bimodal molecular weight distributions (MWD). The resulting viscoelastic (shear storage and loss modulus) and adhesive properties (i.e., loop tack, peel strength and shear strength) were tested and compared to monomodal distributions of either particle size or molecular weight along with bimodal distributions created by post-polymerization blending

Chapter 7. Relating PSA performance properties to adhesion force and energy determined by atomic force microscopy

An exploratory study of the use of atomic force spectroscopy (AFM) for the estimation of nanomechanical properties of PSA films was carried out. The first goal of the study was to evaluate the dependence of adhesion forces obtained by AFM on the molecular weight and/or particle size distribution of PSA samples. A second goal of the study was to evaluate if there was a correlation between the adhesive properties experienced at the nanoscale (i.e., at the film surface) and those at the macroscale (e.g., tack and peel strength).

1.3 REFERENCES

Antonietti, M., Landfester, K., 2002. Polyreactions in miniemulsions. Progress in Polymer Science 27, 689-757.

Asua, J.M., 2002. Miniemulsion polymerization. Progress in Polymer Science 27, 1283-1346.

Aymonier, A., Papon, E., Villenave, J.J., Tordjeman, P., Pirri, R., Gérard, P., 2001. Design of pressure-sensitive adhesives by free-radical emulsion copolymerization of methyl methacrylate and 2-ethylhexyl acrylate. 1. Kinetic study and tack properties. Chemistry of Materials 13, 2562-2566.

Dube, M.A., Amin Sanayei, R., Penlidis, A., O'Driscoll, K.F., Reilly, P.M., 1991. A microcomputer program for estimation of copolymerization reactivity ratios. Journal of Polymer Science Part A: Polymer Chemistry 29, 703-708.

Fabbroni, E.F., Shull, K.R., Hersam, M.C., 2001. Adhesive and mechanical properties of soft nanocomposites: Model studies with blended latex films. Journal of Polymer Science Part B-Polymer Physics 39, 3090-3102.

Fonseca, G.E., McKenna, T.F., Dubé, M.A., 2008. Influence of Particle Nucleation in Pressure Sensitive Adhesive Properties: Miniemulsion versus Emulsion Polymerization. Macromolecular Symposia 271, 83-93.

Geurts, J.M., Lammers, M., German, A.L., 1996. The effect of bimodality of the particle size distribution on film formation of latices. Colloids and Surfaces A-Physicochemical and Engineering Aspects 108, 295-303.

Hua, H., Dubé, M.A., 2001. Off-line monitoring of butyl acrylate, methyl methacrylate and vinyl acetate homo- and copolymerizations in toluene using ATR-FTIR spectroscopy. Polymer 42, 6009-6018.

International Organization for Standardization, 1996. Methods for Determination of Particle Size Distribution Part 8: Photon Correlation Spectroscopy. International Standard ISO13321,

Jovanovic, R., Dubé, M.A., 2004. Emulsion-based pressure-sensitive adhesives: A review. Journal of Macromolecular Science: Polymer Reviews C44, 1-51.

Landfester, K., Bechthold, N., Forster, S., Antonietti, M., 1999. Evidence for the preservation of the particle identity in miniemulsion polymerization. Macromolecular Rapid Communications 20, 81-84.

Lathova, E., Lath, D., Pavlinec, J., 1993. The Behavior of Poly (2-Ethylhexyl Acrylate) in Dilute-Solution - Viscosity Measurements. Polymer Bulletin 30, 713-718.

Maron, S.H., Elder, M.E., Ulevitch, I.N., 1954. Determination of Surface Area and Particle Size of Synthetic Latex by Adsorption .6. Critical Micelle Concentrations of Various Emulsifiers in Latex. Journal of Colloid Science 9, 382-384.

Ouzineb, K., Graillat, C., McKenna, T.F., 2004. Study of compartmentalization in the polymerization of miniemulsions of styrene and butyl methacrylate. Journal of Applied Polymer Science 91, 115-124.

Patnaik, M., Choudhary, V., Varma, I.K., 1992. Structural and thermal characterization of methyl methacrylate/alkyl acrylate copolymers. European Polymer Journal 28, 1433-1439.

Peters, A.C.I.A., Overbeek, G.C., Buckmann, A.J.P., Padget, J.C., Annable, T., 1996. Bimodal dispersions in coating applications. Progress in Organic Coatings 29, 183-194.

Petrie, E.M., 2000. Handbook of Adhesives and Sealants, 1st edition ed. McGraw-Hill, New York.

Pressure Sensitive Tape Council, 2004. Test Methods for Pressure Sensitive Adhesive Tapes, 14th ed. ed. Pressure Sensitive Tape Council, Northbrook, Illinois.

Sasaki, M., Nakamura, Y., Fujita, K., Kinugawa, Y., Iida, T., Urahama, Y., 2005. Relation between phase structure and peel adhesion of poly (styrene-isoprene-styrene) triblock copolymer/tackifier blend system. Journal of Adhesion Science and Technology 19, 1445-1457.

Satas, D., 1989. Acrylic Adhesives, in: Satas, D. (Eds.), Handbook of Pressure-Sensitive Adhesive Technology. Van Nostrand Reinhold, New York, pp. 396-

Schneider, M., 2000. Etude de Procédés de Synthèse de Latex Multipopulés à Haut Extrait Sec.

Stubbs, J.M., Sundberg, D.C., 2005. Measuring the extent of phase separation during polymerization of composite latex particles using modulated temperature DSC. Journal of Polymer Science, Part B: Polymer Physics 43, 2790-2806.

Sung, I.K., Kim, K.S., Chin, I.J., 1998. Dynamic mechanical and morphological study on model pressure sensitive adhesive based on poly (styrene-b-butadiene-b-styrene). Polymer Journal 30, 181-185.

Tobing, S., Klein, A., Sperling, L.H., Petrasko, B., 2001. Effect of network morphology on adhesive performance in emulsion blends of acrylic pressure sensitive adhesives. Journal of Applied Polymer Science 81, 2109-2117.

Tobing, S.D., Klein, A., 2000. Mechanistic studies in tackified acrylic emulsion pressure sensitive adhesives. Journal of Applied Polymer Science 76, 1965-1976.

Tobing, S.D., Klein, A., 2001a. Molecular parameters and their relation to the adhesive performance of acrylic pressure-sensitive adhesives. Journal of Applied Polymer Science 79, 2230-2244.

Tobing, S.D., Klein, A., 2001b. Molecular parameters and their relation to the adhesive performance of emulsion acrylic pressure-sensitive adhesives. II. Effect of crosslinking. Journal of Applied Polymer Science 79, 2558-2564.

Zhang, X.M., Tasaka, S., Inagaki, N., 2003. Adhesion behavior of blends of polybutadiene and tackifiers. Journal of Adhesion Science and Technology 17, 423-434.

CHAPTER 2

THEORETICAL BACKGROUND AND RESEARCH METHODOLOGY

This chapter is divided in two sections. The first offers the reader an overview of emulsion and miniemulsion polymerization as well as the basis needed to understand the performance of pressure-sensitive adhesives (PSAs). The second section focuses on the research methodology employed. It details each one of the preparation and characterization techniques used throughout this study that, due to the concise nature of scientific publications, was not included in subsequent chapters.

2.1 THEORETICAL BACKGROUND

2.1.1 Pressure sensitive adhesives

Adhesives are substances capable of attaching to materials by surface contact through adhesion and cohesion mechanisms in a strong and permanent manner. The adhesion mechanism refers to the attraction of two different substances resulting from intermolecular forces between them; meanwhile the cohesion mechanism involves intermolecular attractive forces within a single substance. Adhesives are primarily classified according to the type of application as structural and non-structural adhesives. PSAs are the most common type of non-structural adhesives. According to the Pressure Sensitive Tape Council (Pressure Sensitive Tape Council, 2004), "a PSA is an adhesive that is aggressively and permanently tacky and adheres without the need of more than a finger or hand pressure. It does not require activation by any energy source, it has sufficient ability to hold onto an adherend and it also has enough cohesive strength to be able to be removed cleanly from the adherend". PSAs are used in a wide range of applications such as tapes, protective films, and labels. They can be produced by hot-melt, radiation-cured, solvent-based and water-based polymerization (emulsion processes). Table 2.1 summarizes some of the advantages and disadvantages of these techniques (Pizzi and Mittal, 2003).

Table 2.1. Advantages and disadvantages of various techniques for the preparation of PSAs (reproduced from Pizzi and Mittal (2003))

Solvent-based	Water-based	Hot-melt
	Advantages	
• Quick drying • Good adhesion to non-polar substrates • Good bond strength to plastics • Versatile	• Easy cleaning • Good adhesion to polar substrates • Good heat and aging resistance • Environmentally acceptable • High solids • Ready to use	• Very fast setting • No solvent waste • Environmentally acceptable • 100% active
	Disadvantages	
• Flammability • Toxicity • Relatively low solids content • Less easy to clean	• Slow drying • Requires heat to dry • Poor adhesion to non-polar substrates	• High equipment cost • Requires heat • Thermal degradation possible • Difficult to clean • Temperatures can affect substrate

Because of their many advantages and due to increasingly stringent regulations regarding volatile organic compounds (VOCs), many companies are switching from solvent-based to latex-based adhesives. Nowadays, latex-based PSAs have a dominant position in the market place (Petrie, 2000). The PSA industry is challenged now to optimize their properties to make them equally good or better than their solvent-based counterparts.

Latex-based PSAs can be prepared from natural or synthetic rubber, acrylics, silicones, polyvinyl ether, polyisobutylene and polybutadiene. In particular, acrylic-based PSA have a large commercial importance since they offer many advantages such as good resistance to temperature; ability to form crosslinks; good resistance to chemicals, UV and oxidation; colour stability; good shear strength and good hydrolysis resistance. They have a few drawbacks such as poor adhesion to low surface energy polymers, initial low tack and poor creep resistance compared to elastomer-based adhesives (Petrie, 2000). The present study is consequently focused on latex-based acrylic PSAs due to their many positive features.

Acrylic water-borne PSAs are usually composed of the following elements (Satas, 1989a; Jovanovic and Dubé, 2004):

- A monomer with a low glass transition temperature (T_g), such as butyl acrylate (BA), 2-ethyl hexyl acrylate (EHA) or iso-octyl acrylate (IOA) are used to impart tack. These monomers are sometimes called "soft" monomers.
- A monomer with a high T_g such as methyl methacrylate (MMA), methyl acrylate (MA) or vinyl acetate (VAc) are used to impart cohesive strength. These compounds are called "hard" monomers.
- A functional monomer such as acrylic acid (AA) or methacrylic acid (MAA) is added to enhance cohesion and provide sites for intermolecular crosslinking. Possible crosslinking reactions include radiation decarboxylation leading to radical formation and crosslinking by polymerization and recombination. Functional monomers also enhance cohesion through an increase of the overall copolymer T_g, since their homopolymers usually exhibit high T_g values (i.e., higher than room temperature). On the other hand, the functional groups (such as carboxylic acids or hydroxyl groups) also help wetting the adherend surface and accelerate the rate of bonding (tack).

2.1.2 Properties of PSAs

As mentioned earlier, the PSA adhesion will depend primarily on three properties that define whether the adhesive is effective or not. An effective adhesive must possess both liquid and solid properties, i.e., it must wet the surface when the bond is formed and must sustain a certain level of stress during debonding. These properties are tack, peel strength and shear strength.

Tack is probably the most important property of PSAs and is defined as the ability of an adhesive to form a bond of measurable strength to another material under conditions of low contact pressure and short contact time (Zosel, 2000). This definition also explains why tack is also one of the most difficult properties to measure in a PSA, since it is not a fundamental property but depends on the test methods and measurement conditions. In other

words, tack is a measurement of how easily and how quickly a given adhesive can be applied to a chosen substrate.

Peel strength is a measure of how difficult it is to remove the adhesive once it has been attached firmly to a substrate (Benedek, 2004). As defined by the Pressure Sensitive Tape Council (Pressure Sensitive Tape Council, 2004), peel strength is the force per unit width required to break the bond between a PSA tape and the surface to which it has been applied when the tape is peeled back at a controlled angle and at a standard rate and condition. There are two common angles at which the tape is peeled off: 90° and 180° (although obvious, it is important to point out here that the values obtained will be different if the angle is at 90° or 180° and therefore, the angle used must be reported along with the experimental conditions).

Shear strength is the shear force required to pull the PSA parallel to the surface to which it is affixed with a definite pressure. Therefore, shear strength is a measure of the cohesive strength, which reflects the ability of the adhesive to be removed from the substrate without leaving a residue.

2.1.3 Factors influencing PSA properties

There are several factors influencing the PSA properties that can be manipulated during a reaction. Tack is strongly influence by the chemical nature and composition of the polymer, which is reflected in the T_g of the adhesive. Considering that most PSAs are used at room temperature, an adequate T_g should be around -50 to -30°C (Créton, 2000). In most cases, lowering the T_g will increase the resulting tack values. For example, Athawale and Rathi (1995) studied the effect of monomer concentration on acrylic PSAs prepared with EHA, butyl methacrylate (BMA) and AA and they found that tack increased with the amount of EHA up to a maximum value of 60 wt.% of this monomer and then decreased. In this case, the T_g of the terpolymer decreased as the amount of EHA increased, which in turn increased tack up to a maximum, wherein the T_g was too low to give proper adhesion.

Tack also increases with the homogeneity in the copolymer composition, i.e., more homogeneous particles lead to higher values of tack (Laureau et al., 2001). Molecular weight also poses an influence on the resulting values of tack. A minimum molecular weight that

gives a storage modulus (G') of ~1 x 10^5 to 1 x 10^6 dyne/cm^2 is needed to impart adhesion (Chu, 1989). However, much higher molecular weights will negatively affect tack since they will not allow the adhesive to wet the surface and bond.

The molecular weight between crosslink points (M_c) and the entanglement molecular weight (M_e) are particularly important in PSA performance. They have a strong influence on tack and in general, over all the PSA properties (Zosel, 1991; Zosel and Ley, 1993; Tobing and Klein, 2000; Tobing et al., 2001; Tobing and Klein, 2001a; Tobing and Klein, 2001b). Crosslinking yields lower tack values but confers high shear resistance (Benedek, 2004). Tobing and Klein (2001b) studied the effect of crosslinking on the PSA properties. Isobutoxy methyl acrylamide (IBMA) was introduced into a polymer backbone of EHA or BA to provide additional crosslinking levels after drying the film at an elevated temperature. In their study, tack was found to decrease after the addition of the crosslinking agent. In a following study, they found that tack was also affected by the molecular properties of the sol polymer (the fraction of polymer that can be dissolved in a testing solvent) (Tobing and Klein, 2001): higher sol fractions gave increased tack and peel strength values because of the increased viscoelastic energy dissipation and more intimate contact with a substrate. In the case of M_e, higher values will favour the formation of fibrils, which are known to lead to a high fracture energy and thus, high tack (Zosel, 1998). Fibrillation is observed with M_e above 1 x 10^4 g/mol. However, care should be taken when designing PSAs since fibrillation is also reduced by crosslinking and completely suppressed when the crosslink density is higher than the entanglement density (Zosel, 1998).

The presence of surfactant also reduces tack since the surfactant may migrate to the interface between adhesive and substrate causing a loss in adhesion (Charmeau et al., 1996; Gerin et al., 1999; Charmeau et al., 1999a; Charmeau et al., 1999b; Laureau et al., 2001; Mallégol et al., 2002). However, surfactants are an essential component in dispersion technologies. In emulsion formulations, surfactants modify the particle size distribution, which also affects the rate of polymerization, latex viscosity and film formation and in turn, tack, peel and shear strength. The presence of surfactants is unavoidable in dispersion technologies; however, the type of surfactant and the concentration used can be modified to attempt to minimize their negative influence on the PSA properties. Cannon and Pethrick (2002a, 2002b) produced BA/MMA and EHA/MMA copolymer latexes and using dynamic

mechanical analysis and atomic force microscopy, they were able to elucidate the effect of different types of surfactants, specifically nonyl-phenol ethoxylated-based surfactants on the mechanisms of film formation. They observed that different types of surfactants can cause different final film structures and different chain lengths of the non-ionic surfactants can cause an effect on the T_g of the polymer and thus, affect storage modulus, which will in turn affect PSA performance.

The testing conditions also influence the resulting tack values, i.e., the coating weight, the testing temperature, the type of carrier, the substrate, peeling speed and dwelling time also have an effect on the final reported values of tack. The coating weight (i.e., the thickness of the adhesive layer once it has been coated), for example, influences the flow conditions and in general, is directly proportional to tack. The testing temperature also influences tack. It has been shown by Zosel (2000) that in the case of polyacrylates, tack increases with testing temperature up to a maximum related to the acrylate structure.

Most of the factors that affect tack also affect peel strength. Peel strength is a function of the chemical nature of the adhesive, the molecular weight of the polymer components, and physical factors such as adhesive layer thickness, type and characteristic of the carrier and dwelling time (Jovanovic and Dubé, 2004). Detailed studies on this topic were presented by Benedek (2004) and Satas (1989).

Shear strength is also influenced by the nature of the monomer. For example, the introduction of a "soft" monomer will decrease shear strength, while increasing the amount of "hard" or polar monomers, e.g., MMA, AA, MAA, will increase it. Shear strength is also positively affected by the molecular weight and will increase if the polymer presents a high molecular weight. The molecular weight distribution (MWD) is also extremely important. A broad MWD will lower the value of shear strength when compared to a polymer with a narrower MWD.

Although tack, peel strength and shear strength are mostly influenced by the same intrinsic or structural properties, it is important to point out that they are not affected in similar proportions, i.e., in most cases, factors that positively influence tack and peel strength will have a negative impact on shear strength and *vice-versa*. Figure 2.1 shows an example of how these properties are influenced in a seemingly contradictory way.

It is apparent from the above discussion that the chemical composition, molecular weight and amount of surfactant are the most influential factors affecting PSA properties. For a detailed review on the factors affecting these properties refer to Benedek (2004), Satas (1989) and Jovanovic and Dubé (2004).

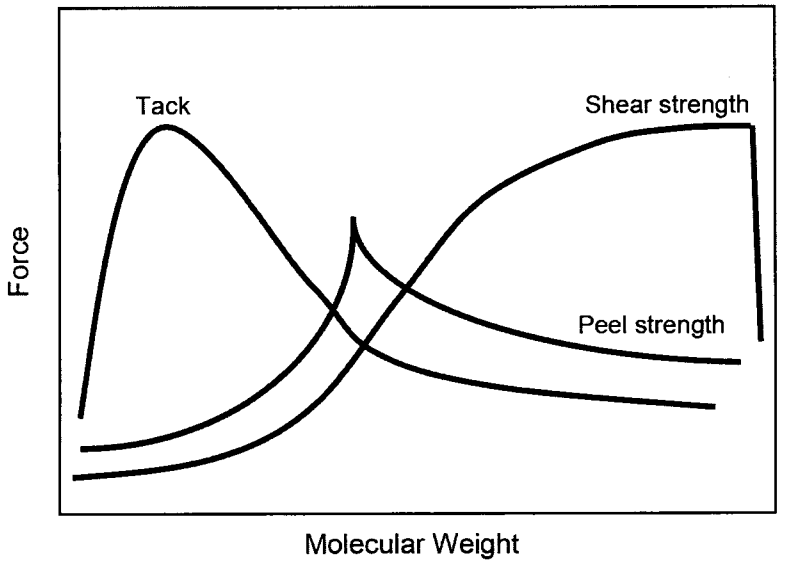

Figure 2.1. PSA properties as a function of molecular weight (Satas, 1989)

The performance of PSAs can also be related to the viscoelastic behaviour of the bulk polymer (Chu, 1989), i.e., to the storage modulus (G'), loss modulus (G") and tan δ. Table 2.2 briefly shows their influence on the adhesive properties (Petrie, 2000). It is acknowledged that the viscoelastic properties are affected by the initial reaction conditions. Nevertheless, knowledge of the viscoelastic properties gives the "big picture" of PSA performance since each region of the viscoelastic spectrum corresponds to different characteristics of the molecular structure (Créton, 2000). For example, the transition from the glassy to the rubbery region is governed by the T_g while the rubbery plateau and viscous flow regions are related to the molecular weight between entanglements, average molecular weight, branching and crosslinking in the polymer.

Various studies have report the use of viscoelastic measurements on PSAs. Aubrey and Sherriff (1980) developed correlations of peel modes with various peel failure modes to different rheological regions of PSAs. Dale et al. (1989) related small-strain and high-strain

measurements to end-use properties (peel strength and shear strength). In their study, they established that the majority of the performance range shown by commercial PSAs is controlled by the bulk mechanical properties of the polymers involved.

Table 2.2. Viscoelastic properties related to PSAs (Reproduced from Petrie (2000))

Property	Effect
Tack	Low tan δ and low G' Low crosslinks (G">G') at 1 Hz of frequency
Shear strength	High G' modulus at low frequencies < 0.1 Hz High viscosity at low shear rates
Peel strength	High G" at higher frequencies > 100 Hz
Cohesive strength	High G' and low tan δ (bulk property)
Adhesive strength	High G" and high tan δ (adhesion with the surface)

2.1.4 Controlling PSA properties

Most research to date focuses on either the effect of the initial polymerization reaction conditions on the intrinsic or microstructural polymer properties or on the effect of changes in polymer properties on the PSA properties. The common approach in these studies has been through trial and error, which can be time consuming. Little work has been focused on understanding how initial polymerization conditions affect the end-use PSA properties. This is likely due to the difficulty in studying large numbers of factors that are known to affect PSA performance. Herein are listed some of the most important studies on this subject.

Elizalde et al. (Elizalde et al., 2002; Elizalde et al., 2004) developed a model relating the adhesive properties with the complete MWD of butyl acrylate (BA)/styrene (STY) latexes with a fixed copolymer composition. The approach consisted of the control of final properties establishing a quantitative relationship between adhesive properties and the MWD. They observed that the latexes with bimodal MWD produced "in-reaction" yielded better results than MWD latexes formed via blending latexes with different MWDs.

Jovanovic et al. (2004a) and Jovanovic and Dubé (2005) developed empirical models relating PSA properties of BA/VAc adhesives to initial reaction conditions such as the chemical composition, AA content, chain transfer agent and surfactant concentrations. A

constrained mixture design was used to investigate the influence of individual monomers on the final adhesive performance. Yet another approach was presented by Aymonier et al. (2003), where they produced a MMA/EHA copolymer to study the correlation between the polymer structure (at the nanoscopic and mesoscopic scales) and the tack properties of the PSA adhesives (macroscopic scale). They used three different polymerization processes: batch, semi-batch with a constant feed rate of monomer mixture and semi-batch with an inversely varying feed rate of the monomers. As expected, the different processes produced different particle morphologies, which in turn resulted in different degrees of composition homogeneity in the polymer particle. The semi-batch process with a constant feed rate of monomer produced a homogeneous statistical copolymer, the batch process adopted an intermediate structure and the semi-batch process with an inversely varying monomer feed rate produced a highly heterogeneous particle with fewer statistical sequences in the chain. The study proved that strict homogeneity does not necessarily result in satisfactory PSA performance. The study carried out by Aymonier et al. (2003) also confirmed the possibility of adjusting the tack properties of PSA by direct synthesis rather than by conventional blending, i.e., by selection of a batch or semi-batch process and the appropriate monomer feed profile needed to produce a specific microstructure..

2.1.5 Emulsion and Miniemulsion polymerization

2.1.5.1 Emulsion polymerization

An emulsion polymerization is a chain growth reaction initiated by free radicals. It is a complex system that involves an inorganic phase (usually water), an organic phase (monomers) and surfactants. One of these phases is dispersed in the other as particles using the surfactant to protect the particles against coalescence electrostatically (ionic surfactants) or by steric hindrance (non-ionic surfactants). A typical emulsion polymerization recipe contains monomers (it can be more than one as in the case of co- or terpolymerizations), surfactants (mixed surfactant systems such as ionic/non-ionic can be present), initiator, chain transfer agent (which modifies the molecular weight of the polymer) and the dispersion medium, which is typically water. Other components can also be added to enhance colloidal

stability, and ultraviolet or oxidation protection, among others. A brief description of each component is presented next:

1. Monomer is the main component in an emulsion polymerization and can be classified as either "soft" or "hard" depending on the T_g of the polymer. The T_g of soft monomers is usually below 0°C and that for hard monomers above 0°C. As mentioned before, the final T_g of a typical PSA could range from -5 to -50°C, depending in the application temperature. It is important to carefully select the monomer(s) to be polymerized, since the T_g of the final product, and thus, many of the adhesive properties will depend on it. Some of the most common monomers used in the fabrication of PSAs are butadiene (BD), STY, vinyl chloride (VC), VAc, vinylidene chloride (VDC), BA, MMA and EHA. Functional monomers can also be found in the formulation of PSA latexes to increase crosslinking or to enhance latex stability. The most common types of functional monomers are from the carboxylic acid family such as AA or MAA. However, groups such as hydroxyl groups, chloride moieties, amine groups, isocyanate groups, derivatives of acrylamide, epoxy groups and sulfonate groups can also act as functional monomers, although not commonly used in the PSA industry (Lovell and El-Aasser, 1997).
2. Initiators are the source of free radicals needed to start the polymerization. While several types of initiators can be used in these reactions, only those that produce free radicals through thermal decomposition are of interest in this study. In conventional emulsion polymerization, the initiator is water-soluble while in miniemulsion polymerization, it can be either water-soluble (e.g., ammonium persulfate, potassium persulfate) or oil-soluble (e.g., benzoyl peroxide, 2,2'-azobisisobutyronitrile).
3. Surfactants are a key component in any emulsion polymerization formulation. They can be divided into four types: electrostatic, steric, electrosteric and polymeric surfactants. The first three types are the most commonly used in latex-based PSA formulations. Electrostatic and electrosteric surfactants can be anionic or cationic surfactants. Surfactants are added to the formulation to lower the interfacial tension and facilitate droplet break-up (Lovell and El-Aasser, 1997; Holmberg, 2003; Karsa, 2003), for particle stabilization and for the creation of nucleation sites in the form of micelles.

4. Buffers are another component in a typical emulsion recipe. They are added to regulate the pH of the mixture. Various monomers present in systems with high pH values can undergo hydrolysis while at low pH values, a number of initiators have faster decomposition rates leading to a reduction in the number of free radicals, which has an impact on monomer conversion.
5. Chain transfer agents are used to control the molecular weight and its distribution in the final product. The most common chain transfer agents are from the mercaptan family due to their high efficiency.

The formulation can also contain other additives to enhance final product properties. Some of these additives include tackifiers, peel modifiers, wetting agents, rheology modifiers and antioxidants.

Emulsion polymerization can present three types of nucleation (although not necessarily all of them). The term "nucleation" refers to the creation of a polymer particle. See Figure 2.2 for a schematic representation of particle nucleation mechanisms. The first type is known as micellar nucleation. In the micellar nucleation mechanism, the free-radicals generated with the decomposition of the initiator react with the monomer dissolved in the aqueous phase to form oligoradicals. Monomer continues to be added to the oligoradicals until they reach a critical length, which renders them insoluble in the aqueous phase. The oligoradicals enter the monomer-swollen micelles where the polymerization continues. Once the polymerization has started, the monomer-swollen micelles become polymer particles. Particle nucleation finishes when the micelles are depleted. This type of nucleation occurs when micelles are present in the reaction mixture and predominates over other types of nucleation because the surface area offered by the surfactant micelles is many times larger than that of the monomer droplets, i.e., it is more likely that a radical or oligoradical will enter a micelle than a monomer droplet. It is expected that monomers with low water-solubility, such as MMA or STY, would nucleate primarily through this type of mechanism.

The second type of nucleation mechanism is homogeneous nucleation. In this case, radicals generated in the aqueous phase propagate with the monomer to form water-soluble oligomers. They continue to propagate in the aqueous phase until they reach their water solubility limit, which causes them to precipitate. The precipitated oligomer particles form

primary particles, which will adsorb surfactant dissolved in the aqueous phase and become stabilized to form polymer particles. The polymer particles created by homogenous nucleation will behave as those created by micellar nucleation. They will grow with the monomer fed by the monomer droplets. A subtype of the homogenous nucleation mechanism, named coagulative nucleation has also been proposed (Lovell and El-Aasser, 1997). In this type of nucleation, primary particles are created by homogenous nucleation,

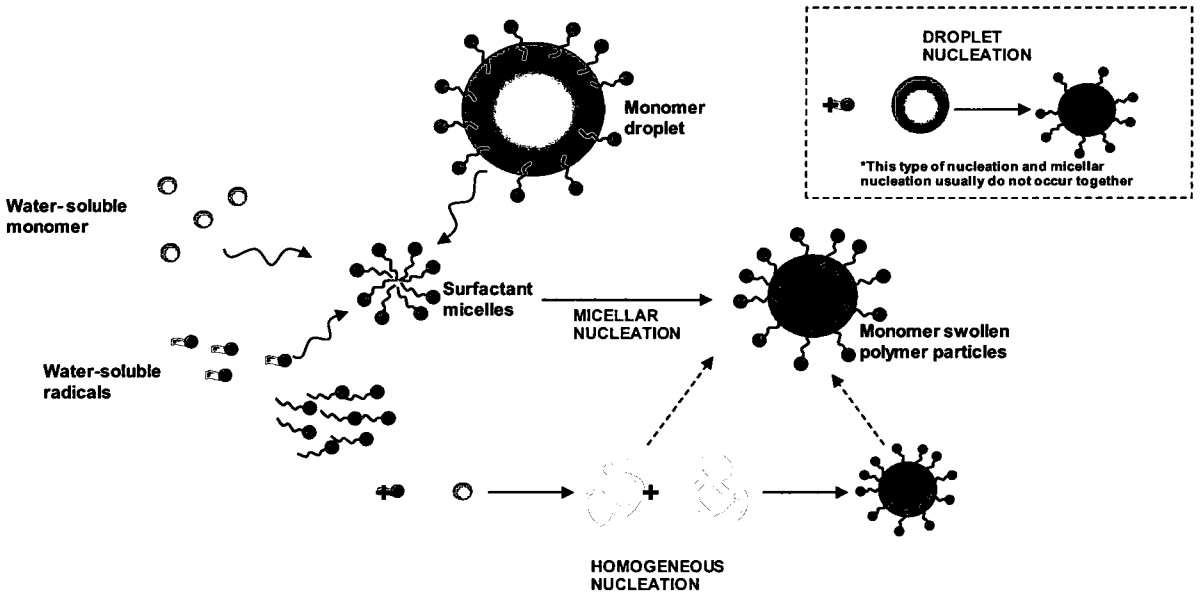

Figure 2.2. Nucleation mechanisms in emulsion polymerization

but due to their small size, which will prevent them from becoming polymer particles after adsorption of surfactant, they will instead coagulate with similar primary particles until their size is big enough to become mature polymer particles. It has been speculated that this nucleation might occur simply because primary particles are more likely to grow by coagulation rather than by propagation due to thermodynamic effects. The homogeneous or coagulative nucleation mechanism is more prevalent in slightly water-soluble monomers such as MMA or VAc.

The last type of nucleation mechanism is known as droplet nucleation. In this mechanism, the free radicals generated by the initiator decomposition enter monomer droplets and propagate within the droplets to form polymer particles. The monomer droplets

are stabilized with available surfactant and become polymer particles, which will grow using only the monomer resident in that droplet.

In conventional emulsion polymerization, the three types of nucleation can occur. However, micellar and homogeneous nucleation are more likely to take place than droplet nucleation since the overall micellar surface area is much larger than that offered by the monomer droplets. On the other hand, particle nucleation in miniemulsion polymerization is dominated by droplet nucleation due to the smaller diameter of the monomer droplets.

Aside from understanding particle nucleation mechanisms, it is also important to visualize the "path" of a polymerization. A typical emulsion polymerization process can be divided into three intervals according to the original theory given by Harkins-Smith-Ewart (Lovell and El-Aasser, 1997). Interval I is the shortest of the three, occurring between 0 and ~10% conversion. As mentioned earlier, prior to the polymerization, the emulsion contains monomer droplets, surfactant molecules, monomer-swollen micelles and initiator molecules. The bulk of the monomer is present as droplets, which are stabilized by some of the surfactant molecules. These droplets have a diameter of 1 - 10 μm and their number density is on the order of 10^9 - 10^{11} dm^{-3}. The monomer droplets will act as monomer reservoirs during the reaction. The remaining surfactant molecules (depending on their concentration) will aggregate into micelles with their hydrophobic core swollen with monomer. They usually have a diameter of 50 - 150 Å and their number density is on the order of 10^{17} to 10^{18} dm^{-3}. These aggregates are present because the surfactant concentration is well above the critical micelle concentration (CMC), which is common in emulsion polymerization. Once the polymerization starts, the initiator molecules dissociate into radicals. These radicals are typically produced at a rate of 10^{16} to 10^{18} radical per dm^3 per second. At this point, the radicals initiate the chain growth reaction by propagating with the monomer molecules dissolved in the aqueous phase to form oligoradicals. This is the beginning of "particle nucleation". The oligoradicals will eventually form polymer particles, which will continue to propagate using monomer supplied by the monomer droplets. It must be noted that typically, monomer has to diffuse from the droplets through the aqueous phase towards the growing polymer particles. The particle number, N_p, and particle size increases and thus will the polymerization rate, R_p (see equations 1 and 2). This will continue until the micelles disappear marking the end of Interval I

$$R_p = \frac{k_p[M]\bar{n}N_p}{N_A} \quad (1)$$

$$N_p = k_i[I]^{0.4}[a_s S]^{0.6} \quad (2)$$

where R_p is the polymerization rate; k_p and k_i are the propagation and initiation rate coefficients; M, I and S are the monomer, initiator and surfactant concentrations; n_{bar} is the average number of radicals per particle; N_p is the number of particles; N_A is Avogadro's number and a_S is the average surface area covered per surfactant molecule.

Interval II takes place between about 10 and 40% conversion. During this interval, the N_p remains constant but the particle size continues to increase. Monomer droplets maintain the monomer concentration in the particles according to a thermodynamic equilibrium. This will continue until the monomer droplets are exhausted and their disappearance marks the end of Interval II. Interval III, takes place from about 40% conversion to the end of the reaction. In this interval, the particle size is more or less constant and the monomer concentration inside the polymer particles starts to decrease. At this point, R_p usually decreases.

2.1.5.2 Miniemulsion polymerization

A miniemulsion is obtained by the mechanical dispersion of an emulsion to form monomer droplets with a droplet size range from 50 to 500 nm. Miniemulsion polymerization has some particularly important characteristics that distinguish it from conventional emulsion polymerization. The most important characteristic of miniemulsion polymerization is that the monomer droplets are much smaller compared to their typical diameter in conventional emulsion polymerization, which gives them a much larger surface. It is important to point out that the final polymer particle size produced by miniemulsion polymerization is about the same diameter as that of conventional emulsion polymerization. Another important characteristic of miniemulsion polymerization is the concentration of the surfactant, which is below the CMC leading to an absence of micelles. Let us note that the surfactant concentration in a miniemulsion is below the CMC because most of the surfactant molecules are stabilizing the monomer droplets, which are an order of magnitude smaller

than the monomer droplets in conventional emulsion polymerization. These two characteristics together promote droplet nucleation. An advantage of droplet nucleation is the possibility to create "compartments", i.e., each droplet can act as a separate reaction vessel allowing it to keep its individuality throughout the reaction. Some authors refer to this phenomenon as "nanoreactors" (Landfester, 2001) and in the present thesis is referred to as maximization of the intra- and extra-particle diffusion resistance.

A miniemulsion recipe typically contains the same components as an emulsion polymerization with one additional compound that is included in the formulation: a hydrophobic compound, which on occasion has been called co-stabilizer. Long chain alcohols such as cetyl alcohol or long chain alkanes such as hexadecane are examples of hydrophobic compounds that have been used in various studies (Bechthold et al., 2000; Asua, 2002; Anderson et al., 2003). However, these types of reagents must be removed after the polymerization since they might have a negative impact on the final product performance. Other studies have considered reagents such as octadecyl acrylate, dodecyl methacrylate or polymeric hydrophobes (Reimers and Schork, 1996b; Ouzineb et al., 2001; Chern and Sheu, 2001; Jovanovic et al., 2004b), which can act as co-monomers and remain part of the polymer chain. In this work, the use of long chain alcohols or alkanes has been avoided and the use of polymeric hydrophobes has been favoured since they do not have to be removed from the final latex.

An emulsion, either a conventional emulsion or a miniemulsion, is a thermodynamically unstable system. Thermodynamic stability in this context means that the emulsion does not change with time and is independent of the preparation technique (Tauer, 2001). However, emulsions can be prepared so that their structure remains unchanged for long periods of time. In this case, the emulsion would be said to be "kinetically stable". When there is a reference to "stable" products in the following, it is in the sense of kinetic stability. To create a stable miniemulsion, the monomer droplets must be stabilized against diffusional degradation processes such as coalescence and Ostwald ripening. Droplet coalescence usually comprises four stages: approach of two droplets at a distance that allows attractive interaction, drainage of the continuous phase film between the droplets, rupture of the film and finally, collapse of the droplets (Tauer, 2001). This mechanism of coalescence is related to that of monomer droplets and not polymer particles. Stabilization against

coalescence is achieved by the addition of appropriate surfactants at a sufficient concentration to impart a surface charge or steric hindrance. Ostwald ripening, on the other hand, is a degradative process where the smaller droplets diffuse into the larger ones, increasing the average droplet size. Ostwald ripening is a direct consequence of the polydispersity of the droplet size distribution.

This degradation process can be explained using thermodynamic principles. The chemical potential of the dispersed phase (μ_{disp}) compared to that of the same bulk material (μ_{bulk}) is increased by $4\sigma v_m/D_d$, so that:

$$\mu_{disp} = \mu_{bulk} + \frac{4\sigma v_m}{D_d} \tag{3}$$

μ_{disp} and μ_{bulk} are the chemical potentials of the dispersed and the bulk phases, σ is the interfacial tension, v_m is the volume of a single molecule and D_d is the diameter of one droplet. However, some of the dispersed-phase species do not reside in the droplets but are instead molecularly dissolved in the continuous phase at a concentration C. The chemical potential of such molecules is equal to:

$$\mu_c = \mu_{c0} + k_B T \ln C \tag{4}$$

where μ_{c0} is a reference value, k_B is the Boltzmann's constant and T is the temperature. At equilibrium $\mu_{disp} = \mu_c$, which means

$$\mu_{bulk} + \frac{4\sigma v_m}{D_d} = \mu_{c0} + k_B T \ln C \tag{5}$$

with

$$\mu_{bulk} - \mu_{c0} = k_B T \ln C_0 \tag{6}$$

After rearrangement of equation (5):

$$\mu_{bulk} - \mu_{c0} = k_B T \ln C - \frac{4\sigma v_m}{D_d} \tag{7}$$

Substituting equation (6) in (7) gives equation (8):

$$k_B T \ln C(D) = k_B T \ln C_0 + \frac{4\sigma v_m}{D_d} \quad (8)$$

where C(D) is the concentration of the dispersed phase at the interface and C_0 is the solubility of the dispersed phase in the continuous medium. Observation of equation (8) leads one to conclude that the smaller the droplet, the higher is C(D). In contrast, if the diameter of the droplets goes to infinity, C(D) will then be equal to C_0. The latter implies that smaller species tend to dissolve, whereas larger species grow by the uptake of matter released from the smaller species. The hydrophobe is added to counteract these effects since it is assumed that the addition of a third component (i.e., the hydrophobic compound) could stabilize the emulsion against Ostwald ripening. Such a component must be highly soluble in the organic phase, because the rate of degradation is controlled by the diffusion rate of the compound with the least water solubility. Consequently, the presence of the hydrophobic compound enhances the stabilization of the emulsion (or more correctly miniemulsion) by decreasing the diffusion rate of the oil phase (Higuchi and Misra, 1962; Asua, 2002).

One can verify whether a miniemulsion can be stable long enough to allow its polymerization using a balance between the Laplace and Osmotic pressures (Landfester et al., 1999; Landfester, 2001). The Laplace pressure (P_L) relates the particle size to the interfacial tension, and the Osmotic pressure (P_O) is indicative of the tendency of the droplets to suffer Ostwald degradation. The P_L can be calculated knowing the surfactant mass as well as the interfacial tension between the two phases:

$$P_L = \frac{2\gamma_{LL}}{r} \quad (9)$$

where γ_{LL} is the interfacial tension of the oil droplet with the aqueous medium and r is the radius of the droplet. γ_{LL} is described by:

$$\gamma_{LL} = \frac{A_d}{A_{surf}} \gamma_{LL,surf} + \left(1 - \frac{A_d}{A_{surf}}\right) \gamma_{LL,naked} \quad (10)$$

where A_d is the surface area of the droplets, A_{surf} is the surface area covered by surfactant, $\gamma_{LL,surf}$ is the interfacial tension between the organic and aqueous phase with surfactant coverage and $\gamma_{LL,naked}$ is the interfacial tension between these two phases without surfactant.

On the other hand, the hydrophobic compound builds up an P_O inside the droplets, which is defined by

$$P_O = \frac{RTC_{hydrophobe}}{M_{hydrophobe}} \quad (11)$$

The P_O counteracts the P_L. Therefore, the key for stabilizing the miniemulsion is to keep the P_O slightly larger than the Laplace pressure, i.e., $P_L < P_O$. By satisfying this condition, it is possible to ensure that a kinetically stable droplet of a useful size has been created. It can also be evaluated in terms of the ratio of number of particles (N_p) by number of initial droplets (N_d), which in an ideal case should be one. However, if the uncertainty of measuring the droplet distributions is accounted for, a range of $N_p/N_d = 1 \pm 0.15$ can be considered as a satisfactory requirement. However, the phenomena involving the maximization of intra- and extra-particle diffusion resistance has been challenged by a number of studies, which claimed that only 20% of N_p was polymerized through droplet nucleation (Choi et al., 1985). Other studies have found that up to 60% of all the monomer droplets were polymerized through this type of nucleation (Chern et al., 1998a; Chern et al., 1998b; Chern and Liou, 1999; Chern and Sheu, 2000; Chern and Sheu, 2001; Chern and Chang, 2003). One study even found that 95% of the droplets could be nucleated (Reimers and Schork, 1996a). In recent years, it was found that using a mixed surfactant stabilization system (sodium dodecyl sulphate/Triton X-405: ionic/steric surfactants) together with octadecyl acrylate (ODA) as hydrophobe, resulted in the N_d at the beginning of the polymerization and the number of polymer particles at the end to be almost identical, confirming that nearly all the monomer droplets were nucleated. It was presumed that the mixed surfactant system provided a synergistic stabilization compared to the use of one surfactant (Ouzineb, 2003; Ouzineb et al., 2004). In their work, they used an anionic surfactant below the CMC and enough non-ionic surfactant to increase the droplet surface coverage, which created an additional stabilization without promoting micellar nucleation.

The advantages of miniemulsion polymerization can be summarized as follows:

i. The polymerization via droplet nucleation provides an approach to incorporate different components inside the droplets without diffusing into other particles. This characteristic can also be used to control various properties of the end-use products. It

can be applied, for example, to create multimodal PSDs or MWDs. It can be hypothesized that the addition of different types and amounts of hydrophobes may lead to a novel approach for controlling polymer microstructure in the final latex particles.

ii. Miniemulsion polymerization can be used to prepare higher solids content latexes than conventional processes without the addition of larger amounts of surfactant and without extended semi-batch operation.

2.2 RESEARCH METHODOLOGY

This section offers details about the preparation and characterization techniques used throughout the research work. As mentioned earlier, each chapter consists of an independent scientific article and may document the experimental details in a more concise way.

2.2.1. Materials

All the reagents were used as supplied by the manufacturer. The monomers used for both MP and CEP reactions were 2-ethyl hexyl acrylate (EHA), methyl methacrylate (MMA) and acrylic acid (AA). Octadecyl acrylate (ODA) was used as the polymerizable hydrophobe and 1-dodecanethiol (DDM) as the chain transfer agent. All of these were reagent grade obtained from Sigma Aldrich. The ionic surfactant used was sodium dodecyl sulphate (SDS) GC grade obtained from Sigma Aldrich and the non-ionic surfactant was Disponil A3065 donated by Cognis Canada, which is a mixture of ethoxylated linear fatty alcohols present as 65% aqueous solution. The reported molecular weight for Disponil was 1022 g/mol (Schneider, 2000). Sodium bicarbonate ($NaHCO_3$) (Aldrich) was used as buffer. Distilled deionized water (DDI H_2O) was used throughout the study. A 0.02 mol L^{-1} hydroquinone solution (HQ) was used as inhibitor to stop conversion in the samples taken along the reactions. Tetrahydrofuran (THF) HPLC grade (EMD Chemicals) was used in the molecular weight determination. Nitrogen gas (Linde Canada) was used to purge the reaction mixture from dissolved oxygen.

2.2.2. Determination of the critical micelle concentration (CMC) and area per surfactant molecule (a_S)

The CMC for SDS and Disponil A3065 in pure water and in surfactant-free latex was determined experimentally using a surface tension (ST) technique (Maron et al., 1954). In this study, ST was measured using a KRUSS K12 tensiometer equipped with a Wilhelmy plate and a dosimeter that allowed testing a range of concentrations from 0 g/L (pure water or pure surfactant-free latex) to 2.5 g of surfactant per litre of solution. The solutions were tested at a temperature of 23 ± 0.2°C. The inflection point in the plot of ST vs. log surfactant concentration was taken as the CMC.

Once the CMC was obtained, it was possible to calculate a_S. The determination of a_S allowed for the quantification of the average particle surface area covered by the surfactant (or surfactants) together with the knowledge of particle size (D_p) and number of particles (N_p). This, in turn, allowed us to formulate the miniemulsion recipe to cover between 35 – 40 % of the total particle surface, which was found to be the most adequate coverage to maximize droplet nucleation (Fonseca et al., 2008). The CMC was also checked for mixtures of anionic/non-ionic surfactants at different molar ratios. For all ratios of the surfactant mixtures studied, the surface tension measurement yielded only one CMC value (see Appendix A).

2.2.3. Preparation of the miniemulsion and emulsion

The organic phase was prepared first. ODA and the three monomers (EHA, MMA and AA) were charged to a 500 mL flask. If the recipe contained DDM as the CTA, it was added at this point. The monomer mixture was stirred using a plate stirrer until it appeared as a homogeneous clear solution. The aqueous phase was prepared separately in a 1 L flask. Disponil and SDS (surfactants) as well as Na_2HCO_3 were dissolved in DDI H_2O. Subsequently, the organic phase was added slowly to the aqueous solution while stirring. The stirring continued until the emulsion appeared as a milky solution. The time required was about 30 min.

The mixture was then sonicated using a Fisher Scientific Sonicator Model 550 with a full load power of 600 W. In order to ensure that sufficient energy was supplied to all the emulsion volume, the total mixture was sonicated in small batches of 100 mL. The mixture

was kept in an ice-bath to avoid an increase in the temperature and possible initiation of the reaction. The sonication time was 4 min at an output amplitude level of 9 (unless otherwise indicated). At the end, the entire volume was mixed and stirred.

In the case of the emulsion used for CEP, the preparation was the same as that for MP, except that the emulsion was not sonicated. It should be noted that ODA was added to both MP and CEP recipes, although previous studies have not done so due to the fact that it is considered merely as the hydrophobic compound. In this work, ODA was acting as a polymerizable hydrophobe and the possibility that this component might pose an influence on the PSA properties was considered, since it would certainly be incorporated into the polymer matrix and could possibly create a bias in the comparison between the adhesive produced by the two techniques.

2.2.4. Polymerization procedure for MP and CEP

The polymerization reactions were performed in a 1.1 L Labmax™ automated stainless steel reactor (Mettler Toledo) equipped with a stirrer, condenser and three feed ports. The initial emulsion or miniemulsion was charged to the reactor and heated to 70°C with stirring. Nitrogen gas was bubbled to the reaction mixture to remove any dissolved oxygen. The temperature and stirring speed were automatically controlled at 70°C and 200 rpm, respectively. The reaction was initiated with the rapid addition of 5 mL of the initiator solution. The reaction time was 120 min. 2 mL samples were taken at different times along the reaction for conversion and D_p analysis. The sampling vials contained a few drops of a HQ solution and were immediately placed in an ice-bath to shortstop the reaction. At the end of the reaction time, the mixture was cooled down to 25°C and transferred to a 1 L jar. The reactivity ratios were calculated using the error-in-variables method (Dubé et al., 1991) using the conversion reported elsewhere (Patnaik et al., 1992). The resulting values were r_{EHA}= 0.426 and r_{MMA}= 1.729.

2.2.5. Droplet and particle size distribution determination

Droplet and particle sizes were obtained using a Dynamic Light Scattering (DLS) instrument (Malvern NanoS Zetasizer) with an angle of 176°. One drop of the emulsion or latex was placed in a 4 mL polystyrene cuvette and diluted with distilled deionized water.

The drop of emulsion or latex was diluted 200 times or until the mean count rate in the DLS equipment was between 200 and 400 kcps (the number of photons detected in kilo counts per second) in order to maximize the accuracy of the results. From visual inspection, the sample appeared more or less turbid. The reported diameter is an intensity weighed average particle size, a.k.a. z-average, made of 3 measurements that were analyzed in 10 runs of 30 s each. It should be mentioned that given the water solubility of some of the monomers used herein (such as vinyl acetate and methyl methacrylate), it is likely that some of the monomer could have been stripped from the sample and dissolved in the water phase, thus decreasing the diameter of the droplet/particle. According to calculations performed to estimate measurement error, there was a 5 to 12% decrease in the droplet diameter (depending on the composition of the co-monomer mixture), which represented an 8 to 15 nm error in particle sizes reported. This is well within the experimental error of the technique and although the error percentage was always present in these measurements, DLS is much better suited than other available methods. Finally, as long as the error of the technique would remain constant, comparisons within our experiments would be valid and allow us to make sound conclusions.

As well, the reported polydispersity index values (PDI) are those given by the instrument and are not conventional PDI values and will be referred to as Malvern Polydispersity Index (M-PI) throughout this work to avoid any misunderstanding. PI values were calculated using a cumulants analysis method of fitting the autocorrelation function (International Organization for Standardization, 1996). The closer the value was to 0.01, the narrower was the distribution. The refractive index used was a weighted-average based on the composition of the mixture and the value was 1.428. The droplet diameter (D_d) was measured immediately after the preparation of the miniemulsion.

2.2.6. Molecular weight distribution

0.1 g of dried polymer was placed in a vial with 5 mL of THF. The vial was closed and placed in a wrist-action shaker for 24 h. The solution was then filtered using a 0.45 μm syringe filter with PTFE membrane (Pall Corporation). The samples were analyzed with a Waters Gel Permeation Chromatography (GPC) instrument equipped with a Differential Refractive Index detector, a manual injector and three Waters Styragel columns (HR6, HR4

and HR3) in series. 200 μL of the solution were withdrawn and injected into a 50 μL loop Rheodyne injector. The flow rate was set at 0.3 mL/min and with an internal temperature of 37°C. The data was analyzed using Empower 2 software from Waters. The calibration curve included a set of 12 standards (EasiCal from Polymer Laboratories) with a range of 162 to 6,035,000 g/mol. The values of K and alpha used for EHA were 1.24 $x10^{-4}$ dL/g and 0.67 while those for MMA were 1.28 $x10^{-4}$ dL/g and 0.69, respectively (Lathova et al., 1993; Hua and Dubé, 2001).

2.2.7. Conversion by gravimetry

Approximately 2 g of latex from the sampling vials taken along the reaction were placed in a 25 mm aluminum dish. The latex was allowed to dry in a fume hood for 24. The dishes were subsequently placed in a vacuum oven at 35°C for 48 h to remove any traces of unreacted monomer and water. The conversion was calculated from the dry polymer weight. Individual conversions were calculated using the total conversion obtained by gravimetry and copolymer compositions obtained by ^{1}H-NMR spectroscopy. Error-in-variables method software was provided by the University of Waterloo (Dubé et al., 1991).

2.2.8. Gel content determination (Tobing and Klein, 2001)

Gel fraction analysis was performed only for the final sample of each reaction. Approximately 200 mg of dry polymer were placed in a pouch formed by two 25 mm-diameter PTFE membranes with a pore size of 0.2 μm. The membranes were heat sealed. The weight of the pouch plus polymer was recorded and the pouch placed in a 100 mL glass jar with 50 to 60 mL of THF. The jars were placed in a shaker for at least 48 h after which time the pouches were removed and allowed to dry. The gel fraction was calculated from the difference between the final and initial weight of the polymer. Each analysis was performed in duplicates and the results reported are the average of those values.

2.2.9. Copolymer composition

Copolymer compositions were determined using ^{1}H-NMR spectroscopy. 200 mg of dry polymer was weighed and placed in a vial. 2 mL of deuterated chloroform (*d*-$CHCl_3$) was added and the vial was shaken for 24 h or until the polymer was visibly dissolved. 1 mL

of the solution was transferred to 5 mm standard NMR tubes. The samples were analyzed using a Bruker AVANCE 400 spectrometer with sample charger. The relative amounts of monomer bound in the copolymer were estimated from the areas corresponding to the absorption peaks of EHA and MMA at 3.90 and 3.60 ppm, respectively. In the case of EHA, the shift corresponds to the protons of OCH_2 group while in the case of MMA, it corresponds to the protons of the OCH3 group (Patnaik et al., 1992; Aymonier et al., 2001).

2.2.10. Glass transition temperature

About 40 mg of dry polymer were weighed into standard DSC hermetic aluminum sample pans. The T_g was determined using a Differential Scanning Calorimeter (DSC) Model Q1000 from TA Instruments equipped with auto sampler, a refrigerated cooling system and nitrogen as the purge gas. The analysis was performed using a modulated DSC method with modulation amplitude of ± 1°C every 60 s. The sample was cooled to -80°C and followed by a heating ramp of 2°C/min. The T_g was calculated from the inflection point in the Reversed Heat Flow curve using the software provided. If the transition was broad and thus the result ambiguous, the T_g was taken as the peak in the curve of the derivative heat capacity (C_p) (Stubbs and Sundberg, 2005).

2.2.11. PSA testing

Tack, peel strength and shear strength were measured according to the Pressure Sensitive Tape Council standards PSTC-6, PSTC-1 and PSTC-7, respectively (Pressure Sensitive Tape Council, 2004). The latex was filtered using glass wool and filtered latex was cast onto a 50 um Mylar® sheet. The cast film was dried at room temperature and conditioned for 24 h at standard conditions of temperature and humidity (23 ± 2°C and 50% ± 2 Relative Humidity). A Universal Instron tester was used to evaluate loop tack and peel strength. PSTC 6 evaluates loop tack. A strip of 25.4 mm x 177.8 mm was cut from the film and was used to form a loop with the adhesive side facing outward. Approximately 25.4 mm at both ends of the strip was masked with tape and inserted into the upper grip. The instrument moved the upper grip downward at a speed of 300 m/min until an area of 25.4 mm^2 came into contact with the stainless steel substrate mounted into the lower grip. Next, the tester moved the upper grip upwards at the same speed while recording the force needed

to debond the loop from the substrate. The maximum force per surface area necessary to remove the adhesive was reported as loop tack. PSTC 1 Test Method A evaluates peel strength at a peel angle of 180°. A specimen of 25.4 mm x 304.8 mm was cut. The strip was laminated onto a stainless steel substrate with the help of a 2040 g roll coater. The roll coater was passed through the film, front to back, twice (i.e., along the length of the film). The dwell time did not exceed one minute. The substrate and the strip were inserted into the grips and the upper grip was set to move upward at a speed of 300 mm/min. The average force per m required to peel the strip from the substrate was recorded and reported as peel strength. Lastly, PSTC 7 measures shear strength. A specimen of 25.4 mm x 152.4 mm of the film was cut. The strip was laminated onto a stainless steel substrate and then placed in a custom-built shear tester using a C-clamp. A 500 g weight was suspended at the end of the strip. The time to failure was recorded automatically using Labview software.

2.2.12. Dynamic Mechanical Analysis

10 to 12 g of latex were placed in a 5 x 5 cm plate, 1-cm height formed using silicone release paper. The latex was left to dry in a fume hood for 2 – 3 days and then transferred to a vacuum oven at 35°C for further drying for 3 – 5 days. The vacuum in the oven was increased slowly to avoid creating bubbles or punctures at the surface of the dry film. A film of 1.5 to 2 mm was obtained after the drying process. The samples were analyzed using a Rheometrics RDA III and 25 mm parallel plate geometry. A 25 x 25 mm specimen was cut and placed between the plates, the gap was closed and the sample was trimmed to the geometry shape.

Two types of analysis were performed. First, for the construction of the master curves, the samples were subjected to isothermal frequency sweeps. The sweep mode was logarithmic with frequencies in a range from 0.1591 Hz to 50 Hz with 20 points per decade in a range of temperatures from -60°C to 80°C with increments of 10°C. The master-curves were built using TA Orchestrator software v.7.2 with manual shifting of the individual curves. The second analysis corresponds to temperature sweeps performed at a frequency of 1.591 Hz from a temperature range from -40°C to 120°C.

2.3 REFERENCES

Anderson, C.D., Sudol, E.D., El Aasser, M.S., 2003. Elucidation of the miniemulsion stabilization mechanism and polymerization kinetics. Journal of Applied Polymer Science 90, 3987-3993.

Asua, J.M., 2002. Miniemulsion polymerization. Progress in Polymer Science 27, 1283-1346.

Aubrey, D.W., Sherriff, M., 1980. Peel Adhesion and Viscoelasticity of Rubber-Resin Blends. Journal of Polymer Science, Part A: Polymer Chemistry 18, 2597-2608.

Aymonier, A., Ledercq, D., Tordjeman, P., Papon, E., Villenave, J.J., 2003. Control of structure and tack properties of acrylic pressure-sensitive adhesives designed by a polymerization process. Journal of Applied Polymer Science 89, 2749-2756.

Aymonier, A., Papon, E., Villenave, J.J., Tordjeman, P., Pirri, R., Gerard, P., 2001. Design of pressure-sensitive adhesives by free-radical emulsion copolymerization of methyl methacrylate and 2-ethylhexyl acrylate. 1. Kinetic study and tack properties. Chemistry of Materials 13, 2562-2566.

Bechthold, N., Tiarks, F., Willert, M., Landfester, K., Antonietti, M., 2000. Miniemulsion polymerization: Applications and new materials. Macromolecular Symposia 151, 549-555.

Benedek, I., 2004. Pressure-Sensitive Adhesives and Applications, 2nd edition ed. Marcel Dekker, Inc., New York.

Cannon, L.A., Pethrick, R.A., 2002a. Comparison of the effect of reactive and non-reactive steric stabilisers on the mechanism of film formation in methyl methacrylate/butyl acrylate copolymers latexes. Part 1. Differential scanning calorimetry, dynamic mechanical analysis and atomic force microscopy. Polymer 43, 6421-6428.

Cannon, L.A., Pethrick, R.A., 2002b. Comparison of the effect of reactive and non-reactive steric stabilisers on the mechanism of film formation in methyl methacrylate/butyl acrylate copolymers latexes. Part 2. Electrical conduction and dielectric spectroscopic investigations. Polymer 43, 6429-6438.

Charmeau, J.Y., Gerin, P.A., Vovelle, L., Schirrer, R., Holl, Y., 1999a. Adhesion of latex films. Part III. Surfactant effects at various peel rates. Journal of Adhesion Science and Technology 13, 203-215.

Charmeau, J.Y., Kientz, E., Holl, Y., 1996. Adhesion of latex films; Influence of surfactants. Progress in Organic Coatings 27, 87-93.

Charmeau, J.Y., Sartre, A., Vovelle, L., Holl, Y., 1999b. Adhesion of latex films. Part II. Loci of failure. Journal of Adhesion Science and Technology 13, 593-614.

Chern, C.S., Chang, H.T., 2003. A competitive particle nucleation mechanism in the polymerization of homogenized styrene emulsions. European Polymer Journal 39, 1421-1429.

Chern, C.S., Chen, T.J., Liou, Y.C., 1998a. Miniemulsion polymerization of styrene in the presence of a water-insoluble blue dye. Polymer 39, 3767-3777.

Chern, C.S., Liou, Y.C., 1999. Styrene miniemulsion polymerization initiated by 2,2 '-azobisisobutyronitrile. Journal of Polymer Science Part A-Polymer Chemistry 37, 2537-2550.

Chern, C.S., Liou, Y.C., Chen, T.J., 1998b. Particle nucleation loci in styrene miniemulsion polymerization using alkyl methacrylates as the reactive cosurfactant. Macromolecular Chemistry and Physics 199, 1315-1322.

Chern, C.S., Sheu, J.C., 2000. Effects of 2-hydroxyalkyl methacrylates on the styrene miniemulsion polymerizations stabilized by SDS and alkyl methacrylates. Journal of Polymer Science Part A-Polymer Chemistry 38, 3188-3199.

Chern, C.S., Sheu, J.C., 2001. Effects of carboxylic monomers on the styrene miniemulsion polymerizations stabilized by SDS/alkyl methacrylates. Polymer 42, 2349-2357.

Choi, Y.T., Elaasser, M.S., Sudol, E.D., Vanderhoff, J.W., 1985. Polymerization of Styrene Miniemulsions. Journal of Polymer Science Part A-Polymer Chemistry 23, 2973-2987.

Chu, S.G., 1989. Viscoelastic Properties of Pressure Sensitive Adhesives, in: Satas, D. (Eds.), Handbook of Pressure-Sensitive Adhesive Technology. Van Nostrand Reinhold, New York, pp. 158-203.

Créton, C., 2000. Materials Science of Pressure-Sensitive Adhesives, in: Meiher, H.E.H. (Eds.), Materials Science and Technology: A Comprehensive Treatment. Wiley-VCH, Weinheim, pp. 707-741.

Dale, W.C., Paster, M.D., Haynes, J.K., 1989. Mechanical-Properties of Acrylic Pressure Sensitive Adhesives and Their Relationships to Industry Standard Testing. Journal of Adhesion 31, 1-20.

Dube, M.A., Amin Sanayei, R., Penlidis, A., O'Driscoll, K.F., Reilly, P.M., 1991. A microcomputer program for estimation of copolymerization reactivity ratios. Journal of Polymer Science Part A: Polymer Chemistry 29, 703-708.

Dubé, M.A., Amin Sanayei, R., Penlidis, A., O'Driscoll, K.F., Reilly, P.M., 1991. A Microcomputer Program for Estimation of Copolymerization Reactivity Ratios. Journal of Polymer Science, Part A: Polymer Chemistry 29, 703-708.

Elizalde, O., Vicente, M., Leiza, J.R., Asua, J.M., 2002. Control of the adhesive properties of n-butyl acrylate/styrene latexes. Polymer Reaction Engineering 10, 265-283.

Elizalde, O., Vicente, M., Plessis, C., Leiza, J.R., Asua, J.M., 2004. Knowledge-based control of emulsion polymerization: Tailoring adhesive properties. JCT Research 1, 45-51.

Fonseca, G.E., McKenna, T.F., Dubé, M.A., 2008. Influence of Particle Nucleation in Pressure Sensitive Adhesive Properties: Miniemulsion versus Emulsion Polymerization. Macromolecular Symposia 271, 83-93.

Gerin, P.A., Grohens, Y., Schirrer, R., Holl, Y., 1999. Adhesion of latex films. Part IV. Dominating interfacial effect of the surfactant. Journal of Adhesion Science and Technology 13, 217-236.

Higuchi, W.I., Misra, J., 1962. Physical Degradation of Emulsions Via Molecular Diffusion Route and Possible Prevention Thereof. Journal of Pharmaceutical Sciences 51, 459-&.

Holmberg, K., 2003. Surfactants and Polymers in Aqueous Solution, 2nd edition ed. John Wiley & Sons, Chichester, England.

Hua, H., Dubé, M.A., 2001. Off-line monitoring of butyl acrylate, methyl methacrylate and vinyl acetate homo- and copolymerizations in toluene using ATR-FTIR spectroscopy. Polymer 42, 6009-6018.

International Organization for Standardization, 1996. Methods for Determination of Particle Size Distribution Part 8: Photon Correlation Spectroscopy. International Standard ISO13321,

Jovanovic, R., Dubé, M.A., 2004. Emulsion-based pressure-sensitive adhesives: A review. Journal of Macromolecular Science: Polymer Reviews C44, 1-51.

Jovanovic, R., Dubé, M.A., 2005. Screening experiments for butyl acrylate/vinyl acetate pressure-sensitive adhesives. Industrial & Engineering Chemistry Research 44, 6668-6675.

Jovanovic, R., McKenna, T.F., Dubé, M.A., 2004a. Empirical modeling of butyl acrylate/vinyl acetate/acrylic acid emulsion-based pressure-sensitive adhesives. Macromolecular Materials and Engineering 289, 467-474.

Jovanovic, R., Ouzineb, K., McKenna, T.F., Dubé, M.A., 2004b. Butyl acrylate/methyl methacrylate latexes: Adhesive properties. Macromolecular Symposia 206, 43-56.

Karsa, D.R., 2003. Surfactants in Polymers, Coatings, Inks and Adhesives, 1st edition ed. John Wiley & Sons, Oxford, England.

Landfester, K., 2001. Polyreactions in miniemulsions. Macromolecular Rapid Communications 22, 896-936.

Landfester, K., Bechthold, N., Tiarks, F., Antonietti, M., 1999. Formulation and stability mechanisms of polymerizable miniemulsions. Macromolecules 32, 5222-5228.

Lathova, E., Lath, D., Pavlinec, J., 1993. The Behavior of Poly(2-Ethylhexyl Acrylate) in Dilute-Solution - Viscosity Measurements. Polymer Bulletin 30, 713-718.

Laureau, C., Vicente, M., Barandiaran, M.J., Leiza, J.R., Asua, J.M., 2001. Effect of the composition profile of 2-ethyl hexyl acrylate/methyl methacrylate latex particles on adhesion. Journal of Applied Polymer Science 81, 1258-1265.

Lovell, P.A., El-Aasser, M.S., 1997. Emulsion Polymerization and Emulsion Polymers, 1st edition ed. John Wiley & Sons, New York.

Mallégol, J., Gorce, J.P., Dupont, O., Jeynes, C., McDonald, P.J., Keddie, J.L., 2002. Origins and effects of a surfactant excess near the surface of waterborne acrylic pressure-sensitive adhesives. Langmuir 18, 4478-4487.

Maron, S.H., Elder, M.E., Ulevitch, I.N., 1954. Determination of Surface Area and Particle Size of Synthetic Latex by Adsorption .6. Critical Micelle Concentrations of Various Emulsifiers in Latex. Journal of Colloid Science 9, 382-384.

Ouzineb, K., 2003. Emulsion and Miniemulsion Polymerization: Stabilization, tubular reactors and practical applications.

Ouzineb, K., Graillat, C., McKenna, T.F., 2004. Study of compartmentalization in the polymerization of miniemulsions of styrene and butyl methacrylate. Journal of Applied Polymer Science 91, 115-124.

Ouzineb, K., Heredia, M.F., Graillat, C., McKenna, T.F., 2001. Stabilization and kinetics in the emulsion copolymerization of butyl acrylate and methyl methacrylate. Journal of Polymer Science Part A-Polymer Chemistry 39, 2832-2846.

Patnaik, M., Choudhary, V., Varma, I.K., 1992. Structural and thermal characterization of methyl methacrylate/alkyl acrylate copolymers. European Polymer Journal 28, 1433-1439.

Petrie, E.M., 2000. Handbook of Adhesives and Sealants, 1st edition ed. McGraw-Hill, New York.

Pizzi, A., Mittal, K.L., 2003. Handbook of Adhesive Technology, 2nd edition ed. Marcel Dekker, New York.

Pressure Sensitive Tape Council, 2004. Test Methods for Pressure Sensitive Adhesive Tapes, 14th ed. ed. Pressure Sensitive Tape Council, Northbrook, Illinois.

Reimers, J.L., Schork, F.J., 1996a. Predominant droplet nucleation in emulsion polymerization. Journal of Applied Polymer Science 60, 251-262.

Reimers, J.L., Schork, F.J., 1996b. Robust nucleation in polymer-stabilized miniemulsion polymerization. Journal of Applied Polymer Science 59, 1833-1841.

Satas, D., 1989a. Acrylic Adhesives, in: Satas, D. (Eds.), Handbook of Pressure-Sensitive Adhesive Technology. Van Nostrand Reinhold, New York, pp. 396-

Satas, D., 1989b. Handbook of Pressure Sensitive Adhesive Technology, 2nd ed. ed. Van Nostrand Reinhold, New York.

Schneider, M., 2000. Etude de Procédés de Synthèse de Latex Multipopulés à Haut Extrait Sec.

Stubbs, J.M., Sundberg, D.C., 2005. Measuring the extent of phase separation during polymerization of composite latex particles using modulated temperature DSC. Journal of Polymer Science, Part B: Polymer Physics 43, 2790-2806.

Tauer, K., 2001. Surface Chemistry in the Polymerization of Emulsion, in: Holmberg, K. (Eds.), Handbook of Applied Surface and Colloid Chemistry. John Wiley & Sons, Chichester; New York, pp. 175-200.

Tobing, S., Klein, A., Sperling, L.H., Petrasko, B., 2001. Effect of network morphology on adhesive performance in emulsion blends of acrylic pressure sensitive adhesives. Journal of Applied Polymer Science 81, 2109-2117.

Tobing, S.D., Klein, A., 2000. Mechanistic studies in tackified acrylic emulsion pressure sensitive adhesives. Journal of Applied Polymer Science 76, 1965-1976.

Tobing, S.D., Klein, A., 2001a. Molecular parameters and their relation to the adhesive performance of acrylic pressure-sensitive adhesives. Journal of Applied Polymer Science 79, 2230-2244.

Tobing, S.D., Klein, A., 2001b. Molecular parameters and their relation to the adhesive performance of emulsion acrylic pressure-sensitive adhesives. II. Effect of crosslinking. Journal of Applied Polymer Science 79, 2558-2564.

Zosel, A., 1991. Effect of Cross-Linking on Tack and Peel Strength of Polymers. Journal of Adhesion 34, 201-209.

Zosel, A., 1998. The effect of fibrillation on the tack of pressure sensitive adhesives. International Journal of Adhesion and Adhesives 18, 265-271.

Zosel, A., 2000. Built to last. Adhesives Age 43, 34-40.

Zosel, A., Ley, G., 1993. Influence of Cross-Linking on Structure, Mechanical-Properties, and Strength of Latex Films. Macromolecules 26, 2222-2227.

CHAPTER 3

Preparation of stable miniemulsions of poly(2-ethyl hexyl acrylate-co-vinyl acetate)

Fonseca, G.E., McKenna, T.F., Dubé, M.A.;
Macromolecular Symposia, accepted (DOI: masy.200900009.R1)

Preparation of stable miniemulsions of poly(2-ethyl hexyl acrylate-co-vinyl acetate)

Gabriela E. Fonseca[1], Timothy F.L. McKenna[2], Marc A. Dubé[1*]

[1]Department of Chemical and Biological Engineering, University of Ottawa, 161 Louis Pasteur Pvt., Ottawa, Ontario, K1N 6N5, Canada; Fax 1(613)5625172; Email: Marc.Dube@uottawa.ca

[2]Department of Chemical Engineering, Queen's University, Kingston, Ontario, K7L 3P4, Canada

ABSTRACT

This paper presents the results of the preparation of miniemulsions as well as the subsequent copolymerizations of 2-ethyl hexyl acrylate and vinyl acetate. The miniemulsions were prepared using a mixture of an anionic and a non-ionic surfactant. Sodium dodecyl sulfate (SDS) was used as the anionic surfactant and two non-ionic surfactants were studied: Triton X-405 and Disponil A3065. The miniemulsions prepared with a 90/10 mol.-% Disponil A3065 were able to reach a kinetically-stable state to yield latexes with 43 wt.-% solids content with a maximum change in the number of particles (N_p) with respect to the number of droplets (N_d) of ~6%. A 2^3 factorial design was then used to discern the influence of monomer, chain transfer agent and surfactant concentration on the droplet size distribution (DSD) and particle size distribution (PSD). Pressure-sensitive adhesive (PSA) properties were also examined.

Keywords: copolymerization, adhesives, vinyl acetate, 2-ethyl hexyl acrylate

3.1. INTRODUCTION

Miniemulsion polymerization is a heterophase polymerization process characterized by its droplet nucleation mechanism. This type of emulsion is produced using a hydrophobic compound that stabilizes the emulsion against Ostwald ripening, together with the use of a high shear homogenization device which breaks down the monomer droplets present in a typical emulsion down to a droplet diameter between 50 and 500 nm. A properly-formulated miniemulsion is able to reach a kinetically-stable state in which the nanometre-sized monomer droplets act as nano-reactors and diffusion of monomer through the aqueous phase could be minimized (Landfester et al., 1999).

Due to the fact that in miniemulsion polymerization monomer droplets are considerably smaller than in conventional emulsion polymerization, polymer nucleation does not proceed via a micellar mechanism and the available surfactant only partially covers the surface area of the monomer droplets. In this case, the monomer droplets do not act as reservoirs and the reaction proceeds under more or less strictly droplet nucleation conditions (Schork et al., 2005).

Miniemulsion polymerization offers a number of benefits that are attractive such as the production of high-solids content and low viscosity latexes (do Amaral and Asua, 2004; Ouzineb et al., 2005), elimination of the oscillatory behaviour in continuous stirred tank reactors (Aizpurua and Barandiaran, 1999), encapsulation of organic and inorganic materials (Antonietti and Landfester, 2002; Bathfield et al., 2005) and synthesis of hybrid nanocomposites (Lopez et al., 2008). Because it is possible to create and design a family of polymer particles with a specific set of properties (it has been called a 1 to 1 copy from monomer droplets to polymer particles (Landfester et al., 1999)), the technique has great potential to generate tailor-made particle structures (Antonietti and Landfester, 2002). The success in miniemulsion polymerization lies in a careful selection of the stabilization system, i.e., the surfactant(s) and the hydrophobic compound, to prevent coalescence and Ostwald ripening. Nevertheless, the addition of the hydrophobic compound per se does not prevent Ostwald ripening completely. The miniemulsion droplet size distribution (DSD) is also critical in attaining a well-stabilized system. Miniemulsions with a broad DSD would inevitably lead to droplet instability due to Ostwald ripening despite the presence of the

hydrophobe. It has been suggested that a narrower DSD would ensure a higher probability of polymerizing under droplet nucleation conditions (Tauer, 2001).

If a miniemulsion has been adequately stabilized, the osmotic pressure (P_O) inside the droplets created by the addition of the hydrophobic compound would be able to counteract the Laplace pressure (P_L) produced by the interfacial energy at the monomer/water interface and the DSD (Landfester, 2000). Ideally, a zero pressure difference would completely stop diffusional degradation. Practically speaking, if this difference is close to zero, it would be sufficient to delay Ostwald ripening so that the miniemulsion could be polymerized.

Ouzineb et al. (Ouzineb et al., 2003; Ouzineb et al., 2004a; Ouzineb et al., 2004b) studied monomer compartmentalization in the homopolymerizations of styrene (STY) and butyl methacrylate (BMA). In one of their studies (Ouzineb et al., 2003), STY and BMA miniemulsions were prepared separately and copolymerized in the same reactor. Using an in-line Attenuated Total Reflectance-Fourier Transform Infrared spectroscopy probe, they found that no significant mass transfer had occurred between the two miniemulsions since no detectable levels of copolymer had been found, i.e., if the monomer compartmentalization had not taken place, a different spectra showing peaks that a copolymer had been formed would have appeared. They also showed that the change from the number of droplets (N_d) to the number of particles (N_p) was the least when the P_O was slightly higher than the P_L.

Miniemulsion polymerization has also been used to polymerize a number of hydrophobic monomers that are not suited for conventional macroemulsion polymerization (Reimers and Schork, 1996; Saethre et al., 1995) and to polymerize different pairs of monomers where at least one of them had a significant solubility in water (Delgado et al., 1986; Jovanovic and Dubé, 2004; Wu and Schork, 2000). Bohórquez and Asua (Bohórquez and Asua, 2008) studied the nucleation mechanism of the miniemulsion copolymerization of VAc and vinyl ester of a highly branched decanoic acid. The influence of hydrophobe and type and concentration of initiator on the nucleation was examined. They observed that droplet nucleation was maximized when miniemulsion stability was improved using stearyl acrylate (SA) and efficient initiators, namely initiators with low water solubility such as lauroyl peroxide (LPO). However, they observed fluctuations in the N_p in most of the recipes prepared with the exception of those polymerized with potassium persulfate (KPS) as

initiator and SA and polyvinyl alcohol (PVOH) as the stabilization system. Even with the latter stabilization system, the final particle diameter was larger than the initial droplet diameter with a ratio of N_d to N_p of ~1.4. It must be pointed out, however, that they obtained stable coagulum-free polyVAc latexes with a high solids content.

Wu and Schork (Wu and Schork, 2000) studied the copolymerization of VAc with butyl acrylate, dioctyl maleate and n-methylol acrylamide, systems with monomer pairs of different water solubilities and reactivity ratios. They found that miniemulsion polymerization was able to compensate for the poor monomer transport of highly water-insoluble monomers in corresponding macroemulsion polymerizations. However, they also observed that only a percentage of the initial droplets were nucleated into polymer particles.

Graillat and Guyot (Graillat and Guyot, 2003) studied the homopolymerization of VAc under different stabilization conditions and found that it was possible to obtain polyVAc latexes in conditions where the final N_p was close to the initial N_d. Nevertheless, these latexes had relatively low solids contents (~20%) and in the case of polyVAc latexes with higher solids contents, the final N_p was lower than the initial N_d, a fact they attributed to the collision of polymer particles with unreacted monomer droplets. However, one can see from their study that even though the conditions for the nucleation of all monomer droplets in a miniemulsion of a slightly water soluble monomer such as VAc are hard to achieve, it is indeed possible to achieve a stable miniemulsion system with a maximized extra-particle monomer diffusion resistance.

The question that arises is whether a miniemulsion can be produced when the copolymer includes a slightly hydrophilic monomer such as VAc. The aim of this paper is to report the miniemulsion copolymerization of a commercial polymer used as PSA: 2-ethyl hexyl acrylate (EHA)/VAc. We first discuss the effect of different stabilization systems on the DSD and PSD of EHA/VAc miniemulsions. The following section shows the results of a 2^3 factorial design used to discern the influence of monomer, chain transfer agent and surfactant concentrations on the DSD and PSD. Finally, the PSA properties obtained for the copolymer EHA/VAc are presented and discussed.

3.2. EXPERIMENTAL DETAILS

3.2.1. Materials

All the reagents were used as supplied by the manufacturer. The monomers used were EHA, VAc and methacrylic acid (MAA). Octadecyl acrylate (ODA) was used as the polymerizable hydrophobe and 1-dodecanethiol (DDM) as the chain transfer agent. All of these were reagent grade obtained from Sigma Aldrich. The ionic surfactant used was sodium dodecyl sulphate (SDS) GC grade (Sigma Aldrich) and the non-ionic surfactants were Disponil A3065 (Cognis Canada) and Triton X-405 (Sigma Aldrich). Sodium bicarbonate ($NaHCO_3$) (Aldrich) was used as buffer. Distilled deionized water (DDI H2O) was used throughout the study. A 0.02 mol L-1 hydroquinone solution was used as inhibitor to stop conversion in the samples. Ammonium persulfate (APS) and benzoyl peroxide (BPO) (Sigma) were used as initiators.

3.2.2. Preparation of the miniemulsion and emulsion

The organic phase was prepared first. ODA, DDM and the monomers were charged to a 500 mL flask. The monomer mixture was stirred until it appeared as a homogeneous clear solution. The aqueous phase was prepared separately in a 1 L flask. The non-ionic surfactant and SDS as well as $NaHCO_3$ (if present) were dissolved in DDI H2O. Subsequently, the organic phase was added slowly to the aqueous solution while stirring until the emulsion appeared as a milky solution. The mixture was sonicated using a Fisher Scientific Sonicator Model 550 with 600 W. In order to ensure that sufficient energy was supplied equally to the entire emulsion volume, the total mixture was sonicated in small batches of 100 mL. The mixture was kept in an ice-bath to avoid an increase in temperature and possible initiation of the reaction. The sonication time was 4 min at an output amplitude level of 9. After the sonication procedure, the entire volume was mixed and stirred.

3.2.3. Polymerization procedure

The polymerization reactions were performed in a 1.1 L Labmax™ automated stainless steel reactor (Mettler Toledo) equipped with a stirrer, condenser and three feed ports. The initial miniemulsion was charged to the reactor and simultaneously heated and mixed. Nitrogen gas was bubbled to the reaction mixture to remove any dissolved oxygen. The temperature and stirring speed were automatically controlled at 60°C and 200 rpm,

respectively. When the reaction temperature was reached, the initiator solution was injected into the reactor. Samples were taken at different times for conversion and D_p analysis. The sampling vials contained a few drops of a hydroquinone solution and were immediately placed in an ice-bath to shortstop the reaction. At the end of the reaction time, the mixture was cooled to 25°C.

3.2.4. Droplet and particle size distribution determination

Droplet and particle diameters were obtained using a Dynamic Light Scattering (DLS) instrument (Malvern NanoS Zetasizer) with a scattering angle of 173°. A drop of the latex was diluted in DDI H_2O and placed in a 4 mL cuvette. The reported diameter is an intensity-weighted average particle size, a.k.a. z-average, made of 3 measurements that were analyzed in 10 runs of 30 s each. For additional details, refer to section 2.2.5.

3.2.5. Polymer property characterization

Molecular weight distributions were determined using Gel Permeation Chromatography (GPC). 0.1 g of dried polymer was placed in a vial with 5 mL of tetrahydrofuran. The vial was closed and placed in a wrist-action shaker for 24 h. The solution was filtered using a 0.45 μm syringe filter with polytetrafluoroethylene membrane (Pall Corporation). The samples were analyzed with a Waters GPC instrument equipped with a Differential Refractive Index detector, a manual injector and three Waters Styragel columns (HR6, HR4 and HR3) in series. The flow rate was set at 0.3 mL/min and with an internal temperature of 37°C. The data was analyzed using Empower 2 software (Waters). The calibration curve included a set of 12 standards (EasiCal from Polymer Laboratories) with a range of 162 to 6,035,000 g/mol. The values of K and alpha used for EHA were 1.24 $x10^{-4}$ dL/g and 0.67 while those for MMA were 1.28 $x10^{-4}$ dL/g and 0.69 (Hua and Dubé, 2001; Lathova et al., 1993), respectively.

Tack, peel strength and shear strength were measured using Pressure Sensitive Tape Council standards PSTC-6, PSTC-1 and PSTC-7, respectively. The latex was filtered using glass wool and cast onto a 50 μm Mylar® sheet. The cast film was dried at room temperature and conditioned for 24 h at standard conditions of temperature and humidity (23 ± 2°C and 50% ± 2 Relative Humidity). A Universal Instron tester was used to evaluate loop tack and peel strength. In the case of loop tack, a strip of 25.4 mm x 177.8 mm was cut from the film

and used to form a loop with the adhesive side facing outward. Approximately 25.4 mm at both ends of the strip was masked with tape and inserted into the upper grip. The instrument moved the upper grip downward at a speed of 300 m/min until an area of 25.4 mm^2 came into contact with the stainless steel substrate mounted into the lower grip. Next, the tester moved the upper grip upwards at the same speed while recording the force needed to debond the loop from the substrate. The maximum force per surface area necessary to remove the adhesive was reported as loop tack.

PSTC 1 Test Method A evaluates peel strength at a peel angle of 180°. A specimen of 25.4 mm x 304.8 mm was cut. The strip was laminated onto a stainless steel substrate with the help of a 2040 g roll coater. The roll coater was passed through the film front to back twice (i.e., along the length of the film). The dwell time did not exceed one minute. The substrate and the strip were inserted into the grips and the upper grip was set to move upward at a speed of 300 mm/min. The average force per m required to peel the strip from the substrate was recorded and reported as peel strength.

Lastly, PSTC 7 was used to measure shear strength. A specimen of 25.4 mm x 152.4 mm of the film was cut. The strip was laminated onto a stainless steel substrate and then placed in a home-built shear tester using a C-clamp. A 500 g weight was suspended at the end of the strip. The time to failure was recorded automatically using Labview software.

3.3. RESULTS AND DISCUSSION

In order to create nanoparticles that can be exploited for applications such as coatings and PSAs, the copolymer EHA/VAc was prepared using different stabilization systems, i.e., a combination of surfactants and hydrophobe that effectively protect monomer droplets against diffusional degradation, were investigated. This particular copolymer involves two challenges that must be dealt with. The first one is the elevated water solubility of VAc monomer of 250 mM (Lovell and El-Aasser, 1997), which might enhance secondary nucleation at the beginning of the polymerization and/or prevent complete polymerization. The second challenge is the large difference in their reactivity ratios (r_{EHA} = 7.5 and r_{VAc} = 0.04 (Brandrup et al., 2005)), which consequently leads to compositional drift. In this work,

the reactions were carried out as batch polymerizations and there is little that can be done to circumvent compositional drift under these conditions.

3.3.1. Stabilization system SDS/Triton X-405

Table 3.1 shows the formulations and the results of the miniemulsion-based latexes polymerized using the stabilization system SDS/Triton X-405 together with ODA as the hydrophobe. The concentrations of ODA and initiator, which in this case was the water-soluble APS, were kept constant at 2.6 and 0.35 phm, respectively, unless otherwise indicated. The ratio between N_p and the initial N_d is also included in Table 3.1 and can be used as a measure of the success of miniemulsion polymerization. Ideally, a properly-stabilized miniemulsion would maintain a N_p/N_d ratio close to unity (Ouzineb et al., 2004b).

Table 3.1. Miniemulsion polymerization of EHA/VAc/MAA using the stabilization system SDS/Triton X-405/ODA

Run	EHA/VAc (wt.-%)	SDS (phm[b])	Triton-X405 (phm)	D_p (nm)	N_d (x 10^{-17})	N_p (x 10^{-17})	N_p/N_d
201	70/30	0.35	4.85	161	0.34	1.50	4.46
202	60/40	0.35	4.85	162	0.55	1.51	2.66
203	70/30	0.35	3.75	214	0.78[c]	0.67	(see [c])
204[a]	70/30	0.35	3.75	221	1.01[c]	0.62	(see [c])
205	70/30	0.40	4.00	127	0.33	1.54	4.93
206	70/30	0.35	3.50	207	0.36[c]	1.22	(see [c])

[a] [Ammonium persulfate] = 0.6 phm
[b] phm = parts per hundred parts monomer
[c] Bimodal DSD observed in the Dynamic Light Scattering measurements

Table 3.1 shows that most of the runs carried out using SDS/Triton X-405 resulted in large deviations from the initial N_d. Figure 3.1a shows the DSD of runs 201, 203, 205 and 206. These formulations were prepared using the same copolymer composition but with different surfactant concentrations. Two of these formulations (runs 203 and 206) displayed a second peak of large droplets, an indication that these miniemulsions were not stabilized properly and it is likely that soon after the sonication, the smaller droplets started to diffuse into the larger ones and that the amount of surfactant used in the formulation was not enough

to stabilize these miniemulsions. Increasing the surfactant concentration to 4.0 and 4.85 phm (runs 205 and 201, respectively) gave a monomodal DSD; however, as can be observed in Figure 3.1b, the final PSDs are broader than the initial DSDs with the presence of smaller particles. This is likely the result of secondary nucleation and the ratio N_p/N_d also supports this idea with values of ~5.

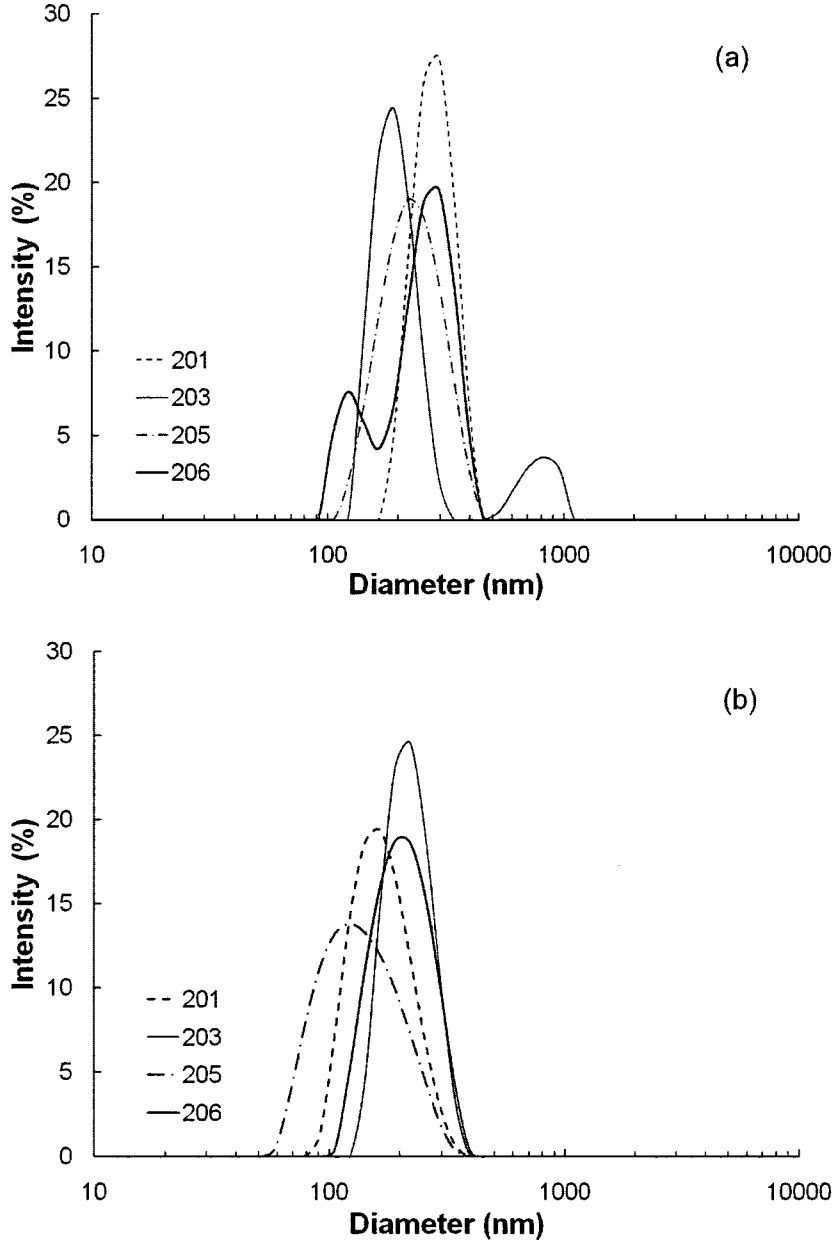

Figure 3.1. a) DSD and b) PSD of miniemulsion runs with different concentrations of surfactant

Figure 3.2 shows the influence of the VAc amount on the DSD and PSD. It is known that surfactant adsorption is determined by the monomer concentration (Hulden and Kronberg, 1994) and thus, it was necessary to verify if a change in the monomer composition in this case could lead to a different DSD. Figure 3.2a shows that larger concentrations of VAc in the formulation (Run 202) led to smaller average D_d. However, it is questionable whether this change is significant or not. It is plausible that with the same surfactant concentration, the droplets with higher VAc amounts need less surface charge density to be stabilized, which could explain the lower D_d. It is also possible that changing the VAc amount poses no effect on the DSD if it is considered that VAc resides on the outermost part of the droplet, thus a change in the VAc amount in the formulation does not really change the nature of the surface. Nevertheless, the reaction did not proceed under droplet nucleation conditions since the final N_p in both runs (201 and 202) was the same, which suggests that it was likely a function of the surfactant and initiator concentrations and proceeded as a conventional emulsion polymerization. It was also observed that the maximum in the rate of polymerization (R_p) was higher for the run with the lower VAc amount, which was expected due to the lower reactivity of VAc.

Figure 3.3 shows the influence of increasing the initiator concentration from 0.35 to 0.6 phm. As can be observed in Figure 3.3b, no effect was observed in the final PSD, although there was an increase in the maxima of the R_p, as expected. The change in initiator concentration was carried out using one of the recipes that had given a bimodal DSD in an attempt to verify whether a portion of the droplets would get nucleated or if the bimodality would serve to enhance a mixed nucleation mechanism. The results showed that doubling the initiator concentration and thus, increasing the radical flux did not have an impact in the final D_p. The lowest APS concentration yielded 214 nm particles while the highest APS concentration resulted in 221 nm particles, which is within the experimental error of the technique. Moreover, the D_p are not much smaller than the D_d in both cases, which suggests that they did not proceed completely as a conventional emulsion polymerization. The final N_p was 0.67×10^{17} and 0.62×10^{17} particle/L for APS concentration of 0.35 and 0.6 phm, respectively. It is interesting to note that doubling APS concentration did not increase the final N_p but it remained almost the same.

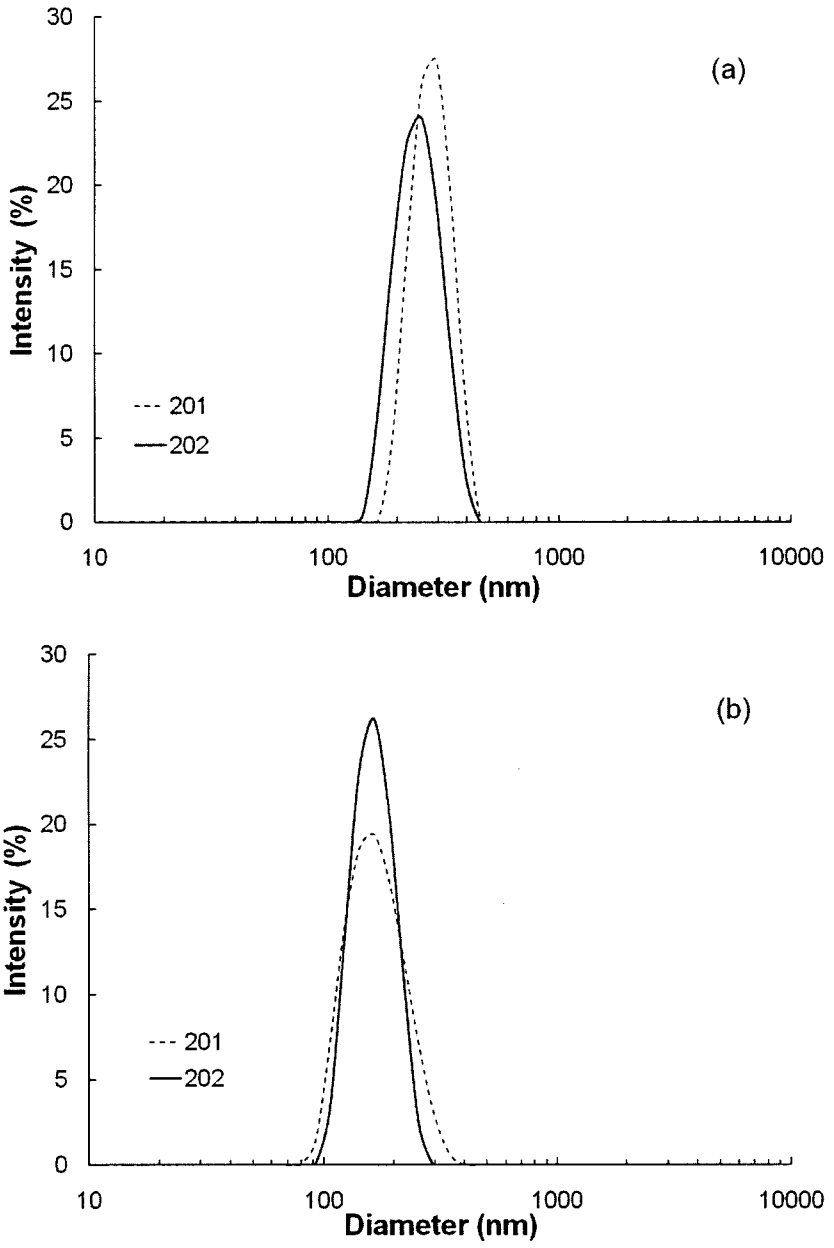

Figure 3.2. a) DSD and b) PSD of miniemulsion runs with different copolymer composition

The results found using the stabilization system SDS/Triton X-405 suggest that only part of the original monomer droplets nucleated while the rest likely served as monomer reservoirs. The main purpose of this study was to find an appropriate stabilization system that could generate nanoparticles that could be tailored for specific applications. The fact that we were unable to achieve compartmentalization with SDS/Triton X-405 even though the P_O

was adjusted slightly above the P_L, suggests that this type of surfactant mixture is not the most appropriate for the EHA/VAc co-monomer system.

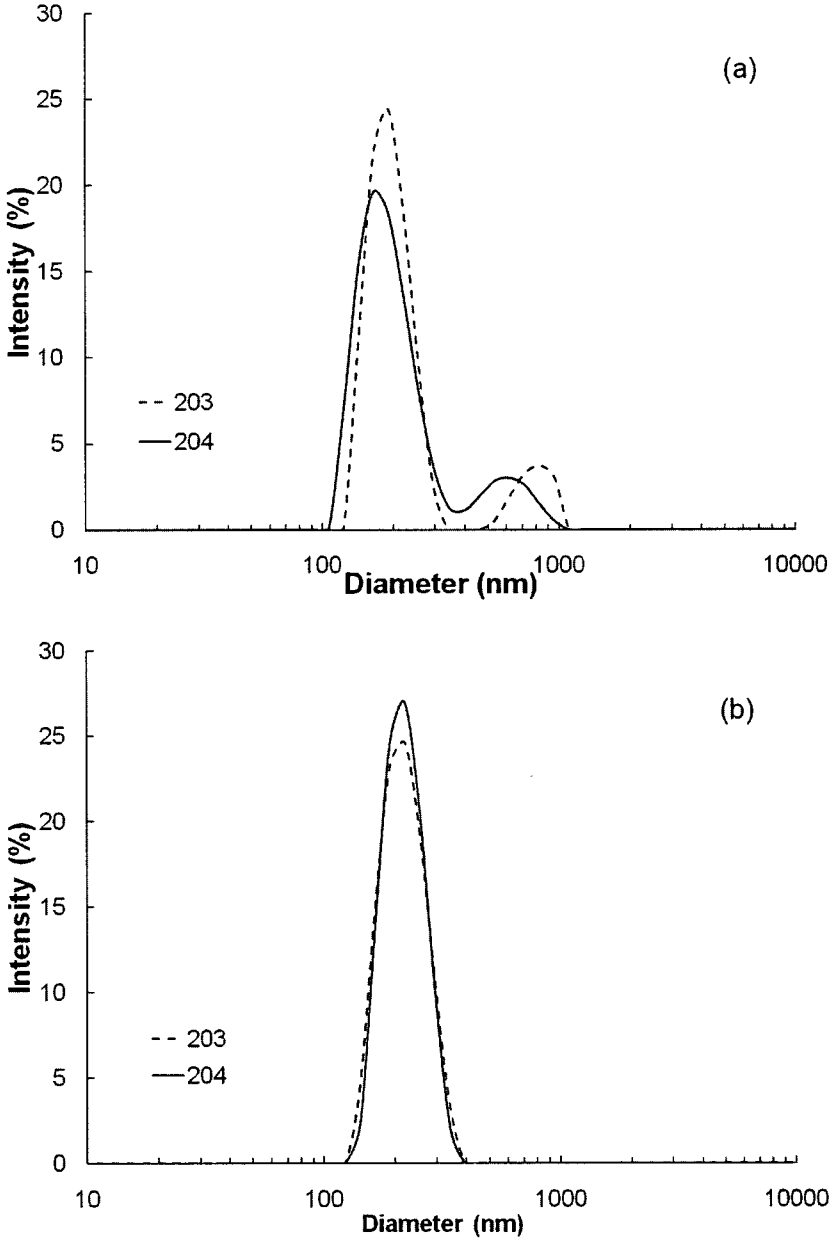

Figure 3.3. a) DSD and b) PSD of miniemulsion runs with different initiator concentration

Graillat and Guyot (Graillat and Guyot, 2003) were able to produce stable poly(VAc) miniemulsion-based latexes using a combination of SDS and Triton X-405 but it is likely that in this work, the inclusion of a highly hydrophobic monomer (i.e., EHA) was

responsible for not achieving stable miniemulsions with this non-ionic surfactant. Triton X-405 has a high hydrophilic-lipophilic balance of ~18 (Erbil, 2000) and it is perhaps more adequate to stabilize miniemulsions of only poly(VAc) (Farzi et al., 2009). However, it must be mentioned that some of the PSD of miniemulsions prepared with this surfactant mixture were as narrow as those usually associated with conventional emulsion polymerization.

3.3.2. Stabilization system SDS/Disponil A3065

The non-ionic surfactant Triton X-405 was substituted for Disponil A3065 to evaluate if an adequate stability of EHA/VAc miniemulsions could be obtained using this particular non-ionic surfactant. Disponil A3065 is a mixture of ethoxylated linear fatty alcohols that do not contain a phenyl group as does Triton X-405. Do Amaral et al. (do Amaral and Asua, 2004) used a combination of Disponil A3065 and an anionic surfactant to stabilize EHA/methyl methacrylate (MMA) miniemulsions. According to their results, the miniemulsions were visually stable for up to a week, although no DSD were reported.

It was also considered that the ODA concentration used in the initial series of runs was not enough to provide a P_O that could prevent or delay Ostwald ripening. In this case, ODA concentration was increased to 4.5 phm in an attempt to increase P_O. Table 3.2 shows the formulations together with the results of the DSD and PSD using the stabilization system SDS/Disponil A3065. The temperature was kept constant at 60°C for all runs in this series.

Runs 301 and 303 were prepared using solely SDS as surfactant while runs 302 and 304 were prepared using Disponil A3065 in order to evaluate how each of these two surfactants was influencing the DSD. Runs 301 and 303 contain the same SDS concentration but they were polymerized using two different initiator concentrations (cf. Table 3.2). Similarly, runs 302 and 304 had the same Disponil A3065 concentration but were polymerized using the same two initiator concentrations as with SDS. As can be observed in Figures 3.4a and b, the measured DSD of both SDS- and Disponil-based miniemulsions were monomodal in nature. However, the formulation prepared with ionic surfactant gave a narrower DSD (run 301) compared to that prepared with the non-ionic surfactant (run 302). Miniemulsions produced with SDS resulted in large increases in the N_p with N_p/N_d values of 2 and 5. It is interesting to note that at the higher APS concentration, (i.e., at 0.35 phm) N_p/N_d was closer to unity

which could be due to more droplets being nucleated at the beginning of the reaction due to higher concentrations of initiator radicals and less new particles generated. However, it is clear that the miniemulsions were not properly stabilized and maximization of the intra- and extra-particle diffusion resistance was not achieved.

Table 3.2. Miniemulsion polymerization of EHA/VAc/MAA using the stabilization system SDS/Disponil A3065/ODA

Run	[SDS] (phm)	[Disponil A3065] (phm[a])	[Initiator[b]] (phm)	D_p (nm)	N_d (x 10^{17})	N_p (x 10^{17}]	N_p/N_d
301	1.0	0.0	0.30 (A)	124	0.69	1.37	2.00
302	0.0	2.30	0.30 (A)	280	0.15	0.13	0.86
303	1.0	0.0	0.15 (A)	113	0.36	2.02	5.60
304	0.0	2.30	0.15 (A)	230	0.28	0.23	0.82
305	0.22	3.00	0.15 (A)	165	0.48	0.68	1.42
306	0.11	3.30	0.15 (A)	180	0.48	0.56	1.16
307	0.11	3.30	0.15 (B)	208	0.53	0.38	0.72
308	0.11	3.30	0.60 (B)	257	0.40	0.22	0.55
309[c]	0.11	3.30	0.15 (A)	201	0.61	0.65	1.06

[a] phm = parts per hundred parts monomer
[b] A = Ammonium persulfate; B = benzoyl peroxide
[c] Solids content was 43% for run 309 and for runs 301 to 308 was 30%

Runs 305 and 306 were prepared using a mixture of ionic and non-ionic surfactants in a 80/20 and 90/10 mole ratio of Disponil A3065/SDS. These ratios were chosen since formulations with SDS led to large values of N_p/N_d while formulations with Disponil gave N_p/N_d ratios below 1, an indication that in the first case, generation of new particles occurred and in the second case, particles coalesced. It was hypothesized that a stabilization system with a higher amount of Disponil A3065 could avoid the generation of new particles while the presence of SDS could stabilize the recipe against coalescence. Figure 3.5 shows the results of runs 305 and 306. One can see that a mixture of Disponil A3065/SDS led to narrower DSD compared to the previous run prepared where only one surfactant was used. However, there was not a significant difference when the Disponil A3065/SDS ratio was changed from a molar ratio of 80/20 to 90/10.

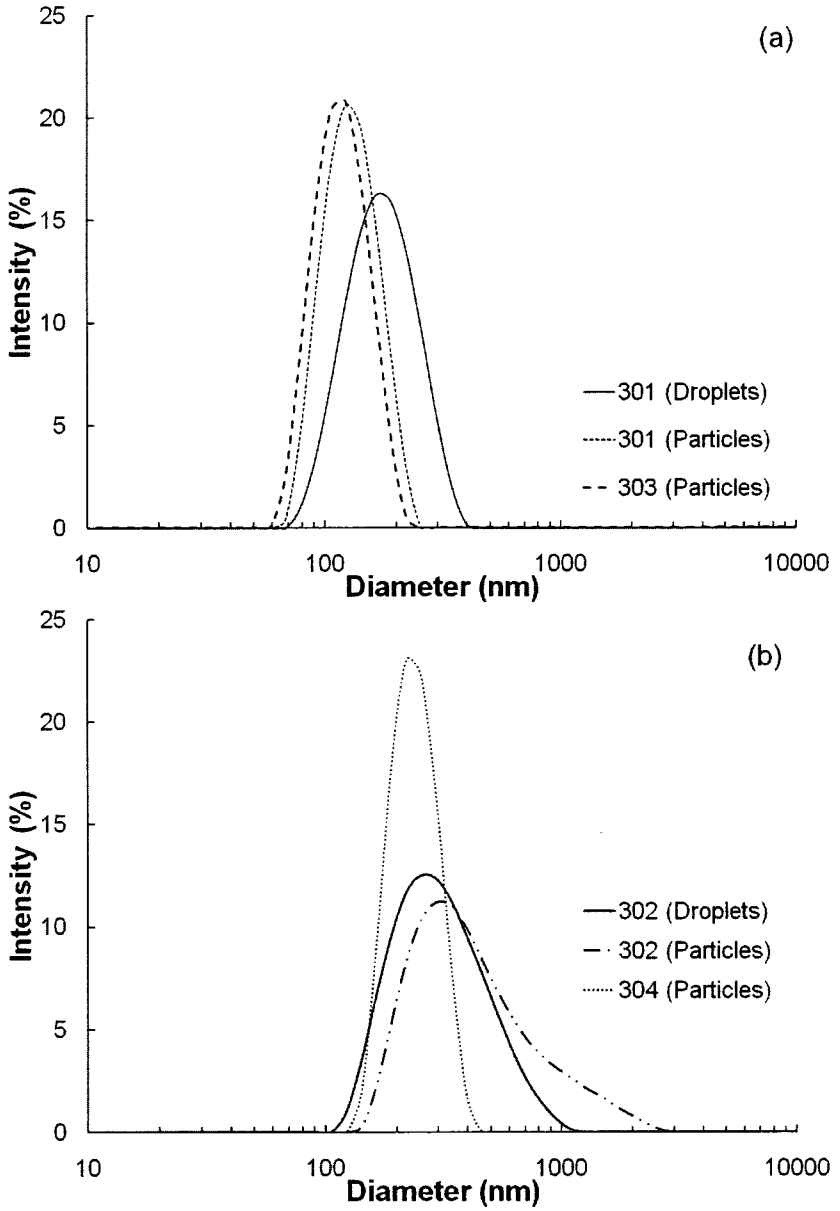

Figure 3.4. a) DSD and PSD of runs 301 and 303 prepared using SDS as the sole stabilizer and b) DSD and PSD of runs 302 and 304 prepared using Disponil A3065 as the sole stabilizer

Although the miniemulsions gave N_p/N_d values closer to unity, they were not behaving as compartmentalized systems, in the sense that maximization of the intra- and extra-particle diffusion resistance was not achieved. Figure 3.6 shows the evolution of N_p/N_d throughout the reaction. It can be observed that in run 306, which gave a value of N_p/N_d

closest to unity at the end of the polymerization (c.f. Table 3.2), the N_p actually increased ~80% after the initiator was injected (this sample was taken after 4 min). This result suggests a combined nucleation mechanism where new particles were generated at the beginning of the reaction as well as the nucleation of a portion of the initial droplets. However, there was not enough surfactant to stabilize the newly generated polymer particles causing some of those particles to coalesce and thus, the average D_p increased again to a value very close to the initial D_d.

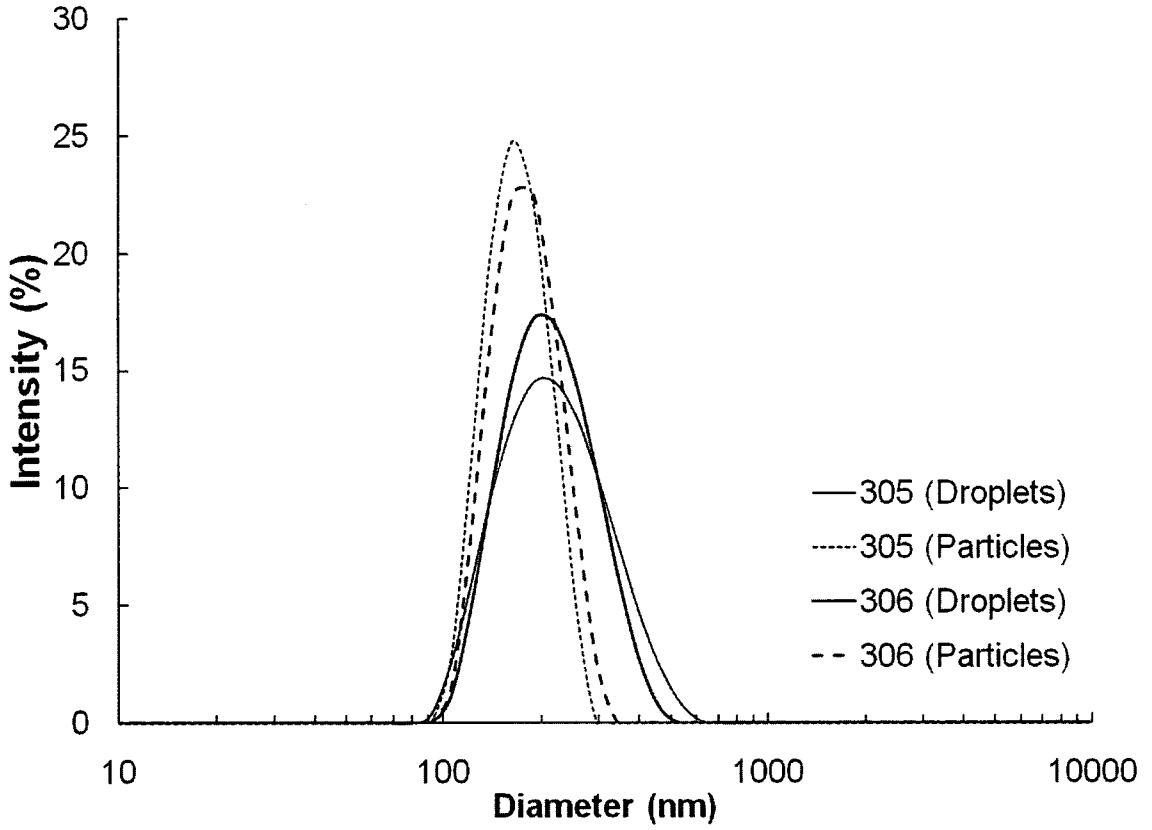

Figure 3.5. DSD and PSD of runs 305 and 306 using a mixture of 80/20 mol.-% and 90/10 mol.-% Disponil/SDS, respectively

Figure 3.7 shows the DSD and PSD for runs 307 and 308, which were polymerized using the oil-soluble initiator BPO. BPO, a water-insoluble compound (water solubility of ~0.012 mM) is also thought to act as a hydrophobe improving miniemulsion stability. As a matter of fact, there was an increase of ~4% and ~12% in the P_O. As can be observed in

Figure 3.7, the final PSD of run 307 is reasonably close to its initial DSD and although N_p/N_d is below 1, it does not fluctuate as much as previous runs (c.f. Figure 3.6). However, the maximum conversion attained in run 307 was ~57 wt.-% after 3 h likely due to the low efficiency of this initiator, which led to low values of $\bar{n}$. Therefore, it was decided to carry out run 308 with a higher initiator concentration and longer reaction time. The DSD and PSD of run 308 are also shown in Figure 3.7 and as can be seen, they are reasonably close to each other. The maximum conversion in run 308 after 7 h was ~67 wt.-%. The conversion profile (not shown here) displayed a plateau at 67 wt.-% after 4 h of reaction without appreciable change afterwards. An analysis of the copolymer composition by 1H-NMR spectroscopy showed that most of the polymer in the particles was EHA homopolymer. This is consistent with the reactivity ratios (discussed earlier) which favour EHA homopolymer production and the relatively high water solubility of VAc.

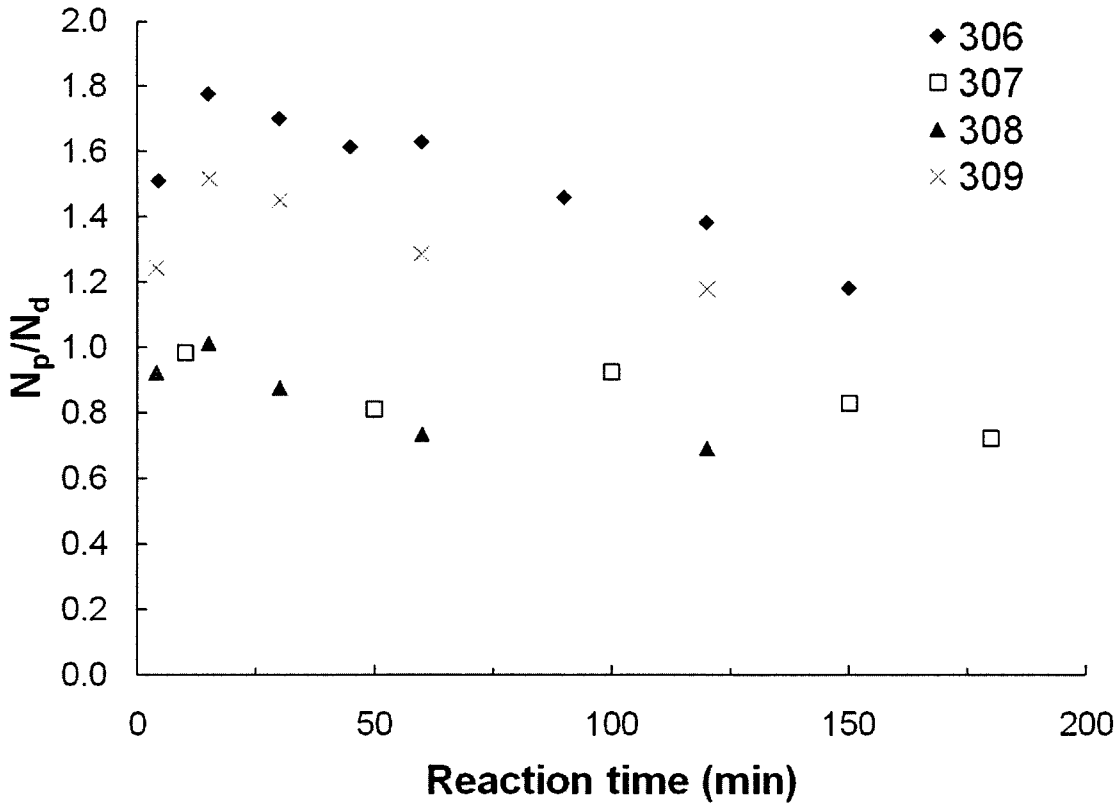

Figure 3.6. Evolution of N_p/N_d for runs 306 to 309

The miniemulsion prepared for run 306 was the most stable miniemulsion prepared up to this point with a conversion above 95%. However, the formulation contained 30 wt.-% solids, which is a relatively low solids content. Run 309 was prepared with a solids content of 43 wt.-% in order to test the stability of the miniemulsion. Figure 3.8 shows the DSD of run 309 immediately after sonication as well as after 1, 2 and 9 days. It also shows the final PSD of the latex, which was polymerized using the miniemulsion right after sonication. Figure 3.8 shows that the DSD did not change significantly after 2 days, which strongly suggest that the miniemulsion was stable and that the higher solids content did not impede the preparation of a kinetically-stable miniemulsion. It was also observed that the measurement taken after 9 days showed two peaks, where one of them had approximately the same diameter as that initially reported. The second peak (large particles) is evidently the result of degradation processes.

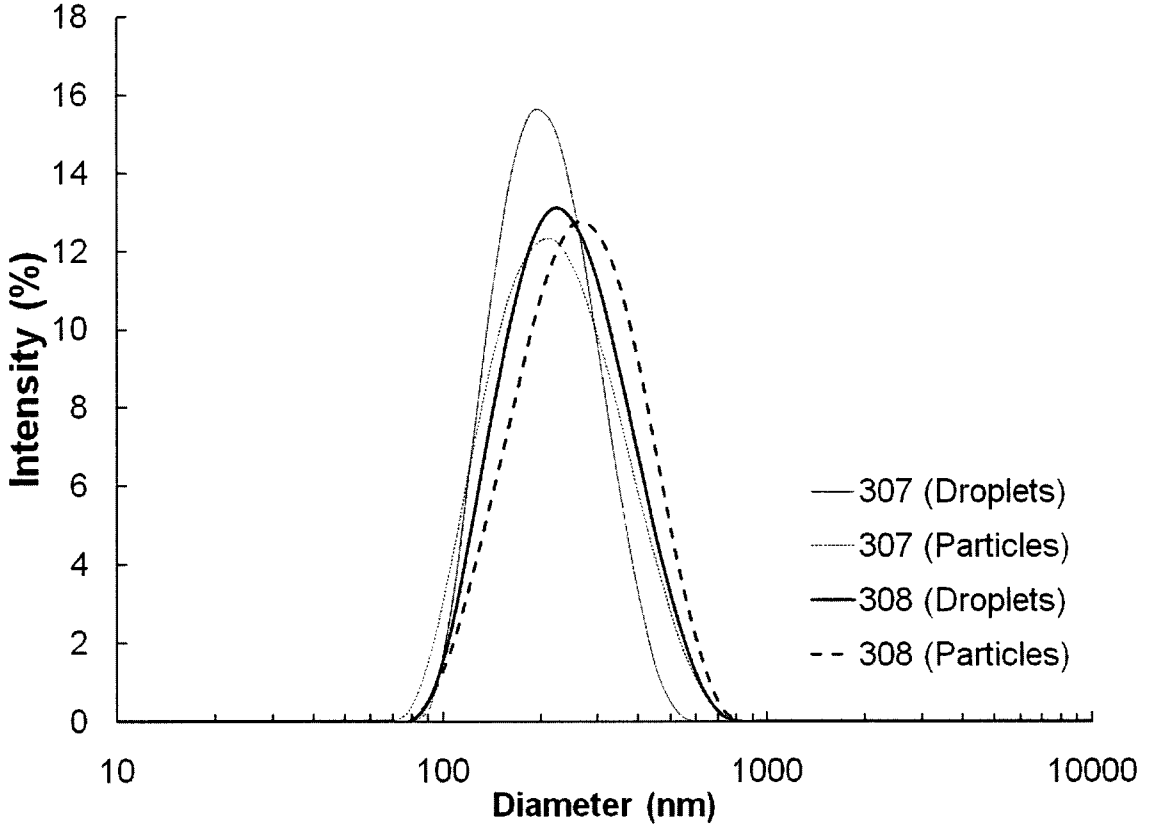

Figure 3.7. DSD and PSD of runs 307 and 308 polymerized using 0.15 and 0.60 phm of BPO as initiator

3.3.3. Influence of co-monomer, surfactant and DDM concentration

Once a set of conditions that gave a kinetically-stable miniemulsion was found, a 2^3 factorial design was carried out to evaluate the influence of the copolymer, surfactant and DDM concentration on D_d, D_p, N_p/N_d and afterwards, their influence on the three main PSA properties: tack, peel strength and shear strength (Zosel, 1998). The statistical analysis was carried out using an α value of 0.05 for statistical significance. α is known as a type-1 error, which is the maximum acceptable level of risk for rejecting a true null hypothesis and is expressed as a probability ranging between 0 and 1. Table 3.3 shows the levels for each factor as well as the results of D_p, N_p/N_d, the maximum conversion (X_{max}) attained and the maximum deviation observed from an ideal N_p/N_d of 1 (be it at any point during the reaction).

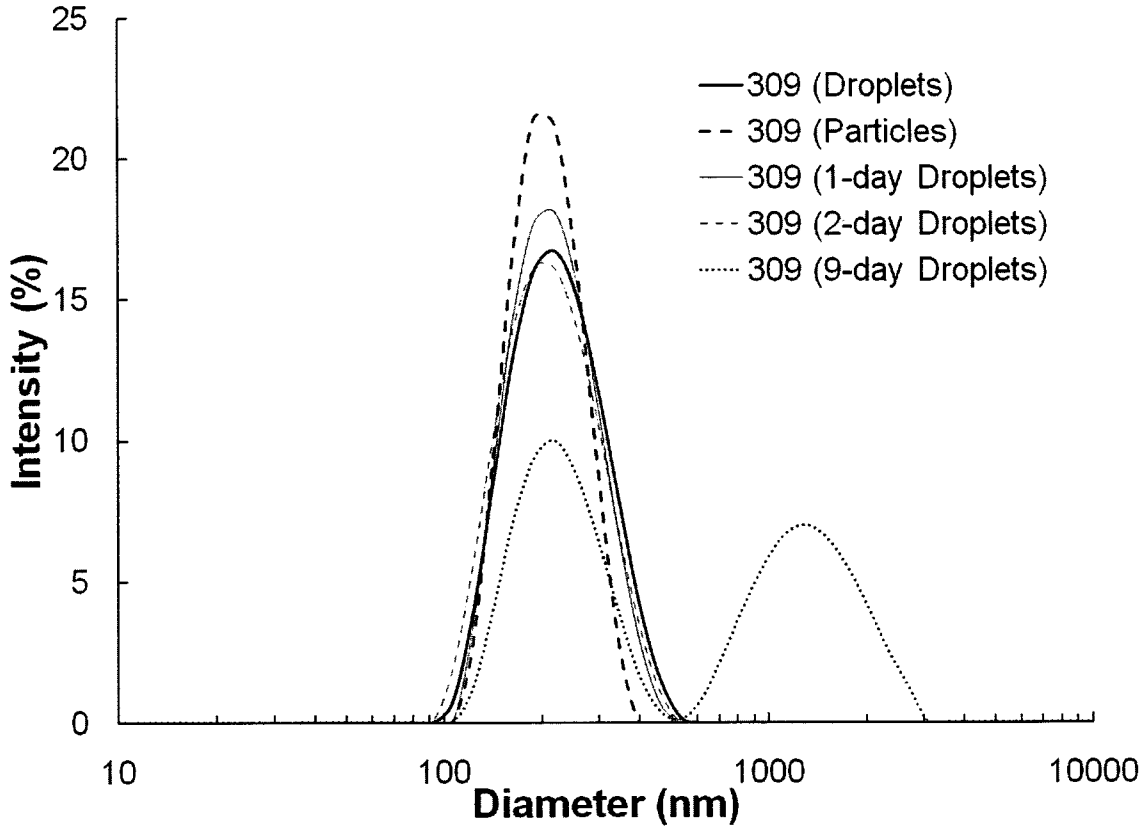

Figure 3.8. DSD and PSD of run 309 using a mixture of 96/4 wt.-% of Disponil/SDS and with 43% solids content

The statistical analysis showed that D_d was strongly influenced by the monomer and surfactant concentrations with p-values of 0.007 and 0.01, respectively. P-values are used to determine which of the effects in the model are statistically significant and are compared against α-values: if the p-value is less than or equal to α, then the effect is significant. It was expected that the surfactant concentration would play a role in determining D_d; however, it was not anticipated that the monomer composition would have a significant influence. It was then noticed that the N_d was larger for those recipes containing a monomer composition of 65/35 wt.-% of EHA/VAc, i.e., higher levels of VAc, which in turn decreased D_d.

Table 3.3. 2^3 factorial design of the miniemulsion polymerization of EHA/VAc/MAA

Run	MC (wt.-%)	[S] (phm)	[DDM] (phm)	D_p (nm)	X_{max} (wt.-%)	N_p/N_d	Max. dev.[b] (%)	M_w (g mol^{-1})
401	85/15	3.5	1.0	217	86	0.99	13	58,800
402	85/15	4.5	0.5	188	88	1.09	11	120,600
403	65/35	4.5	0.5	184	93	0.86	11	200,000
404	65/35	4.5	1.0	169	75	1.21	30	37,000
405	65/35	3.5	0.5	189	76	1.07	16	63,200
406	85/15	4.5	1.0	191	92	1.16	31	64,000
407	85/15	3.5	0.5	215	91	1.07	17	112,600
408	65/35	3.5	1.0	199	77	0.97	3	47,200

[a] MC = Monomer composition as EHA/VAc; S = Surfactant; DDM = Dodecyl mercaptan
[b] Maximum deviation of N_p/N_d from 1.0

There were a number of runs that did not reach full conversion (cf. Table 3.3) and it was observed that the maximum conversion was strongly correlated to the VAc content, which is likely due to the low reactivity of this monomer. This raised the question on how much the lower values of conversion influenced miniemulsion polymerization. The evolution of N_p/N_d throughout the reaction in each one of the reactions was analyzed and the largest deviation observed was recorded (also shown in Table 3.3). It was noted that the largest deviations were not correlated with the VAc nor were DDM concentrations significant in obtaining lower deviation values. It was initially thought that a higher DDM concentration would build up P_O and in turn, have an influence on stability. However, the surfactant concentration was the only statistically significant factor. Figure 3.9 shows the initial N_d and

the evolution of N_p for runs 406 and 408. Run 406 presented the largest deviation from an ideal N_p/N_d of 1, with a change of ~30% with respect to N_d while run 408 presented the lowest deviation of ~3%. It must be mentioned that a deviation of 3% at the beginning of the reaction can represent a miniemulsion that is stabilized properly.

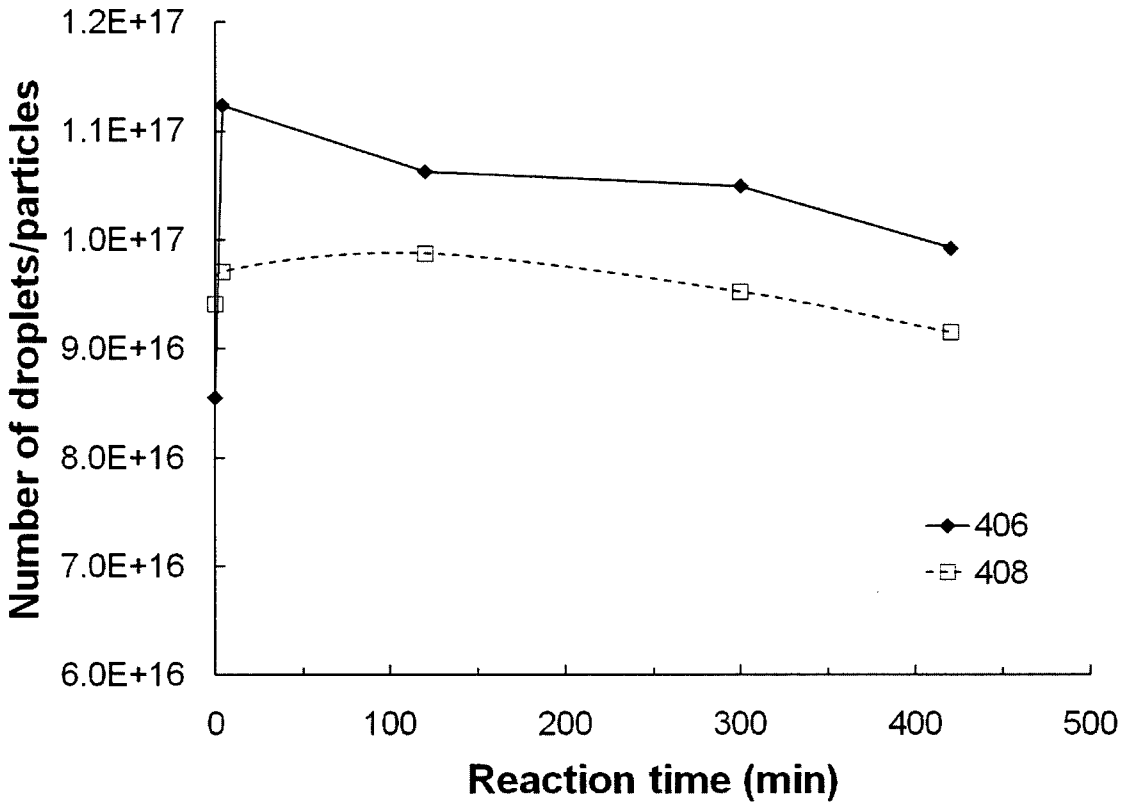

Figure 3.9. Initial N_d and evolution of the N_p for miniemulsion-based runs 406 and 408

3.3.4. Pressure-sensitive adhesive properties

Figure 3.10 shows the results of loop tack, peel strength and shear strength obtained in the factorial design. However, it was difficult to assess the influence of the copolymer composition on the PSA properties due to the fact that a number of the runs did not reach full conversion and the polymer particles were mostly comprised of homopolymer of EHA. Nevertheless, it was observed that those latexes prepared with a monomer mixture of EHA/VAc of 85/15 wt.% gave higher values of loop tack and lower values of peel strength. Conversely, shear strength did not seem to be affected by the copolymer composition.

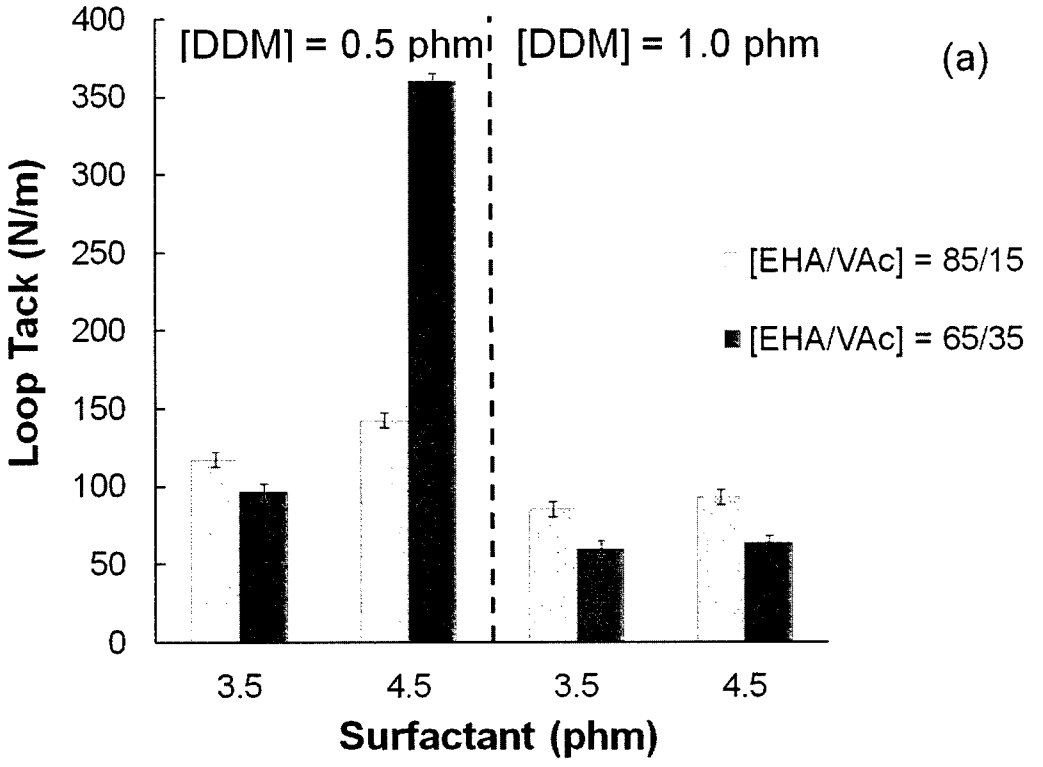
[DDM] = 0.5 phm
[DDM] = 1.0 phm
(a)
Loop Tack (N/m)
400
350
300
250
200
150
100
50
0
[EHA/VAc] = 85/15
[EHA/VAc] = 65/35
3.5
4.5
3.5
4.5
Surfactant (phm)

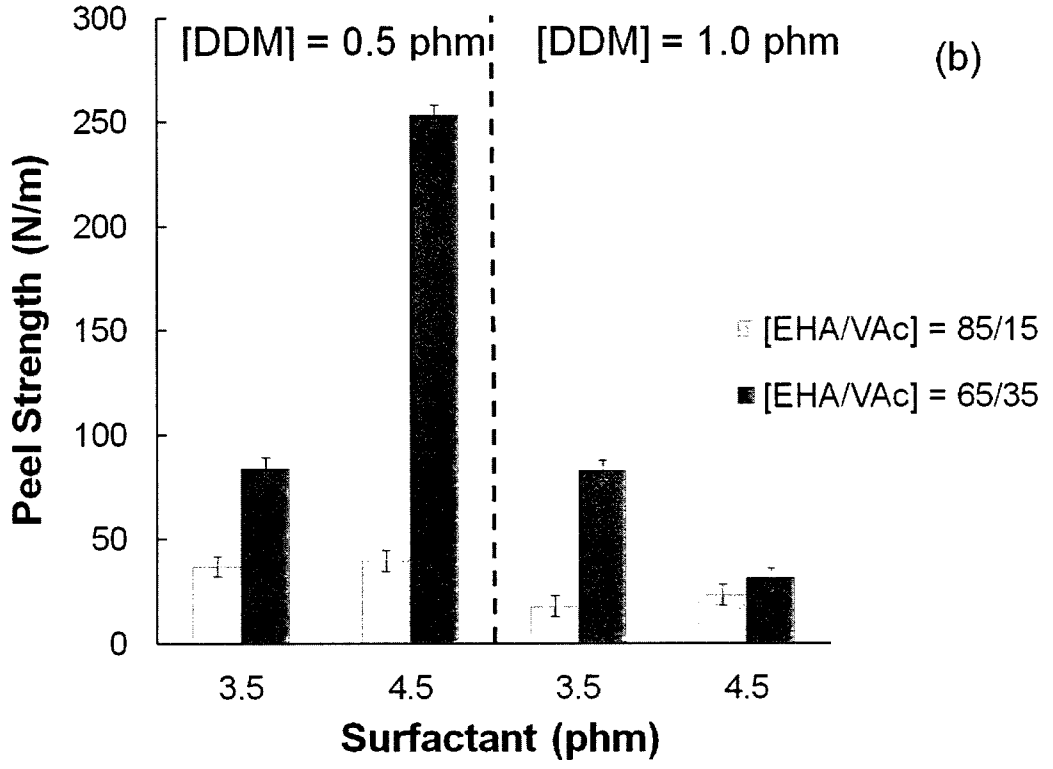
[DDM] = 0.5 phm
[DDM] = 1.0 phm
(b)
Peel Strength (N/m)
300
250
200
150
100
50
0
[EHA/VAc] = 85/15
[EHA/VAc] = 65/35
3.5
4.5
3.5
4.5
Surfactant (phm)

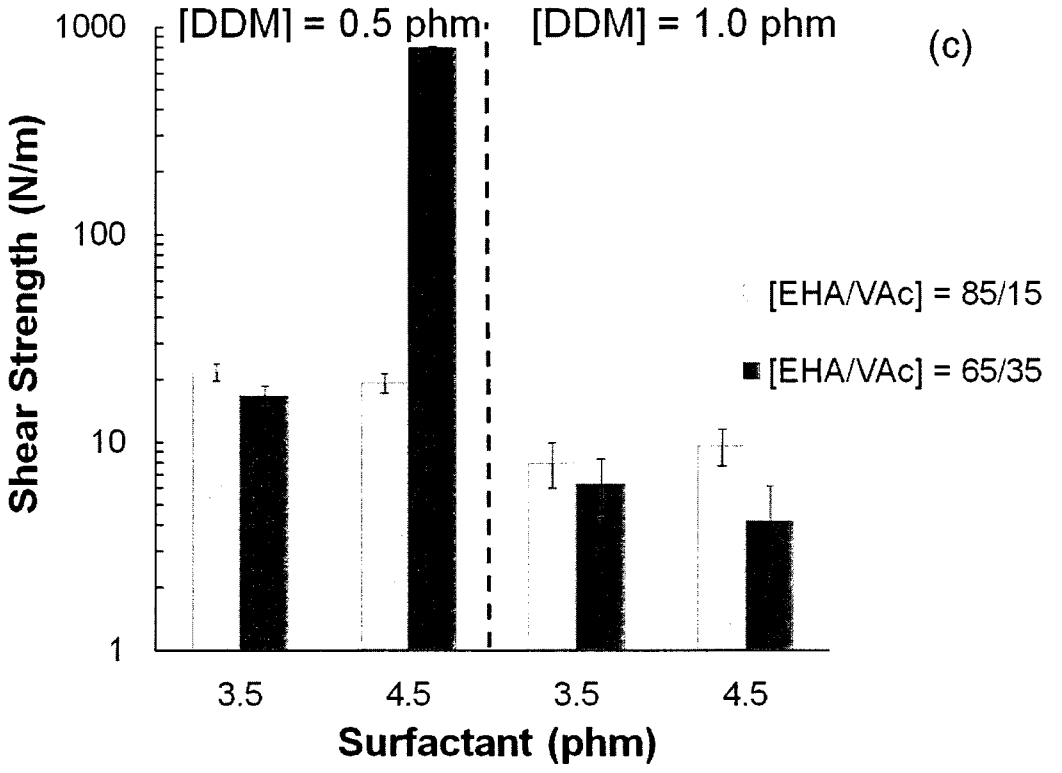

Figure 3.10. Influence of EHA/VAc polymer composition, surfactant and DDM concentration on a) loop tack, b) peel strength and c) shear strength (log scale)

On the other hand, DDM concentration had a strong influence on the determination of the three PSA properties. At the levels of M_w produced within the range of experimental conditions, loop tack, peel and shear strength increased with a decrease of DDM concentration. Figure 3.11 shows how loop tack was strongly correlated to M_w with a linear increase towards larger loop tack values with higher molecular weights. A similar trend was observed for peel and shear strength (not shown here). One can see that highest loop tack values were attained at a M_w above 1 x 10^5 g mol^{-1}, which observed an adhesive failure, while those below this M_w limit displayed cohesive failure. It is likely that at this M_w, fibrils started forming, which have been suggested to be responsible for adequate levels of tack in PSAs (Zosel, 1998).

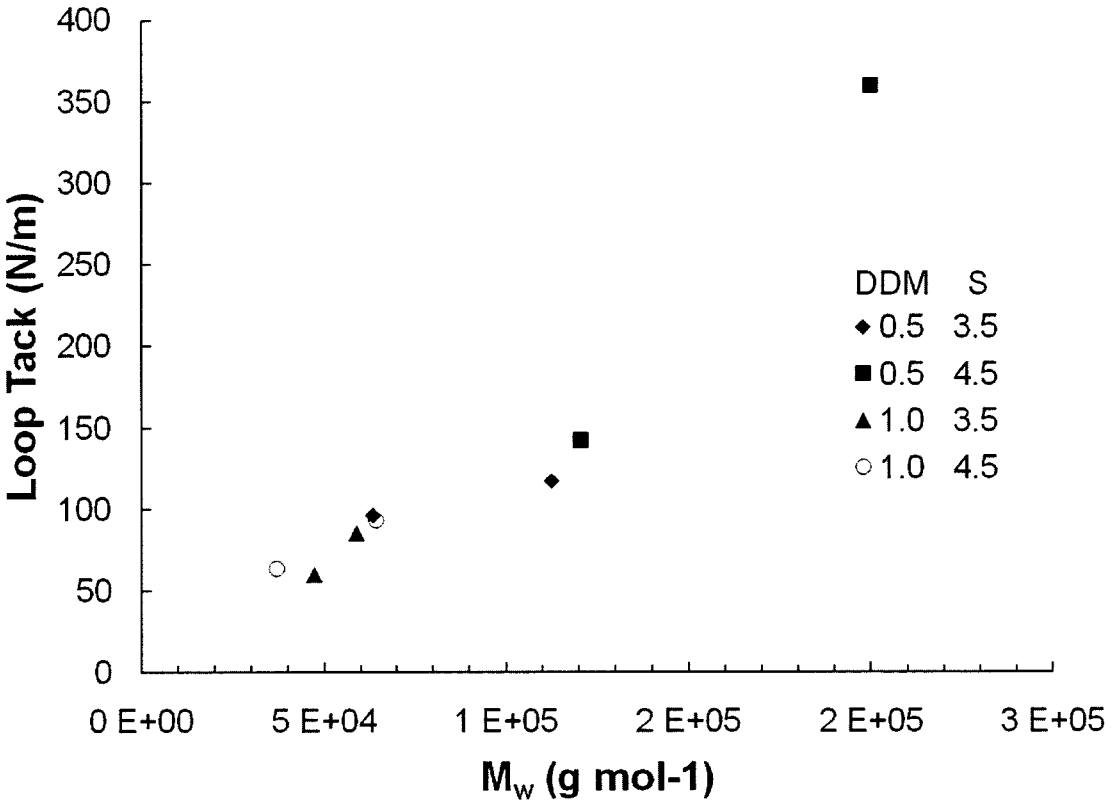

Figure 3.11. Loop tack versus M_w (S = Surfactant; DDM = Dodecyl mercaptan)

3.4. CONCLUSIONS

The preparation of stable miniemulsion-based latexes of poly(EHA/VAc) was studied. Two surfactant mixtures were investigated: SDS/Triton X-405 and SDS/Disponil A3065. The first mixture contained Triton X-405, a non-ionic surfactant with a high content of water soluble groups. The results showed that SDS/Triton X-405 was not able to adequately stabilize the miniemulsions to ensure maximization of intra- and extra-particle diffusion resistance, even though the ODA concentration had been adjusted to give a P_O slightly higher than the P_L. The second surfactant mixture contained Disponil A3065, an ethoxylated linear fatty alcohol surfactant with a lower amount of water soluble groups compared to Triton X-405. Through the screening experiments, we found that a 10/90 mol.-% ratio of SDS/Disponil A3065 with an ODA concentration of 4.5 phm were able to adequately stabilize the miniemulsion resulting in 43% solids-content latexes. The final

N_p/N_d obtained in the most stable recipe was 1.06 with a maximum deviation in the N_p at the beginning of the polymerization of ~3%.

Once a stable range of conditions was identified, a 2^3 factorial design was carried out to understand the influence of changes in co-monomer, surfactant and DDM concentration on the DSD and PSD and later, in the PSA properties (loop tack, peel strength and shear strength). The analysis showed that the DSD was strongly influenced by the co-monomer and surfactant concentrations. It was also noted that the change in DDM concentration did not contribute to the miniemulsion stability in the range studied in this work nor did it represent a significant factor in determining the DSD and PSD. However, the statistical analysis was unable to identify the influence of the co-monomer concentration on the final PSD due to the fact that 5 out of 8 runs in the factorial design did not reach full conversion (conversions between 71 and 91 wt.-%). This was likely due to the water solubility of VAc monomer combined with its low reactivity compared to EHA. This is typical of VAc-containing systems and it continues to represent a significant challenge for industrial applications. Typically, semi-continuous monomer feed strategies are employed to counteract this effect; however, as mentioned by Schork et al. (2005), the semi-continuous monomer feed in miniemulsion polymerization would not differ from that obtained in conventional emulsion polymerization.

The DDM concentration did not affect DSD or PSD but it played a strong role in the determination of M_w. Within the range of DDM and surfactant concentrations studied in this work, the M_w varied from 40,000 to 200,000 g mol^{-1}. As a consequence, DDM concentration had a strong influence on loop tack, peel strength and shear strength. A linear relationship between tack and M_w was observed, i.e., higher M_w resulted in higher loop tack. Similar trends were observed for peel and shear strength.

3.5. ACKNOWLEDGMENTS

The authors gratefully acknowledge the financial support of the Natural Science and Engineering Research Council (NSERC) of Canada and the National Council of Science and Technology (CONACYT) of Mexico.

3.6. REFERENCES

Aizpurua, I., Barandiaran, M.J., 1999. Comparison between conventional emulsion and miniemulsion polymerization of vinyl acetate in a continuous stirred tank reactor. Polymer 40, 4105-4115.

Antonietti, M., Landfester, K., 2002. Polyreactions in miniemulsions. Progress in Polymer Science 27, 689-757.

Bathfield, M., Graillat, C., Hamaide, T., 2005. Encapsulation of high biocompatible hydrophobe contents in nonionic nanoparticles by miniemulsion polymerization of vinyl acetate or styrene: Influence of the hydrophobe component on the polymerization. Macromolecular Chemistry and Physics 206, 2284-2291.

Bohórquez, S.J., Asua, J.M., 2008. Particle nucleation in high solids batch miniemulsion polymerization stabilized with a polymeric surfactant. Journal of Polymer Science, Part A: Polymer Chemistry 46, 6407-6415.

Brandrup, J., Immergut, E.H., Grulke, E.A., Abe, A., Bloch, D.R., 2005. Polymer Handbook, 4th edition ed. Wiley, New York.

Delgado, J., Elaasser, M.S., Vanderhoff, J.W., 1986. Miniemulsion Copolymerization of Vinyl-Acetate and Butyl Acrylate .1. Differences Between the Miniemulsion Copolymerization and the Emulsion Copolymerization Processes. Journal of Polymer Science Part A-Polymer Chemistry 24, 861-874.

do Amaral, M., Asua, J.M., 2004. Synthesis of large, high-solid-content latexes by miniemulsion polymerization. Journal of Polymer Science, Part A: Polymer Chemistry 42, 4222-4227.

Erbil, H.Y., 2000. Vinyl Acetate Emulsion Polymerization and Copolymerization With Acrylic Monomers, 1st. edition ed. CRC Press, Boca Raton, USA.

Farzi, G., Bourgeat-Lami, E., McKenna, T.F.L., 2009. Miniemulsions Using Static Mixers: A Feasibility Study Using Simple In-Line Static Mixers. Journal of Applied Polymer Science 114, 3875-3881.

Graillat, C., Guyot, A., 2003. High solids vinyl acetate polymers from miniemulsion polymerization. Macromolecules 36, 6371-6377.

Hua, H., Dubé, M.A., 2001. Off-line monitoring of butyl acrylate, methyl methacrylate and vinyl acetate homo- and copolymerizations in toluene using ATR-FTIR spectroscopy. Polymer 42, 6009-6018.

Hulden, M., Kronberg, B., 1994. Mixed Adsorption of Anionic and Nonionic Surfactants on Latex Particles. Journal of Coatings Technology 66, 67-77.

Jovanovic, R., Dubé, M.A., 2004. Butyl acrylate/vinyl acetate miniemulsion polymerization: A study on compartmentalization. Macromolecular Chemistry and Physics 205, 958-965.

Landfester, K., 2000. Recent developments in miniemulsions - Formation and stability mechanisms. Macromolecular Symposia 150, 171-178.

Landfester, K., Bechthold, N., Forster, S., Antonietti, M., 1999. Evidence for the preservation of the particle identity in miniemulsion polymerization. Macromolecular Rapid Communications 20, 81-84.

Lathova, E., Lath, D., Pavlinec, J., 1993. The Behavior of Poly(2-Ethylhexyl Acrylate) in Dilute-Solution - Viscosity Measurements. Polymer Bulletin 30, 713-718.

Lopez, A., Chemtob, A., Milton, J.L., Manea, M., Paulis, M., Barandiaran, M.J., Theisinger, S., Landfester, K., Hergeth, W.D., Udagama, R., McKenna, T., Simal, F., Asua, J.M., 2008. Miniemulsification of monomer-resin hybrid systems. Industrial & Engineering Chemistry Research 47, 6289-6297.

Lovell, P.A., El-Aasser, M.S., 1997. Emulsion Polymerization and Emulsion Polymers, 1st edition ed. John Wiley & Sons, New York.

Ouzineb, K., Graillat, C., Dubé, M.A., Jovanovic, R., McKenna, T.F., 2004a. Compartmentalisation in miniemulsions: Exploration of compartmentalisation and some interesting end-uses. Macromolecular Symposia 206, 107-119.

Ouzineb, K., Graillat, C., McKenna, T.F., 2004b. Study of compartmentalization in the polymerization of miniemulsions of styrene and butyl methacrylate. Journal of Applied Polymer Science 91, 115-124.

Ouzineb, K., Graillat, C., McKenna, T.F., 2005. High-Solid-Content Emulsions. V. Applications of Miniemulsions to High Solids and Viscosity Control. Journal of Applied Polymer Science 97, 745-752.

Ouzineb, K., Hua, H., Jovanovic, R., Dubé, M.A., McKenna, T.F., 2003. Monomer compartmentalisation in miniemulsion polymerisation studied by infrared spectroscopy. Comptes Rendus Chimie 6, 1343-1349.

Reimers, J.L., Schork, F.J., 1996. Miniemulsion copolymerization using water-insoluble comonomers as cosurfactants. Polymer Reaction Engineering 4, 135-152.

Saethre, B., Mork, P.C., Ugelstad, J., 1995. Preparation of poly (vinyl chloride) latexes by polymerization of stabilized monomer droplets. Journal of Polymer Science, Part A: Polymer Chemistry 33, 2951-2959.

Schork, F.J., Luo, Y., Smulders, W., Russum, J.P., Butte, A., Fontenot, K., 2005. Miniemulsion Polymerization. Advances in Polymer Science 175, 129-255.

Tauer, K., 2001. Surface Chemistry in the Polymerization of Emulsion, in: Holmberg, K. (Eds.), Handbook of Applied Surface and Colloid Chemistry. John Wiley & Sons, Chichester; New York, pp. 175-200.

Wu, X.Q., Schork, F.J., 2000. Batch and semibatch mini/macroemulsion copolymerization of vinyl acetate and comonomers. Industrial & Engineering Chemistry Research 39, 2855-2865.

Zosel, A., 1998. The effect of fibrillation on the tack of pressure sensitive adhesives. International Journal of Adhesion and Adhesives 18, 265-271.

CHAPTER 4

Influence of particle nucleation in pressure sensitive adhesive properties: miniemulsion *versus* emulsion polymerization

---

Fonseca, G.E., McKenna, T.F., Dubé, M.A.;
Macromolecular Symposia 271, 83 – 93 (2008)

Influence of particle nucleation in pressure sensitive adhesive properties: miniemulsion versus emulsion polymerization

Gabriela E. Fonseca[1], Timothy F. L. McKenna[2] and Marc A. Dubé[1*]

[1]Department of Chemical and Biological Engineering,
University of Ottawa, Ottawa, Ontario, K1N 6N5, Canada
E-mail: Marc.Dube@UOttawa.ca, Fax: +1 (613) 5625172

[2]Department of Chemical Engineering, Queen's University, Kingston, Canada

ABSTRACT

Miniemulsion polymerization is a promising approach to produce and tailor pressure sensitive adhesives. In this paper, a systematic comparison of the adhesives properties of latexes produced by miniemulsion and conventional emulsion polymerization is presented. Specifically, the influence of the total surfactant concentration, chain transfer agent concentration and chemical composition on the final adhesive properties of the polymer 2-ethyl hexyl acrylate/methyl methacrylate/acrylic acid was discerned using a 2^3 factorial design for each polymerization method. In addition to the adhesive properties (i.e., loop tack, peel strength and shear strength), molecular weight distribution, particle size distribution (PSD) and glass transition temperature were analyzed. The results show that under the conditions used in this work, it is possible to produce pressure sensitive adhesives using miniemulsion polymerization carried out mostly by droplet nucleation. The change in polymerization process produced certain differences such as larger particles sizes. Focusing on the films that exhibited adhesive failure, miniemulsion displayed higher values of loop tack and peel strength compared to conventional emulsion polymerization. Shear strength results were strongly dependent on the amount of gel content and sol molecular weight for both cases.

Keywords: miniemulsion polymerization; 2-ethyl hexyl acrylate; methyl methacrylate; pressure sensitive adhesives

4.1 INTRODUCTION

A global need for environmentally friendly technologies and products has led to the replacement of volatile organic compounds (VOCs) used in the production of pressure sensitive adhesives (PSAs), for water. Water-based technologies such as emulsion polymerization are now widely used in PSA production. In particular, water-based PSAs produced with acrylic polymers are now common commercial products (Satas, 1989).

The performance of these pressure sensitive products (PSPs) is characterized by their adhesive and cohesive behaviour, which is defined by three main application properties, namely, tack, peel strength and shear strength. Tack represents the ability to form an instant bond; peel strength represents the resistance to removal from the adherend and shear strength is a measure of the cohesive strength (Jovanovic and Dubé, 2004). However, there is a known conflict between these three application properties since an increase in tack and peel strength (adhesive component) often leads to a decrease in shear strength (cohesive component) and vice versa (Benedek, 2004). Depending on the application, it is usually desirable to find a means to decouple this property interdependence.

The behaviour of a PSP is a consequence of its viscoelastic properties which are influenced by several polymer properties such as the molecular weight distribution (MWD), particle size distribution (PSD) and glass transition temperature (T_g), which in turn are affected by the type of process, reaction conditions, monomers used and addition of other components (surfactants, initiator, crosslinkers, etc.).

It is also known that broad or multimodal MWDs can help in the improvement of PSA properties (Satas, 1989). For example, tack and peel strength improve with an increase in molecular weight (up to a maximum); however, they can be further improved by adding a fraction of low molecular weight polymer. In addition, it is recognized that multimodal PSDs can promote the achievement of higher solids contents latexes at a reduced viscosity, which is beneficial from a processing and economics point of view (Chu et al., 1998; Schneider et al., 2002).

Emulsion polymerization is a heterogeneous polymerization process wherein monomer droplets are suspended in an aqueous phase containing surfactant micelles. The surfactant also stabilizes the monomer droplets. Typically, an emulsion polymerization

system consists of three phases, namely a monomer droplets phase, a continuous phase (surfactant, micelles, a free-radical initiator and other components dissolved in the water) and the polymer particles phase. Micelles will be present in the continuous phase if the surfactant concentration is above the critical micelle concentration (CMC) and these are normally the setting for the nucleation of polymer particles. Usually, the main locus of the reaction takes place inside the polymer particles (i.e., the nucleated monomer-swollen micelles (Gilbert, 1995).

Miniemulsion polymerization has gained interest in the last twenty years because of its potential for commercial polymer production. This type of polymerization is formulated to change the particle nucleation location from monomer-swollen micelles to the monomer droplets. This is accomplished by using an appropriate surfactant system and a highly hydrophobic compound, together with the use of high shear mixing. The hydrophobic compound decreases the monomer droplets' solubility and the combination of high shear mixing and a stabilizer serves to adjust or control the droplet sizes and their distribution. Together, these will delay Ostwald ripening, creating a kinetically stable emulsion and producing so-called "particle compartmentalization" (Antonietti and Landfester, 2002). In a miniemulsion, the mean monomer droplet diameter is considerably smaller (50 – 500 nm) than in conventional emulsions (>1 μm), which greatly increases the droplets' surface area. Also, the amount of surfactant present in the medium is kept well below the CMC. The larger surface area occupied by the monomer droplets and the absence of micelles cause the nucleation of polymer particles to occur in the droplets as opposed to micelles. The result is that monomer droplets act as independent batch nano-reactors keeping their individual characteristics throughout the reaction, wherein no significant amount of material is transferred between the droplets or towards the continuous aqueous phase. This could allow the simultaneous polymerization of various sets of particles with different characteristics, and potentially, the fine-tuning of PSA properties.

Previous studies have established the viability of producing miniemulsion-based PSA with multimodal MWDs and PSDs and confirmed that extra-particle monomer diffusion resistance can be maximized (Ouzineb et al., 2003; Jovanovic et al., 2004). The aim of this study was to evaluate the difference between the PSA produced by the two polymerization processes, i.e., miniemulsion and conventional emulsion polymerization. The ultimate goal

was to increase one property (i.e., loop tack) without decreasing another (i.e., shear strength). Miniemulsion polymerization could help in this goal, but in order to do so, it was necessary to know if different nucleation mechanisms would lead to different PSA application properties or if the more stable miniemulsion polymerization was producing different polymer microstructures, e.g., lower molecular weights or broader particle size distributions. In other words, it was indispensable to identify the range of PSA properties achievable by miniemulsion polymerization and how they were compared to those produced by similar conditions in conventional emulsion polymerization.

Herein, we present the results of a systematic comparison of the adhesive properties obtained by miniemulsion and conventional emulsion polymerization. A factorial design was used to discern the effects of chain transfer agent concentration (CTA), total surfactant concentration (TS) and copolymer composition (CC), which are three important parameters that affect the polymer properties and in turn, the PSA and viscoelastic properties.

4.2 EXPERIMENTAL DETAILS

4.2.1 Materials and Preparation

The monomers used in this study were 2-ethyl hexyl acrylate (EHA) (Aldrich), methyl methacrylate (MMA) (Aldrich) and acrylic acid (AA) (Aldrich). The hydrophobe used was octadecyl acrylate (ODA) (Aldrich) and the initiator was ammonium persulfate (APS) (Sigma-Aldrich). 1-dodecanethiol (DDM) (Aldrich) was used as chain transfer agent (CTA). The surfactant system consisted of a mixture of an ionic (Sodium dodecyl sulphate (SDS) (Sigma-Aldrich) and a non-ionic surfactant (Disponil® A3065) (donated by Cognis Canada). Sodium bicarbonate ($NaHCO_3$) (Sigma-Aldrich) was used as buffer. Distilled deionized water was used in all the experiments as the continuous phase. All ingredients were used without further purification.

The conventional emulsions and miniemulsions were prepared by mixing the aqueous phase, which contained SDS, Disponil® A3065, $NaHCO_3$ and water, with the organic phase which contained EHA, MMA, AA, ODA and DDM. The organic phase was slowly added to the aqueous phase and stirred until a homogeneous emulsion was obtained. For the miniemulsion polymerization, the emulsion was then sonicated for 4 min using a Fisher

Scientific Sonic Dismembrator model 550 at level 9. It should be noted that ODA was added to both the miniemulsion and conventional emulsion recipes, although previous studies have not done so due to the fact that it is considered merely as the hydrophobic compound. In this work, the possibility that this component might pose an influence in the PSA properties was considered, since it would certainly be incorporated into the polymer matrix and could possibly create a bias in the comparison between the two adhesives. Therefore, the ODA concentration was kept constant for both polymerization methods.

The polymerization reactions were performed in a 1.1L Labmax™ automated stainless steel reactor (Mettler Toledo) equipped with a stirrer, condenser and three feed ports. The temperature and stirring speed were automatically controlled at 70°C and 200 rpm, respectively. Conversion was obtained from gravimetric measurements. Droplet and particle sizes for the monomodal distributions were obtained using a Dynamic Light Scattering (DLS) instrument (Malvern NanoS Zetasizer) with an angle of 176°. Two drops of the latex were diluted and placed in a polystyrene cuvette and analyzed 3 times. The reported diameter is the z-average (intensity-based) of 3 measurements that were analyzed in 10 runs of 30 s each. The number of particles and number of droplets were calculated based on the average polymer particle or monomer droplet diameter obtained from DLS and conversion measurements. The osmotic pressure (P_O) and Laplace pressure (P_L) were calculated according to the method used by Ouzineb et al. (2004). The P_O considers only the concentration of ODA and do not includes that of DDM.

4.2.2 Characterization

The MWDs were obtained using Gel Permeation Chromatography (Waters). A small sample of dry polymer was dissolved in tetrahydrofuran (THF) to give a concentration of ~0.015 g/mL. The solution was then filtered with a 0.45 μm filter to eliminate the presence of large particles and gel. The instrument is equipped with a refractive index detector and three Waters Styragel columns used in series (10^3, 10^4 and 10^6 Å). THF was used as the eluent at a flow rate of 0.3 mL/min. The calibration was done with polystyrene standards with molecular weights ranging from 1.3 x 10^3 to 3.15 x 10^6 g/mol. The analysis of the data was done using the Universal Calibration method with Empower2 software (Waters). The

Mark-Houwink constants used are K = 0.0001254 dL/g and α = 0.67 for poly (2-ethyl hexyl acrylate) (Lathova et al., 1993) and K = 0.000128 dl/g and α = 0.69 for poly (methyl methacrylate) (Brandrup et al., 2005).

Copolymer compositions were obtained using ^{1}H-NMR spectroscopy (Bruker). Each sample of dry polymer was dissolved in d-CCl_4 at a concentration of 5% w/v. Further details about the procedure can be found in Jovanovic and Dubé (Jovanovic and Dubé, 2001).

Adhesive testing was performed following Pressure Sensitive Tape Council (PSTC) standards PSTC-1, PSTC-6 and PSTC-7 for peel strength, loop tack and shear strength, respectively (Pressure Sensitive Tape Council, 2004). The latexes were cast on a 50 μm Mylar® film using a Meyer rod to obtain approximately 65 g/m^2 (dry basis) of applied adhesive and were conditioned under controlled temperature (23±2°C) and humidity (50±5%) for 24 h prior to testing. The substrate used for these tests was stainless steel.

A 2^3 factorial design with 2 center points was used to discern the effect of CC, CTA and TS in both, miniemulsion and conventional emulsion polymerization (see Table 4.1) for a total of 20 runs. Statistical analysis was performed with the statistical software Minitab® version 14.

\

Table 4.1. Miniemulsion recipes

Factor	Levels		
	-1	0	1
Chemical composition EHA/MMA wt.%]	65/35	75/25	85/15
CTA [phm[a]]	0.50	0.75	1.00
Surfactant [phm]	4.50	5.00	5.50
Initiator [phm]	0.30		
Buffer [phm]	0.15		
AA [phm]	2.00		
ODA [phm]	4.00		

4.3 RESULTS AND DISCUSSION

The goal of this work was to determine the range of properties that a true miniemulsion polymerization could achieve and make an unbiased comparison between the PSA properties produced by both miniemulsion and conventional emulsion polymerization. As a first step, it was first necessary to evaluate whether the miniemulsion reactions had proceeded via droplet nucleation and if the presence of secondary nucleation could also influence the PSA application properties in a way that would be more in line with conventional emulsion polymerization than miniemulsion polymerization.

Table 4.2.MiniemulsionMiniemulsion and conventional emulsion polymerization: stability and particle diameter

Run ID	N_p/N_d	P_O [bar]	P_L [bar]	MP D_p [nm]	CEP D_p [nm]
1	1.145	2.91	1.65	177	160
2	1.005	2.89	1.64	182	153
3	1.307	2.92	1.52	170	138
4	1.099	2.95	1.64	197	155
5	0.884	2.91	1.5	191	138
6	1.073	2.92	1.77	196	150
7	1.140	2.86	1.77	162	100
8	1.139	2.92	1.64	160	125
9	1.220	2.86	1.6	178	124
10	1.084	2.9	1.64	180	154

In order to make such an evaluation, the ratio between the number of polymer particles and number of droplets (N_p/N_d) was calculated (see Table 4.2). From these results, it was observed that the ratio N_p/N_d was sensitive to the amount of surfactant involved in the recipes and to a lesser extent to the amount of EHA (see Figure 4.1).

In order to get a better idea of this dependence, the amount of the polymer particle surface covered by surfactant, which was calculated according to a method used by Fortuny-Heredia (2002), was investigated. Figure 4.2 illustrates the dependence of N_p/N_d with the particle surface covered by surfactant. This figure shows that in order to obtain a relatively

stable miniemulsion, the amount of surfactant would have to be kept at concentrations that would result in surface coverage of no more than 38%, which could possibly restrict the particle sizes achievable. As mentioned before, it was seen that N_p/N_d was sensitive to the amount of EHA present in the emulsion (see Figure 4.1). Table 4.2 also shows the values of the resulting P_O and P_L. One could think that high EHA level runs would require a lower amount of ODA to be stable. This could be explained by looking at the difference between P_O and P_L. A plot of the differences between these two pressures was generated (see Figure 4.3) to corroborate this reasoning. As it can be observed, moving to a higher amount of EHA increases the difference between P_O and P_L, leaning towards the limits of colloidal stability. A decrease of P_O by means of decreasing the ODA concentration would likely overcome this effect. Also, moving to a higher surfactant concentration decreases this difference and in this case, an increase in P_O to compensate for it would be recommended. In the end, a judicious balance between these two pressures must be achieved to yield a stable miniemulsion.

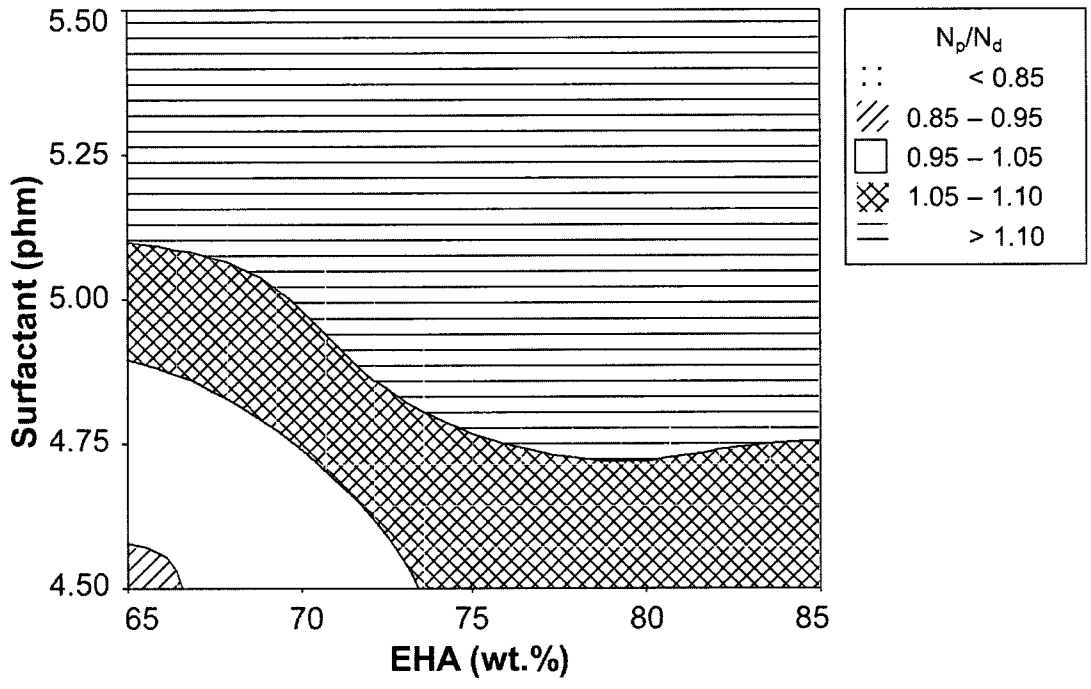

Figure 4.1. Relationship between N_p/N_d versus amount of EHA and TS.

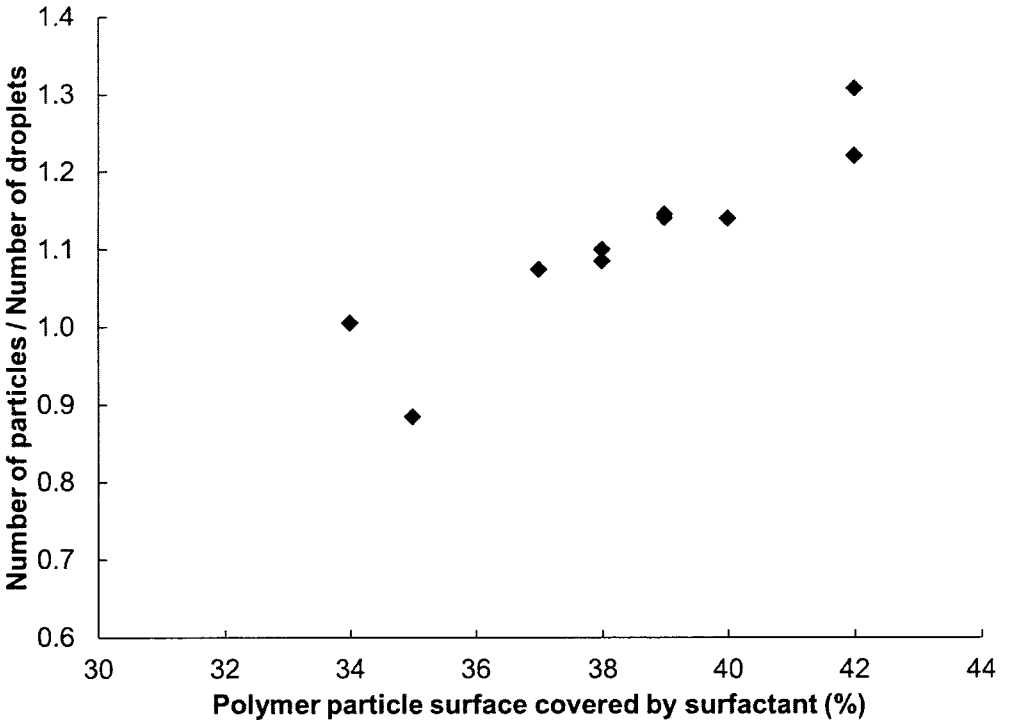

Figure 4.2. Polymer particle surface covered by surfactant

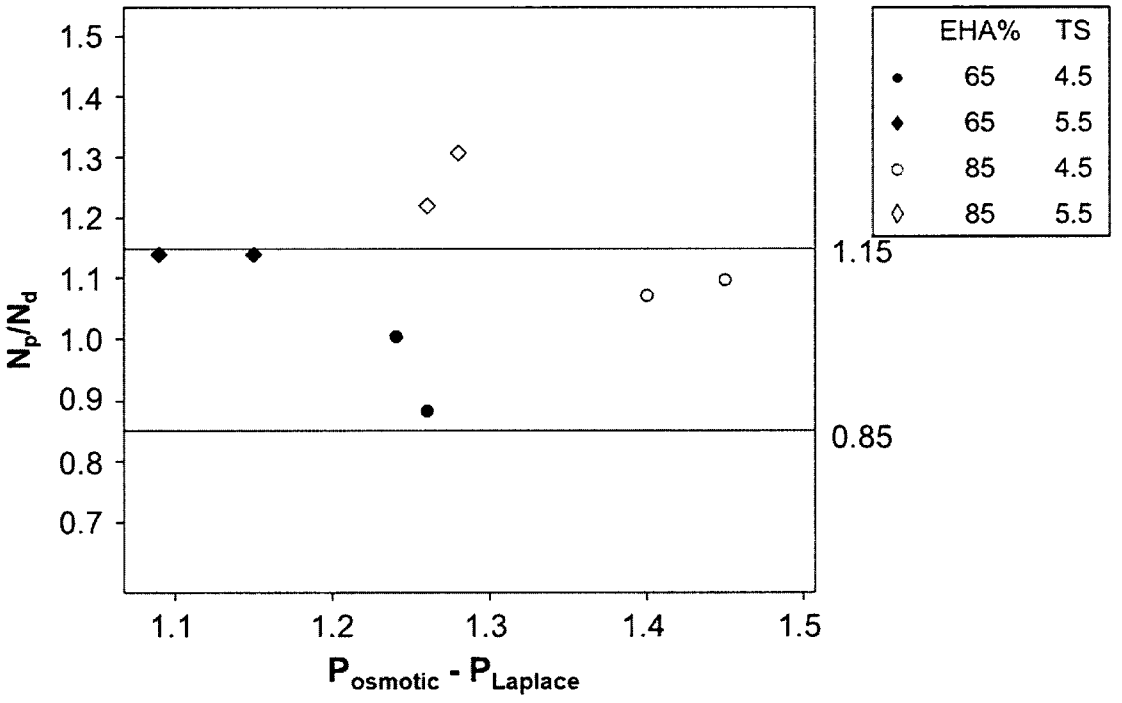

Figure 4.3. Plot of (P_O - P_L) vs. N_p/N_d at two EHA levels (65 and 85 wt%) and two TS levels (4.5 and 5.5 phm)

In summary, eight out of ten of the runs were polymerized within the stability limits. The results of the miniemulsion and conventional emulsion polymerization showed some important differences. First of all, the miniemulsion polymerizations resulted in somewhat larger particles compared to the conventional emulsion polymerizations. Table 4.2 shows the results for the particle diameters.

A statistical analysis suggests that in the case of miniemulsion polymerization, both TS and CC amounts influenced the final D_p, while in the case of conventional emulsion polymerization, the three factors studied (i.e., CTA, TS and CC) all affected the final D_p. In both cases, TS was the major effect, a result that was expected since particle size is usually manipulated by the concentration of surfactant. Figure 4.4 shows how a change in TS results in different final distributions for the two techniques. This figure also shows how conventional emulsion polymerization produced a narrower PSD at the high level of TS compared to miniemulsion polymerization. As well, the effect of a change in surfactant is more pronounced for conventional emulsion polymerization, where the PSD is determined by the particle formation and subsequent growth, while in the miniemulsion polymerization case, the PSD is determined prior to the reaction. The PSD produced by miniemulsion polymerization was dependent on the initial droplet size distribution (DSD), which in turn was influenced by TS, the high shear applied to the miniemulsion and to a lesser extent in the CC. Figure 4.5 shows the effect of a change in CTA for both polymerization techniques. There is no significant effect in miniemulsion case while in conventional emulsion polymerization, the effect is small but observable. This could imply that the PSD can be manipulated independently of MWD in a miniemulsion polymerization, i.e., it could be possible to modify a priori the PSD without changing MWD or to modify MWD without changing PSD.

In the case of the weight- and number-average molecular weights, M_w and M_n respectively, it was found that there was no significant statistical influence other than the CTA concentration for both polymerization methods. However, the miniemulsion polymerizations produced higher values of M_n and narrower PDI indexes compared to the conventional emulsion polymerizations, as can be seen in Figures 4.6 and 4.7. It is thought that a possible reason for the lower sol M_w and narrower polydispersity encountered in miniemulsion based latexes could be due to a lower transfer between the particles.

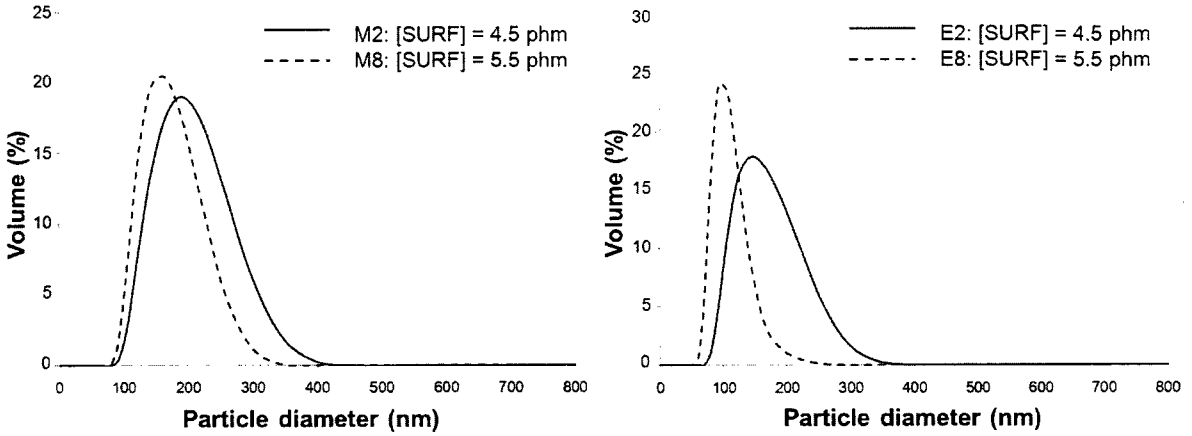

Figure 4.4. PSD for miniemulsion (above) and conventional emulsion (below) polymerization

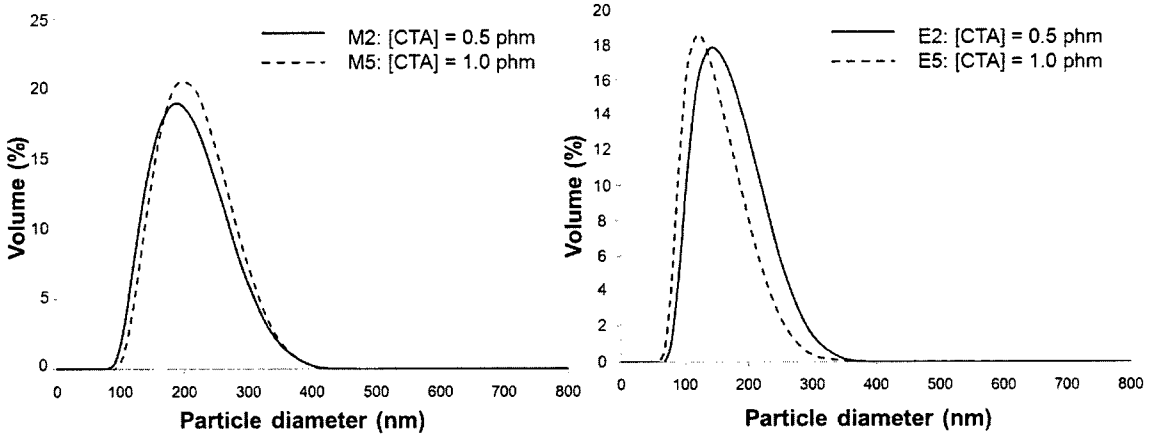

Figure 4.5. PSD for miniemulsion (above) and conventional emulsion (below) polymerization

The next step in the analysis was the evaluation of the PSA properties and how the different particle nucleation mechanisms had impacted the results. Table 4.3 shows results for the three main PSA properties for both the miniemulsion and conventional emulsion polymerizations. Some of these runs presented a cohesive failure characterized by transfer of adhesive material to the substrate. Only those latexes prepared with an EHA/MMA composition of 65/35 wt.% presented adhesive failure (no residue was left on the substrate) in both techniques. The reason for having a cohesive failure in this case is related to the T_g of the polymer, which could be low for the testing temperature, i.e., at room temperature (see

Table 4.3) or the gel content of those latexes was considerably low giving not sufficient cohesion to the adhesive.

Analyzing first loop tack, it was seen that it was primarily influenced by the EHA concentration, which was expected since it is known that changes in CC will modify the glass transition temperature, which in turn affects tack. Since a good PSA is related to adhesive failure, it was decided to look at the influence of the other factors using only those runs that presented adhesive failure.

Figure 4.7 shows the influence of M_n, M_w and gel content in loop tack for both polymerization techniques. It was found out that higher values of M_n and M_w resulted in higher loop tack. However, miniemulsion polymerization gave higher values compared to conventional emulsion polymerization, even though the latter produced higher M_w.

When gel content was considered to see if it was posing an effect in this property, it was established that there was not any relation between loop tack and gel content, which can be due in part to the low levels of gel content produced in this work, which may not be high enough to display this dependence. The other factor that could be influencing loop tack and creating this difference in the adhesive results is the PSD since conventional emulsion polymerization produced narrower distributions with smaller mean particle diameters compared to miniemulsion polymerization.

Peel strength, on the other hand, is known to be affected mainly by the modulus through the molecular weight. In this work, miniemulsion polymerization gave higher values of peel strength compared to conventional emulsion polymerization (see Figure 4.8), although it had lower or equivalent values of the M_w. The reason attributed to this lies in the amount of gel content, which was higher for miniemulsion based films than it was for conventional emulsion based films. A sample with a higher amount of gel content would present less polymer mobility, which would improve its cohesion and peel strength at these levels of gel content. It should also be mentioned that miniemulsion-based latexes exhibited narrower MWD than the conventional emulsion-based latexes, fact that could contribute to an improvement of the cohesive strength even though the former exhibited somewhat higher values of M_w.

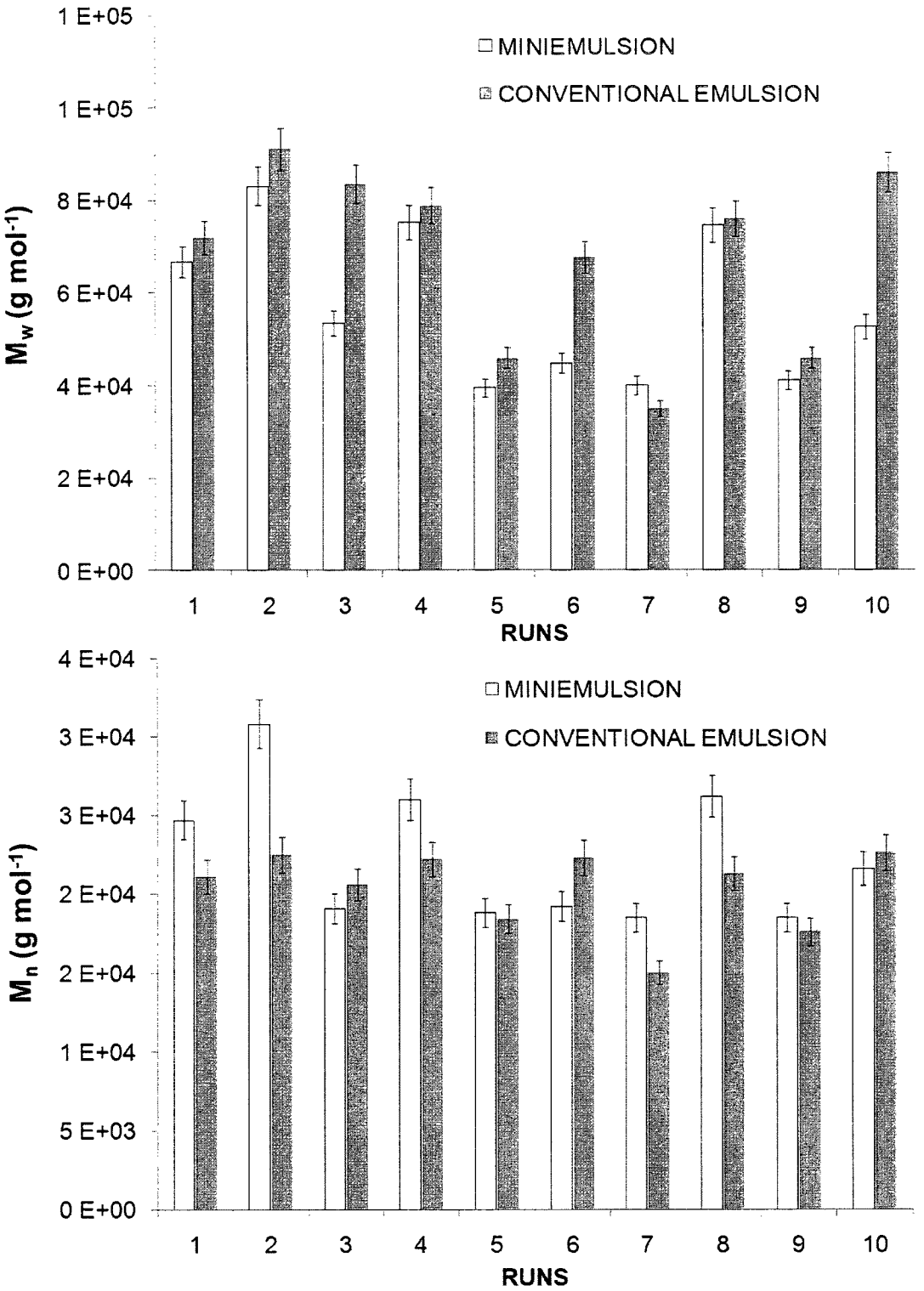

Figure 4.6. Weight- and number-average molecular weight results

Table 4.3. Loop tack, peel strength and shear strength results for miniemulsion (MP) and conventional emulsion polymerization (CEP).

	MP				CEP			
Run	Loop tack [N/cm^2]	Peel strength [N/10 mm]	Shear strength [min]	T_g [°C]	Loop tack [N/cm^2]	Peel strength [N/10 mm]	Shear strength [min]	T_g [°C]
1	0.49	0.189	0.47	-52	1.46	0.964	1.31	-52
2	2.48	3.133	3.15	-47	1.06	0.552	22.00	-52
3	0.50	0.213	0.39	-57	1.66	1.582	1.25	-57
4	0.70	0.279	0.74	-56	1.11	0.824	1.22	-57
5	1.39	5.545	3.59	-43	0.57	0.446	1.48	-51
6	0.35	0.156	0.16	-57	0.50	0.223	0.15	-55
7	1.45	1.066	1.38	-46	0.35	0.288	0.19	-65
8	1.81	5.299	5.12	-50	1.08	0.874	0.84	-52
9	0.32	0.173	0.13	-57	0.26	0.174	0.16	-60
10	0.86	0.638	1.70	-48	0.55	0.346	2.71	-52

Finally, both polymerization methods showed similar trends for shear strength (see Figure 4.9). In both cases, it can be seen that shear strength values increased with M_w and gel content since higher cohesive strength is attained when the polymer chains are not able to move as freely, which is possible when molecular weight is increased or under the presence of gel or a network. If considering only those films that presented adhesive failure, miniemulsion polymerization produced higher values of gel content compared to conventional emulsion polymerization. However, the resulting values of shear strength depended on the combination of both parameters, which does not allow for a straightforward conclusion regarding whether one technique is improved over the other. The presence of higher amounts of gel content in miniemulsion could be caused by a larger presence of intermolecular chain transfer to polymer which could lead to the formation of microgel structures within the particles.

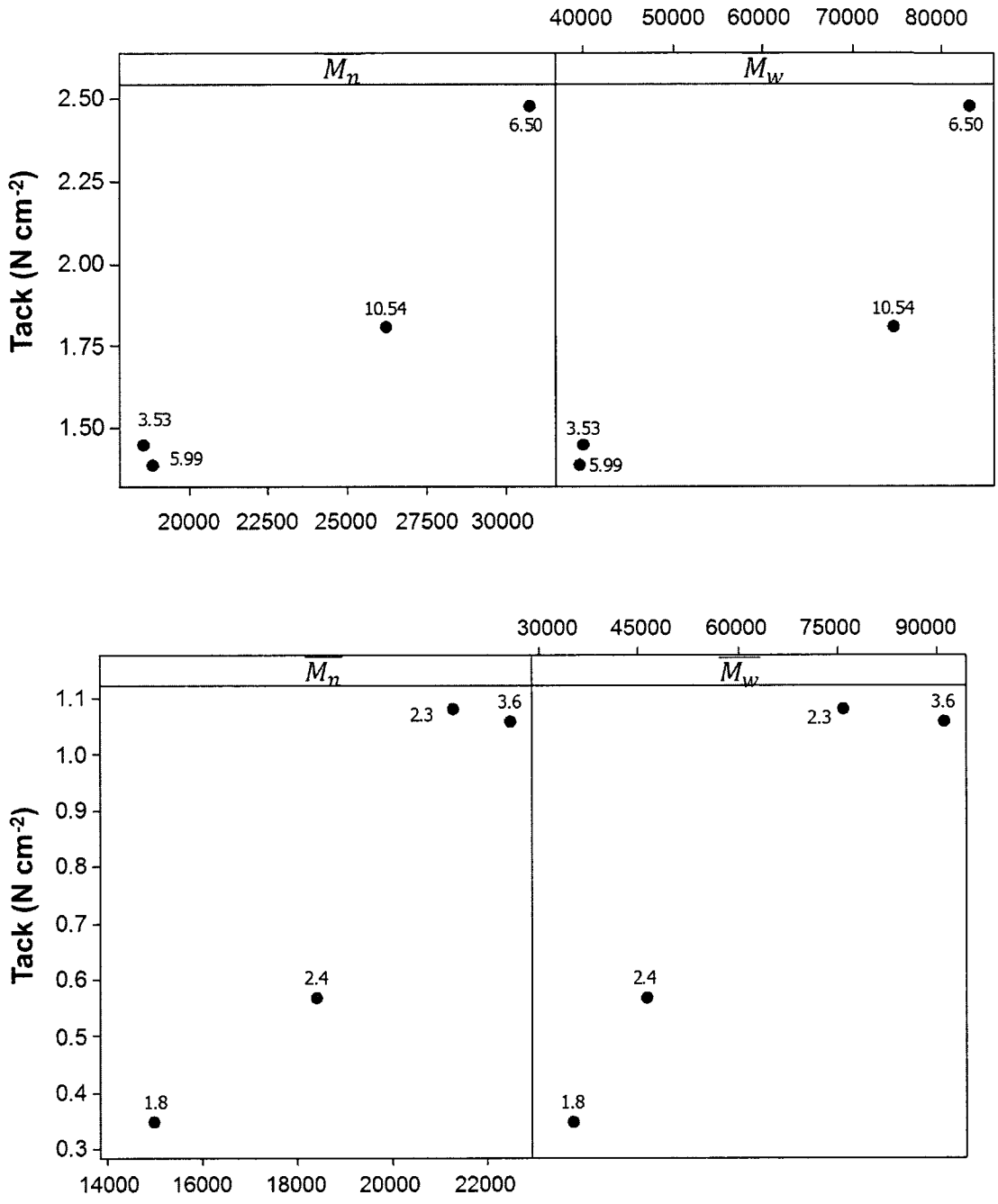

Figure 4.7. Scatterplot of loop tack vs. M_n and M_w for miniemulsion (upper graph) and conventional emulsion polymerization (bottom graph) (Adhesive failure only). Values next to points indicate gel fractions

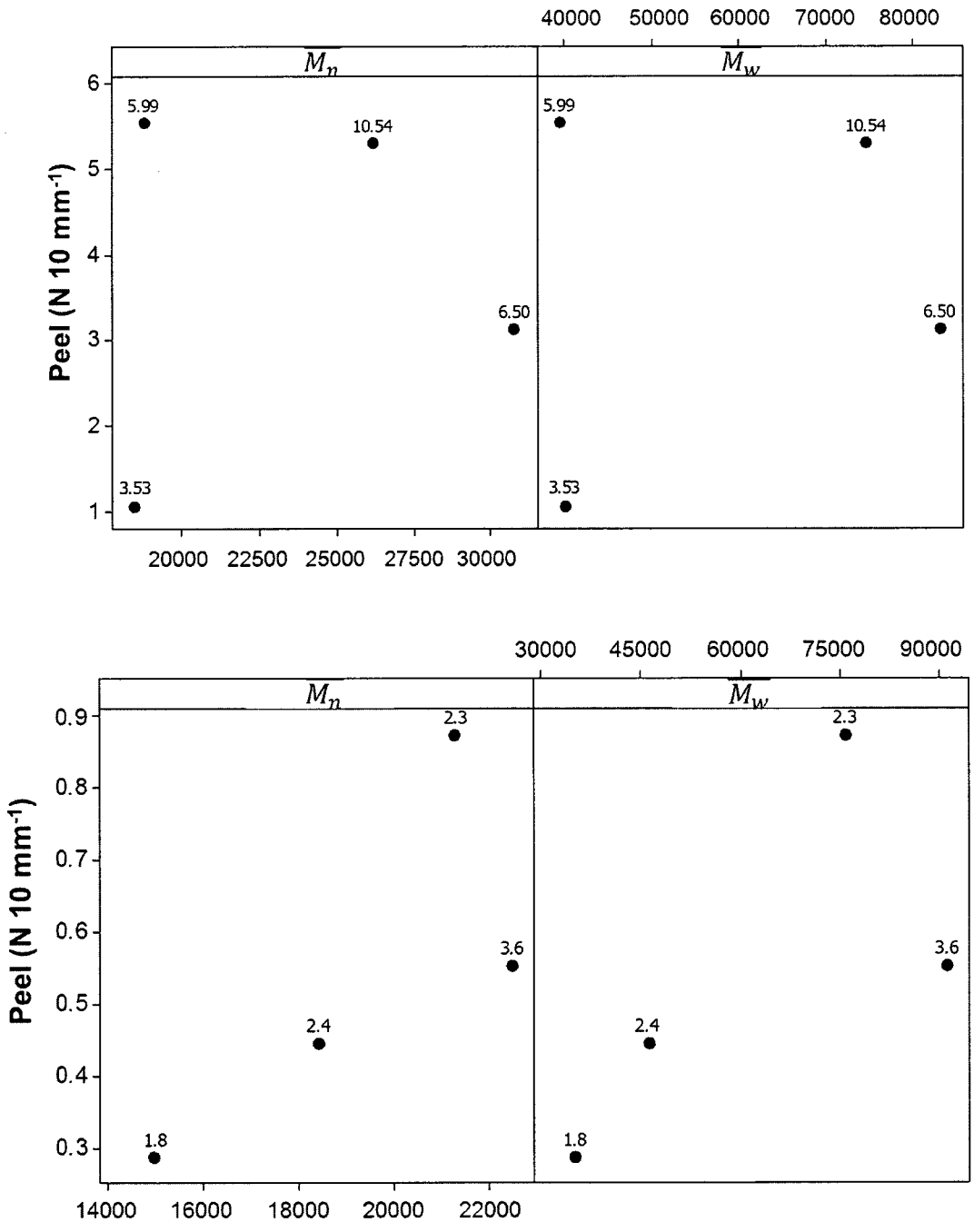

Figure 4.8. Scatter plot of peel strength vs. M_n and M_w for miniemulsion (upper graph) and conventional emulsion polymerization (bottom graph) (Adhesive failure only). Values next to points indicate gel fractions.

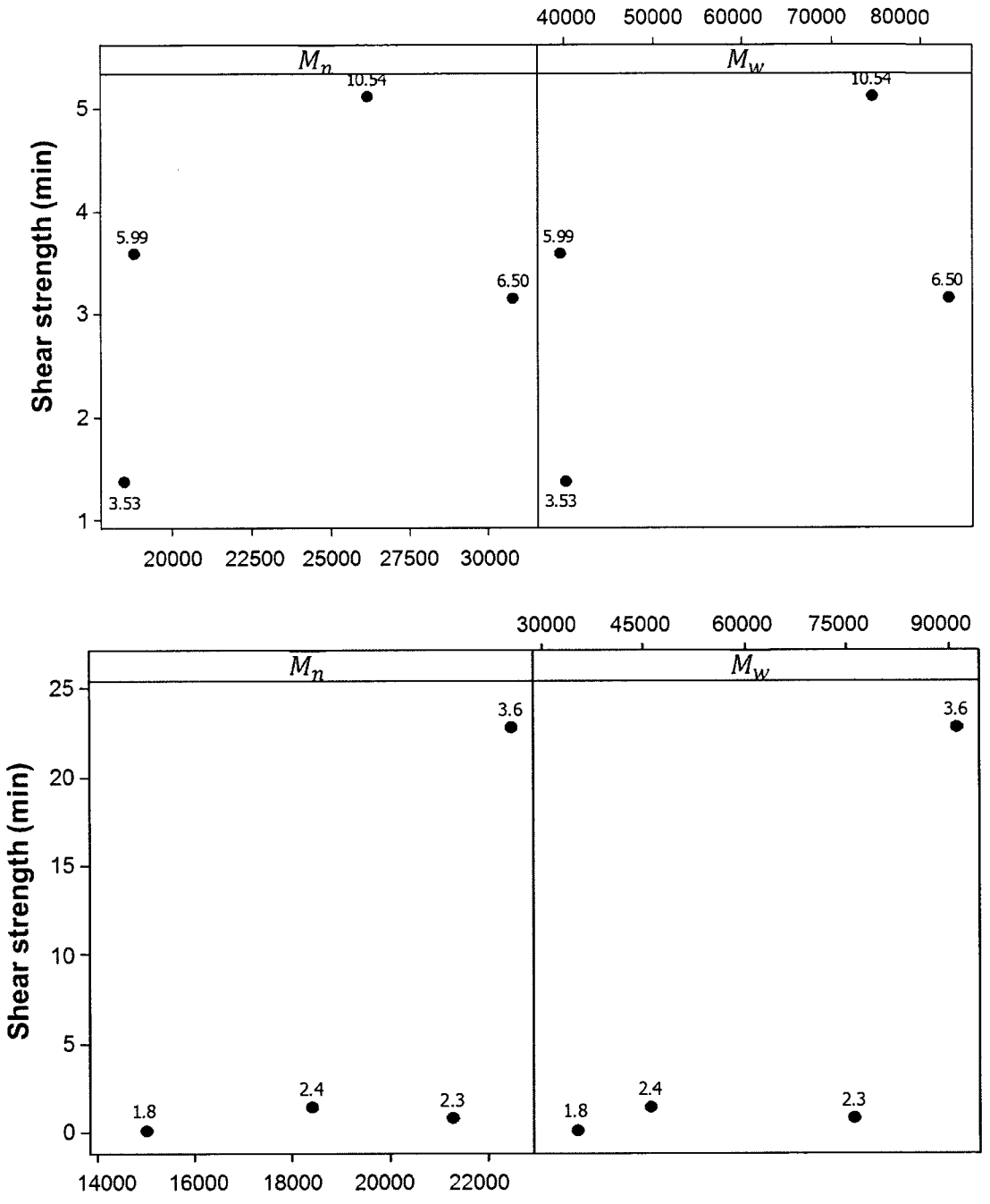

Figure 4.9. Scatterplot of shear strength vs. M_n and M_w for miniemulsion (upper graph) and conventional emulsion polymerization (bottom graph). Values next to points indicate gel fractions.

4.4 CONCLUSIONS

The aim of this study was to carry out a comparison between PSAs produced by miniemulsion and conventional emulsion polymerization. The analysis proved to be useful in discerning the range of properties for miniemulsion based latexes and to highlight the differences between PSAs created by two polymerization techniques with different nucleation mechanisms (droplet *vs.* micellar nucleation).It was shown that miniemulsion stability strongly relies on a judicious balance between the P_O and P_L and it should be kept in mind that if one wants to modify the size of the polymer particles (e.g., through a modification of TS or composition), the concentration of the hydrophobe, in this case ODA, must be modified to adjust this pressure balance and obtain a stable miniemulsion.

In general, miniemulsion based EHA/MMA adhesives yielded higher values of loop tack and peel strength to those produced by its counterpart. This can be attributed in part to the differences in the PSD, which were broader with higher mean particle diameter for those films cast from conventional emulsion-based latexes. It can be speculated that somewhat larger particles and a larger polydispersity contributed to higher loop tack values. Also, miniemulsion-based latexes showed narrower MWD, lower M_w and somewhat larger gel contents. These characteristics could be the reason for the higher values of peel strength exhibited by those films prepared by the miniemulsion polymerization technique. Finally, shear strength results were dependent on the amount of gel content, which was expected. However, gel content values of miniemulsion polymerization samples were generally higher when compared to those produced by conventional emulsion polymerization. The films cast from conventional emulsion-based latexes that displayed higher shear strength values also displayed a larger M_w than its counterpart, which could be well the reason for the higher cohesion in that film.

4.5 ACKNOWLEDGMENTS

The authors wish to gratefully acknowledge the financial support from the Natural Science and Engineering Research Council (NSERC) of Canada, the University of Ottawa International Creative Research Initiative and the National Council for Science and Technology of Mexico (CONACYT).

4.6 REFERENCES

Antonietti, M., Landfester, K., 2002. Polyreactions in miniemulsions. Progress in Polymer Science 27, 689-757.

Benedek, I., 2004. Pressure-Sensitive Adhesives and Applications, 2nd edition ed. Marcel Dekker, Inc., New York.

Brandrup, J., Immergut, E.H., Grulke, E.A., Abe, A., Bloch, D.R., 2005. Polymer Handbook, 4th edition ed. Wiley, New York.

Chu, F.X., Guillot, J., Guyot, A., 1998. Study of poly(St/BA/MAA) copolymer latexes with trimodal particle size distribution. Polymers for Advanced Technologies 9, 844-850.

Cognis, 2009. Disponil(R) A3065. Disponil_r_A_3065_E

Dow Chemical Company, 2009. Triton^{TM} X-405 (70%) Surfactant. Form No.119-01889-1107

Fortuny Heredia, M., 2002. Modélisation de Procédés pour la synthèse de latex multipopules.

Gilbert, R.G., 1995. Emulsion Polymerization: A Mechanistic Approach, Academic Press Inc., San Diego, CA.

Jovanovic, R., Dubé, M.A., 2001. Off-line monitoring of butyl acrylate and vinyl acetate homopolymerization and copolymerization in toluene. Journal of Applied Polymer Science 82, 2958-2977.

Jovanovic, R., Dubé, M.A., 2004. Emulsion-based pressure-sensitive adhesives: A review. Journal of Macromolecular Science: Polymer Reviews C44, 1-51.

Jovanovic, R., Ouzineb, K., McKenna, T.F., Dubé, M.A., 2004. Butyl acrylate/methyl methacrylate latexes: Adhesive properties. Macromolecular Symposia 206, 43-56.

Lathova, E., Lath, D., Pavlinec, J., 1993. The Behaviour of Poly (2-Ethylhexyl Acrylate) in Dilute-Solution-Viscosity Measurements. Polymer Bulletin 30, 713-718.

Ouzineb, K., Graillat, C., McKenna, T.F., 2004. Study of compartmentalization in the polymerization of miniemulsions of styrene and butyl methacrylate. Journal of Applied Polymer Science 91, 115-124.

Ouzineb, K., Hua, H., Jovanovic, R., Dubé, M.A., McKenna, T.F., 2003. Monomer compartmentalisation in miniemulsion polymerisation studied by infrared spectroscopy. Comptes Rendus Chimie 6, 1343-1349.

Pressure Sensitive Tape Council, 2004. Test Methods for Pressure Sensitive Adhesive Tapes, 14th ed. ed. Pressure Sensitive Tape Council, Northbrook, Illinois.

Satas, D., 1989. Handbook of Pressure Sensitive Adhesive Technology, 2nd ed. ed. Van Nostrand Reinhold, New York.

Schneider, M., Claverie, J., Graillat, C., McKenna, T.F., 2002. High solids content emulsions. I. A study of the influence of the particle size distribution and polymer concentration on viscosity. Journal of Applied Polymer Science 84, 1878-1896.

CHAPTER 5

Miniemulsion *versus* conventional emulsion polymerization for pressure-sensitive adhesives production

---

Fonseca, G.E., McKenna, T.F., Dubé, M.A.;
Chemical Engineering Science 65 (9), 2797 – 2810 (2010)

Miniemulsion vs. conventional emulsion polymerization for pressure-sensitive adhesives production

Gabriela E. Fonseca[1], Timothy F.L. McKenna[2], Marc A. Dubé[1*]

[1]Department of Chemical and Biological Engineering, University of Ottawa, 161 Louis Pasteur Pvt., Ottawa, Ontario, K1N 6N5, Canada; Fax 1(613)5625172; Email: Marc.Dube@uottawa.ca

[2]Department of Chemical Engineering, Queen's University, Kingston, Ontario, K7L 3P4, Canada

ABSTRACT

A systematic study of the production of poly (2-ethyl hexyl acrylate/methyl methacrylate/acrylic acid) pressure-sensitive adhesives (PSAs) via conventional emulsion and miniemulsion polymerization was carried out in order to discern and compare the influence of copolymer composition, chain transfer agent (CTA) and surfactant concentrations on the kinetics and microstructure of the resulting adhesive films. The results showed that miniemulsion polymerization proceeded solely under droplet nucleation for a certain set of initial reaction conditions. The miniemulsion-based latexes presented a polymer microstructure that was different to that found in latexes produced by conventional emulsion polymerization, as observed in the frequency master curves and PSA performance analysis. Batch miniemulsion polymerization was able to produce films with entanglement densities (M_w/M_e) from 2 up to 11, which were strongly correlated with loop tack, peel strength and shear strength. Conversely, under the same reaction conditions, batch conventional emulsion polymerization was only able to produce M_w/M_e ratios below 2.

Keywords: Miniemulsion polymerization, methyl methacrylate, 2-ethyl hexyl acrylate, pressure-sensitive adhesives

5.1 INTRODUCTION

Pressure-sensitive adhesives (PSA) are viscoelastic materials, which in their dry state are aggressively and permanently tacky at room temperature and can adhere to a variety of surfaces with the application of slight pressure (Pressure Sensitive Tape Council, 2004). PSAs are used in a wide number of applications that range from tapes and labels to drug-delivery patches (Benedek, 2006), markets that generate billions of dollars. Nevertheless, they also release volatile-organic compounds (VOCs) in large amounts since solvent-based polymerization remains one of the main PSA production technologies. Thus, a global need for greener technologies together with increasingly stringent environmental regulations has led the PSA industry to move to solvent-less technologies, such as water-based polymerization and hot-melt extrusion. Water-based technologies such as emulsion polymerization are now used in commercial PSA production.

However many waterborne PSAs still underperform their solvent-borne counterparts, which is one of the reasons why industry has not shifted entirely to this technology. This is mainly because PSAs are complex materials that are not yet fully understood, with molecular structures that are challenging to control and thus, to optimize and tailor. Their performance depends on a considerable number of factors (Jovanovic and Dubé, 2004) that can be divided into two main categories: those influencing the interfacial interaction between the PSA and the substrate, and those influencing the viscoelastic behaviour. The interfacial interaction component involves the wetting behaviour, surface tension and testing conditions. The viscoelastic component refers to all the nanoscopic and mesoscopic polymer characteristics that influence the bulk structure of a PSA. When a PSA is put to the test, it must first intimately wet the surface (bonding step), which would require a material that is able to flow under low stresses and secondly, it must be able to dissipate energy when it is being removed (debonding step) and not leave residue on the substrate, which would require a material that has high cohesive strength. The result is a set of conflicting properties where improvements to the adhesive component often result in a decrease in the cohesive component and *vice versa*.

The microstructure of a PSA can be modified through the copolymer composition, feeding policies, chain transfer agent and crosslinker concentrations, variations that are

reflected in the glass transition temperature (T_g) and molecular weight distributions (MWD) (Satas, 1989). It is well-known that modification of the copolymer composition has a substantial influence on PSA behaviour. For example, a homogeneous composition throughout the polymer particle versus a gradient composition can lead to different PSA performance properties (i.e., while maintaining the same ratio of the polymers involved (Aymonier et al., 2003)) as will the modification of the copolymer composition (i.e., changing the ratio of "hard" *versus* "soft" polymers) (Athawale and Rathi, 1995; Gower and Shanks, 2004b). The polymer microstructure reflected in the MWD, is also one of the most significant factors affecting PSA end-use properties. Studies have found that that the concentration of CTA has a strong influence on the static shear strength of the PSA (Gower and Shanks, 2004a), e.g., an increase in CTA level would decrease the gel fraction and in turn, decrease shear strength. It was also noted that at lower gel fractions, the influence of the gel content decreased and the influence of copolymer composition became predominant. Other studies have focused on the development of quantitative models constructed using partial least squares regression relating peel strength and shear strength of a butyl acrylate/styrene (BA/Sty)-based PSA with the complete MWD (Elizalde et al., 2002). The model proposed can predict the adhesive properties based on a given MWD and the MWD can then be produced by using a control strategy (Vicente et al., 2001).

Molecular weight between crosslink points (M_c), entanglement molecular weight (M_e) and gel content must also be considered when defining PSA performance (Tobing and Klein, 2001a). Shear strength, for example, is very much influenced by entanglement and crosslinking. These entanglements and crosslinks will increase viscosity which prevents flow and in turn, increases shear strength. There is a strong correlation between M_e and fibrillation: above certain values of M_e, adhesives will show fibril formation. Fibrillation is critical to having PSAs with high values of peel strength and tack (Zosel, 1998).

Particle size distribution (PSD) is another parameter that influences PSA performance. For commercial purposes, there is a need for latexes with high solids-contents and low viscosities. Several studies have looked into the production of these latexes through different approaches (Boutti et al., 2005; do Amaral et al., 2005; Greenwood et al., 1998; Schneider et al., 2002). They have succeeded in minimizing the viscosity of the dispersions using bimodal or multimodal PSDs. Nevertheless, to our knowledge, only two studies have

looked into the effect of PSD on the final PSA properties (do Amaral et al., 2005; Roberge and Dubé, 2006).

PSA performance is also greatly dependent on the viscoelastic properties of the polymer (Chang, 1997). According to the Dalhquist criterion (Chu, 1989), the storage modulus should be less than 3 x 10^6 dyne/cm^2 to ensure that the PSA has enough tack. As well, the flow region in a typical frequency master curve should not fall off too quickly to ensure an adequate level of shear strength (Satas, 1989). In fact, tack, peel strength and shear strength have been correlated qualitatively to the viscoelastic properties (storage modulus, loss modulus and tan δ) and to a lesser degree in a quantitative way (Du et al., 2004; Gower and Shanks, 2006; Jovanovic and Dubé, 2007; Plaut et al., 2001; Yarusso, 1999).

PSAs can be produced using conventional emulsion polymerization (CEP). In this study, the word *conventional* will be used to refer to the common water-based polymerization (a.k.a. macroemulsion polymerization). Typically, the main locus of the reaction in CEP is inside the polymer particles (i.e., the nucleated monomer-swollen micelles). Miniemulsion polymerization (MP) is another water-based polymerization. The difference between MP and CEP lies in the nucleation mechanism, i.e., MP is formulated to change the locus of particle nucleation from the monomer-swollen micelles to the monomer droplets. This is accomplished by using an appropriate surfactant and a highly hydrophobic compound, together with the use of high shear mixing. The hydrophobic compound decreases driving force for monomer desorption from the droplets. Thus delays Ostwald ripening, creating a "kinetically-stable" emulsion and producing so-called particle compartmentalization (Antonietti and Landfester, 2002; Schork et al., 2005), which refers to the maximization of intra- and extra-particle diffusion resistance. The combination of high shear mixing and surfactant serves to adjust and control the droplet size distribution.

Some of the benefits that MP offers over CEP are mainly the production of moderate solids content in one-step formulations (Ouzineb et al., 2005) as well as the incorporation or encapsulation of hydrophobic materials such as magnetic particles and dyes (for biological applications like genetic detection and cell labelling) as well as effective incorporation of pigments (Boehm et al., 2003; Landfester and Ramirez, 2003; Tronc et al., 2004).

Previous studies have compared MP and CEP in terms of their kinetics, PSD and number of particles (Aizpurua and Barandiaran, 1999). To our knowledge, the work by Jovanovic et al. (Jovanovic et al., 2004b) remains the only study that compared adhesive properties (i.e., tack, peel strength and shear strength) of PSAs prepared with MP and CEP. They reported on structure-property relationships between adhesive properties and, M_w and particle size. Their primary objective was to obtain a bimodal PSD and MWD using MP and CEP, and they presented the final properties of two latexes obtained with the two techniques but with different MWDs.

The aim of this study was two-fold. The first goal was to systematically compare the polymer microstructure and adhesive properties of latexes prepared by MP and CEP. A factorial design was used to determine the effect of chain transfer agent concentration (CTA), total surfactant concentration and monomer composition on the polymer properties (i.e., MWD, PSD and polymer composition) and then, how changes in these polymer properties affect the final PSA properties, i.e., tack, peel strength and shear strength. The second goal of this study was to quantify the range of properties that MP-based latexes offer within a given set of initial reaction conditions so that one can modify these conditions to suit particular product performance needs. It is important to state that before running the factorial design, the study focused on finding formulation conditions that would ensure the preparation of a kinetically-stable miniemulsion, in the sense that the polymerization loci remains mainly in the monomer droplets, which in turn would allow an unbiased comparison of the two techniques (Fonseca et al., 2008).

5.2 EXPERIMENTAL DETAILS

5.2.1 Materials

The monomers used for both MP and CEP reactions were 2-ethyl hexyl acrylate (EHA), methyl methacrylate (MMA) and acrylic acid (AA). Octadecyl acrylate (ODA) was used as the polymerizable hydrophobe and 1-dodecanethiol (DDM) as the CTA. All of these were reagent grade obtained from Sigma Aldrich. The ionic surfactant used was sodium dodecyl sulphate (SDS; GC grade, Sigma Aldrich) and the non-ionic surfactant was Disponil A3065 (Cognis Canada). Sodium bicarbonate ($NaHCO_3$) (Aldrich) was used as buffer.

Distilled deionized water (DDI H_2O) was used throughout the study. A 0.02 mol L^{-1} hydroquinone solution (HQ) was used as inhibitor to stop conversion in the samples. Tetrahydrofuran (THF) (HPLC grade, EMD Chemicals) was used in the molecular weight determination. Nitrogen gas (Linde Canada) was used to purge the reaction mixture from dissolved oxygen. All the reagents were used as supplied by the manufacturer.

5.2.2 Preparation of the miniemulsion and emulsion

ODA and the three monomers (EHA, MMA and AA) were charged to a 500 mL flask. If used, DDM as the CTA was added at this point. The aqueous phase was prepared separately in a 1 L flask. Disponil and SDS (surfactants) as well as Na_2HCO_3 were dissolved in DDI H_2O. Subsequently, the organic phase was added slowly to the aqueous solution while stirring. The stirring continued until the emulsion appeared as a milky solution (~30 min). The mixture was then sonicated in 100 mL batches using a Fisher Scientific Sonicator Model 550 for 4 min each batch at an output amplitude level of 9. At the end, the entire volume was combined and stirred.

In the case of the emulsion used for CEP, the preparation was the same as that for MP, except that the emulsion was not sonicated. The solids content for both formulations was kept at ~50 wt.-%. In some cases, solids content differences between the MP and CEP latexes existed due to the production of coagulum. These differences were compensated for by adjusting the film thickness when casting the latex. It should be noted that ODA was added to both MP and CEP recipes, although previous studies have not done so, due to the fact that it was considered merely as the hydrophobic compound. In this work, ODA was acting as a polymerizable hydrophobe and the possibility that this component might influence the PSA properties was considered, since it would certainly be incorporated into the polymer matrix and could possibly create bias in the comparison of the adhesive properties from each of the two techniques.

5.2.3 Polymerization procedure for MP and CEP

The polymerizations were performed in a 1.1 L Labmax™ automated stainless steel reactor (Mettler Toledo) equipped with a stirrer, condenser and three feed ports. The initial emulsion or miniemulsion was charged to the reactor and heated to 70°C with stirring. Nitrogen gas was bubbled through the reaction mixture to remove any dissolved oxygen. The

total volume of the initial emulsion or miniemulsion was ~700 to 800 mL. The temperature and stirring speed were automatically controlled at 70°C and 200 rpm, respectively. The reaction was initiated by charging the initiator solution when the reaction temperature was reached. The reaction time was 120 min. 2 mL samples were taken at different times along the reaction trajectory for conversion and D_p analysis. The sampling vials contained a few drops of an HQ solution and were immediately placed in an ice-bath to shortstop the reaction.

5.2.4 Characterization

Droplet and particle sizes were obtained using a Dynamic Light Scattering (DLS) instrument (Malvern NanoS Zetasizer) with a scattering angle of 176°. The reported diameter is an intensity-weighted average particle size, a.k.a. z-average, comprised of 3 measurements analyzed in 10 runs of 30 s each. The reported polydispersity index values (PDI) are those given by the instrument and are not conventional PDI values. They are referred to as Malvern Polydispersity Index (M-PI) throughout this work to avoid any misunderstanding. A value closer to 0.01 indicates a narrower distribution. The droplet diameter (D_d) was measured immediately after the preparation of the miniemulsion.

Molecular weight averages and distributions were measured with a Waters Gel Permeation Chromatography (GPC) instrument equipped with a Differential Refractive Index detector, a manual injector and three Waters Styragel columns (HR6, HR4 and HR3) in series. The flow rate was set at 0.3 mL/min and the measurements were conducted at 37°C. The data were analyzed using Empower 2 software from Waters. The calibration curve included a set of 12 standards (EasiCal from Polymer Laboratories) with a range of 162 to 6,035,000 g/mol. The values of the Mark-Houwink constants, K and alpha, used for EHA were 1.24 $x10^{-4}$ dL/g and 0.67 while those for MMA were 1.28 $x10^{-4}$ dL/g and 0.69, respectively (Hua and Dubé, 2001; Lathova et al., 1993).

Monomer conversion was measured using a standard gravimetric method and was based on dried polymer weight (see Chapter 2 for a more detailed account of monomer conversion estimation). Individual monomer conversions were calculated using the total conversion obtained by gravimetry and copolymer compositions obtained by ^{1}H-NMR spectroscopy.

Gel fraction analysis was performed on the final sample for each run using a modification to the method described by Tobing and Klein (Tobing and Klein, 2001a). Approximately 200 mg of dry polymer was placed in a pouch formed by two 25 mm-diameter PTFE membranes with a pore size of 0.2 μm. The membranes were heat sealed. The weight of the pouch plus polymer was recorded and the pouch was placed in 50 to 60 mL of THF. The jars were placed in a shaker for at least 48 h after which time the pouches were removed and allowed to dry. The gel fraction was calculated from the difference between the final and initial weight of the polymer. Each analysis was performed in duplicate and the results reported are the averages.

Copolymer compositions were determined using ^{1}H-NMR spectroscopy on a Bruker AVANCE 400 spectrometer. The relative amounts of monomer bound in the copolymer were estimated from the areas corresponding to the absorption peaks of EHA and MMA at 3.90 and 3.60 ppm, respectively. In the case of EHA, the shift corresponded to the protons of the OCH_2 group while in the case of MMA, it corresponded to the protons of the OCH_3 group (Aymonier et al., 2001; Patnaik et al., 1992).

The glass transition temperature (T_g) was determined using a Differential Scanning Calorimeter (DSC) Model Q1000 from TA Instruments. The analysis was performed using a modulated DSC method with a modulation amplitude of ± 1°C every 60 s. The sample was cooled to -80°C followed by heating at 2°C/min. The T_g was calculated from the inflection point in the Reversed Heat Flow curve using the software provided. If the transition was broad and the results ambiguous, the T_g was taken as the peak in the curve of the derivative heat capacity (Stubbs and Sundberg, 2005).

Tack, peel strength and shear strength were measured according to the Pressure Sensitive Tape Council standards PSTC-6, PSTC-1 and PSTC-7, respectively (Pressure Sensitive Tape Council, 2004). Details of the procedure are also given in Jovanovic and Dubé (Jovanovic et al., 2004a).

For the dynamic mechanical analysis, 10 to 12 g of latex was placed in a 5 x 5 cm plate lined with silicone release paper. The latex was left to dry in a fume hood for 2 – 3 days and then transferred to a vacuum oven at 35°C for further drying for 3 – 5 days. A film of 1.5 to 2 mm was obtained after the drying process. The samples were analyzed using a

Rheometrics RDA III and 25 mm parallel plate geometry. First, for the construction of the master curves, the samples were subjected to isothermal frequency sweeps. The sweep mode was logarithmic with frequencies in a range from 0.1591 Hz to 50 Hz with 20 points per decade in a range of temperatures from -60°C to 80°C with increments of 10°C. The master-curves were built using TA Orchestrator software v.7.2 with manual shifting of the individual curves. A second analysis corresponded to temperature sweeps performed at a frequency of 1.591 Hz from a temperature range from -40°C to 120°C.

5.2.5 Design of experiments

Two 2^3 factorial designs were used to discern the effect of copolymer composition, and CTA and surfactant concentrations in miniemulsion and conventional emulsion polymerization: one factorial design for each polymerization technique for a total of 16 runs (8 runs for miniemulsion and 8 runs for conventional emulsion polymerization). 2 centre points were added to each factorial design to check for process stability and possible curvature for a total of 20 runs in the first stage (c.f. Table 5.1). An additional CTA level (0.1 phm as the lower level and 0.3 phm as center point) was further included to better observe the effect of MWD and other molecular parameters. Statistical analysis was performed with Minitab® software version 14.

Table 5.1: MP and CEP factorial design

Factor	Levels		
EHA/MMA [wt.-%]	65/35	75/25[b]	85/15
CTA [phm]	0.50	0.75[b]	1.00
Surfactant [phm]	4.50	5.00	5.50

[a] For all experiments: [APS] = 0.30 phm, [$NaHCO_3$] = 0.15 phm, [AA] = 2.00 phm, [ODA] = 4.00 phm; T_r = 70°C, Stirring speed = 200 rpm
[b] Reaction levels for the center point runs.

5.3 RESULTS AND DISCUSSION

To find an adequate surfactant mixture that would provide a D_p of ~200 nm with a narrow DSD, a screening design was used. It was found that a mixed surfactant system using Disponil and SDS at a ratio of 93/7 mol.-% provided excellent droplet stability and

maximized droplet nucleation. More details on the screening design can be found in Fonseca et al. (2008).

In the present study, droplet nucleation was evaluated through the evolution of the number of polymer particles (N_p), i.e., the difference between the final N_p and the initial number of monomer droplets (N_d). A ratio of N_p/N_d of approximately one would indicate that most of the monomer droplets were preserved and it could be assumed that the polymerization proceeded by droplet nucleation. It is acknowledged that an ideal droplet nucleation (i.e., $N_p/N_d=1$) is indeed improbable and a ratio between 0.85 and 1.15 was considered sufficient to ensure that most of the droplets had become polymer particles.

The factorial designs for MP and CEP and their results are shown in Tables 5.2 and 5.3, respectively. In the case of MP, an additional CTA concentration of 0.1 phm is shown in Table 2 (runs M11 to M15). This additional CTA concentration was also tested in CEP but unfortunately, coagulation in the CEP runs was such that it was not possible to characterize the latexes (~50% of the initial polymer mass coagulated in the corresponding CEP runs). The additional CTA level was included in the design after the results of the initial factorial design had been obtained (i.e., runs M1 to M9), which indicated that the CTA concentration range used could be masking interactions between the reaction conditions and polymer properties.

It was observed in the results that a number of the MP runs had fluctuations in the evolution of N_p/N_d that could be considered outside of the optimum range (i.e., runs M3, M9, M12 and M13). It is likely that secondary nucleation had occurred in those runs, creating new particles. It appears that MP can proceed by a droplet nucleation mechanism under a strict set of conditions and this must be considered when making comparisons. For example, in the present study, the surfactant concentration was varied, since it was expected to affect D_p and PSD, and in turn, the resulting adhesive properties. However, the concentration of ODA (which determines the osmotic pressure (P_O)) was not varied. As a consequence, the Laplace pressure (P_L) likely increased for the levels with higher surfactant concentrations (and hence smaller D_d), but the P_O remained the same. As a consequence, some formulations presented conditions where a miniemulsion would be able to reach a kinetically-stable state and others where the conditions would not be achieved (Landfester, 2001).

In order to quantify the fluctuations in the N_p/N_d for each one of the MP runs, a normalized standard deviation was calculated for each run using Equation (1):

$$Normalized\ standard\ deviation = \frac{\sqrt{\frac{1}{N}\Sigma_{i=0}^{N}(x-y)^2}}{y} \quad (1)$$

Table 5.2. Experimental design and final polymer properties for Miniemulsion Polymerization

Run	Monomer feed composition	CTA	Surfactant	X_{max}	T_g	M_w x10^{-3}	M_n x10^{-3}	N_p/N_d	D_p[a]
	EHA/MMA wt.-%	phm	phm	wt.fr.	°C	g/mol	g/mol		nm
M1	75/25	0.75	5.0	0.9897	- 52	66.7	24.7	1.18	177 (0.05)
M2	65/35	0.50	4.5	0.9512	- 47	83.1	30.8	1.08	182 (0.04)
M3	85/15	0.50	5.5	0.9937	- 57	53.5	19.1	1.31	170 (0.04)
M4	85/15	0.50	4.5	0.9970	- 55	75.3	26.0	1.10	197 (0.05)
M5	65/35	1.00	4.5	0.9777	- 43	39.5	18.8	0.90	190 (0.02)
M6	85/15	1.00	4.5	0.9854	- 56	44.8	19.2	1.07	196 (0.05)
M7	65/35	1.00	5.5	0.9314	- 45	40.0	18.5	1.14	162 (0.03)
M8	65/35	0.50	5.5	0.9297	- 50	74.6	26.2	1.16	160 (0.03)
M9	85/15	1.00	5.5	0.9793	- 56	41.0	18.5	1.22	178 (0.06)
M11	75/25	0.30	5.0	0.9622	- 50	113.0	31.0	0.91	204 (0.07)
M12	65/35	0.10	4.5	0.9699	- 48	293.0	78.7	0.80	224 (0.03)
M13	85/15	0.10	5.5	0.9917	- 47	280.0	49.8	1.27	181 (0.04)
M14	85/15	0.10	4.5	0.9894	- 55	313.5	58.2	0.87	214 (0.02)
M15	65/35	0.10	5.5	0.9391	- 49	269.5	75.7	0.95	187 (0.05)

[a]The values in parentheses represent the polydispersity indices given by the DLS instrument Malvern NanoS. See experimental details for further information

where N is the number of samples taken in a MP run, x is the N_p/N_d obtained for each one of those samples taken along a reaction and y would be equal to one since an ideal case would not present fluctuations of the N_p with respect to the N_d. The results showed that the normalized standard deviation was strongly influenced by the surfactant concentration as can be observed in Figure 5.1. The runs polymerized at the higher surfactant concentration presented large fluctuations, especially at the beginning of the reaction leading to large values of normalized standard deviation. Higher surfactant concentrations are used to decrease the droplet diameter and in turn, the final particle diameter but care should be exercised in doing so since it could also lead to large increases in the N_p with respect to the N_d. These fluctuations must be taken into consideration when comparing MP latexes to their CEP counterparts.

Differences in conversion and R_p between MP and CEP have been comprehensively studied in the past for other polymerization systems (Asua, 2002; Schork et al., 2005) and it must be pointed out that the current study is not a comprehensive investigation of the kinetic differences between the two polymerization techniques; however, some differences must be highlighted.

Table 5.3. Experimental design and final polymer properties for Conventional Emulsion Polymerization

Run	Monomer feed composition	CTA	Surfactant	Conversion	T_g	M_w x10^{-3}	M_n x10^{-3}	D_p[a]
	EHA/MMA wt.-%	phm	phm	wt.fr.	°C	g/mol	g/mol	nm
E1	75/25	0.75	5.0	0.9877	- 53	72.0	21.1	185 (0.04)
E2	65/35	0.50	4.5	0.9665	- 52	91.1	22.5	153 (0.06)
E3	85/15	0.50	5.5	0.9782	- 58	83.5	20.6	138 (0.02)
E4	85/15	0.50	4.5	0.9680	- 58	78.8	22.2	155 (0.02)
E5	65/35	1.00	4.5	0.9428	-52	46.0	18.4	138 (0.06)
E6	85/15	1.00	4.5	0.9670	- 55	67.6	22.3	150 (0.05)
E7	65/35	1.00	5.5	0.9226	- 66	35.0	15.0	100 (0.06)
E8	65/35	0.50	5.5	0.9364	- 52	76.0	21.3	124 (0.08)
E9	85/15	1.00	5.5	0.9670	- 61	46.0	17.6	124 (0.08)

[a]The values in parentheses represent polydispersity index given by the DLS instrument Malvern NanoS

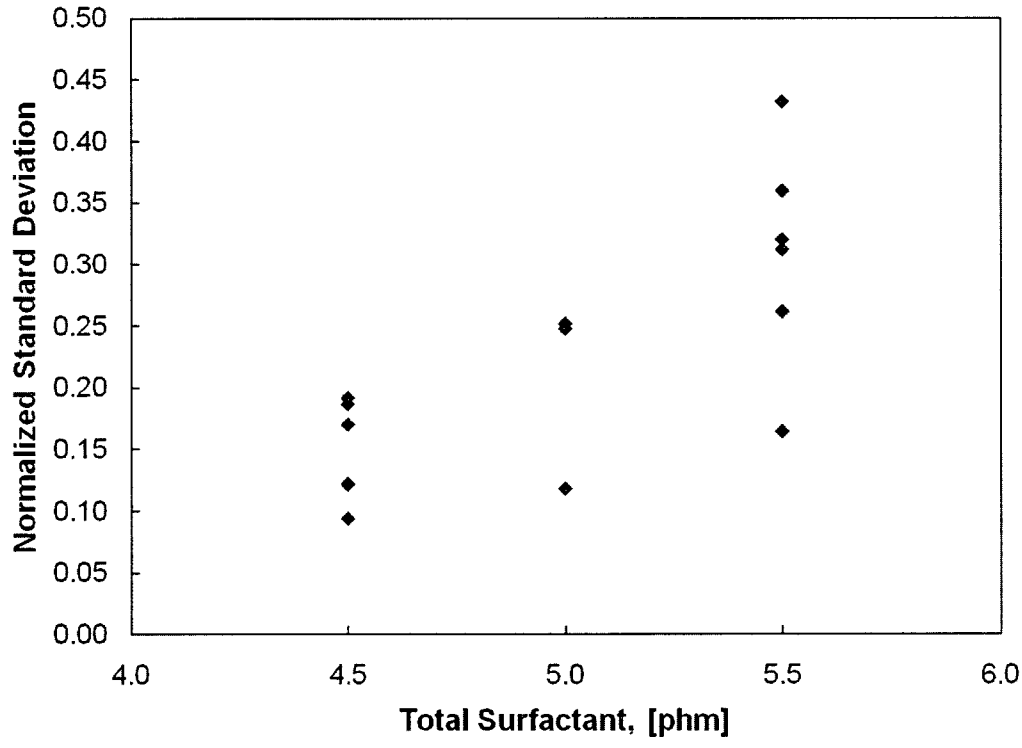

Figure 5.1. Normalized standard deviation of the ratio N_p/N_d for the miniemulsion polymerizations

The analysis showed that the surfactant concentration constituted the most important effect in the CEP runs. This result was not surprising since the surfactant concentration strongly influences the N_p, which in turn influences conversion and the rate of polymerization (R_p). The CTA concentration had a smaller influence on the conversion while the copolymer composition had no significant influence. However, we observed that the three factors influenced MP kinetics differently. In the first place, the surfactant concentration did not have as strong an effect on the conversion within the range of concentrations studied, which was expected due to the fact that MP proceeds under droplet nucleation conditions. Figure 5.2a shows the conversion curves for reactions 5 and 7 carried out at surfactant concentrations of 4.5 phm and 5.5 phm, respectively, in both MP (label M) and CEP (label E). This pair was chosen because run M5 had the lowest normalized standard deviation of all the MP runs. Run M7 was prepared with the same copolymer composition and CTA concentration differing only in the surfactant concentration. As can be observed in Figure 5.2a, during the first 60 min of reaction, there is a significant difference between run E5 and E7 when increasing the surfactant concentration. However, the same surfactant concentration increase does not result in different conversion trajectories for the case of MP. The trend observed in Figure 5.2a for the pair run 5/run 7 was also observed in the other reactions (not shown here) except for runs M3 and M9. These latter two runs presented the highest normalized standard deviation, where it was evident that the MP runs proceeded not only under droplet nucleation conditions, but likely via a combination of droplet and homogeneous nucleation.

Copolymer composition, on the other hand, did present an influence on the conversion of MP, i.e., the higher the amount of EHA (and lower MMA), the higher was the conversion at a certain point in time (see Figure 5.2b), which is due to the fact that the propagation rate coefficient for EHA is an order of magnitude higher than it is for MMA (Plessis et al., 2001b). Finally, changes in the CTA concentration did not produce any observable differences in the kinetic behaviour.

In order to get a better idea of the differences between CEP and MP, the fractional conversion of the recipe with the lowest normalized standard deviation (i.e., M5) was plotted and compared to its CEP counterpart (i.e., E5) in Figure 5.3. The lowest normalized standard

deviation would mean that a lower number of new particles were generated through secondary nucleation and a closer scenario to all the droplets being nucleated. One can see in Figure 5.3 that MMA was rapidly polymerized and preferentially incorporated in the copolymer chain in both CEP and MP compared to EHA, which was expected due to their reactivity ratios (r_{EHA} = 0.426 and r_{MMA} = 1.729 as recalculated using the error-in-variables method (Dubé et al., 1991) from literature data (Patnaik et al., 1992)). From Figure 5.3, one can conclude that although MP presented slower reaction rates, it followed the same compositional drift as in a batch CEP.

The kinetic results showed that care should be exercised in the following sections when making comparisons of miniemulsion– and conventional emulsion–based latexes since the variations (mainly in the surfactant concentration) inherent in a factorial design led to polymerizations that proceeded under a combination of nucleation mechanisms.

5.3.1 Polymer microstructure

M_w and MWD are two of the most important molecular parameters affecting PSA behaviour. The analysis showed that the CTA concentration represented the only significant influence for both techniques, i.e., the surfactant concentration and copolymer composition did not have a significant effect in the MWD. The range of M_w attained was similar for both techniques in the range of CTA concentration from 0.5 to 1.0 phm. The lower range of CTA concentration studied (i.e., 0.1 to 0.3 phm) led to M_w's in the range of 113,000 to 313,000 g/mol in the case of MP. Unfortunately, the latexes obtained by CEP presented large amounts of coagulum (more than 50 wt.-% of the initial mass) and M_w could not be reported. It should be noted that for the same CTA concentration level of 0.1 phm, all of the miniemulsion-based latexes were stable and the amount of coagulation obtained after filtering the latex at this CTA concentration was ~2 wt.-%.

There were a number of differences in the MWD between the latexes produced by CEP and MP. For example, MP produced latexes with narrower MWDs and lower M_w's compared to CEP. Figure 5.4a shows the MWD of the latexes prepared with a copolymer composition of 85/15 wt.-% EHA/MMA and 4.5 phm of surfactant concentration (the same trend was observed with a copolymer composition of 65/35 wt.-% EHA/MMA at the same surfactant concentration). It was observed that in the case of MP, decreasing the CTA

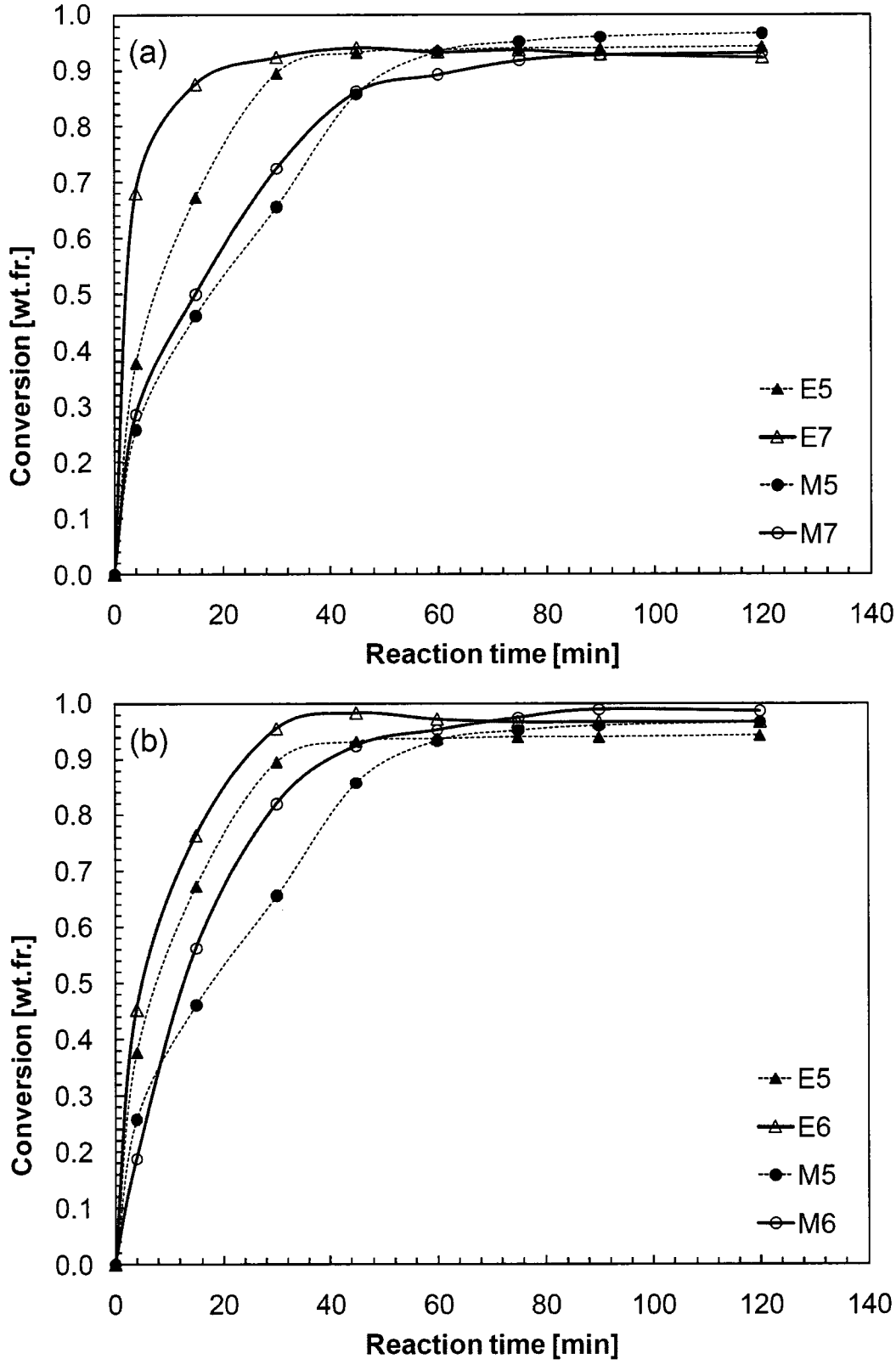

Figure 5.2. Overall conversion curves of polymerization runs a) M5 and M7 (different surfactant concentration) and b) M5 and M6 (different copolymer composition)

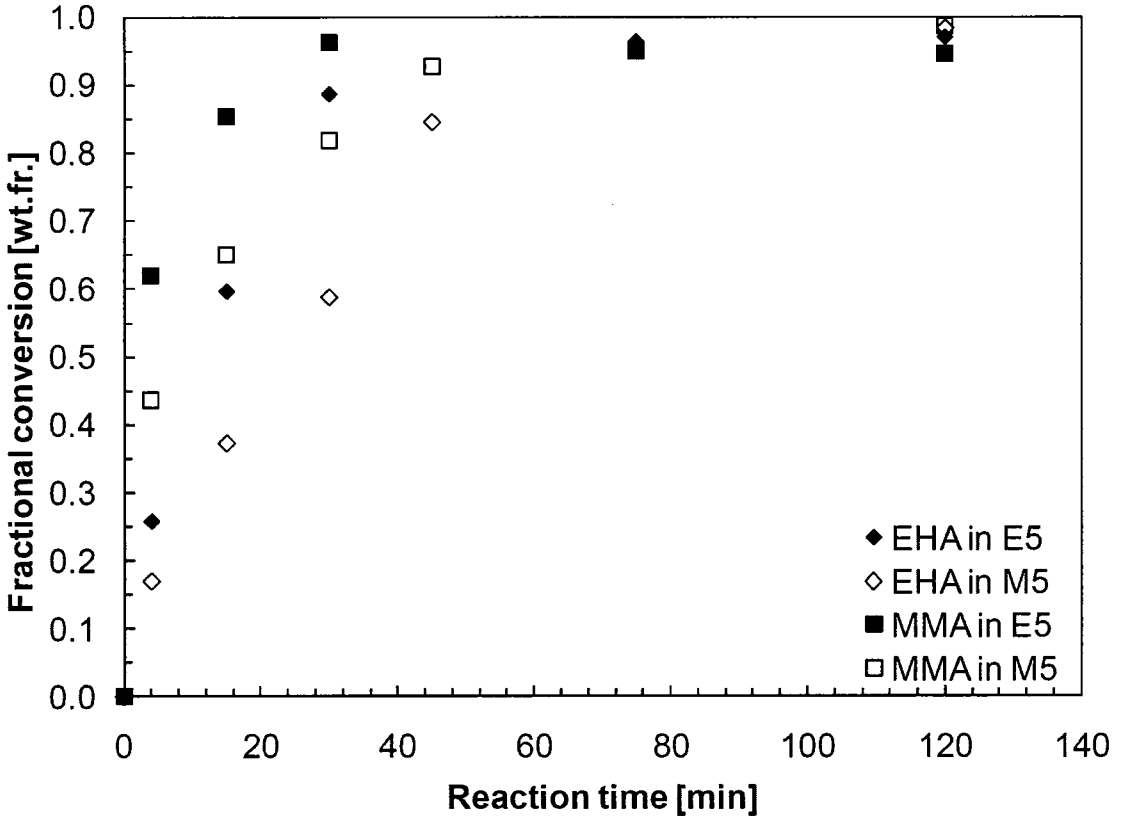

Figure 5.3. Fractional conversion versus reaction time for run E5 and M5. EHA (diamonds) and MMA (squares) in CEP (filled symbols) and MP (empty symbols)

concentration from 1.0 phm to 0.5 phm changed the M_w from 45,000 to 75,000 g/mol while the same variation in the CTA concentration in the case of the CEP runs changed the M_w from 67,000 to 78,800 g/mol. This is, the increase in the M_w is three times higher in the case of MP. This can be partly attributed to the different nucleation mechanisms and the fact that the CEP created three times more particles compared to MP, which evidently resulted in different D_p's. Another aspect that should be considered is the fact that the monomer concentration in the particles is intrinsically different at the beginning of the polymerization due to their respective nucleation mechanism, i.e., a higher monomer concentration (in this case, MP) leads to a lower probability of intermolecular and intramolecular chain transfer or chain transfer to polymer, which in turn could lead to lower M_w for MP runs (Plessis et al., 2000; Plessis et al., 2001a).

Figure 5.4b shows the MWD of latexes prepared with the same copolymer composition of 85/15 wt.-% EHA/MMA but with a surfactant concentration of 5.5 phm. As can be observed in this case, the change in CTA concentration increased the M_w from 41,000

to 53,000 g/mol with a polydispersity of ~2.5 for MP-based latexes while for CEP-based latexes, a change in CTA concentration from 1.0 to 0.5 phm increased the M_w from 46,000 to 83,000 g/mol with a much broader polydispersity of 4.0 compared to its miniemulsion counterpart. The molecular weight between entanglements, M_e, is another important parameter that must be considered in the evaluation of PSA performance. A material with no or very few entanglements will not present adequate PSA behaviour. It has been suggested that a polymer with entanglement lengths above 1 to 1.5 $x10^4$ g/mol would be sufficient for the formation of fibrils (Zosel, 1998). However, a high entanglement length is not sufficient *per se* to produce adequate PSA behaviour and often the ratio M_w/M_e is used to indicate the material's entanglement density. A minimum ratio of ~2 is suggested to indicate that polymer chains would entangle enough to provide sufficient cohesive strength so that the material could be used as a PSA (Tobing and Klein, 2000). In other words, a material with enough entanglement length but low M_w would not form a satisfactory microstructure nor would a material with high M_w but very few entanglements. In order to obtain an appropriate network, the M_w would have to be at least twice as large as M_e.

M_e for MP and CEP latexes were calculated using Equation (2) shown below (Tobing and Klein, 2000):

$$M_e = \frac{\rho_P RT}{G_n^0} \tag{2}$$

where ρ_P is the density of the polymer estimated as 1.1 g/cm^3, T is the temperature of the onset of the rubbery plateau, R is the gas constant and G_n^0 is the rubbery plateau modulus. G_n^0 can be determined from isochronal temperature sweeps obtained by DMA analysis. If the rubbery plateau was not clearly identified, M_e was estimated using the plasticizer model (Tobing and Klein, 2001a) (c.f. Equation 3):

$$M_{e,polydisperse} = \frac{M_{e,monodisperse}}{\varphi^{2.3}} \tag{3}$$

where $M_{e,monodisperse}$ and $M_{e,polydisperse}$ are the entanglement molecular weight for a monodisperse and a polydisperse sample, respectively; and φ is the weight fraction of polymer species with molecular weight higher than $M_{e,monodisperse}$. φ can be obtained from the GPC cumulative MWD. $M_{e,monodisperse}$ for EHA and MMA were taken as 37,432 g/mol (Tobing and Klein, 2001a) and 10,013 g/mol (Fetters et al., 1994), respectively. The amount

of each monomer in the copolymer was used to obtain an average $M_{e,monodisperse}$ to be used in Equation (3). It was found that for latexes M1 to M9 in both MP and CEP (with the exception of latex M2), the rubbery plateau region in the DMA plot was relatively short and thus, the M_e was estimated following the plasticizer model. For the remaining latexes (i.e., M2 and M12 to M15), the rubbery plateau modulus was obtained from the DMA plot.

Table 5.4 shows the results of M_e and M_w/M_e calculated for the CEP and MP polymers. It can be seen that the latexes M2, M12, M13, M14 and M15 presented values of M_w/M_e above a value of 2, which suggests that the PSA cast from these latexes presented a network with enough entanglement density to provide a good basis for adequate PSA performance. However, for those runs prepared with a CTA concentration higher than 0.5 phm (i.e., with a M_w below ~80,000 g/mol and very large M_e's), M_w/M_e became very small, an indication of a poor entanglement density. Some of the latexes actually gave values of M_w/M_e as small as 0.1 suggesting that they completely lacked an entangled structure.

It is interesting to note that there appeared to be a suitable range of M_e that would provide an adequate microstructure. All of the M_e values obtained in this study were above 10,000 g/mol; however, those latexes with an M_e between 10,000 and 40,000 g/mol produced networks with entanglement densities above 2 making the network "entangled enough" to create fibrils and give adequate PSA properties. However, those latexes with a M_e above 70,000 g/mol created entanglement densities with M_w/M_e values below 2, which meant that these networks would be too loose to have enough cohesion and form fibrils and this most certainly would have a negative impact on the PSA properties.

Comparing the two techniques, it is noted that some of the MP-based latexes presented networks with larger values of M_w/M_e than their CEP counterparts. For example, looking at the latexes M2 and E2, the value of M_e obtained in MP is half of that obtained in CEP with a M_w/M_e of ~2.4, which means that MP produced polymer chains that were able to inter-diffuse and entangle with other polymer chains. The CEP method, on the other hand, produced a slightly higher M_w with a broader polydispersity and due to the fact its M_e was higher than the M_e of M2, we can see that CEP produced a looser network. The question that arises is what factors are influencing M_e in each of these two techniques that lead to two different microstructures.

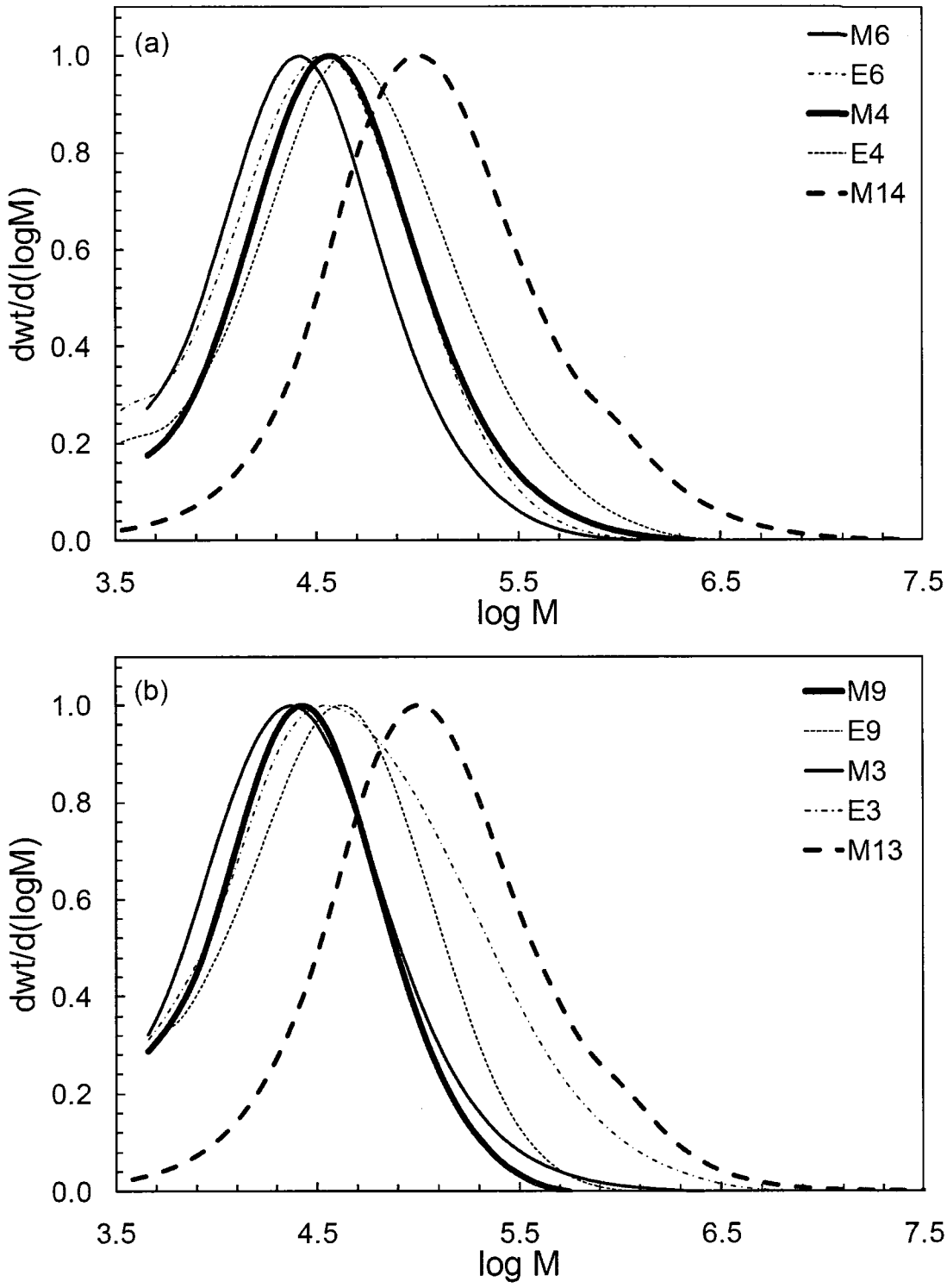

Figure 5.4. MWD for runs with a 85/15 wt.-% EHA/MMA copolymer composition with a) 4.5 phm of surfactant concentration and b) 5.5 phm of surfactant concentration

Table 5.4. Entanglement molecular weight (M_e) and M_w/M_e for MP and CEP latexes

Run	$M_e \times 10^{-3}$	M_w/M_e	Run	$M_e \times 10^{-3}$	M_w/M_e
	g/mol			g/mol	
M1	121	0.50	E1	146	0.50
M2	34	2.40	E2	90	1.00
M3	251	0.20	E3	235	0.35
M4	126	0.60	E4	174	0.45
M5	148	0.30	E5	117	0.40
M6	320	0.15	E6	158	0.40
M7	160	0.25	E7	304	0.10
M8	74	1.00	E8	98	0.80
M9	378	0.10	E9	487	0.10
M12	26	11.10			
M13	38	7.40			
M14	39	8.15			
M15	25	10.50			

On one hand, the M_e in CEP was influenced by the three factors studied, i.e., copolymer composition, surfactant and CTA concentration with surfactant concentration having the largest effect with a p-value of 0.011 (an alpha of 0.05 was used in the statistical analysis). On the other hand, M_e in MP was influenced only by copolymer composition and CTA concentration. Since the surfactant concentration had a large effect in CEP, the effect of D_p into M_e was analyzed and it was observed that the smaller the D_p, the larger was the M_e. A similar analysis was done with the MP results and no such trend was observed. This can be due to the fact that under the given set of surfactant concentrations, the range of D_p's obtained in MP was narrow compared to the range obtained in CEP.

5.3.2 Particle size distribution (PSD)

PS and PSD are also known to affect PSA properties. Consequently, knowledge of how to control and tailor the PSD is an essential part in the bigger goal of tailoring PSA performance.

The analysis showed that in the case of CEP, the final D_p was mainly influenced by the surfactant and CTA concentrations while in the case of MP, D_p was affected by copolymer composition and surfactant concentration, which is consistent with our previous findings. It was expected that surfactant concentration had a significant influence since it

determined the D_d and together with the miniemulsion stability, they determined the final D_p. On the other hand, CTA concentration did not show a significant influence on D_p as opposed to the CEP case.

In order to explain how much the change of technique would affect the PSD, the results from latexes M5 and E5 were plotted in Figure 5.5. As can be observed, MP produced a similar PSD but with larger average D_p. It is important to point out that the PSD obtained by MP was comparable to that obtained by CEP. The polydispersity values obtained were 0.04 and 0.06 for MP and CEP, respectively. One should note that we are able to produce narrower distributions using CEP if it is carried out in a semi-continuous mode instead of a batch mode. Figure 5.5 also shows latexes M2 and E2, which were prepared with the same copolymer composition and surfactant concentration but with a lower CTA concentration. It was observed that a decrease in the CTA amount did not change the PSD in MP but it did shift the PSD of CEP-based latexes towards larger D_p's.

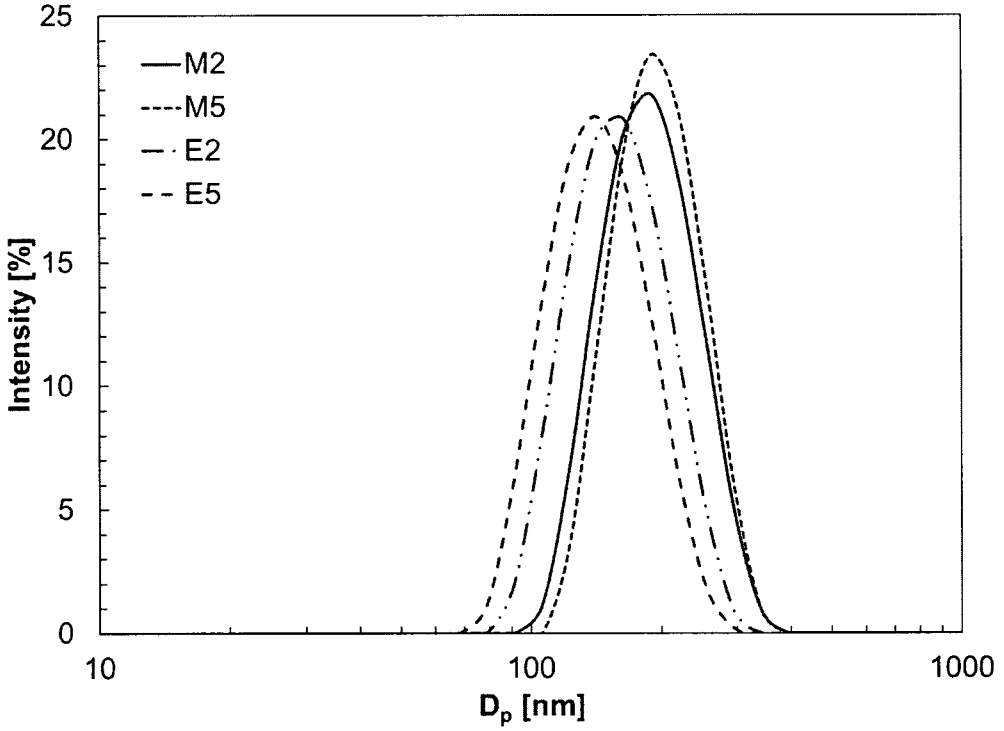

Figure 5.5. Particle size distribution of runs 2 and 5 in MP and CEP prepared using a copolymer composition of 65/35 wt.-% EHA/MMA and a surfactant concentration of 4.5 phm but using 0.5 phm (recipe 2) and 1.0 phm (recipe 5)

Figure 5.6 shows the PSD obtained for latexes M12, M13, M14 and M15 prepared with the lowest CTA concentration (c.f. Table 5.2 for details of the recipes). One can see that the main factor affecting the PSD was again the surfactant concentration since M12 and M14 were prepared with a surfactant concentration of 4.5 phm while M13 and M15 were prepared with 5.5 phm. Even though both surfactant and copolymer compositions were significant, surfactant was the only factor effectively affecting PSD with very small changes in PSD due to copolymer composition. On the other hand, CTA concentration affected D_d as discussed previously, but once D_d was set, the CTA concentration did not affect the final PSD.

5.3.3 Glass transition temperature (T_g)

It is known that the T_g is affected by copolymer composition and by the type of distribution of the two polymers, i.e., whether the particle has a homogeneous or heterogeneous morphology. DSC analysis was performed to test the effect of producing a latex via MP or CEP on their resulting morphology. The values of the T_g for each latex are presented in Tables 5.2 and 5.3 for MP and CEP, respectively.

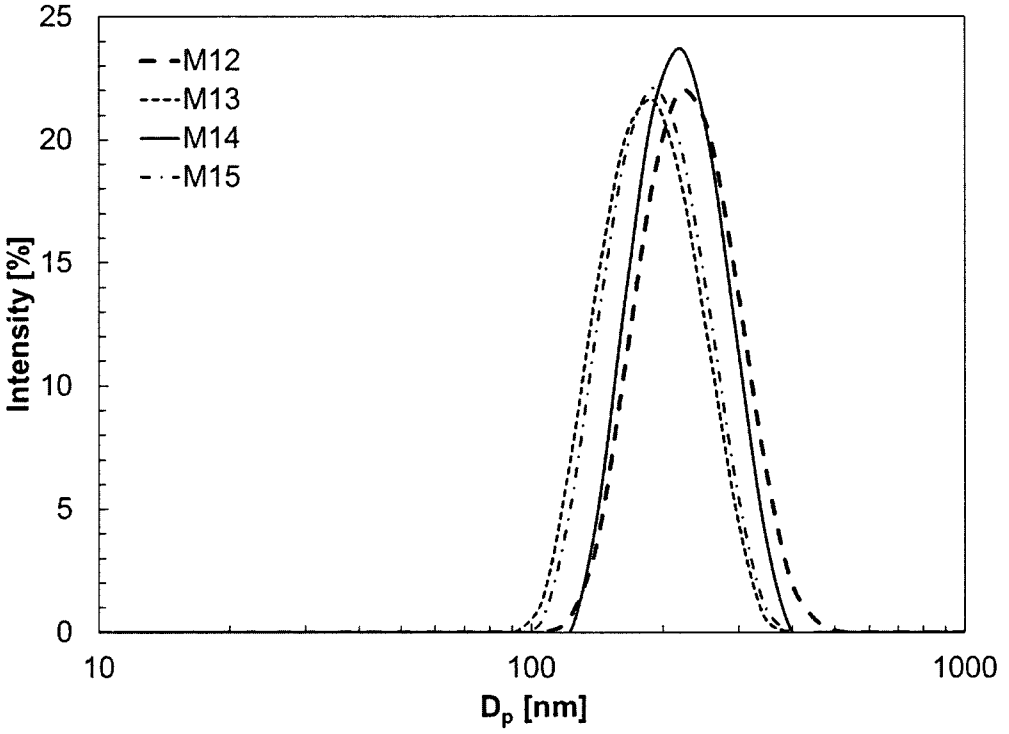

Figure 5.6. Particle size distributions of the recipes carried out in MP using a CTA concentration of 0.1 phm

The thermographs of the polymers produced with recipes M5 and E5 are shown in Figure 5.7a. This particular recipe was prepared with a monomer composition of 65/35 wt.-% EHA/MMA. As can be observed, the T_g of the polymers produced with this composition were ill-defined. If the entire temperature range is considered as the transition, the T_g of MP-based polymers is higher than that produced by CEP: -43° C for M5 and -52°C for E5. However, it appears that E5 contains two transitions in the temperature range between -70 and 0°C. If the derivative with respect to temperature of the reversible heat capacity is plotted (Rev C_p), one can see that E5 has indeed a T_g at around -50°C and a second broad transition that continues until approximately 0°C. On the other hand, M5 appears to have one main transition at approximately -52°C and a smaller second transition between -40°C and -20°C that is not as broad as that displayed by E5. The same trend was observed for all the recipes prepared at this copolymer composition. These results suggest that MP produced polymer particles with two compositions, one portion richer in EHA (likely the particle center) than a second portion (likely the outer layer of polymer particle). CEP produced a portion rich in EHA but it also has another portion of the polymer particle with a gradient copolymer composition as seen from the broad transition. An additional melting temperature transition peak was also observed at around 30°C in both MP and CEP. This peak, which indicated a melting point, was present in all the polymers produced at approximately the same temperature range (25 to 30°C). The peak belongs to the non-ionic surfactant Disponil A3065, for which a melting transition appears typically at 30°C (cf. Appendix A).

Figure 5.7b shows the thermographs of the polymers prepared with recipes M6 and E6. In this case, the polymers were prepared with a monomer composition of 85/15 wt.-% EHA/MMA with the same surfactant and CTA concentration as M5 and E5, i.e., 4.5 phm and 1.0 phm, respectively. As can be observed in Figure 5.7b, in this recipe the T_g transition was much narrower compared to M5 and E5 and there was no appreciable difference between the polymer particles produced by MP and CEP in contrast to Figure 5.7a. The copolymer compositions of recipes 5 and 6 were evaluated by ^{1}H-NMR spectroscopy at different conversions in order to follow the evolution of the composition in the two cases. Figures 5.8a and b show the copolymer composition evolution versus conversion for these recipes prepared by MP and CEP, where one can see that even though both techniques

produced polymers with a composition drift, there was not a significant difference between the two techniques.

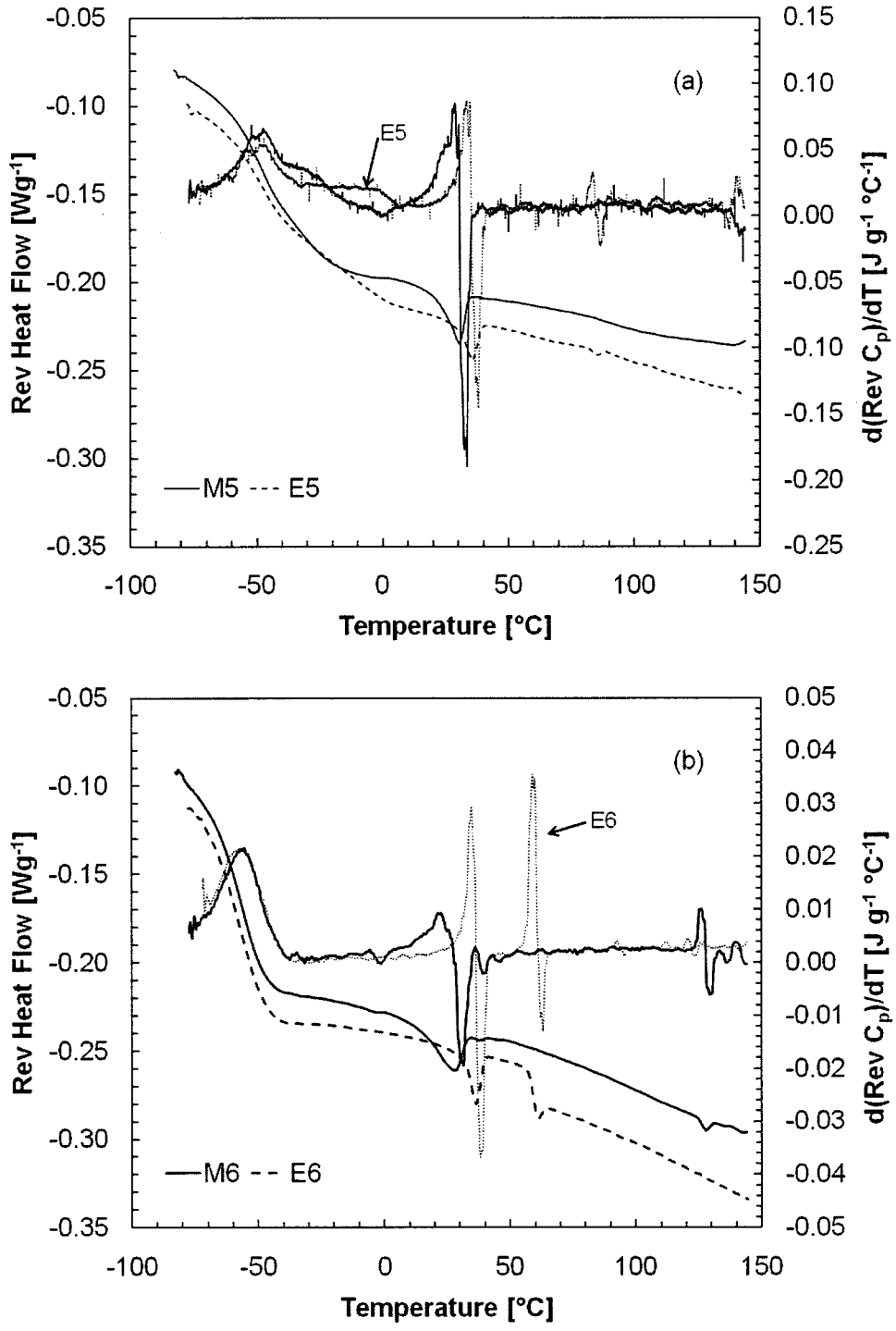

Figure 5.7. DSC thermographs of polymers produced in runs a) M5 (solid line) and E5 (dashed line) and b) M6 (solid line) and E6 (dashed line)

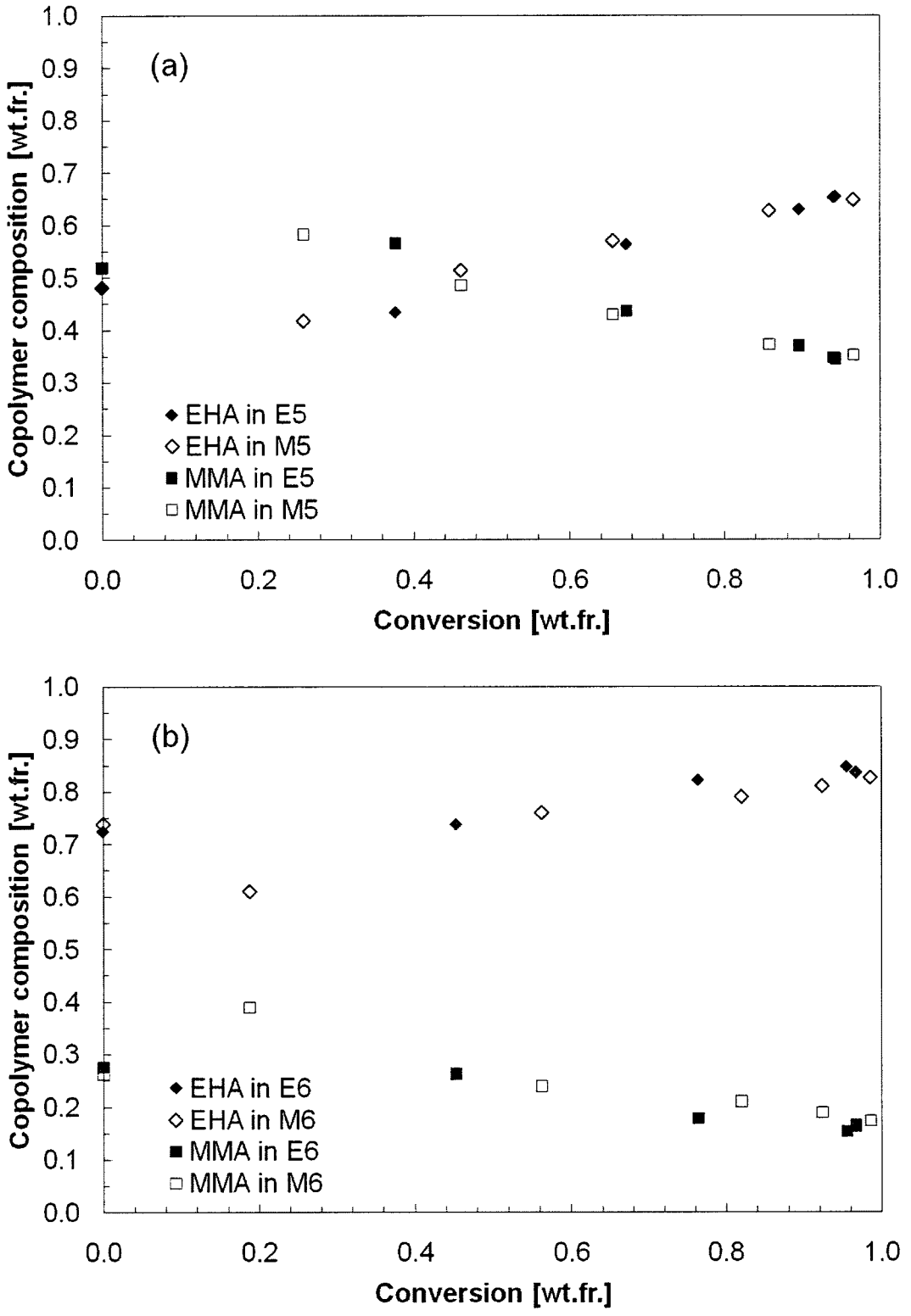

Figure 5.8. Copolymer composition versus conversion of recipes (a) 5 and (b) 6: EHA (diamonds) and MMA (squares) in CEP (filled symbols) and MP (empty symbols)

5.3.4 Viscoelastic properties

Examination of the viscoelastic behaviour of the polymers produced by both CEP and MP revealed certain differences. The different regions of a frequency master curve (i.e., glassy, rubbery plateau and terminal zone) can be related to different microstructural aspects of the polymer (Ferry, 1980). Figures 5.9a and b, respectively, show master curves of the storage (G') and loss (G") shear modulus versus frequency ($\omega \cdot a_T$) obtained for the polymers prepared with recipes M2 and E2 (similar trends were observed in the rest of the factorial design runs). The master curves were constructed using the Boltzmann superposition principle by applying horizontal shift factors (a_T) to superimpose the curves at a reference temperature of 25°C. The data was fitted using the well-known William-Landel-Ferry (WLF) equation and the WLF coefficients (C_1 and C_2) were calculated for each of the polymers (Ferry, 1980).

The results of the coefficients show two different materials. M2 gave a C_1 of 9.26 and a C_2 of 150.97 while E2 gave a C_1 of 10.3 and a C_2 of 131.38. This difference in the coefficients indicates that these two polymers produced using the same formulation but via two different nucleation mechanisms resulted in two different bulk structures. The smaller value of C_1 of M2 with respect to E2 would correspond to a larger free volume at the reference temperature. As can be observed in Figure 5.12a and b, the polymer prepared by MP (i.e., M2) displayed a much lower G' and G" in all the frequency range compared to the polymer prepared by CEP. The value of G' differs by almost a decade in magnitude. This could be an indication that producing a polymer by MP changed the microstructure as observed from the M_e values discussed earlier. It was expected that a polymer with a higher M_e (in this case E2) would present a lower G' and G". However, the opposite was found in this analysis. Certainly, other factors such as T_g and MWD have to be taken into consideration. E2 presented a wider T_g (similar as run E5 presented in Figure 5.7a), as observed from the DSC thermographs, which likely had an impact on the free volume and increased G' and G". Polymers prepared with recipes E2 and M2 also presented different M_w's (91,000 and 83,000 g/mol, respectively) and polydispersities, which could also be increasing G' and G" and compensating for the effect of a decrease in these two physical properties due to the higher M_e.

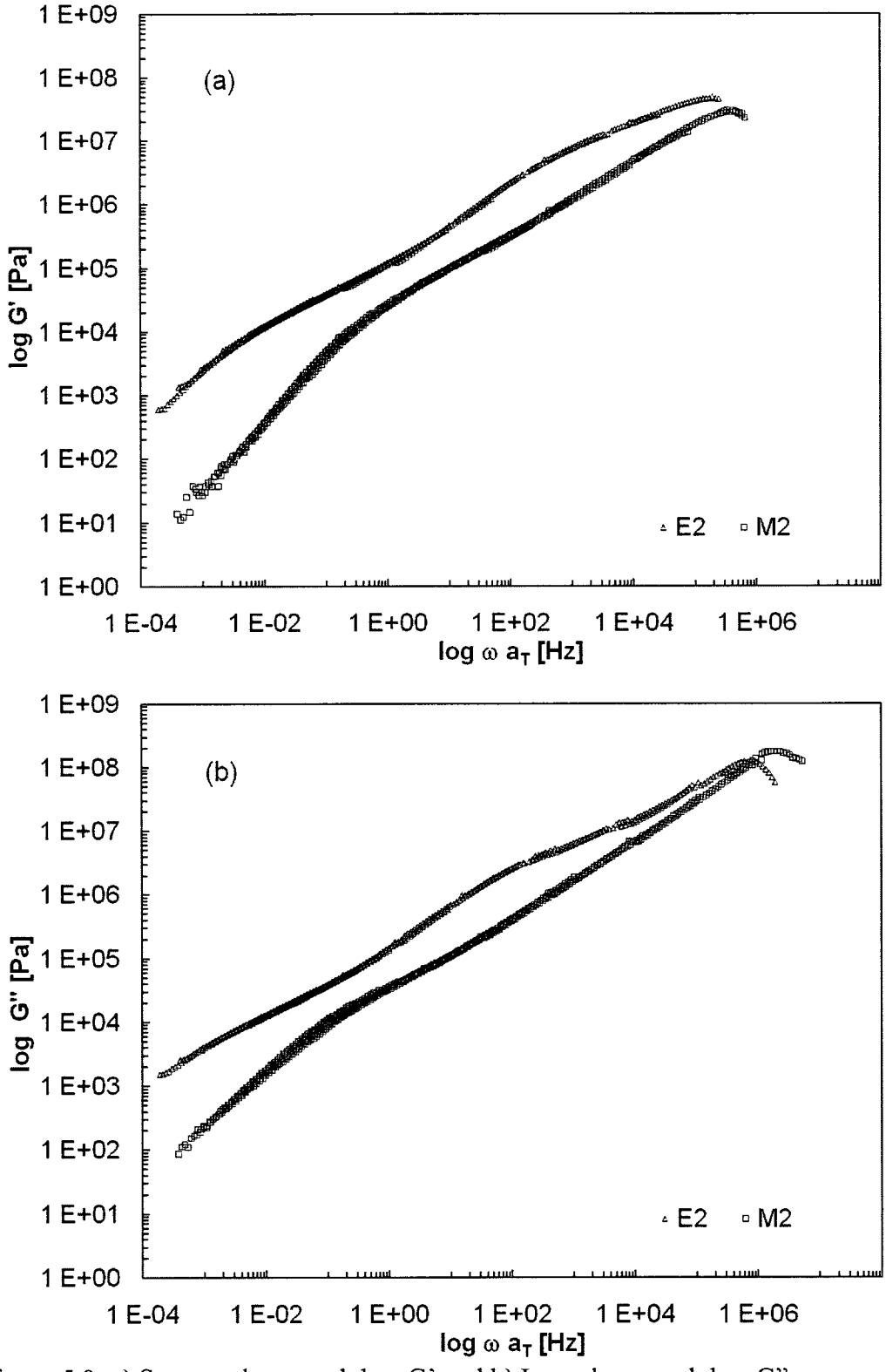

Figure 5.9. a) Storage shear modulus, G' and b) Loss shear modulus, G" versus ωa_T for polymers produced in runs M2 (solid line) and E2 (dashed line)

Figures 5.10a and b show G' and a_T, respectively, for three polymers produced by MP. These three polymers were chosen because they have very different entanglement densities (c.f. Table 5.6). M2 was a loose network with a M_w of 83,000 g/mol, which was over twice the value of M_e giving an entanglement density of ~2.4. M14 had the largest M_w with 313,500 and an M_e that was 8.15 times lower. Finally, M15 had an intermediate M_w of 269,500 g/mol but with the lowest M_e of the three polymers giving the highest M_w/M_e value of the three with 10.5. Examination of the curves shows that the rubbery plateau and terminal regions increased with increasing entanglement densities. One part is understandably due to the increase of M_w: it can be appreciated how the rubbery plateau becomes more evident in M14 and M15 compared to M2, which not only has lower M_w but also narrower polydispersity. The terminal region also increased to higher values of G'. Usually, this region increases with M_w but in this case, the M_w of M15 was somewhat lower than that of M14. However, the M_e of sample M15 was lower, producing a more entangled network, a possible reason for the larger G' in the terminal region, which is consistent with previous studies (Yarusso, 2002). This is also reflected in Figure 5.10b, where a_T for the same three polymers was plotted against the temperature. It can be seen that below room temperature, an increase in the entanglement density led to an increase in a_T which indicates that below room temperature the relaxation times of M15 (higher M_w/M_e) were much higher than the relaxation time of M2 (low M_w/M_e).

The next question was how much the initial reaction conditions modified the resulting network. For example, in order to go from a loose network (M2) to a more entangled one (M14), the CTA concentration was decreased 5 times but the amount of the "soft" monomer, i.e., EHA, was increased from 65 wt.-% to 85 wt.-%. In order to achieve even higher entanglement densities (M15), the CTA concentration was the same as that for M14 but the amount of EHA in the system was decreased to 65 wt.-%. This together with a smaller D_p (the surfactant concentration for M15 was at the highest level, i.e., at 5.5 phm) gave the highest of the entanglement densities found within the range of conditions investigated in this study.

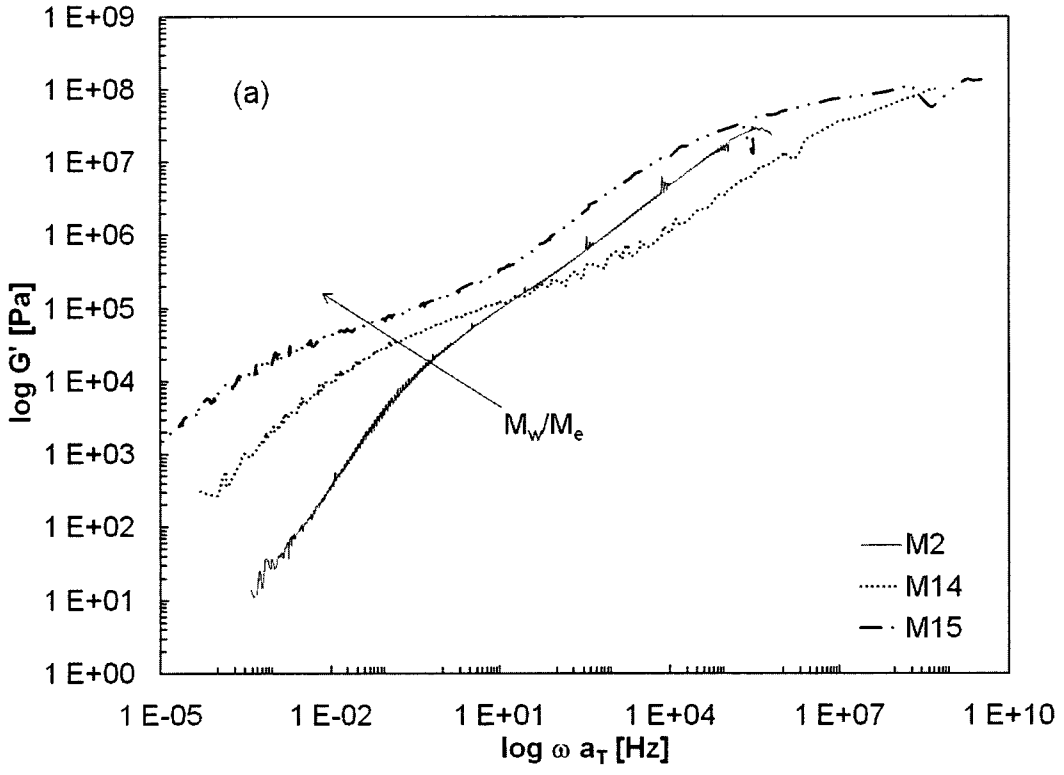

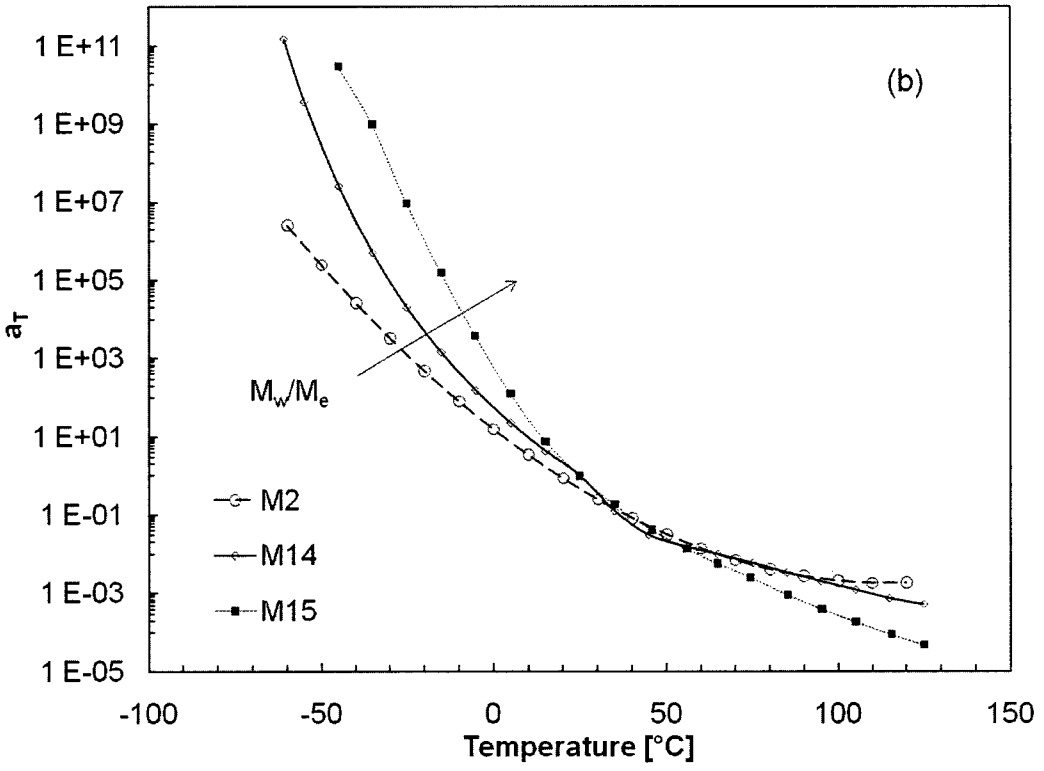

Figure 5.10. a) Storage shear modulus, G' versus ωa_T and b) Shift factor (log a_T) versus Temperature for polymers with three different entanglement densities

5.3.5 PSA properties

Tables 5.5 and 5.6 present the results of the PSA characterization for films cast from latexes produced by MP and CEP, respectively. The results include the type of failure exhibited in the loop tack and peel strength tests for each one of the samples. The resulting properties for MP-based and CEP-based films were different. It is possible to see in some cases, such as in M2, that MP gave higher values of loop tack and peel strength compared to CEP, which was a result of a higher entanglement density (i.e., M_w/M_e). On the other hand, M2 exhibited lower shear strength than E2. The latter was expected since lower values of G' in the terminal region obtained in the DMA analysis suggested a lower cohesive strength.

Table 5.5. PSA properties results of Miniemulsion-based latexes

LATEX	Loop tack maximum	Loop tack plateau	Type of failure	Peel strength	Type of failure	Shear strength	PSA coating weight
	N/m	N/m	(for loop tack)	N/m	(for peel strength)	s	g/m^2
M1	79.58	38.58	A	18.05	C	38.0 (1)	35.1
M2	405.48	271.97	A	185.43	C	280.0 (55)	29.1
M3	100.39	30.51	C	16.73	C	40.0 (4)	34.2
M4	115.65	52.17	C	23.62	C	50.0 (2)	33.9
M5	158.24	81.59	A	93.95	A	241.0 (6)	33.8
M6	86.94	32.81	C	17.22	C	10.0 (1)	35.0
M7	182.96	69.23	C/A	64.28	C	107.0 (11)	36.8
M8	314.82	153.29	A	217.57	A	300.0 (18)	32.9
M9	67.66	18.72	C	11.90	C	12.0 (1)	31.6
M11	385.09	155.02	A	310.04	A	1140 (60)	32.3
M12	226.38	182.09	A	252.62	A	286500 (1050)	33.5
M13	426.92	314.96	A	285.43	C	1058 (66)	28.6
M14	339.57	182.09	A	259.11	A	3300 (200)	30.8
M15	178.40	76.28	A	121.39	A	130200 (900)	33.6

C = Cohesive Failure; A = Adhesive Failure; C/A = combination of both failures with the presence of fibrils
LT = loop tack; PS = Peel Strength
Standard deviation values are reported in parenthesis besides the results

In order to evaluate how the bonding behaviour changed with the different levels of the three factors used in this study, loop tack curves were plotted as the force versus detachment distance for the different initial reaction conditions (c.f. Figure 5.11a-b). These curves reflect the force needed during the initial phases of debonding (loop tack plateau) and the maximum force needed to completely detach the loop from the substrate (loop tack maximum) (Woo et al., 2004). Full loop tack-displacement curves show in a more detailed

way the differences between those films cast from MP- and CEP-produced latexes. The values obtained in these curves are those shown in Tables 5.5 and 5.6 as loop tack plateau and loop tack maximum.

Table 5.6. PSA properties results of Conventional Emulsion-based latexes

LATEX	Loop tack maximum	Loop tack plateau	Type of failure	Peel strength	Type of failure	Shear strength	PSA coating weight
	N/m	N/m	(for loop tack)	N/m	(for peel strength)	s	g/m^2
E1	316.47	242.30	C W/F	100.55	C W/F	94	38.0
E2	166.48	121.97	A	37.09	A	1557	40.0
E3	323.89	234.88	A	158.24	A	90	40.0
E4	258.37	178.02	C	76.65	C	128	40.5
E5	118.77	62.99	A	24.88	A	97	40.0
E6	103.84	32.48	C	14.76	C	30	42.2
E7	94.53	22.68	C	13.26	C	13	40.0
E8	180.12	135.83	C	47.00	C	60	40.5
E9	80.71	25.10	C	12.55	A	15	40.0

C = Cohesive Failure; A = Adhesive Failure; C/A = combination of both failures with the presence of fibrils

In the case of MP-based films, the analysis showed that the CTA concentration was the main factor affecting loop tack (plateau and maximum) followed by the copolymer composition. The surfactant concentration had very little effect. As a matter of fact, the copolymer composition was the only statistically significant factor in the loop tack plateau, i.e., the T_g and particle microstructure played a role in the initial stages of debonding but had less impact on the final force required to detach or completely break the fibrils from the substrate. The difference between these two techniques can be better appreciated in Figure 5.11a, where the complete force versus detachment distance was plotted for four PSA films: M2 and E2 (films cast from latexes prepared using 65/35 wt.-% EHA/MMA) and M4 and E4 (films cast from latexes prepared using 85/15 wt.-% EHA/MMA). The large increase in the force, both at the plateau and at the maximum point that is created due to the relatively small change in D_p for the case of MP-based films is noted: M2 has a D_p of 182 nm while M4 has a D_p of 197 nm. Nevertheless, it is evident that a smaller D_p favoured larger values of loop tack. On the other hand, films cast from latexes E2 and E4 had very similar D_p's (153 nm and 155 nm, respectively) while still displaying a significant difference in the loop tack curve. In this case, the increase in the loop tack curve was likely due to the difference in

weight-average M_w between these two latexes that accounted for about 12,000 g/mol between them.

The CTA and surfactant concentrations alone did not account for all the differences found. Noting that each technique produced a different entanglement density, it was then verified whether larger values of M_w/M_e were correlated with higher values of loop tack. In Figure 5.11a, M2 displays the highest force values (equivalent to the highest loop tack for the films shown in Figure 5.11a) with a M_w/M_e equal to 2.45 (c.f. Table 5.4) while M4 displays the lowest force values with a M_w/M_e of 0.6. It is clear that those films with M_w/M_e values below 2 will not form fibrils and they will produce films with poor values of loop tack.

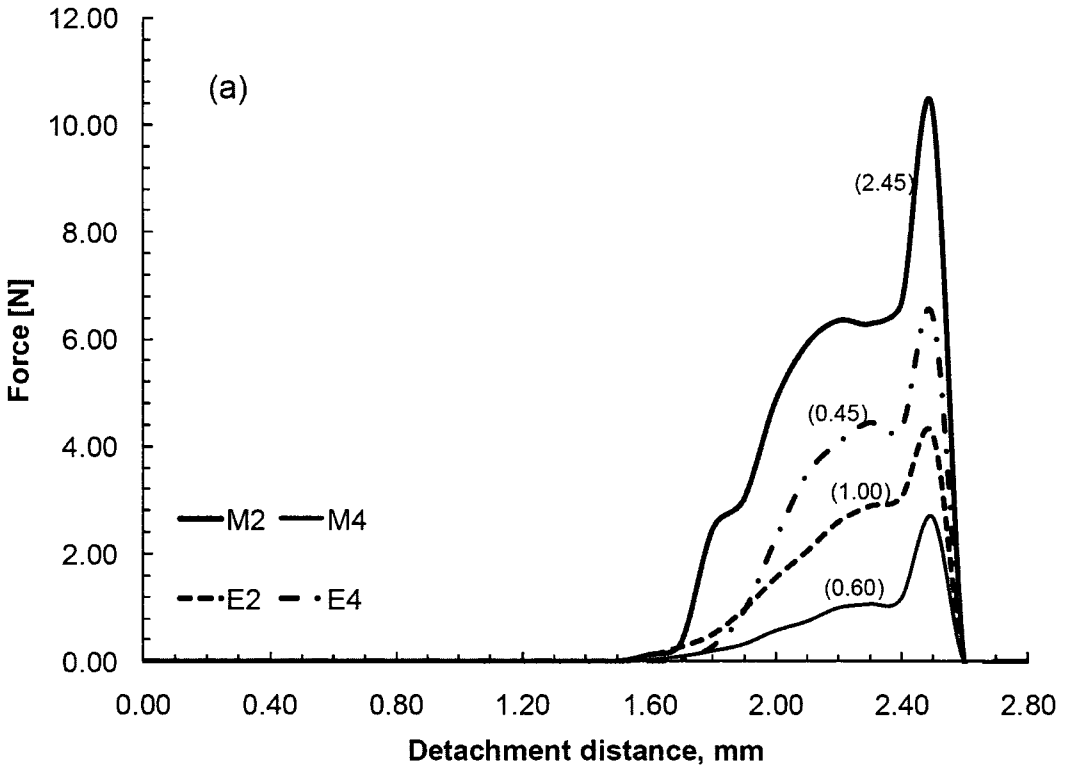

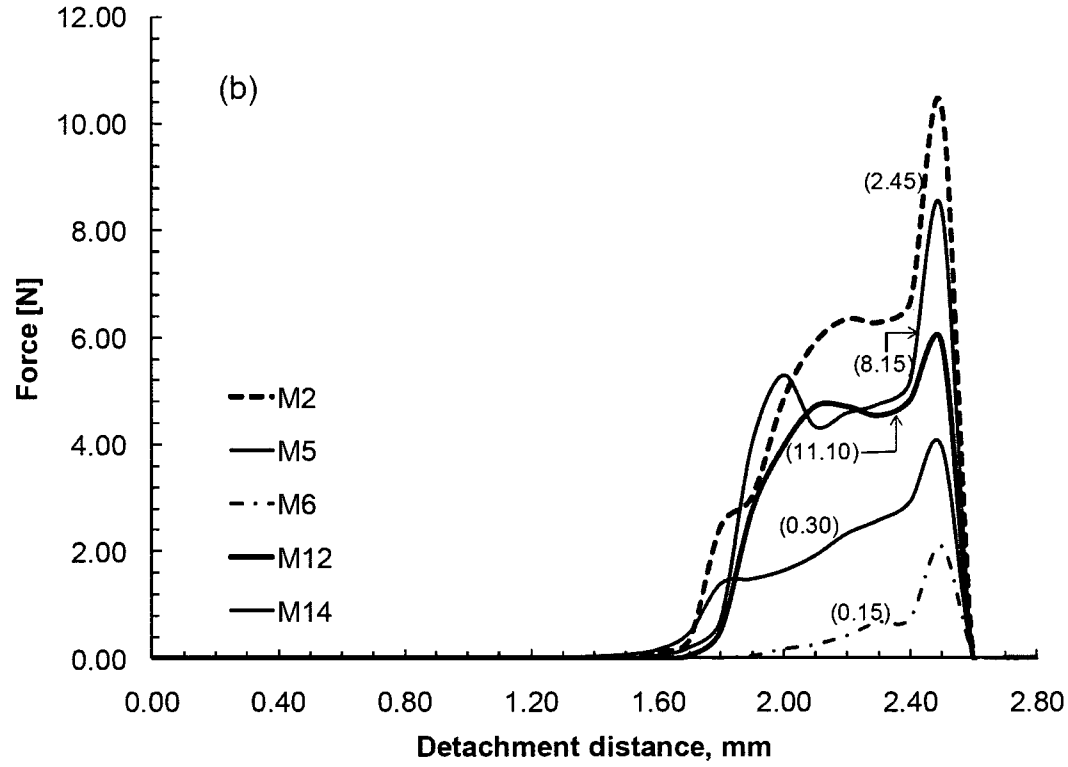

Figure 5.11. Detachment Force versus Detachment Distance for films cast from latexes a) M2, M4, E2 and E4 and b) M2, M5, M6, M12 and M14

If a broader range of CTA concentrations is included, higher M_w/M_e values were found as reported on Table 5.4, which led to higher values of loop tack. Figure 5.11b shows the full force versus detachment distance for films with different entanglement densities. As can be observed in Figure 5.11b, the force values increased with an increase in M_w/M_e from a series of films with low loop tack values and displaying cohesive failure (CF) to a maximum of 10 N exhibited by the film M2 followed by a decrease in force values with higher values of M_w/M_e. In order to assess whether there was an optimum entanglement density that could achieve a maximum value of loop tack, the values of loop tack maximum were plotted versus M_w/M_e in Figure 5.12. The figure displays a maximum value of loop tack of 430 N/m with a M_w/M_e of ~7.5 followed by a decrease in the values of loop tack with higher values of M_w/M_e. It is also interesting to point out those points below $M_w/M_e = 1$ exhibited complete cohesive failure while those above a value of 1 exhibited adhesive failure.

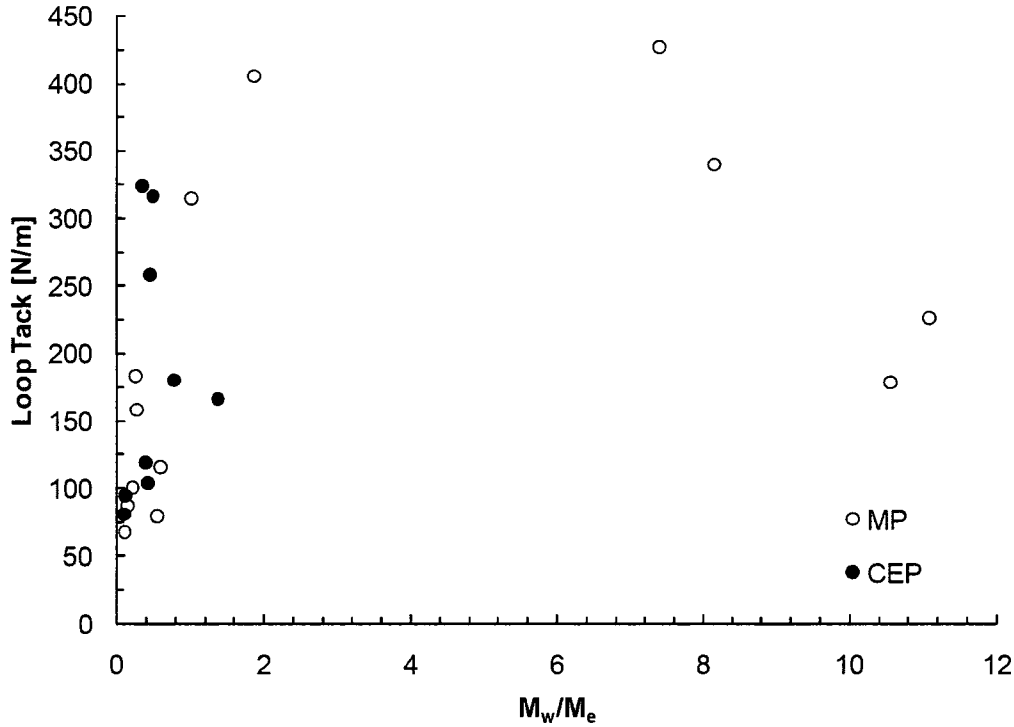

Figure 5.12. Loop tack versus M_w/M_e for MP and CEP-based films

A similar analysis was made with the results obtained for peel strength and shear strength. In the case of MP-based films, the CTA concentration was the main factor affecting peel strength. Surfactant concentration was also significant but to a lesser degree. For CEP-based films, the resulting values of peel strength were more difficult to assess since it appeared that only the CTA concentration was posing an influence on this property. A plot of peel strength versus M_w/M_e was plotted to evaluate the influence of the entanglement density on this PSA property and this is shown in Figure 5.13. As can be seen in Figure 5.13, there is also a trend with a maximum value of peel strength of ~275 N/m at M_w/M_e around 7 to 7.5. This is consistent with reported results that found that very high values of M_w/M_e reduced the loop tack and peel strength significantly due to a decrease in the energy the polymer is able to dissipate due to tighter microstructure (Tobing and Klein, 2001a). The reported values of M_w/M_e for continuous networks found in the literature for emulsion-based PSAs produced by a semi-continuous process are in the same order as those found herein for MP-based PSAs produced in a batch process.

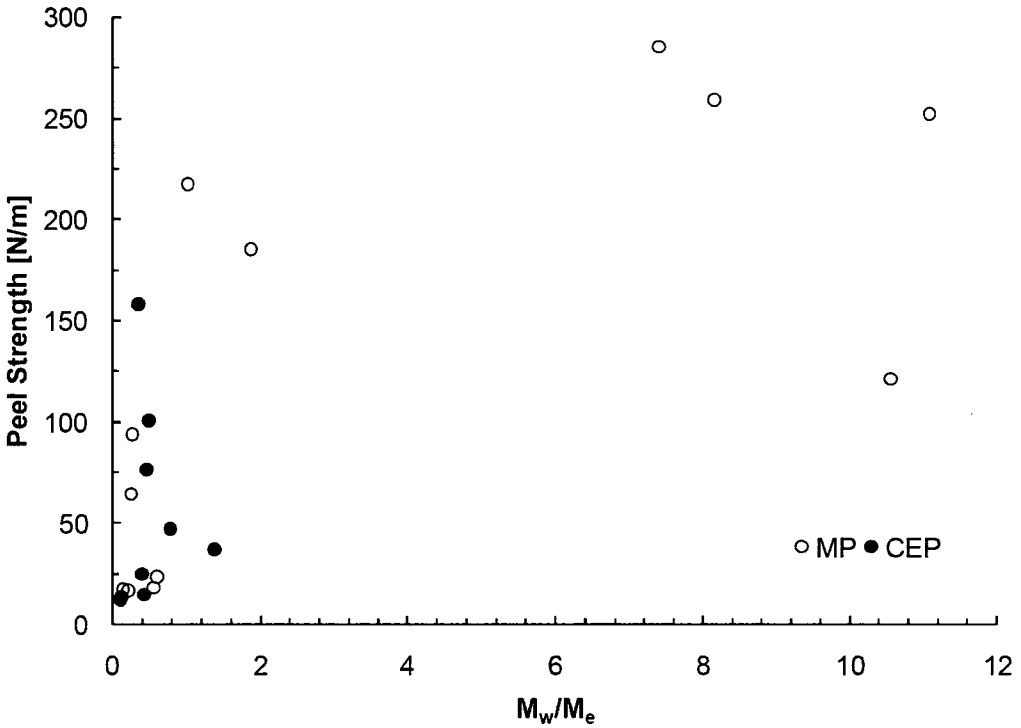

Figure 5.13. Peel strength versus M_w/M_e for MP and CEP-based films

Shear strength was expected to be mainly affected by M_w and M_e, which were in turn affected by the three factors studied, i.e., by copolymer composition, CTA and surfactant concentration. Analysis of the main effects led to the conclusion that increasing the levels of the three factors would cause a decrease in shear strength for both MP and CEP. Similarly as with loop tack and peel strength, shear strength versus M_w/M_e was plotted and it is shown in Figure 5.14. Since the copolymer composition has an influence over shear strength, only those latexes with a composition of 65/35 wt.-% EHA/MMA were plotted. However, the same trend was observed in the case of latexes prepared at a copolymer composition of 85/15 wt.-% EHA/MMA. A closer examination of the graph in Figure 5.14 reveals that there is a definite linear relationship between these two properties: higher entanglement densities led to higher values of shear strength. This is due to the fact that a more entangled network morphology would lead to lower resistance to flow. The trend for CEP-based films is not as evident because it was not possible to produce stable latexes with CTA concentrations below 0.5 phm using a batch process and thus their M_w/M_e ratios were rather low. It is known that similar results could be achievable by the use of a semi-continuous process as presented in a number of studies (Tobing et al., 2001; Tobing and Klein, 2001a; Tobing and Klein, 2001b).

Nevertheless, it must be highlighted that MP is capable of achieving stable latexes with these entanglement densities and shear strength values using a batch process. At the M_w/M_e levels where loop tack and peel strength showed maxima, i.e., at a value of ~7 or 8, shear strength already displays values over 3 x 10^3 s.

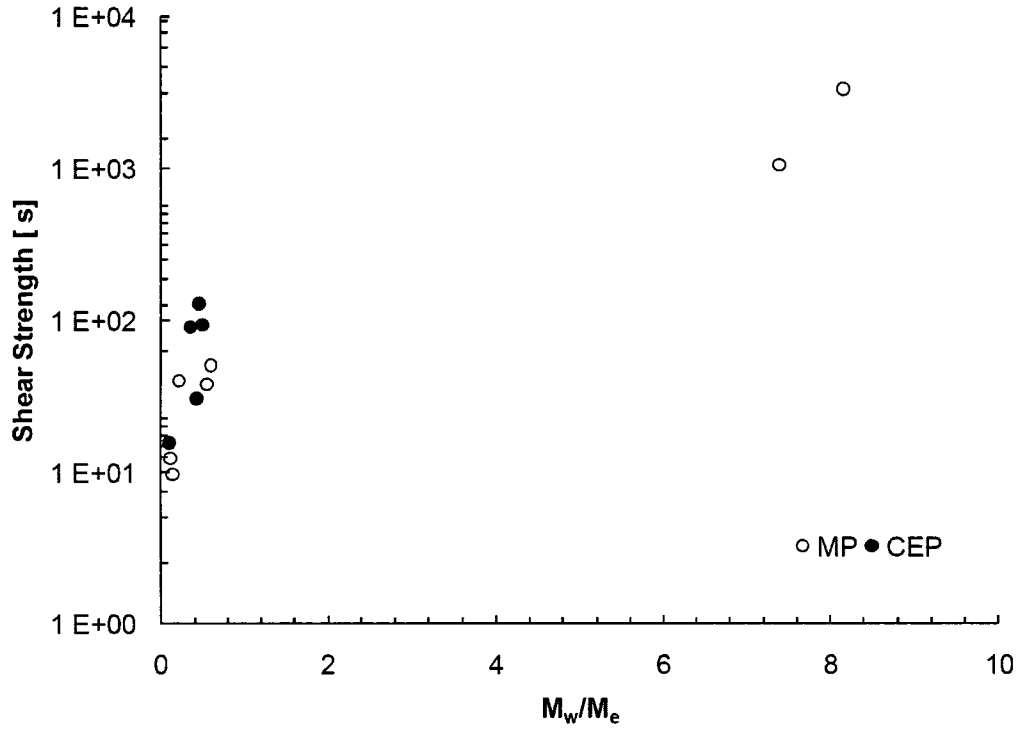

Figure 5.14. Shear strength versus M_w/M_e for MP and CEP-based films for a 65/35 wt.-% EHA/MMA copolymer composition

5.4 CONCLUSIONS

The influence of monomer composition, chain transfer agent and surfactant concentration on the kinetics, structural (e.g., molecular weight and particle size) and adhesive properties of poly (EHA/MMA/AA) latexes prepared via MP and CEP were each systematically studied using separate 2^3 factorial designs. Significant kinetic and microstructural differences between the latexes (or films) produced by these two techniques were found due to the different particle nucleation mechanisms. The most significant difference between the films obtained by MP and CEP was shown via the viscoelastic analysis wherein MP-based films displayed a much lower G' and G" compared to those produced by CEP, indicating a different microstructure. Analysis of the films showed that a

number of the MP-based latexes presented more entangled networks compared to CEP-based ones even though the M_w was generally lower for the MP latexes.

It was possible to exert a certain degree of control over the entanglement densities with MP polymerization. High entanglement densities values were obtained using low CTA concentrations (0.1 phm) and EHA amounts of 65 wt.-% giving a maximum M_w/M_e value of ~11, which produced a PSA with a shear strength of ~80 h. However, maximum values of loop tack and peel strength were found at M_w/M_e of ~7. The M_w/M_e ratio was strongly correlated with the PSA properties. Our ability to control entanglement densities and, as a result the PSA properties, makes miniemulsion polymerization an ideal technique for tailoring the properties of PSA materials.

5.5 ACKNOWLEDGMENTS

The authors gratefully acknowledge the financial support of the University of Ottawa, the Natural Science and Engineering Research Council (NSERC) of Canada and the National Council of Science and Technology (CONACYT) of Mexico.

5.6 REFERENCES

Aizpurua, I., Barandiaran, M.J., 1999. Comparison between conventional emulsion and miniemulsion polymerization of vinyl acetate in a continuous stirred tank reactor. Polymer 40, 4105-4115.

Antonietti, M., Landfester, K., 2002. Polyreactions in miniemulsions. Progress in Polymer Science 27, 689-757.

Asua, J.M., 2002. Miniemulsion polymerization. Progress in Polymer Science 27, 1283-1346.

Athawale, V.D., Rathi, S.C., 1995. Effect of Monomer Concentration on the Adhesive Properties of Acrylic Pressure-Sensitive Adhesives. Journal of Adhesion Science and Technology 9, 899-905.

Aymonier, A., Ledercq, D., Tordjeman, P., Papon, E., Villenave, J.J., 2003. Control of structure and tack properties of acrylic pressure-sensitive adhesives designed by a polymerization process. Journal of Applied Polymer Science 89, 2749-2756.

Aymonier, A., Papon, E., Villenave, J.J., Tordjeman, P., Pirri, R., Gerard, P., 2001. Design of pressure-sensitive adhesives by free-radical emulsion copolymerization of methyl methacrylate and 2-ethylhexyl acrylate. 1. Kinetic study and tack properties. Chemistry of Materials 13, 2562-2566.

Benedek, I., 2006. Developments in Pressure-Sensitive Products, 2nd ed. ed. CRC Press, Boca Raton, Florida.

Boehm, A.J., Glaser, A., Koch, O., 2003. Nanocolorants - More than colored nanoparticles. 2, 2419-2422.

Boutti, S., Graillat, C., McKenna, T.F., 2005. High solids content emulsion polymerisation without intermediate seeds. Part II. In situ generation of bimodal latices. Polymer 46, 1211-1222.

Chang, E.P., 1997. Viscoelastic properties of pressure-sensitive adhesives. Journal of Adhesion 60, 233-248.

Chu, S.G., 1989. Viscoelastic Properties of Pressure Sensitive Adhesives, in: Satas, D. (Eds.), Handbook of Pressure-Sensitive Adhesive Technology. Van Nostrand Reinhold, New York, pp. 158-203.

do Amaral, M., Roos, A., Asua, J.M., Créton, C., 2005. Assessing the effect of latex particle size and distribution on the rheological and adhesive properties of model waterborne acrylic pressure-sensitive adhesives films. Journal of Colloid and Interface Science 281, 325-338.

Du, J., Lindeman, D.D., Yarusso, D.J., 2004. Modeling the peel performance of pressure-sensitive adhesives. Journal of Adhesion 80, 601-612.

Dubé, M.A., Amin Sanayei, R., Penlidis, A., O'Driscoll, K.F., Reilly, P.M., 1991. A Microcomputer Program for Estimation of Copolymerization Reactivity Ratios. Journal of Polymer Science, Part A: Polymer Chemistry 29, 703-708.

Elizalde, O., Vicente, M., Leiza, J.R., Asua, J.M., 2002. Control of the adhesive properties of n-butyl acrylate/styrene latexes. Polymer Reaction Engineering 10, 265-283.

Ferry, J.D., 1980. Viscoelastic Properties of Polymers, 3rd edition ed. John Wiley and Sons, New York, USA.

Fetters, L.J., Lohse, D.J., Richter, D., Witten, T.A., Zirkel, A., 1994. Connection Between Polymer Molecular-Weight, Density, Chain Dimensions, and Melt Viscoelastic Properties. Macromolecules 27, 4639-4647.

Fonseca, G.E., McKenna, T.F., Dubé, M.A., 2008. Influence of Particle Nucleation in Pressure Sensitive Adhesive Properties: Miniemulsion versus Emulsion Polymerization. Macromolecular Symposia 271, 83-93.

Gower, M.D., Shanks, R.A., 2004a. The effect of chain transfer agent level on adhesive performance and peel master-curves for acrylic pressure sensitive adhesives. Macromolecular Chemistry and Physics 205, 2139-2150.

Gower, M.D., Shanks, R.A., 2004b. The effect of varied monomer composition on adhesive performance and peeling master curves for acrylic pressure-sensitive adhesives. Journal of Applied Polymer Science 93, 2909-2917.

Gower, M.D., Shanks, R.A., 2006. Acrylic acid level and adhesive performance and peel master-curves of acrylic pressure-sensitive adhesives. Journal of Polymer Science, Part B: Polymer Physics 44, 1237-1252.

Greenwood, R., Luckham, P.F., Gregory, T., 1998. Minimising the viscosity of concentrated dispersions by using bimodal particle size distributions. Colloids and Surfaces A: Physicochemical and Engineering Aspects 144, 139-147.

Hua, H., Dubé, M.A., 2001. Off-line monitoring of butyl acrylate, methyl methacrylate and vinyl acetate homo- and copolymerizations in toluene using ATR-FTIR spectroscopy. Polymer 42, 6009-6018.

Jovanovic, R., Dubé, M.A., 2004. Emulsion-based pressure-sensitive adhesives: A review. Journal of Macromolecular Science: Polymer Reviews C44, 1-51.

Jovanovic, R., Dubé, M.A., 2007. Butyl acrylate/vinyl acetate emulsion-based pressure-sensitive adhesives: Empirical modelling of final properties. Canadian Journal of Chemical Engineering 85, 341-349.

Jovanovic, R., McKenna, T.F., Dubé, M.A., 2004a. Empirical modeling of butyl acrylate/vinyl acetate/acrylic acid emulsion-based pressure-sensitive adhesives. Macromolecular Materials and Engineering 289, 467-474.

Jovanovic, R., Ouzineb, K., McKenna, T.F., Dubé, M.A., 2004b. Butyl acrylate/methyl methacrylate latexes: Adhesive properties. Macromolecular Symposia 206, 43-56.

Landfester, K., 2001. Polyreactions in miniemulsions. Macromolecular Rapid Communications 22, 896-936.

Landfester, K., Ramirez, L.P., 2003. Encapsulated magnetite particles for biomedical application. Journal of Physics: Condensed Matter 15, S1345-S1361.

Lathova, E., Lath, D., Pavlinec, J., 1993. The Behavior of Poly(2-Ethylhexyl Acrylate) in Dilute-Solution - Viscosity Measurements. Polymer Bulletin 30, 713-718.

Ouzineb, K., Graillat, C., McKenna, T.F., 2005. High-Solid-Content Emulsions. V. Applications of Miniemulsions to High Solids and Viscosity Control. Journal of Applied Polymer Science 97, 745-752.

Patnaik, M., Choudhary, V., Varma, I.K., 1992. Structural and thermal characterization of methyl methacrylate/alkyl acrylate copolymers. European Polymer Journal 28, 1433-1439.

Plaut, R.H., Williams, N.L., Dillard, D.A., 2001. Elastic analysis of the loop tack test for pressure sensitive adhesives. Journal of Adhesion 76, 37-53.

Plessis, C., Arzamendi, G., Alberdi, J.M., Agnely, M., Leiza, J.R., Asua, J.M., 2001a. Intramolecular chain transfer to polymer in the emulsion polymerization of 2-ethylhexyl acrylate. Macromolecules 34, 6138-6143.

Plessis, C., Arzamendi, G., Leiza, J.R., Schoonbrood, H.A.S., Charmot, D., Asua, J.M., 2000. A decrease in effective acrylate propagation rate constants caused by intramolecular chain transfer. Macromolecules 33, 4-7.

Plessis, C., Arzamendi, G., Leiza, J.R., Schoonbrood, H.A.S., Charmot, D., Asua, J.M., 2001b. Kinetics and polymer microstructure of the seeded semibatch emulsion copolymerization of n-butyl acrylate and styrene. Macromolecules 34, 5147-5157.

Pressure Sensitive Tape Council, 2004. Test Methods for Pressure Sensitive Adhesive Tapes, 14th ed. ed. Pressure Sensitive Tape Council, Northbrook, Illinois.

Roberge, S., Dubé, M.A., 2006. The effect of particle size and composition on the performance of styrene/butyl acrylate miniemulsion-based PSAs. Polymer 47, 799-807.

Satas, D., 1989. Handbook of Pressure Sensitive Adhesive Technology, 2nd ed. ed. Van Nostrand Reinhold, New York.

Schneider, M., Claverie, J., Graillat, C., McKenna, T.F., 2002. High solids content emulsions. I. A study of the influence of the particle size distribution and polymer concentration on viscosity. Journal of Applied Polymer Science 84, 1878-1896.

Schork, F.J., Luo, Y., Smulders, W., Russum, J.P., Butte, A., Fontenot, K., 2005. Miniemulsion Polymerization. Advances in Polymer Science 175, 129-255.

Stubbs, J.M., Sundberg, D.C., 2005. Measuring the extent of phase separation during polymerization of composite latex particles using modulated temperature DSC. Journal of Polymer Science, Part B: Polymer Physics 43, 2790-2806.

Tobing, S., Klein, A., Sperling, L.H., Petrasko, B., 2001. Effect of network morphology on adhesive performance in emulsion blends of acrylic pressure sensitive adhesives. Journal of Applied Polymer Science 81, 2109-2117.

Tobing, S.D., Klein, A., 2000. Mechanistic studies in tackified acrylic emulsion pressure sensitive adhesives. Journal of Applied Polymer Science 76, 1965-1976.

Tobing, S.D., Klein, A., 2001a. Molecular parameters and their relation to the adhesive performance of acrylic pressure-sensitive adhesives. Journal of Applied Polymer Science 79, 2230-2244.

Tobing, S.D., Klein, A., 2001b. Molecular parameters and their relation to the adhesive performance of emulsion acrylic pressure-sensitive adhesives. II. Effect of crosslinking. Journal of Applied Polymer Science 79, 2558-2564.

Tronc, F., Winnik, M.A., Kaul, B.L., Graciet, J.C., 2004. Polycarbonate Particles and Dye-Labelled Particles by Miniemulsion Polymerization. Journal of Polymer Science, Part A: Polymer Chemistry 42, 1999-2009.

Vicente, M., Leiza, J.R., Asua, J.M., 2001. Simultaneous central of copolymer composition and MWD in emulsion copolymerization. AIChE Journal 47, 1594-1606.

Woo, Y., Plaut, R.H., Dillard, D.A., Coulthard, S.L., 2004. Experiments and inelastic analysis of the loop tack test for pressure-sensitive adhesives. Journal of Adhesion 80, 203-221.

Yarusso, D.J., 1999. Quantifying the relationship between peel and rheology for pressure sensitive adhesives. Journal of Adhesion 70, 299-320.

Yarusso, D.J., 2002. Effect of Rheology on PSA Performance, in: Dillard, D.A., Pocius, A.V. (Eds.), The Mechanics of Adhesion. Elsevier, Amsterdam, pp. 499-533.

Zosel, A., 1998. The effect of fibrillation on the tack of pressure sensitive adhesives. International Journal of Adhesion and Adhesives 18, 265-271.

CHAPTER 6

Bimodal particle size and molecular weight distributions using a one-pot two-step miniemulsion polymerization strategy

---

Fonseca, G.E., McKenna, T.F., Dubé, M.A.;
Industrial & Engineering Chemistry Research, submitted

Bimodal particle size and molecular weight distributions using a one-pot two-step miniemulsion polymerization strategy

Gabriela E. Fonseca[1], Timothy F.L. McKenna[2], Marc A. Dubé[1*]

[1]Department of Chemical and Biological Engineering, University of Ottawa, 161 Louis Pasteur Pvt., Ottawa, Ontario, K1N 6N5, Canada; Fax 1(613)5625172; Email: Marc.Dube@uottawa.ca

[2]Department of Chemical Engineering, Queen's University, Kingston, Ontario, K7L 3P4, Canada

ABSTRACT

A one-pot two-step miniemulsion polymerization approach was successfully used to create poly (2-ethyl hexyl acrylate/methyl methacrylate/acrylic acid) pressure sensitive adhesives with well-defined and predictable bimodal particle size distributions (PSD) or bimodal molecular weight distributions (MWD). The resulting viscoelastic (shear storage and loss modulus) and adhesive properties (i.e., loop tack, peel strength and shear strength) were tested and compared to monomodal distributions of either particle size or molecular weight along with bimodal distributions created by post-polymerization blending. The results indicated that in-situ bimodal MWD offered superior values of PSA properties when compared to either monomodal MWD or post-polymerization blends. Viscoelastic analysis of the in-situ bimodal MWD samples showed that the proposed approach can effectively vary the MWD and crosslinking densities of the resulting PSAs, thus tailoring the final properties. In comparison, the in-situ bimodal PSD latexes did not show significant differences in viscoelastic behaviour but exhibited large differences in PSA properties.

Keywords: Miniemulsion polymerization, methyl methacrylate, 2-ethyl hexyl acrylate, pressure-sensitive adhesives, bimodal, particle size distributions, molecular weight distributions

6.1 INTRODUCTION

Pressure sensitive adhesives (PSA) are used in applications ranging from ordinary tapes and labels to highly complex structures such as those used in drug delivery technology (Satas, 1989).Their ability to adhere to practically any surface with slight pressure, commonly referred to as tack, is likely the main reason for the extensive application of this category of adhesives (Pressure Sensitive Tape Council, 2004). Up until very recently, they were most commonly produced using solution polymerization, a process that requires the monomers to be reacted in a solvent such as toluene or xylene, among others. They can also be produced by water-based polymerization (e.g., suspension, conventional emulsion, microemulsion and miniemulsion polymerization), where the monomers are dispersed in water as opposed to organic solvents, making these techniques more environmentally friendly. Stringent environmental regulations have influenced a push towards the reduction of volatile organic compounds in PSA products. As a consequence, a great deal of research has been carried out to attempt to understand the differences in the microstructure of polymers formed by solvent-based versus water-based polymerizations (Tobing and Klein, 2000; Tobing and Klein, 2001b).

In addition to tack, which represents the ability of an adhesive to bond to a substrate, PSAs must exhibit a certain peel strength (i.e., the ability to debond easily from the substrate) and shear strength (i.e., the cohesive strength to resist flow and be removed without leaving a residue) (Satas, 1989). This set of properties is usually tailored to a specific application through adjustment of the molecular microstructure. In the case of water-based polymerization, this is achieved by modification of the molecular features [molecular weight distribution (MWD), glass transition temperature (T_g), entanglement molecular weight (M_e) and molecular weight between crosslinks (M_c)] (Jovanovic and Dubé, 2004) as well as the particle size distribution (PSD). While the PSD mainly influences film formation and latex viscosity (Schneider et al., 2002a), it has also been shown to affect adhesive properties (Roberge and Dubé, 2006; Qu et al., 2009). Nevertheless, care should be taken when modifying the molecular microstructure as, most often, increasing the properties associated with adhesion (tack and peel strength) tends to decrease cohesion (shear strength) (Satas, 1989).

In order to compensate for the decrease in cohesion, it has been suggested that a small fraction of high molecular weight material can make a substantial contribution to shear strength (Satas, 1989). A number of studies have reported on the influence of broad (Baus and Swift, 1985) or blended multimodal (O'Connor and Willenbacher, 2004) MWDs on different polymer or adhesive properties. A comparison of adhesive properties for films produced from latex blends to achieve a bimodal MWD with films produced from latexes with an "in-reaction" bimodal MWD showed that the latter yielded better PSA properties (Elizalde et al., 2002).

There are several means to produce multimodal MWDs besides post-polymerization blending. These include various semi-batch monomer-feed strategies (Sayer et al., 2000; Vicente et al., 2001) as well as sequential polymerization processes (Lenzi et al., 2005). Ouzineb et al. (2004) presented an approach using a miniemulsion/semi-batch emulsion polymerization technique to create latexes with high molecular weight followed by the addition of another miniemulsion to create the low molecular weight portion of the same polymer.

Broad or multimodal PSD latexes offer advantages over narrow PSD latexes such as high solids contents and reduced viscosity (Schneider et al., 2002b). Multimodal distributions have been achieved by post-polymerization blending of two or more latex types (i.e., different particle sizes) into a film so that the desired final PSA properties are achieved (Steward et al., 2000). Latexes with bimodal PSDs have been shown to exhibit improved rheological and film formation properties compared to their monomodal counterparts (Geurts et al., 1996; Peters et al., 1996). The influence of the latex PSD of model acrylic PSAs with monomodal and post-polymerization blended bimodal PSDs on tack was studied (do Amaral et al., 2005). Blends with 40 wt.-% or more of small particles yielded films with superior adhesive properties compared to that of the parent monomodal particle distributions. However, the M_w of the two particle populations they produced were different. Nevertheless, for a fixed copolymer composition, it was possible to influence the adhesive properties by changing the latex PSD. A number of approaches have been investigated to produce multimodal PSD systems without post-polymerization blending such as seeded semi-batch processes (Chu et al., 1998a; Chu et al., 1998b; Chu et al., 1998c; Schneider et al., 2002b),

unseeded multi-step processes (Boutti et al., 2005) and by exploiting miniemulsion polymerization techniques (Ouzineb et al., 2005).

Jovanovic et al. (Jovanovic et al., 2004b) compared the PSA performance of latexes prepared by either conventional emulsion or miniemulsion polymerization. Although they were successful in creating bimodal MWD/PSD latexes, the peaks of particle size and molecular weight obtained by conventional emulsion and miniemulsion were different and thus, it was not easy to discriminate between the effects that a different PSD or MWD had on these PSA properties. Overall, these studies showed that it is possible to affect the PSA performance through careful modification of the multimodal PSD or MWD. They also showed that multimodal distributions generated during the reaction produced higher tack, peel and shear strength values compared to latex blends. However, the decoupling of the MWD and PSD effects on PSA properties has yet to be studied.

Miniemulsion polymerization is especially attractive for the production of latexes since it can provide a means to finely control the MWD and PSD due to its nucleation mechanism (Ouzineb et al., 2003; Ouzineb et al., 2004). Miniemulsion polymerization differs from conventional emulsion polymerization in that the reaction proceeds under droplet nucleation conditions and not via micellar or homogeneous nucleation. Proceeding under droplet nucleation conditions favours so-called compartmentalization in miniemulsion polymerization, which refers to a maximization of the intra- and extra-particle monomer diffusion resistance. A properly-formulated miniemulsion is able to reach a kinetically-stable state in which the nanometre-sized monomer droplets act as nano-reactors and diffusion of monomer through the aqueous phase could be minimized (Landfester et al., 1999). It is this characteristic that could allow for the production of a bimodal MWD or PSD in situ without the need of multiple seeds. Some of the added benefits of miniemulsion polymerization over conventional emulsion polymerization are the production of moderate solids content latexes in one-step polymerizations and the encapsulation of hydrophobic materials such as highly water-insoluble monomers as well as pigments and dyes (Asua, 2002).

In this work, a one-pot two-step miniemulsion polymerization strategy is presented for the production of bimodal MWD or bimodal PSD latexes. The impact of the bimodal MWD or PSD on PSA properties is presented. As opposed to previous studies, the initial

reaction conditions were carefully designed so that for bimodal PSD latexes, the molecular weight and gel fraction were identical for small and large particles. Similarly, for the bimodal MWD latexes, the surfactant and monomer concentrations were carefully selected to produce identical particle diameters for the low and high molecular weight polymer fractions. Thus, the effects of the MWD and PSD on PSA properties were decoupled.

6.2 EXPERIMENTAL DETAILS

6.2.1 Materials

All of the materials were reagent grade, were used as supplied by the manufacturer, and were obtained from Sigma Aldrich, unless otherwise indicated. The monomers were 2-ethyl hexyl acrylate (EHA), methyl methacrylate (MMA) and acrylic acid (AA). Octadecyl acrylate (ODA) was used as the polymerizable hydrophobe and 1-dodecanethiol (DDM) as the chain transfer agent. The ionic surfactant was sodium dodecyl sulphate (SDS) (GC grade) and the non-ionic surfactant was Disponil A3065 donated by Cognis Canada. Sodium bicarbonate ($NaHCO_3$) was used as a buffer. Distilled deionized water (DDI H_2O) was used throughout the study.

6.2.2 Preparation of the miniemulsion

ODA, DDM and the three monomers (EHA, MMA and AA) were mixed until they formed a homogeneous, clear solution. Disponil A3065, SDS and $NaHCO_3$ were dissolved in DDI H_2O. Subsequently, the organic phase was added slowly to the aqueous phase and stirred until the emulsion appeared as a milky solution. 100 mL-batches were then sonicated in an ice-bath for 4 min each at an output amplitude level of 9 using a Fisher Scientific Sonicator Model 550. Finally, the total volume was combined in one vessel.

6.2.3 Polymerization procedure for bimodal molecular weight distributions

The polymerization reactions were performed in a 1.1 L Labmax™ automated stainless steel reactor (Mettler Toledo) equipped with a stirrer, condenser and three feed ports. The two miniemulsions, each with different CTA concentrations, were prepared

separately prior to the reaction. The first miniemulsion was charged to the reactor and heated while stirring. Nitrogen gas was bubbled through the reaction mixture to remove any dissolved oxygen. The temperature and stirring speed were automatically controlled at 70°C and 200 rpm, respectively. The reaction was initiated with a single shot of the initiator solution. The first miniemulsion was left to polymerize for 180 min, after which time the second miniemulsion was added to the reactor with a second shot of initiator solution. The total reaction volume was then left to polymerize for an additional 180 min. It is important to note that the second miniemulsion was not a seed but rather a miniemulsion. The resulting latexes will be referred to as in-situ bimodal MWD latexes to distinguish them from typical post-polymerization blends. The five latexes in this set of experiments are labelled HL (high/low M_w). The two monomodal MWD latexes are considered the extremes and are labelled as HL1 and HL5. The three bimodal MWD latexes are referred to as HL2, HL3 and HL4 depending on the formulation.

All the miniemulsion polymerizations carried out in this study were prepared using the recipe shown in Table 6.1. The monomer composition and the ODA concentration (which acted as the hydrophobic compound delaying Ostwald ripening) were kept constant. The difference in terms of preparation between miniemulsions with high M_w and miniemulsions with low M_w lay solely in the CTA concentration, i.e., the first miniemulsion contained no CTA while the second contained 0.5 phm CTA, as shown in Table 6.1.

6.2.4 Polymerization procedure for bimodal particle size distributions

The polymerization reactions to produce latexes with a bimodal PSD were performed in the same reactor as mentioned above (see Table 6.1). The first miniemulsion was prepared to produce monomer droplets with a diameter of ~200 nm. This miniemulsion was charged to the reactor, heated to 70°C and the reaction was initiated with an initiator shot. The miniemulsion was left to polymerize for 180 min and at this point, monomer and surfactant solutions (cf. Table 6.1) were fed semi-continuously until the required particle diameter was achieved (~450 nm). The second miniemulsion with an average monomer droplet diameter of ~200 nm was then charged to the reactor and the polymerization continued for 180 min. Similar to the bimodal MWD case, the five latexes of this set are labelled LS (large/small

D_p). The two monomodal PSD latexes are referred to as LS1 and LS5, while the three bimodal PSD latexes are referred to as LS2, LS3 and LS4.

Table 6.1. Bimodal MWD and PSD : detailed experimental recipes

		First population	Second population	
		Step 1	Step 2	
Bimodal MWD	EHA [wt.-%]	63.0	63.0	
	MMA [wt.-%]	35.0	35.0	
	AA [wt.-%]	2.0	2.0	
	ODA [phm]	4.0	4.0	
	DDM	0	0.5	
	SDS [phm]	0.09	0.09	
	Disponil A3065 [phm]	4.57	4.57	
	$NaHCO_3$ [phm]	0.15	0.15	
	APS [phm]	0.30	0.30	
		First population		Second population
		Step 1	Step 2	Step 3
Bimodal PSD	EHA [wt.-%]	63.0	63.0	63.0
	MMA [wt.-%]	35.0	35.0	35.0
	AA [wt.-%]	2.0	2.0	2.0
	ODA [phm]	4.0	0.0	4.0
	DDM	0.20	0.30	0.20
	SDS [phm]	0.09	0.0	0.09
	Disponil A3065 [phm]	4.57	1.20	4.57
	$NaHCO_3$ [phm]	0.15	0.15	0.15
	APS [phm]	0.30	0.40	0.30

6.2.5 Sample characterization

Monomer conversion was obtained using conventional gravimetric procedures. Droplet and particle sizes were obtained using a NanoS Dynamic Light Scattering instrument (Malvern Instruments) with a scattering angle of 174° for the monomodal distributions and a

Laser Diffraction LS 13320 multi wavelength particle analyzer (Beckman Coulter) for the bimodal particle size distributions. The polydispersity indices given throughout this study are those reported by the Malvern dynamic light scattering instrument and are not the same as those reported more commonly elsewhere. The polydispersity indices given by this instrument indicate that a family of particles with a polydispersity under 0.01 is considered being monodisperse. MWDs were analyzed by Gel Permeation Chromatography (Fonseca et al., 2008). The universal calibration curve included a set of standards (EasiCal from Polymer Laboratories) with a range of 162 to 6,035,000 g/mol. The values of K and alpha used for EHA were 1.24 $x10^{-4}$ dL/g and 0.67 while those for MMA were 1.28 $x10^{-4}$ dL/g and 0.69, respectively (Lathova et al., 1993; Hua and Dubé, 2001).

Gel fraction was analyzed on the final latex samples. 200 mg of dry polymer was placed in a pouch formed by two 25 mm-diameter PTFE membranes with a pore size of 0.2 μm. The membranes were heat sealed and placed in a glass jar with 50 mL of THF. The jars were placed in a shaker for at least 48 h after which time the pouches were removed and allowed to dry. The gel fraction was calculated from the difference between the final and initial weight of the polymer. T_g was determined using a Differential Scanning Calorimeter (DSC) Model Q1000 (TA Instruments). The analysis was performed using a modulated DSC method with modulation amplitude of ± 1°C every 60 s. The sample was cooled to -80°C and followed by a heating ramp of 2°C/min. The T_g was calculated from the inflection point in the Reversed Heat Flow curve using the software provided. If the transition was broad and thus, the result ambiguous, the T_g was taken as the peak in the curve of the derivative heat capacity (C_p). Mastercurves and temperature sweeps were carried out by Dynamic Mechanical Analysis (DMA) (Rheometrics RDA III).

Tack, peel strength and shear strength were measured according to the Pressure Sensitive Tape Council standards PSTC-6, PSTC-1 and PSTC-7, respectively (Pressure Sensitive Tape Council, 2004; Jovanovic et al., 2004a). The latex was filtered using glass wool and cast onto a 50 um Mylar® sheet. The cast film was dried at room temperature and conditioned for 24 h at standard conditions of temperature and humidity (23 ± 2°C and 50% ± 2 Relative Humidity).

6.3 RESULTS AND DISCUSSION

The key to a successful miniemulsion polymerization lies in the careful selection of the stabilization system, i.e., the surfactants, which protect the miniemulsion against coalescence, and the hydrophobic compound, which protects the miniemulsion against diffusional degradation such as Ostwald ripening. Certainly, a miniemulsion with a perfectly monodisperse droplet size distribution (DSD) would not require the presence of a hydrophobic compound since Ostwald ripening would not occur. Let us recall that Ostwald ripening is a direct consequence of the DSD: the larger the difference in droplet diameter (D_d), the larger will be the difference in chemical potential and consequently, Ostwald ripening would occur (Tauer, 2001). The miniemulsion DSD is critical in attaining a well-stabilized system. Subsequently, the key for droplet nucleation to prevail as the main nucleation mechanism is a miniemulsion with a narrow DSD. Figure 6.1 presents the initial DSD and the evolution of the PSD of a typical run in this study. All of the miniemulsion polymerizations exhibited the same trend as that shown in Figure 6.1.

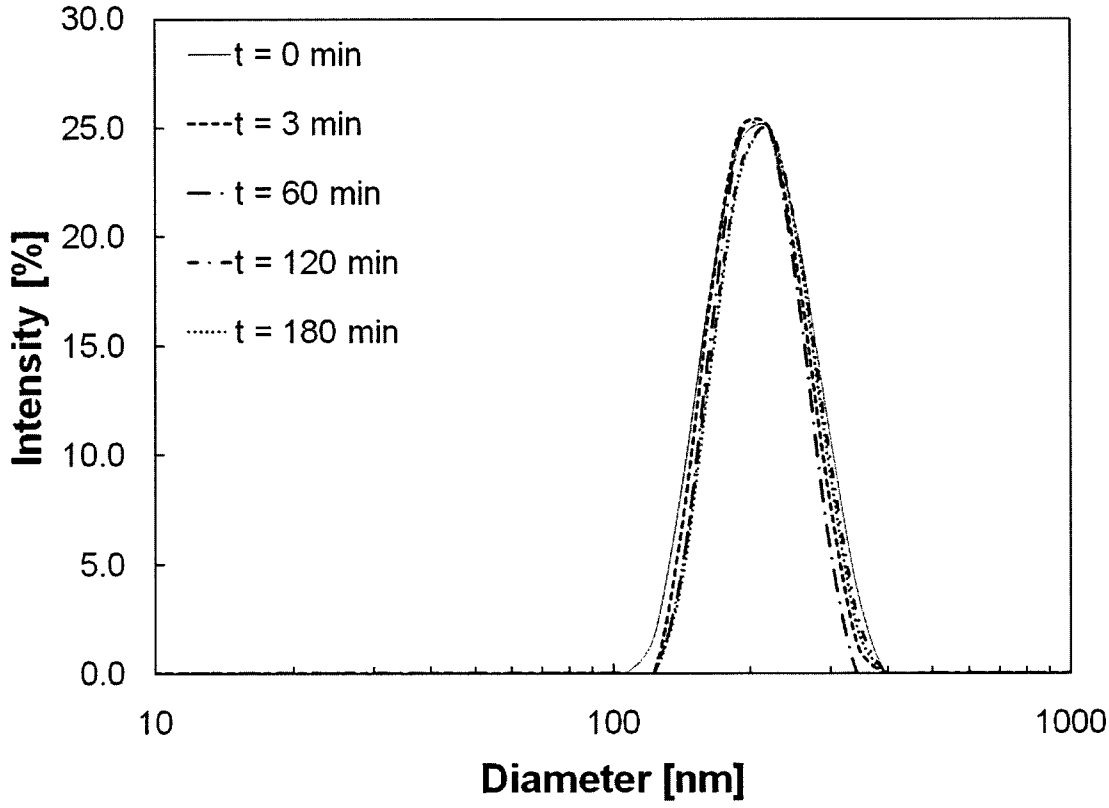

Figure 6.1. Droplet Size and Evolution of Particle Size Distribution of reaction HL1

The initial D_d of sample 't=0' (cf. Figure 6.1) is 202 nm and the average D_p did not change significantly throughout the reaction, exhibiting a final value of 220 nm. These results led us to presume that the reactions indeed proceeded via droplet nucleation since there was no indication of secondary nucleation despite the presence of MMA and AA (monomers with appreciable water solubility) and thus, this formulation was used for the production of bimodal distributions.

6.3.1 Bimodal Molecular Weight Distributions

Table 6.2 summarizes the weight fractions and the ratio between the number of particles with high M_w and low M_w. Our goal was to evaluate the influence of the concentration of high M_w domains (which would be expected to be highly elastic and provide high shear strength) and low M_w domains (which would be viscous and be able to dissipate energy easily) on PSA performance. As shown in Table6.2, three ratios were tested to assess the changes in viscoelastic behaviour and adhesive properties. Along with that of the bimodal MWD films, the properties of films cast from monomodal MWD latexes were measured. As mentioned earlier, the copolymer composition was fixed at 63/35/2 wt.-% EHA/MMA/AA so that the only observable effect on the PSA properties would be that of the molecular weight. In order to verify that the PSD did not change after addition of the second unreacted miniemulsion, the PSD was measured before and after charging the second miniemulsion. The miniemulsions were designed to have a D_p of approximately 200 nm and any significant deviation from this value would indicate that a "true" miniemulsion polymerization did not take place. The z-average D_d of the two miniemulsions were 210 and 213 nm, respectively. The sample taken just prior to the addition of the second miniemulsion presented a conversion of ~95 wt.-% and the D_p was equal to 218 nm. The next sample was taken 30 min after the addition of the second unreacted miniemulsion. Upon addition of the unreacted miniemulsion, the PSD did not show any indication of secondary nucleation, which would likely appear as smaller particles or as a broader distribution, i.e., the addition of the miniemulsion did not change the z-average diameter or the polydispersity. The DSD of the final sample of this latex was, in fact, close to that of the initial miniemulsion with a z-average diameter of 225 nm.

Table 6.2. Composition of latexes for the monomodal and in-situ bimodal distributions

	Run	Mass %[a] High M_w		Mass % Low M_w	
Bimodal MWD	HL1	100		0	
	HL2	75		25	
	HL3	50		50	
	HL4	25		75	
	HL5	0		100	
	Run	Mass %[a] Small D_p	Number % Small D_p	Mass % Large D_p	Number % Large D_p
Bimodal PSD	LS1	100	100	0	0
	LS2	27	75	73	25
	LS3	11	50	89	50
	LS4	4	25	96	75
	LS5	0	0	100	100

[a] The solids content of all miniemulsion-based latexes prepared was ~52 wt.% and since D_p's in the bimodal MWD latexes were equal, volume and number percentages were used interchangeably.

Figure 6.2 shows the final PSD of the in-situ bimodal MWD latexes as well as that of the monomodal MWD latexes. The PSDs of the latexes were all comparable, thus eliminating any effect that particle size could have on the PSA properties. Copolymer composition could also have an effect on the adhesive properties. Figure 6.3 shows the DSC thermographs of both monomodal and in-situ bimodal MWD polymers. There was no significant difference between the copolymer compositions of the five latexes, thus eliminating its influence. The monomodal and in-situ bimodal MWD of the five samples are shown in Figures 6.4a and b, respectively. As shown in Table 6.1, the monomodal MWD with low M_w polymer was produced using a CTA concentration of 0.5 phm producing a weight-average M_w of ~121,000 g/mol while the high M_w polymer was produced without the addition of CTA, giving a weight-average M_w of ~878,000 g/mol as seen in Figure 6.4a. The production of the in-situ bimodal MWD was carried out in two steps as outlined earlier. The first step involved a miniemulsion designed to produce a polymer with the same M_w as sample HL1 in Figure 6.4a. The reactor contents were allowed to react until most of the monomer in the first population had reacted. At this point, the second unreacted miniemulsion was introduced to the reactor. This miniemulsion was prepared to produce a polymer with the same M_w as sample HL5.

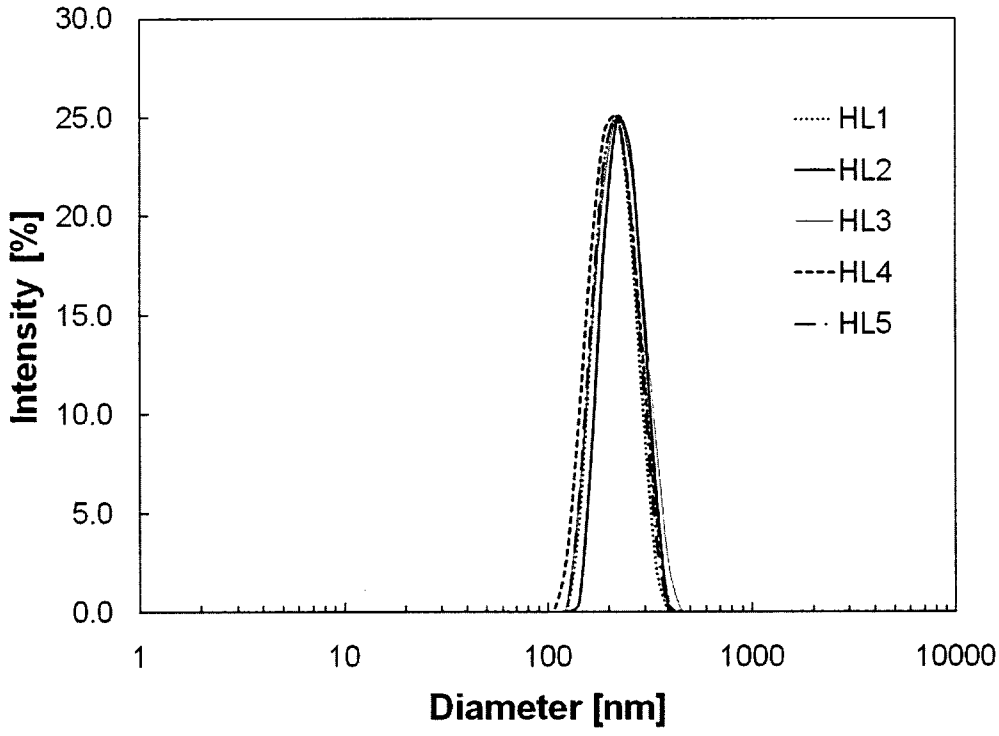

Figure 6.2. PSD of the bimodal MWD (HL2, HL3 and HL4) and monomodal MWD (HL1 and HL5)

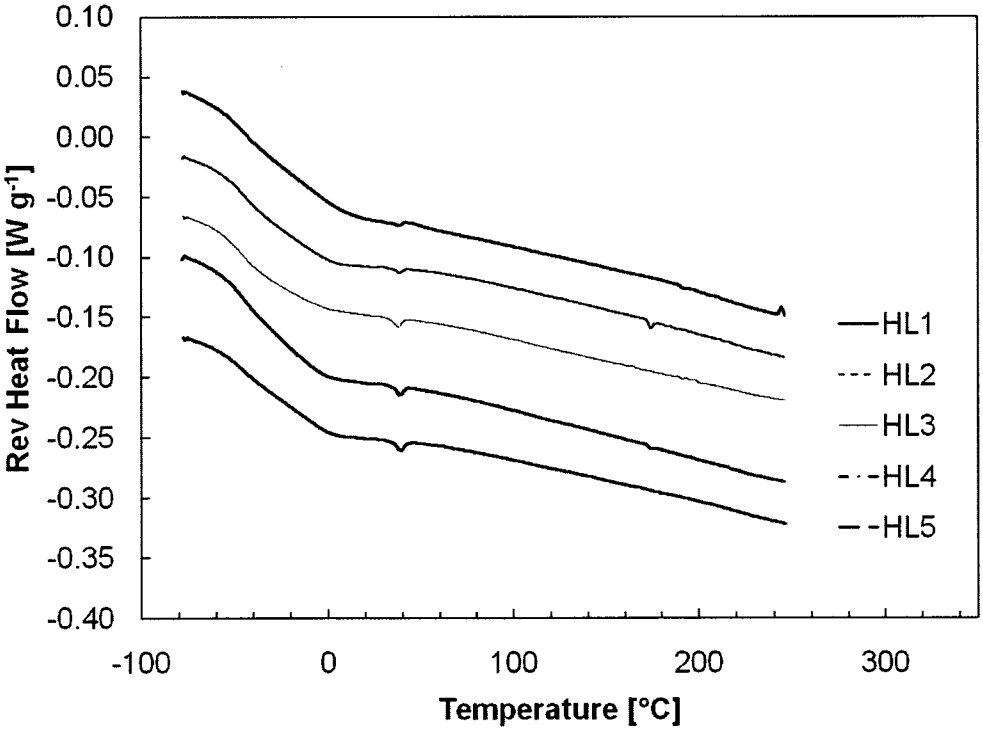

Figure 6.3. DSC thermographs of polymers with monomodal MWD (HL1 and HL5) and in-situ bimodal MWD (HL2, HL3, HL4)

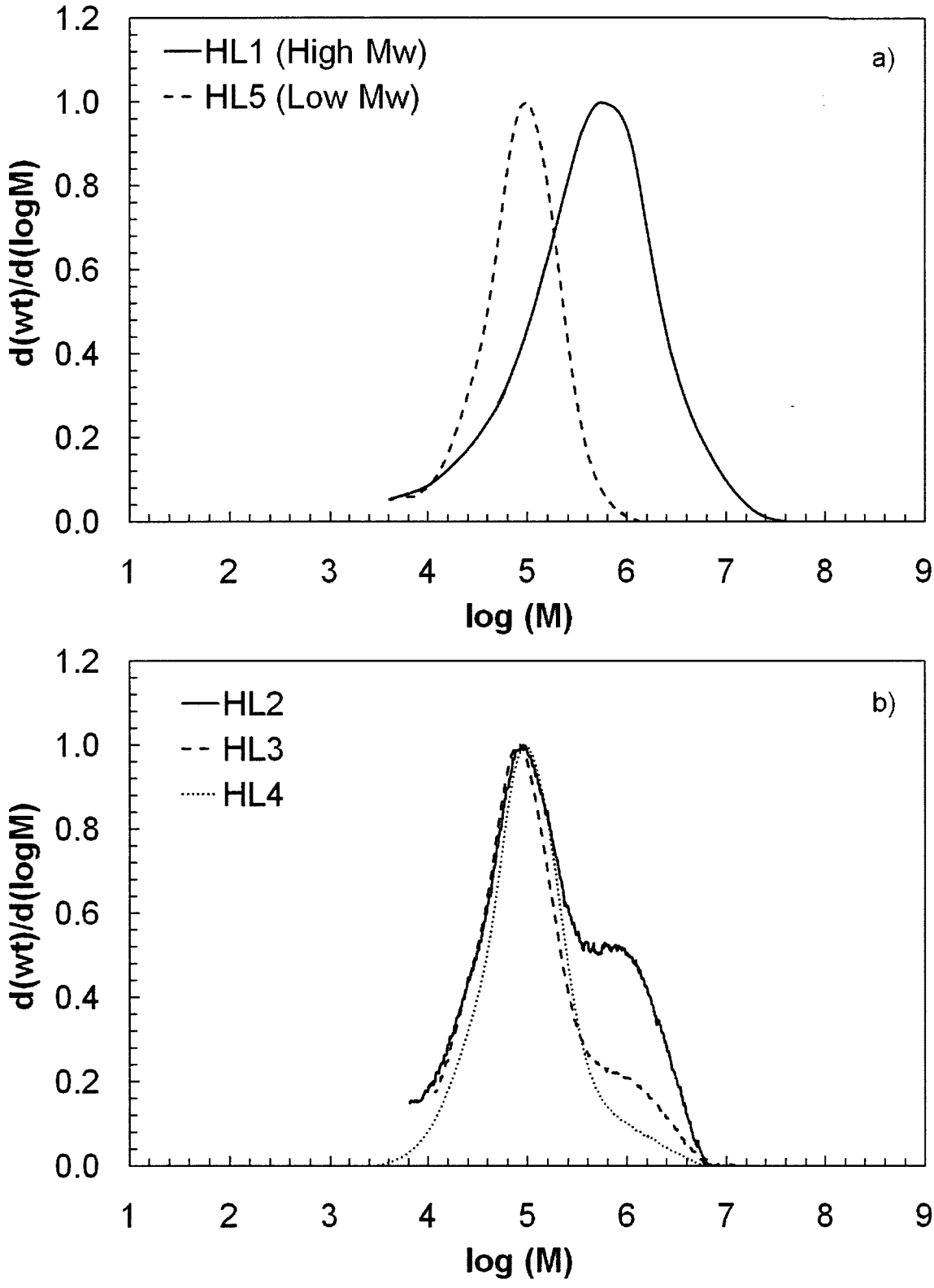

Figure 6.4. a) Monomodal MWD of runs HL1 (Low M_w) and HL5 (High M_w) and b) in-situ bimodal MWD of latexes HL2, HL3 and HL4 (Ratios of high-to-low M_w are 3, 1 and 0.3, respectively)

Figure 6.4b shows the GPC results of the in-situ bimodal MWD and offers two pieces of information. First, it shows that there was no transfer between the two populations of particles since the location of the two peaks in the in-situ bimodal MWDs corresponds to the location of the peaks obtained in the monomodal MWDs when only one population of particles was used. This was also corroborated by the PSD of the in-situ bimodal MWD latexes shown in Figure 6.2, which did not display evidence of transfer. Second, it also shows that the peak that corresponds to the high M_w decreases as the weight fraction decreases. However, the high M_w peak was also considerably smaller than the peak that corresponds to the low M_w even though the mass fraction (or N_p) in two of the runs was at least equal to or larger than the mass fraction of low M_w. In this case, this is due to the fact that no CTA was added to the high M_w miniemulsion, which in turn produced high gel fractions, which were likely separated from the fraction that is soluble in the GPC mobile phase solvent (in this case, tetrahydrofuran) during the sample preparation process. The peaks were also not completely separated from each other due to the relatively small difference between the two M_w's. However, the M_w's were chosen keeping in mind the final application as PSAs.

It is known that in water-borne acrylic polymers, intermolecular chain transfer to polymer contributes to the formation of gel fractions and this effect decreases in the presence of a CTA. Figure 6.5 shows the gel fractions for the monomodal and in-situ bimodal MWD polymer samples. The gel fraction of the monomodal MWD with high M_w (sample HL1) was ~0.56 and the gel fraction for the monomodal MWD with low M_w (sample HL5) was ~0.03. Gel fractions for the bimodal MWD had values in between these two extremes and gel fractions increased with the weight fraction of the high M_w particles, which was expected since the high M_w domains increased. These results were compared to gel fractions obtained for latexes with a bimodal MWD obtained by post-polymerization blending of latexes HL1 and HL5 using the same weight fractions as for the in-situ bimodal MWD. These samples are referred to as post-polymerization blends and the corresponding sample name is designated with an X.

Surprisingly, the results showed that the gel fractions of the post-polymerization blends were lower for samples HL2X and HL3X and about the same value for HL4X. Molecular weight and particle size results suggest that compartmentalization (referring to a

maximization of the intra- and extra-particle diffusion resistance) indeed took place or that it remained compartmentalized. However, it has been reported that the number of 'gel-forming events' increases with feeding time because the polymer chains are subjected for a longer period of time to the action of the radicals (Gonzalez et al., 2006). The difference in gel fractions between the "in-situ bimodal MWD" and the post-polymerization blends lies likely in the additional intermolecular chain transfer reactions of the population of particles that contained no CTA (high M_w particles), which remained inside the reactor for a longer period of time after the addition of the second miniemulsion.

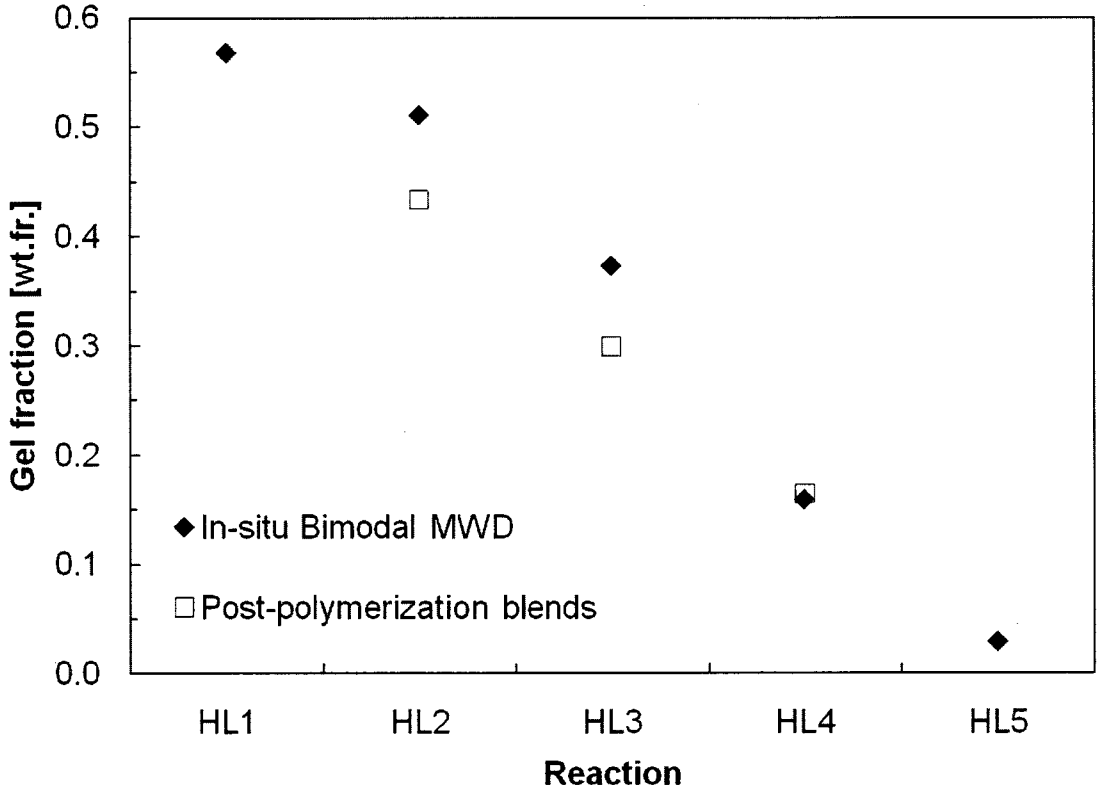

Figure 6.5. Gel fraction of in-situ bimodal MWD (filled diamonds) and post-polymerization blended bimodal MWD (empty squares)

Figures 6.6a and b show the storage (G') and loss shear modulus (G") for the monomodal and in-situ bimodal MWD. The transition region showed no significant variation between the different samples indicating similar copolymer compositions, which was consistent with DSC measurements. The differences between the five curves appeared exclusively in the rubbery plateau and terminal regions, where it is known that changes in M_w and MWD are strongly noticeable. One can see that the rubbery plateau region of sample

HL1 extended further to lower frequencies without a clear presence of the terminal region. The rubbery plateau region becomes more evident for samples HL2, HL3 and HL4 while sample HL5 showed a very short rubbery plateau region and decayed into the terminal region at a much higher frequency. These results indicate that sample HL1 had a higher M_w (which is also known from GPC measurements) and the absence of the terminal region gives an indication of a crosslinked structure (Ferry, 1980). G' sequentially decreased with lower weight fractions of the high M_w miniemulsion indicating that crosslinking sequentially decreased. It is beyond the aim of this study to quantify the molecular weight between crosslink points but the extent of crosslinking can be seen from the curves and qualitatively compared. From Figure 6.6a, one can see that G' in the rubbery plateau region of sample HL1 is higher than that for sample HL2. Both of them are crosslinked but HL1 is likely more crosslinked since its values of G' are higher and the terminal region starts to decay at a much lower frequency compared to sample HL2. Overall, the three bimodal MWD samples had characteristics of the high and low M_w monomodal MWD. It is expected that samples HL2, HL3 and HL4 offer the characteristics of, on the one hand, high compliance and good contact with the surface, while on the other hand, of a crosslinked network that will give the necessary cohesion.

Figures 6.7 to 6.9 present the results of the PSA properties (loop tack, peel strength and shear strength) for the monomodal MWD (grey bars), in-situ bimodal MWD (black bars) and post-polymerization bimodal MWD blends (white bars). As can be seen in Figure 6.7, the loop tack values of the films cast from monomodal MWD latexes were lower compared to those films cast from in-situ bimodal MWD latexes. The higher values of loop tack were attributed to two effects. The first effect was due to the bimodality of the MWD since all other factors had been kept constant (e.g., copolymer composition, D_p and adhesive testing conditions). Sample HL2 exhibited the highest loop tack values of the three samples at a ratio of high-to-low M_w of 3, which means that most of the polymer particles in sample HL2 had a very high M_w with only a portion of the particles with low M_w acting to provide a high compliance. Figure 6.7 also shows that loop tack values decreased as the weight fraction of low M_w increased. The second effect offered by these results is noticed when they are compared against the bimodal MWD prepared by post-polymerization blending, which

displayed a lower loop tack values. If the bimodality of the MWD was the only effect responsible for the higher values of loop tack, then it would be expected that the bimodal

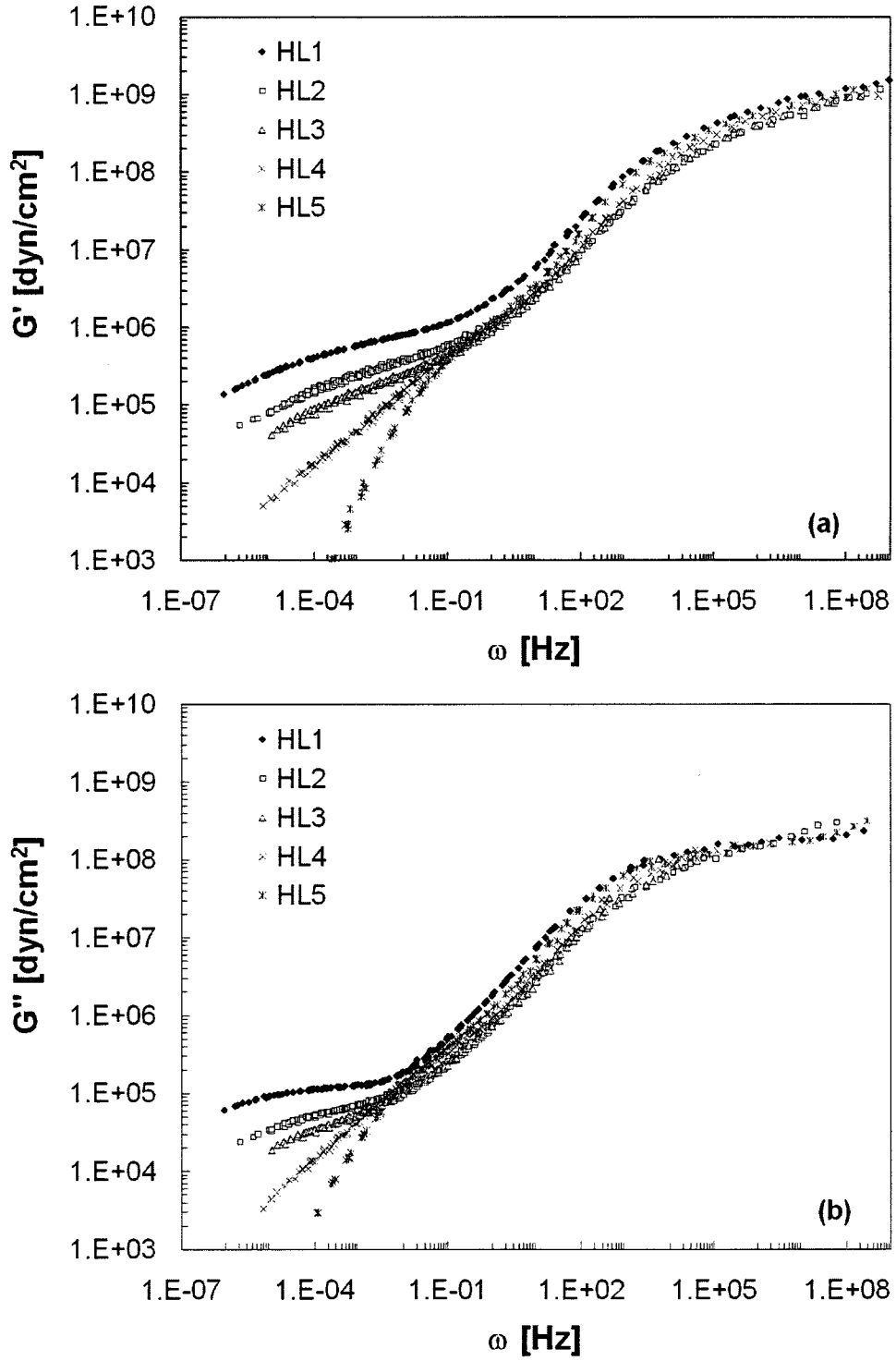

Figure 6.6. Frequency master curves of a) storage and b) loss modulus (G') for monomodal MWDs of high (HL1) and low M_w (HL5), and in-situ bimodal MWD (HL2, HL3 and HL4)

MWD latexes obtained by post-polymerization blending would have similar values. As can be observed in Figure 6.7, the post-polymerization blends had considerably lower values compared to the in-situ bimodal MWD samples. This behaviour was likely due to the lower gel fraction observed earlier. In general, the results observed for the in-situ bimodal MWD samples are due to a combined effect of the bimodality of the distribution and the in-situ process itself, which led to higher gel fractions. Both characteristics improved loop tack values.

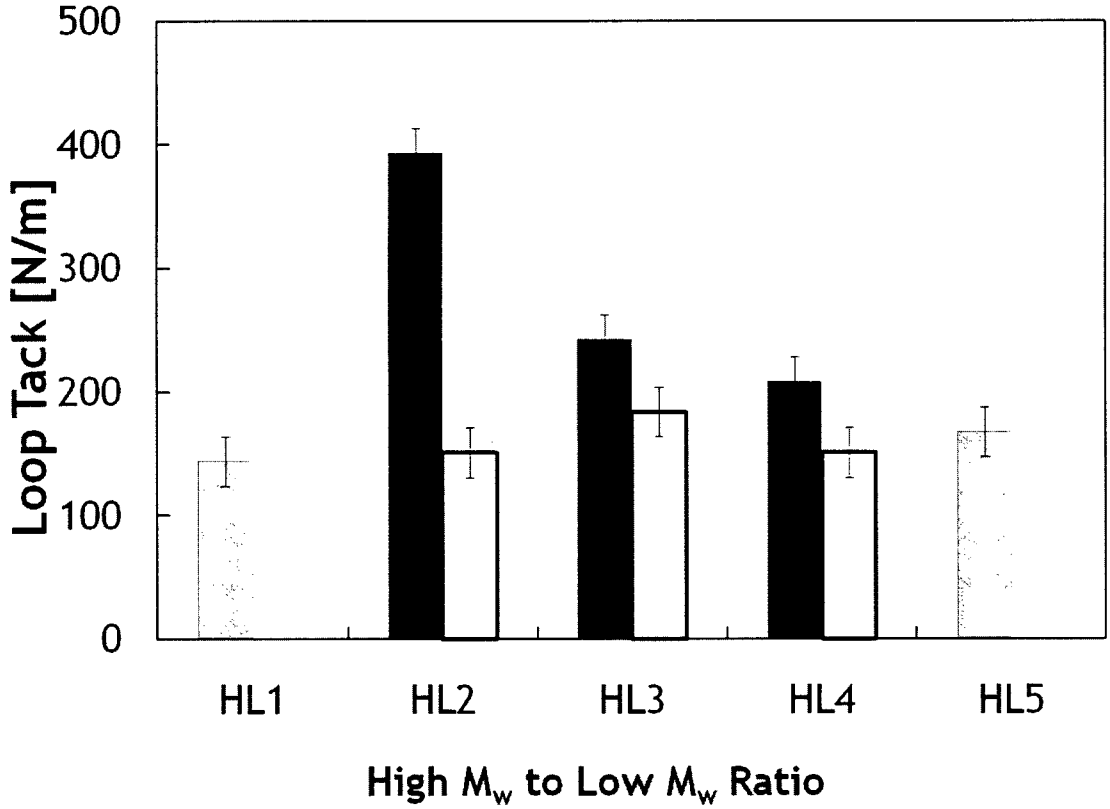

Figure 6.7. Loop Tack results for monomodal MWD (grey), in-situ bimodal MWD (black) and post-polymerization blended bimodal MWD (white). Ratios represent the N_p of High M_w by N_p of low M_w

Similarly, Figure 6.8 shows the peel strength results for the in-situ bimodal MWD samples (black bars), post-polymerization blends (white bars) and monomodal MWD (grey bars) samples. The difference in peel strength between the two monomodal MWD samples (HL1 and HL5) was clearly due to their M_w and gel fraction, where HL1 presented a much higher value of both, M_w and gel fraction, effectively decreasing the peel strength (Satas,

1989). The in-situ bimodal MWD samples, on the other hand, displayed significantly higher values of peel strength, which is again attributed to the bimodality of the MWD and gel fractions. The sample with the lowest weight fraction of low M_w particles (i.e., HL4) displayed the highest peel strength. In this sample, the low M_w domains acted as a plasticizer. The low M_w domains and a gel fraction of 0.16 were sufficient to provide cohesive strength but not high enough to provide high levels of crosslinking (Plessis et al., 2001), which would markedly diminish peel strength as also observed in the viscoelastic measurements. As crosslinking levels presumably increased (cf. Figure 6.6a and b) with higher weight fractions of the high M_w domains, peel strength values clearly decreased. The post-polymerization bimodal MWD blends exhibited lower values of peel strength compared to the in-situ bimodal MWD samples.

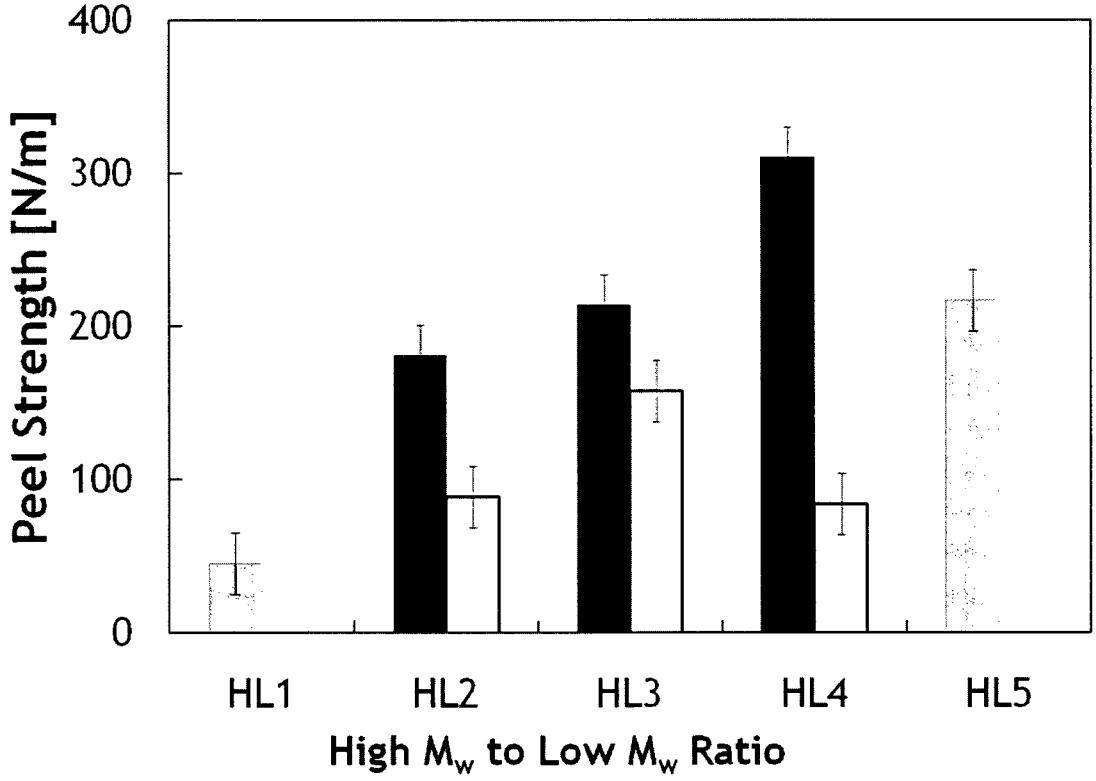

Figure 6.8. Peel Strength results for monomodal MWD (grey), in-situ bimodal MWD (black) and post-polymerization blended bimodal MWD (white). Ratios represent the N_p of High M_w by N_p of low M_w

Finally, Figure 6.9 shows the results of shear strength for the three types of samples: monomodal, in-situ bimodal MWD and post-polymerization blended bimodal MWD. It is

known that shear strength is directly proportional to the amount of crosslinking and entanglement (Tobing and Klein, 2001). It has also been reported that the concentration of CTA has a strong influence on the static shear strength (Gower and Shanks, 2004). As can be observed in Figure 6.9, shear strength values decreased as the weight fraction of high M_w particles decreased, i.e., as gel fractions became small. The results showed that the PSA properties can be tailored and improved using the approach proposed herein.

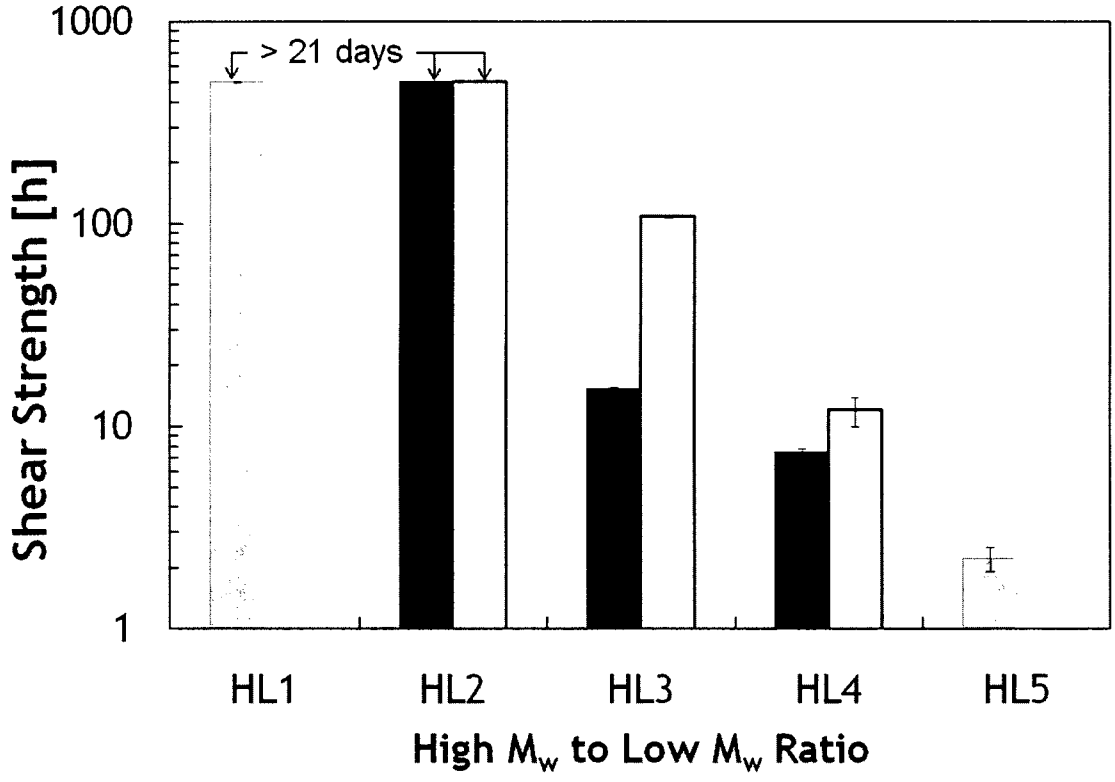

Figure 6.9. Shear Strength results for monomodal MWD (grey), in-situ bimodal MWD (black) and post-polymerization blended bimodal MWD (white). Ratios represent the N_p of High M_w by N_p of low M_w

6.3.2 Bimodal Particle Size Distributions

Once it was established that miniemulsion polymerization facilitated the production of bimodal MWD latexes, bimodal PSD latexes were also produced using a similar, three-step one-pot miniemulsion polymerization approach (cf. Table 6.1). A miniemulsion with a small D_d (~200 nm) was prepared first and charged to the reactor. Once the particles reached a high conversion (>95 wt.-%), additional monomer and surfactants were added in a semi-continuous fashion to increase the D_p to ~450 nm. As soon as the particles reached the

specified diameter, a second miniemulsion with a small D_d (~200 nm) was loaded to the reactor and the two populations (i.e., small and large D_p particles) were left to polymerize to full conversion. Table 6.1 in the experimental section shows the recipe for the production of the bimodal PSD.

In order to test the influence of having more or less small D_p particles, similarly as in the bimodal MWD case, three ratios of small to large D_p particles were tested and the corresponding weight fractions are shown in Table 6.2. The CTA concentrations were adjusted to produce medium weight-average M_w gel-free samples (gel fraction of ~3 wt.-%) that would still ensure good PSAs properties but with the same MWD in both, small and large D_p particle populations. A change in the MWD would likely affect the PSA properties (Chauvet et al., 2005) and it would not be possible to differentiate between the effect of the MWD and that of the PSD. It is known that a certain amount of gel is required to produce PSAs. Moreover, any significant difference between the crosslinking of two given samples would difficult our understanding of the influence of particle size. Figure 6.10 shows the MWD of the five samples, i.e., the monomodal PSD of small and large D_p and the in-situ bimodal PSD. Finally, the copolymer composition was another aspect that was carefully considered in the preparation of the bimodal PSD. There were not observable deviations in the T_g of the three in-situ bimodal PSD latexes measured by DSC (not shown here).

The initial miniemulsion followed the same PSD trend as that exhibited previously for the bimodal MWD case (cf. Figure 6.1) and it is thus not shown again here. Figure 6.11 shows the final PSDs of the small and large D_p populations. The difference between the two D_p's was constrained by the typical particles sizes used in PSA applications which ranged from 100 to 1000 nm (Benedek, 2004). The average D_p for the two populations were 167 nm and 310 nm, respectively. These values were obtained using a laser diffraction multi wavelength particle analyzer (Beckman Coulter). The PSD of monomodal PSD samples were analyzed using a dynamic light scattering instrument (Malvern Instrument). The D_p's obtained using the laser diffraction multi wavelength particle analyzer were smaller than the measurements carried out previously by dynamic light scattering (such as the PSD reported earlier in this study), which has been observed before (Schneider and McKenna, 2002).

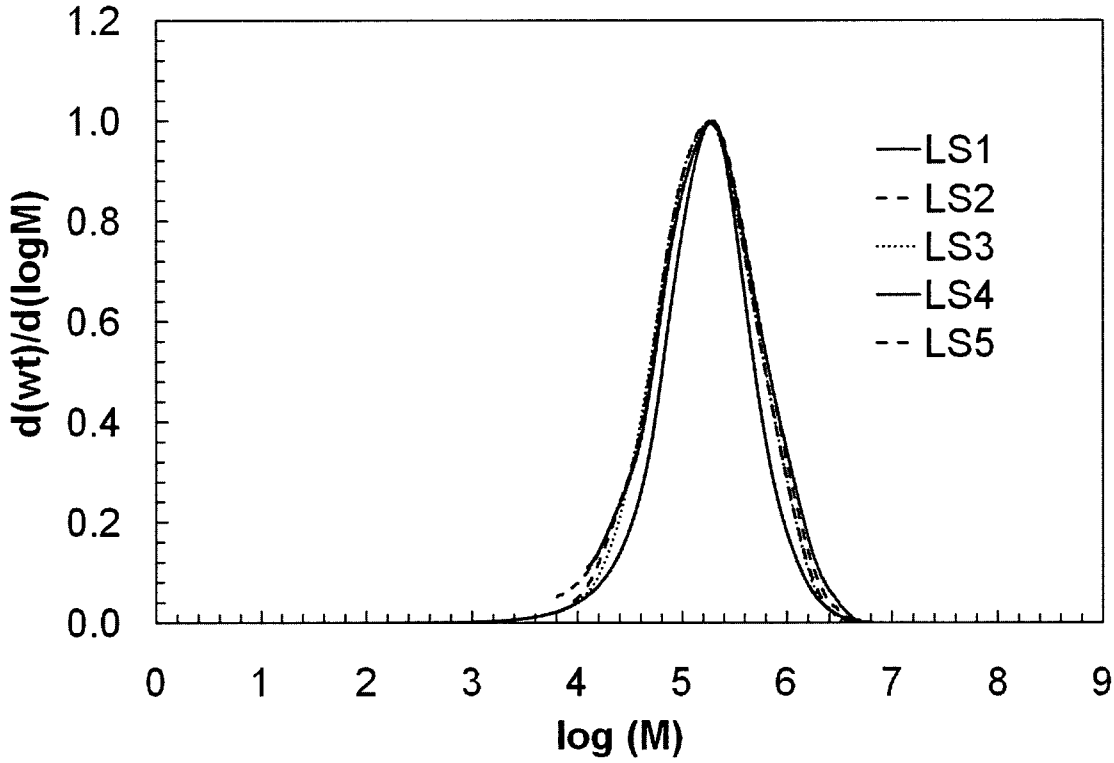

Figure 6.10. MWD of monomodal PSD for the small (LS1) and large (LS5) particle diameters and in-situ bimodal PSDs (LS2, LS3, LS4)

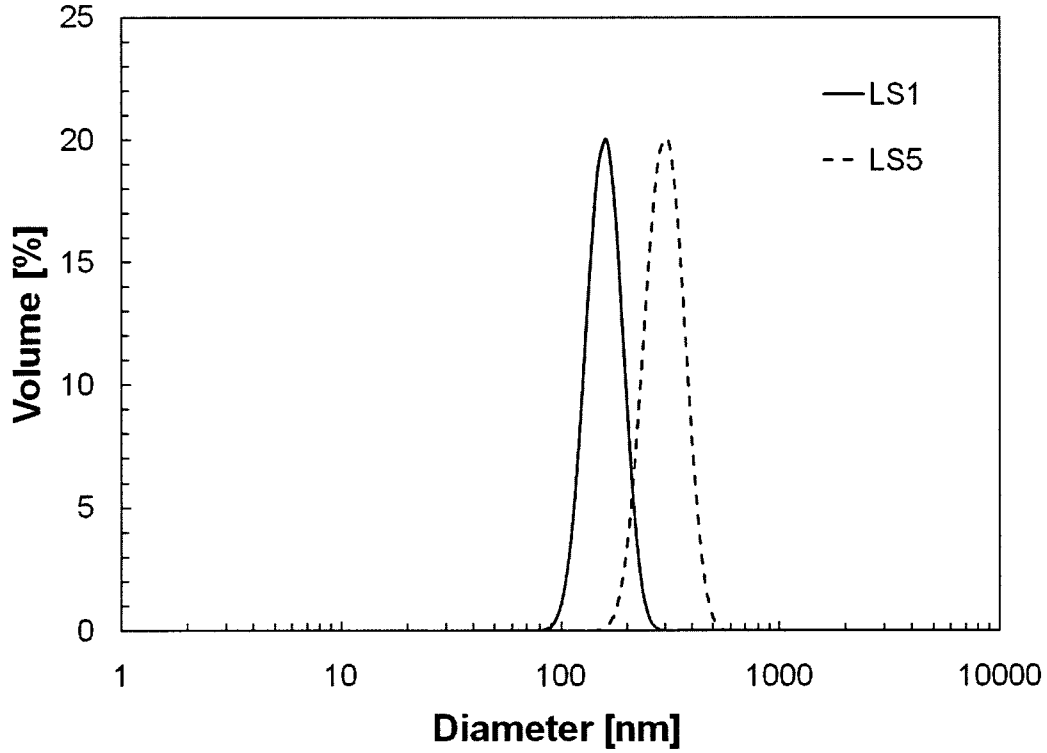

Figure 6.11. Particle size distribution of small D_p (LS1) and large D_p (LS5) polymer particles prepared by miniemulsion polymerization

Figure 6.12 shows the particle size analysis of the three samples with in-situ bimodal PSD. As can be observed in the plot, the samples with 75 and 50% in number (or 27 and 11 wt.-%) of small D_p particles were evidently bimodal distributions. However, sample LS4 did not exhibit a peak of the smaller D_p particles possibly due to the fact that this sample contained the lowest weight percentage of the small D_p particles (4 wt.-%). It is likely that the amount of these particles was low enough to avoid detection by the laser diffraction instrument.

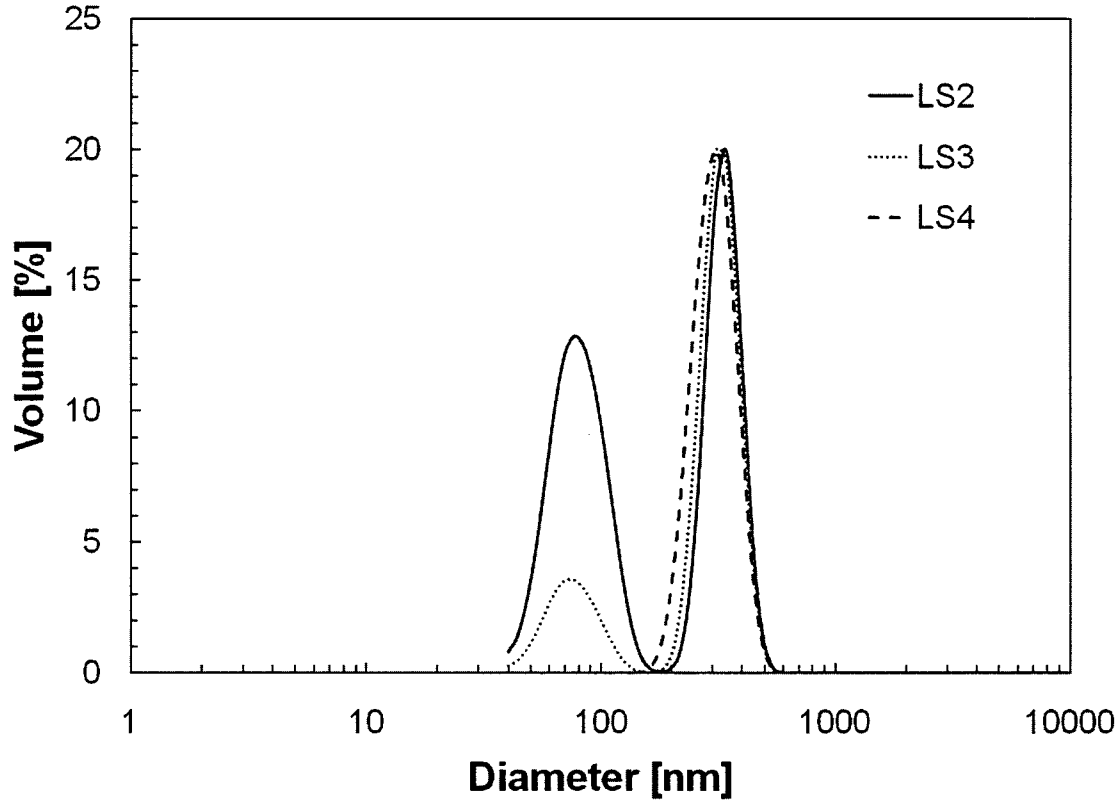

Figure 6.12. Particle size distribution of in-situ bimodal latexes (LS4, LS3 and LS2)

Once it was confirmed that the latexes had indeed a bimodal PSD, the viscoelastic and adhesive behaviours were measured. Figure 6.13 showed G' and G" of the monomodal PSD of the small (LS1) and large (LS5) D_p's and of the in-situ bimodal PSDs. Surprisingly, there was no difference in the viscoelastic behaviour in the transition, rubbery plateau or terminal region of the samples analyzed. These results differ from those found by do Amaral et al. (do Amaral et al., 2005), who found a significant difference between the viscoelastic

behaviour of post-polymerization latex blends prepared from small D_p and large D_p latexes. However, it is difficult to draw conclusions from their study since the adhesives were prepared by two different polymerization techniques (conventional emulsion and miniemulsion polymerization), which produced two different MWDs and likely two different microstructures. Since the rheology is very sensitive towards M_w and MWD (Benedek, 2004), it is clear that in this study, all of the samples had the same M_w and MWD and particle size did not contribute to their viscoelastic behaviour. In other words, all the particles (large and small) had the same bulk properties.

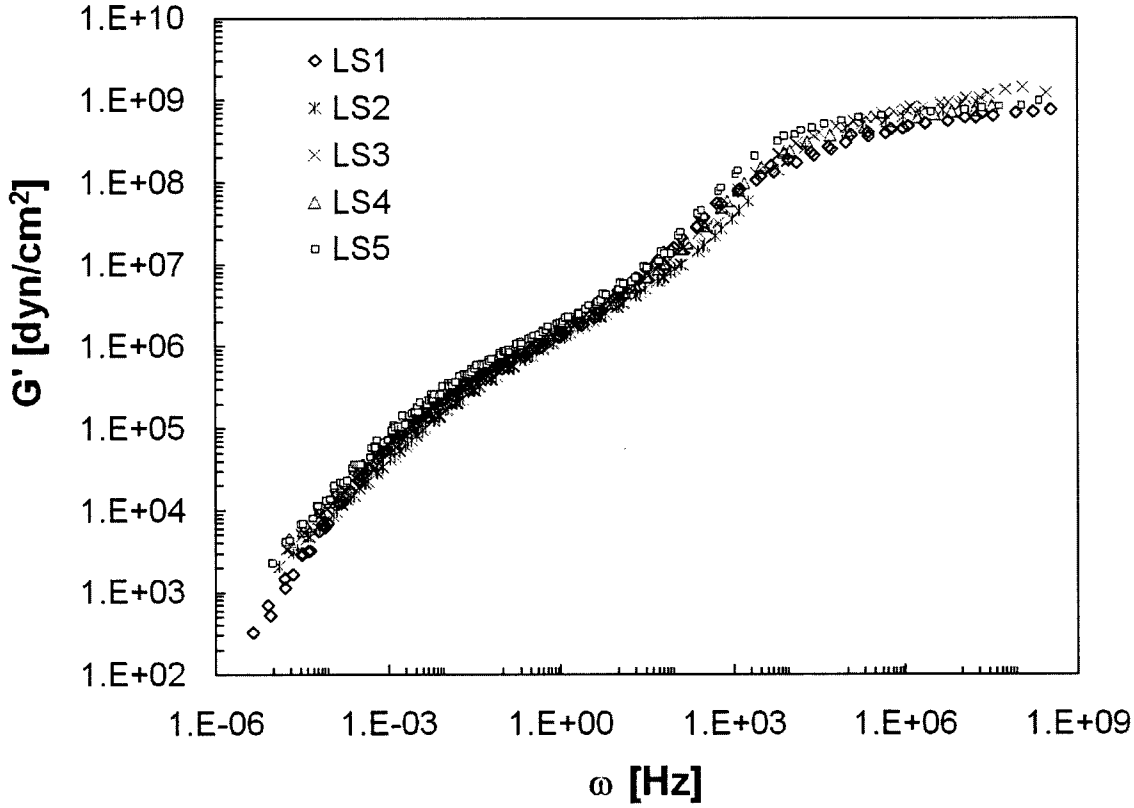

Figure 6.13. Frequency master curves of storage modulus (G') for polymer with monomodal PSD of small D_p (LS1) and large D_p (LS5) and for polymers with in-situ bimodal PSD

Figures 6.14 to 6.16 show the results of the PSA properties of the monomodal, in-situ bimodal and post-polymerization blended bimodal PSDs latexes. As can be observed, while loop tack and shear strength exhibited considerable differences between the three types of latexes, this was not the case for peel strength, either for in-situ bimodal or post-polymerization blended bimodal PSDs. Differences were only encountered between the peel strength of monomodal small and large D_p latexes. Even though the overall copolymer

composition, gel content and MWD were the same for all the latexes studied herein, it is likely that the semi-continuous feeding stage introduced different compositional drift in the larger particles. It is evident from Figure 6.14 that the latexes with smaller particles gave lower values of loop tack compared to the larger particles. As well, it was those blends with the highest number of large particles that resulted in much larger values of loop tack. Moreover, the values of loop tack of films cast from in-situ bimodal PSD latexes were larger than the post-polymerization blend bimodal PSD latexes. However, as can be seen in Figure 6.14, the values of loop tack for the bimodal PSD latexes were not an average of the loop tack values obtained for the two monomodal PSDs. Since the viscoelastic behaviour shows no difference between the samples analyzed, i.e., the PSD (either monomodal or bimodal) had no effect on the viscoelastic behaviour (not to be confused with the influence that PSD has on the latex rheology which is of large industrial importance), the differences in the resulting values of loop tack are likely due to an interfacial phenomena. In terms of film formation, it has been reported that smaller particles deform faster and take less time to fill interstitial voids while larger particles showed only superficial deformation in the same time frame because in larger particles, the polymer chains have to flow over longer distances (Eckersley and Rudin, 1996; DuChesne et al., 1999). This means that the three bimodal PSD latexes prepared in this study led to various film formation paths and thus, different particle surfaces which in turn affected loop tack. It has to be also considered that small and large particles could contain different surfactant amounts. Even though, the polymerization was designed to cover approximately the same surface area for both diameters, it is acknowledged that larger particles had a larger monomer to surfactant ratio compared to the smaller particles (39 versus 22). Nevertheless, the monomer to surfactant ratios between the three in-situ bimodal PSD latexes and their respective post-polymerization blends counterparts should be equal and thus, the monomer to surfactant ratios *per se* did not account for the differences observed. It was then concluded that a combination of the bimodality of PSD and the proposed in-situ polymerization method were the main factors contributing synergistically to the improved loop tack values.

Peel strength, on the other hand, did not show discernible differences between the bimodal PSDs, as mentioned previously. Nevertheless, we can see in Figure 6.15 that there was a noteworthy difference between the two monomodal distributions. For example, sample

LS1 (monomodal PSD with small particles) exhibited a peel strength value of ~258 N/m while sample LS5 (monomodal PSD with large particles) had a peel strength value of ~475 N/m, which is about twice as much as the former. This difference was the result of similar reasons as in the loop tack results, i.e., differences in composition drift between the large and small particles or different film formation paths leading to different contact area or different roughness at the interface with the substrate since all other variables (copolymer composition, MWD, gel content) were kept equal. As for the bimodal PSDs (in-situ or post-polymerization blends), it was noticeable that they gave a peel strength closer to the value obtained from large particles, which could be due to the fact that the mass fraction of the large particles was considerably larger than the small particles.

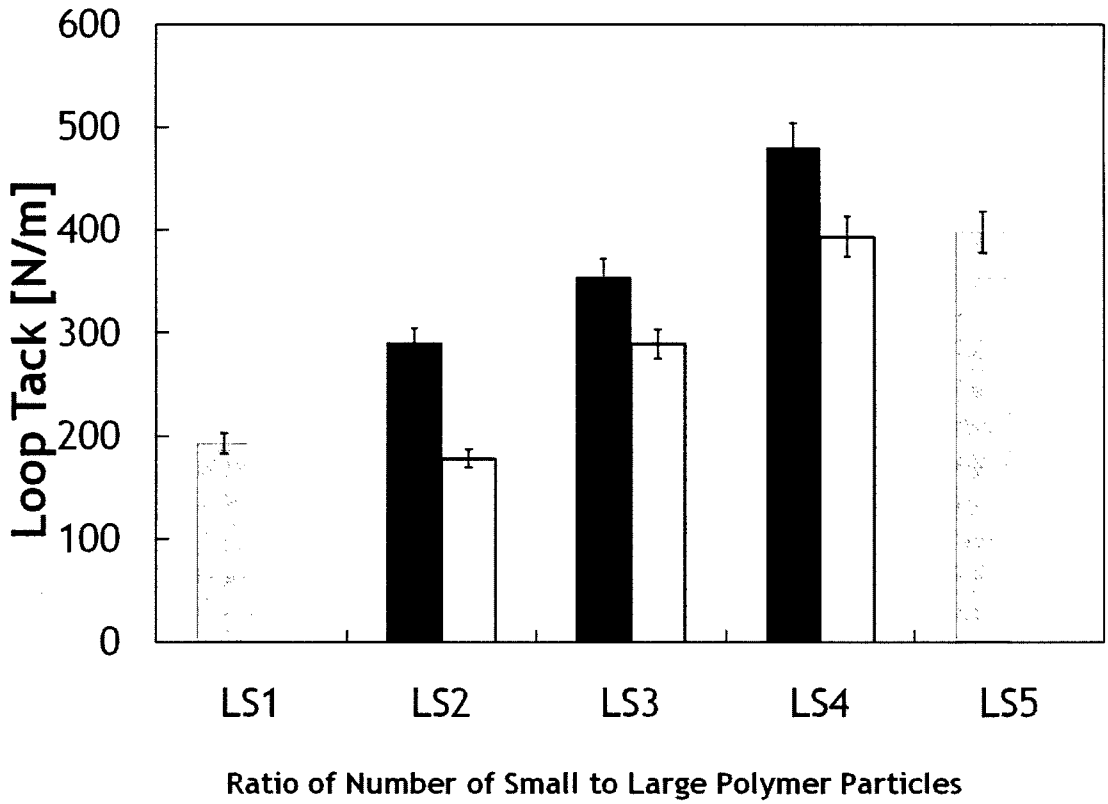

Figure 6.14. Loop tack results for monomodal PSD of small and large D_p (grey); in-situ bimodal PSD (black) and post-polymerization blended bimodal PSD (white)

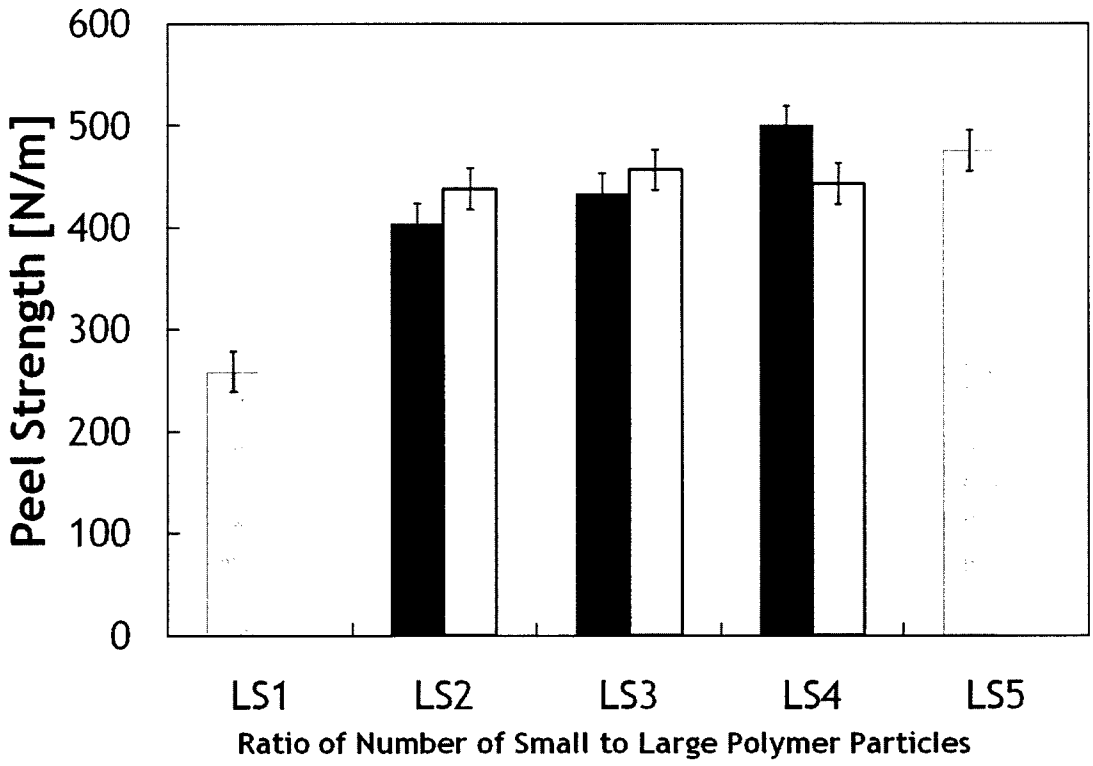

Figure 6.15. Peel strength results for monomodal PSD of small and large D_p (grey); in-situ bimodal PSD (black) and post-polymerization blended bimodal PSD (white)

Finally, the results displayed in Figure 6.16 show the films cast from bimodal PSDs latexes. As can be observed, the bimodal PSD sample with the highest number of large particles (LS4) displayed the highest shear strength values while the monomodal PSD exhibited much lower values. The differences in shear strength observed between the in-situ bimodal MWD and post-polymerization blended bimodal MWD latexes were likely within experimental error. Nevertheless, one can see that higher amounts of large particles led to an increase in shear strength. At this point, it is still not clear what PSD or film formation-related mechanisms were playing a role on the resulting shear strength values of the PSAs produced, a subject which may require further investigation.

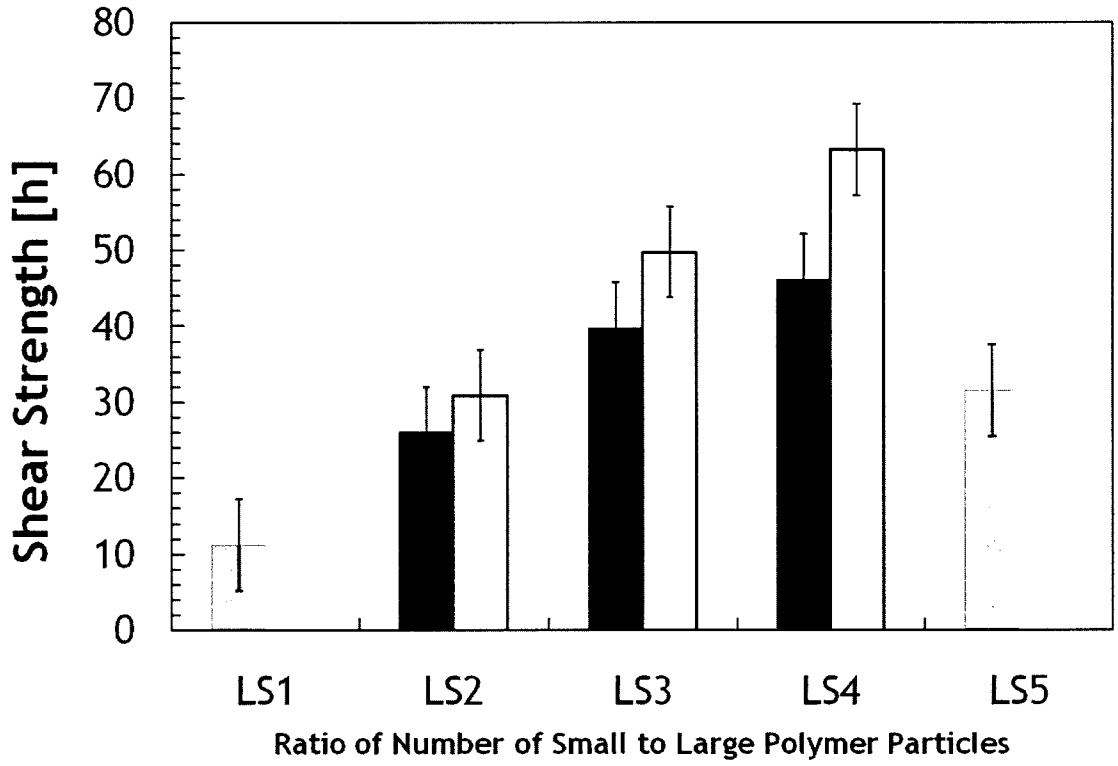

Figure 6.16. Shear strength results for monomodal PSD of small and large D_p (grey); in-situ bimodal PSD (black) and post-polymerization blended bimodal PSD (white)

6.4 CONCLUSIONS

The study described in this paper detailed a one-pot two-step miniemulsion polymerization strategy for the production of well-defined bimodal MWD or bimodal PSD latexes. The strategy exploits the droplet nucleation mechanism of miniemulsion polymerization to create populations of polymer particles of either different particle diameter or different molecular weight. The latexes produced by this approach were termed in-situ bimodal and their viscoelastic and PSA properties were compared to the properties of monomodal distributions as well as bimodal distributions produced via post-polymerization blending.

The results indicated that gel fractions of the in-situ bimodal MWD latexes were higher than those obtained by post-polymerization blending suggesting that additional intermolecular chain transfer reactions occurred during the miniemulsion polymerization. It was speculated that these additional reactions occurred inside the first population of particles,

which did not contain CTA, during the second step of the polymerization that subjected this particle population to a longer time inside the reactor. The viscoelastic analysis clearly showed that increasing the fraction of particles with low M_w modified the microstructure from a crosslinked structure (as noted in the rubbery plateau region of sample HL2) to a lightly crosslinked structure (as noted in the terminal region in sample HL4). PSA performance analysis showed that the loop tack and peel strength results exhibited higher values when the latexes were prepared in-situ as opposed to post-polymerization blending. They also displayed higher values than the monomodal MWDs. This effect was attributed to the higher gel fractions as well as to the bimodality of the MWD since all other properties (e.g., T_g and PSD) were carefully kept equal.

Bimodal PSD latexes were also successfully prepared using a similar approach. There were no significant differences in the viscoelastic behaviour when comparing the different in-situ bimodal PSD latexes (i.e., different ratios of large-to-small particles) or when compared to the monomodal PSD samples. Nevertheless, two of the PSA properties (loop tack and shear strength) were significantly different depending on the ratio of large-to-small particles used and in most of the cases, they displayed values larger than their corresponding monomodal PSD. Peel strength, on the other hand, did not exhibited differences between the different ratios and it was only observed that the bimodal PSD took on a value similar to the large particle population. The in-situ bimodal PSD latexes were also compared to post-polymerization blends similarly and it was found that they both fell within the same range. It is important to stress out that the benefit offered by the in-situ bimodal distributions lies in the preparation technique since it uses a one-pot two-step approach as opposed to the post-polymerization blends. The polymer produced in this study had the same copolymer composition but it is suggested that it can also be used to create PSAs (or latexes for that matter) with different compositions. The approach can also be used to create PSAs with bimodal MWD and PSD simultaneously.

6.5 ACKNOWLEDGMENTS

The authors gratefully acknowledge the financial support of the Natural Science and Engineering Research Council (NSERC) of Canada and the University of Ottawa. G.E.F.

thanks the National Council of Science and Technology (CONACYT) of Mexico for the doctoral scholarship provided.

6.6 REFERENCES

Asua, J.M., 2002. Miniemulsion polymerization. Progress in Polymer Science 27, 1283-1346.

Baus, R.E., Swift, G., 1985. Emulsion polymer of heterogeneous molecular weight and preparation thereof. 499127,

Benedek, I., 2004. Pressure-Sensitive Adhesives and Applications, 2nd edition ed. Marcel Dekker, Inc., New York.

Boutti, S., Graillat, C., McKenna, T.F., 2005. High solids content emulsion polymerisation without intermediate seeds. Part II. In situ generation of bimodal latices. Polymer 46, 1211-1222.

Chauvet, J., Asua, J.A., Leiza, J.R., 2005. Independent control of sol molar mass and gel content in acrylate polymer/latexes. Polymer 46, 9555-9561.

Chu, F.X., Graillat, C., Guyot, A., 1998a. High solid content multisized emulsion copolymerization of styrene, butyl acrylate, and methacrylic acid. Journal of Applied Polymer Science 70, 2667-2677.

Chu, F.X., Guillot, J., Guyot, A., 1998b. Study of poly(St/BA/MAA) copolymer latexes with bimodal particle size distribution. Polymers for Advanced Technologies 9, 851-857.

Chu, F.X., Guillot, J., Guyot, A., 1998c. Study of poly(St/BA/MAA) copolymer latexes with trimodal particle size distribution. Polymers for Advanced Technologies 9, 844-850.

do Amaral, M., Roos, A., Asua, J.M., Créton, C., 2005. Assessing the effect of latex particle size and distribution on the rheological and adhesive properties of model waterborne acrylic pressure-sensitive adhesives films. Journal of Colloid and Interface Science 281, 325-338.

DuChesne, A., Bojkova, A., Rottstegge, J., Glasser, G., Neher, D., Krieger, S., 1999. Film formation of heterogeneous latex systems - a comparative study by mechanical testing, electron microscopy, interferometry and solid state NMR. Physical Chemistry Chemical Physics 1, 3871-3878.

Eckersley, S.T., Rudin, A., 1996. Film formation of acrylic copolymer latices: A model of stage II film formation. Film Formation in Waterborne Coatings 648, 2-21.

Elizalde, O., Vicente, M., Leiza, J.R., Asua, J.M., 2002. Control of the adhesive properties of n-butyl acrylate/styrene latexes. Polymer Reaction Engineering 10, 265-283.

Ferry, J.D., 1980. Viscoelastic Properties of Polymers, 3rd edition ed. John Wiley and Sons, New York, USA.

Fonseca, G.E., McKenna, T.F., Dubé, M.A., 2008. Influence of Particle Nucleation in Pressure Sensitive Adhesive Properties: Miniemulsion versus Emulsion Polymerization. Macromolecular Symposia 271, 83-93.

Geurts, J.M., Lammers, M., German, A.L., 1996. The effect of bimodality of the particle size distribution on film formation of latices. Colloids and Surfaces A: Physicochemical and Engineering Aspects 108, 295-303.

Gonzalez, I., Leiza, J.R., Asua, J.M., 2006. Exploring the limits of branching and gel content in the emulsion polymerization of n-BA. Macromolecules 39, 5015-5020.

Gower, M.D., Shanks, R.A., 2004. The effect of chain transfer agent level on adhesive performance and peel master-curves for acrylic pressure sensitive adhesives. Macromolecular Chemistry and Physics 205, 2139-2150.

Hua, H., Dubé, M.A., 2001. Off-line monitoring of butyl acrylate, methyl methacrylate and vinyl acetate homo- and copolymerizations in toluene using ATR-FTIR spectroscopy. Polymer 42, 6009-6018.

Jovanovic, R., Dubé, M.A., 2004. Emulsion-based pressure-sensitive adhesives: A review. Journal of Macromolecular Science: Polymer Reviews C44, 1-51.

Jovanovic, R., McKenna, T.F., Dubé, M.A., 2004a. Empirical modeling of butyl acrylate/vinyl acetate/acrylic acid emulsion-based pressure-sensitive adhesives. Macromolecular Materials and Engineering 289, 467-474.

Jovanovic, R., Ouzineb, K., McKenna, T.F., Dubé, M.A., 2004b. Butyl acrylate/methyl methacrylate latexes: Adhesive properties. Macromolecular Symposia 206, 43-56.

Landfester, K., Bechthold, N., Forster, S., Antonietti, M., 1999. Evidence for the preservation of the particle identity in miniemulsion polymerization. Macromolecular Rapid Communications 20, 81-84.

Lathova, E., Lath, D., Pavlinec, J., 1993. The Behavior of Poly(2-Ethylhexyl Acrylate) in Dilute-Solution - Viscosity Measurements. Polymer Bulletin 30, 713-718.

Lenzi, M.K., Cunningham, M.F., Lima, E.L., Pinto, J.C., 2005. Producing Bimodal Molecular Weight Distribution Polymer Resins Using Living and Conventional Free-Radical Polymerization. Industrial & Engineering Chemistry Research 44, 2568-2578.

O'Connor, A.E., Willenbacher, N., 2004. The effect of molecular weight and temperature on tack properties of model polyisobutylenes. International Journal of Adhesion and Adhesives 24, 335-346.

Ouzineb, K., Graillat, C., McKenna, T.F., 2004. Study of compartmentalization in the polymerization of miniemulsions of styrene and butyl methacrylate. Journal of Applied Polymer Science 91, 115-124.

Ouzineb, K., Graillat, C., McKenna, T.F., 2005. High-Solid-Content Emulsions. V. Applications of Miniemulsions to High Solids and Viscosity Control. Journal of Applied Polymer Science 97, 745-752.

Ouzineb, K., Hua, H., Jovanovic, R., Dubé, M.A., McKenna, T.F., 2003. Monomer compartmentalisation in miniemulsion polymerisation studied by infrared spectroscopy. Comptes Rendus Chimie 6, 1343-1349.

Peters, A.C.I.A., Overbeek, G.C., Buckmann, A.J.P., Padget, J.C., Annable, T., 1996. Bimodal dispersions in coating applications. Progress in Organic Coatings 29, 183-194.

Plessis, C., Arzamendi, G., Leiza, J.R., Alberdi, J.M., Schoonbrood, H.A.S., Charmot, D., Asua, J.M., 2001. Seeded semibatch emulsion polymerization of butyl acrylate: Effect of the chain-transfer agent on the kinetics and structural properties. Journal of Polymer Science, Part A: Polymer Chemistry 39, 1106-1119.

Pressure Sensitive Tape Council, 2004. Test Methods for Pressure Sensitive Adhesive Tapes, 14th ed. ed. Pressure Sensitive Tape Council, Northbrook, Illinois.

Qu, X.W., Wang, N.Y., Lovell, P.A., 2009. Preparation and Characterization of the Latexes with Different Particle Sizes by Semibatch Emulsion Polymerization and the Influence on Properties of Waterborne Pressure-Sensitive Adhesives. Journal of Applied Polymer Science 112, 3030-3040.

Roberge, S., Dubé, M.A., 2006. The effect of particle size and composition on the performance of styrene/butyl acrylate miniemulsion-based PSAs. Polymer 47, 799-807.

Satas, D., 1989. Handbook of Pressure Sensitive Adhesive Technology, 2nd ed. ed. Van Nostrand Reinhold, New York.

Sayer, C., Lima, E.L., Pinto, J.C., Arzamendi, G., Asua, J.M., 2000. Molecular weight distribution in composition controlled emulsion copolymerization. Journal of Polymer Science, Part A: Polymer Chemistry 38, 1100-1109.

Schneider, M., Claverie, J., Graillat, C., McKenna, T.F., 2002a. High solids content emulsions. I. A study of the influence of the particle size distribution and polymer concentration on viscosity. Journal of Applied Polymer Science 84, 1878-1896.

Schneider, M., Graillat, C., Guyot, A., McKenna, T.F., 2002b. High solids content emulsions. III. Synthesis of concentrated latices by classic emulsion polymerization. Journal of Applied Polymer Science 84, 1916-1934.

Schneider, M., McKenna, T.F., 2002. Comparative study of methods for the measurement of particle size and size distribution of polymeric emulsions. Particle & Particle Systems Characterization 19, 28-37.

Steward, P.A., Hearn, J., Wilkinson, M.C., 2000. An overview of polymer latex film formation and properties. Advances in Colloid and Interface Science 86, 195-267.

Tauer, K., 2001. Surface Chemistry in the Polymerization of Emulsion, in: Holmberg, K. (Eds.), Handbook of Applied Surface and Colloid Chemistry. John Wiley & Sons, Chichester; New York, pp. 175-200.

Tobing, S.D., Klein, A., 2000. Mechanistic studies in tackified acrylic emulsion pressure sensitive adhesives. Journal of Applied Polymer Science 76, 1965-1976.

Tobing, S.D., Klein, A., 2001a. Molecular parameters and their relation to the adhesive performance of acrylic pressure-sensitive adhesives. Journal of Applied Polymer Science 79, 2230-2244.

Tobing, S.D., Klein, A., 2001b. Molecular parameters and their relation to the adhesive performance of emulsion acrylic pressure-sensitive adhesives. II. Effect of crosslinking. Journal of Applied Polymer Science 79, 2558-2564.

Vicente, M., Leiza, J.R., Asua, J.M., 2001. Simultaneous central of copolymer composition and MWD in emulsion copolymerization. AIChE Journal 47, 1594-1606.

CHAPTER 7

Relating PSA performance properties to adhesion force and energy determined by atomic force microscopy

Fonseca, G.E., McKenna, T.F., Dubé, M.A.;

Relating PSA performance properties to adhesion force and energy determined by atomic force microscopy

Gabriela E. Fonseca[1], Timothy F. L. McKenna[2] and Marc A. Dubé[1*]

[1]Department of Chemical and Biological Engineering,
University of Ottawa, Ottawa, Ontario, K1N 6N5, Canada
E-mail: Marc.Dube@UOttawa.ca
Fax: +1 (613) 5625172

[2]Department of Chemical Engineering,
Queen's University, Kingston, Canada

ABSTRACT

Atomic Force Microscopy (AFM) was used to acquire adhesion-force curves to investigate the effect of monomodal and bimodal distributions of molecular weight (M_w) and particle size on the adhesion force and energy at the nanoscale. The results revealed that in the case of samples with monomodal molecular weight distributions (MWDs), the adhesion-force curves displayed large differences depending on the weight-average M_w, while those adhesion-force curves obtained from samples with monomodal particle size distributions (PSD) did not exhibit significant differences. Conversely, the acquisition of adhesion-force curves on the bimodal distributions showed that (i) the adhesion force decreased as the fraction of particles with low M_w increased in the sample and (ii) the adhesion force increased with higher fractions of particles with small D_p. The study showed that AFM force curves can distinguish microstructural changes in PSA films with monomodal and bimodal distributions.

Keywords: Miniemulsion polymerization, methyl methacrylate, 2-ethyl hexyl acrylate, pressure-sensitive adhesives, atomic force microscopy, force curves

7.1 INTRODUCTION

Pressure-sensitive adhesives (PSA) are soft, viscoelastic materials that bond to a surface upon the application of slight pressure. Presently, hot-melt, solvent-based and water-based polymerizations are the main PSA production technologies; however, increasing environmental regulations have prompted the use of more environmentally friendly technologies such as water-based emulsion polymerization (Jovanovic and Dubé, 2004). Emulsion polymerization also offers other benefits such as overcoming heat transfer and viscosity problems found in solution polymerization as well as the possibility of obtaining high molecular weight polymers. Nevertheless, PSAs produced by emulsion polymerization have lower performance compared to their solvent-based counterparts due to the presence of surfactants and to the formation of microgels (Tobing and Klein, 2000).

Miniemulsion polymerization is one of the water-based technologies available to potentially produce PSAs. Miniemulsion polymerization employs an emulsification process, which involves the use of mechanical energy to produce a dispersion of monomer droplets with a diameter range of about 50 to 500 nm. The monomer droplets are stabilized against diffusional degradation and coalescence processes by the addition of surfactants and a highly hydrophobic compound (Asua, 2002). We have previously used miniemulsion polymerization to produce latexes with bimodal particle size distributions (PSD) or bimodal molecular weight distributions (MWD) using a one-pot two-step polymerization approach (refer to Chapter 6). The PSA properties and viscoelastic behaviour of the bimodal latexes produced were analyzed and a clear influence of the bimodal MWD on the shear storage and loss modulus, and PSA performance was observed. Surprisingly, the viscoelastic behaviour of the bimodal PSD latexes did not change significantly. However, the analysis of their resulting PSA properties showed a clear influence of the PSD.

Atomic force microscopy (AFM) has become an important tool in the investigation of surface morphology at the atomic level due to its potential to provide information not only through the images obtained with this instrument but also by providing information on different local interactions, such as sample elastic modulus and adhesion forces, among others (Raiteri et al., 1999; Leite and Herrmann, 2005). These interactions can be estimated through the acquisition of force-distance curves, wherein single-point force curves are taken

along a specified area of a sample and the resulting interactions are evaluated. This type of analysis has been called local force spectroscopy (LFS), where a cantilever tip is approached to a sample until it makes contact and is subsequently retracted as depicted in Figure 7.1. At a sufficiently large distance (see point A in Figure 7.1), there is no interaction between the sample and the cantilever tip and thus, there is no cantilever deflection. The sample is approached to the tip until attractive forces (e.g., long-range interactions, Van der Waals and capillary forces) start to act upon the tip (point B). The line between points A and B is referred to as the "zero line" (cf. Figure 7.1). When these forces are stronger than the stiffness of the cantilever, the tip "jumps" into contact with the sample (point C). The line between points B and C is referred to as "jump-to-contact" or "snap-in force". From point C to D, the cantilever is forced into the sample and from point D to E, the cantilever is retracted. At point E the cantilever tip releases from the sample. The lines between points C, D and E represent the indentation of the cantilever into the sample. The slope of the contact region is a function of the elasticity of the material. The hysteresis observed when lines C-D and D-E are not parallel to each other gives information on the plastic deformation of the sample (Leite and Herrmann, 2005). Finally, the segment between E and F corresponds to the point where the spring force of the cantilever surpasses the adhesion forces and the tip detaches from the sample. The line between points E and F is referred to as "jump-off-contact" or "snap-off force". The snap-off force is thought to be related to the adhesive forces between the material and the cantilever tip (Drelich and Mittal, 2005).

AFM has typically been used in the polymer colloids field strictly as an imaging technique of the surface morphology (Sommer et al., 1995; Steward et al., 2000; Aymonier et al., 2003; Lei et al., 2007; Schantz et al., 2007; Xu et al., 2008). There are also a number of studies that have used this instrument to study film formation mechanisms in latex blends (Geurts et al., 1996; Lam et al., 1997; Tzitzinou et al., 2000; Vorobyova and Winnik, 2001). They found that films cast from blends with different proportions of particles with smaller and larger diameters tended to organize differently, which led to different film formation behaviour (Geurts et al., 1996).

AFM has also been used to image waterborne acrylic PSAs. Mallégol et al. (Mallégol et al., 2001; Mallégol et al., 2002; Mallégol et al., 2003) and Lei et al. (2007) reported the first systematic studies of AFM parameters required to obtain informative images of freshly-

cast waterborne acrylic PSA films. They used high tapping amplitudes to impart enough energy to the cantilever tip to pull it from the adhesive surface with a high set point ratio to minimize indentation of the tip and reduce deformation of the soft surface. Their work established a basis to obtain images that could lead to a deeper understanding of film formation behaviour and their correlation with macroscopic properties.

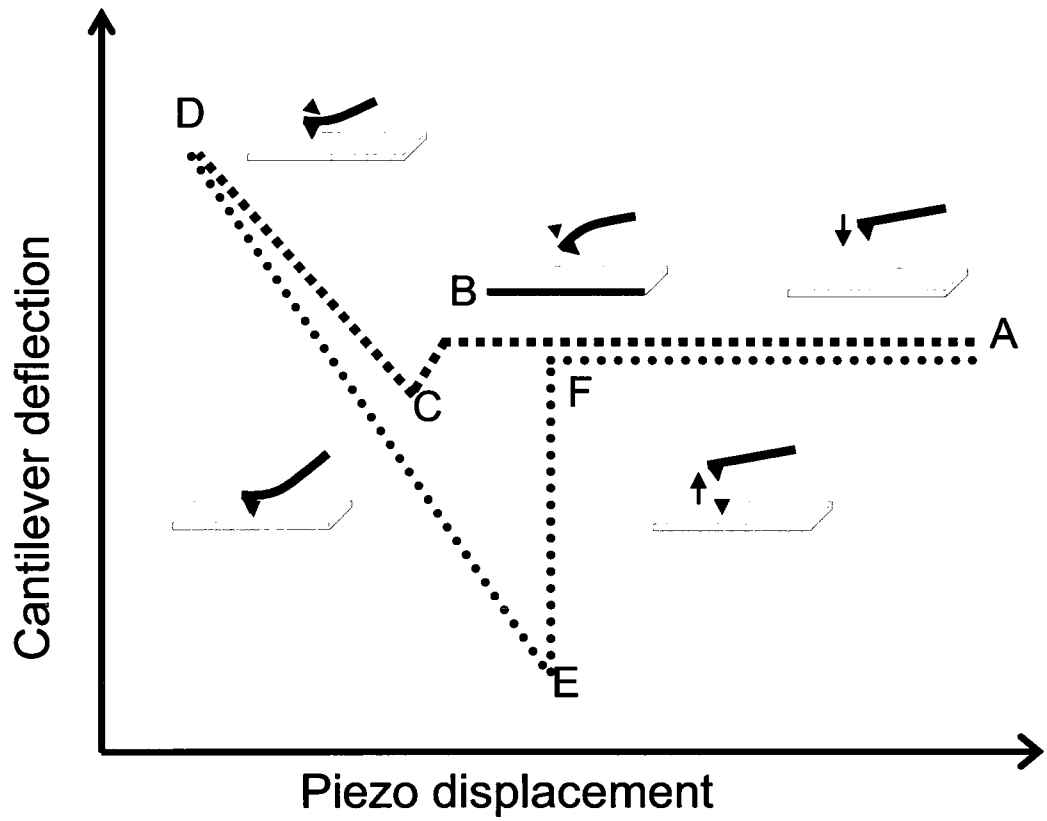

Figure 7.1. Typical force-distance curve in a local force spectroscopy experiment

As mentioned earlier, AFM also allows for the acquisition of force curves that can give information on molecular interactions and mechanical properties at the nanoscale. A number of studies have successfully obtained quantitative information on the mechanical and adhesive responses on nanolithographed poly(methyl methacrylate) (Cappella et al., 2002), the distribution of rubber in high impact poly(propylene) (Bouzid et al., 2005) and adhesion force mapping of phase-separated blends (Eaton et al., 2000). Other studies have collected AFM force curves to study the tackifier influence on PSA adhesion (Paiva et al., 2000; Paiva

and Foster, 2001; Paiva et al., 2001; Canetta et al., 2009) and the pH dependence of macroscale and nanoscale adhesive properties (Wang et al., 2009). Portigliatti et al. (Portigliatti et al., 2000a; Portigliatti et al., 2000b) conducted an interesting "nano-tack" experiment using AFM. They showed that a quantitative analysis of the adhesive behaviour of PSA films can be carried out using AFM. Others have also looked at the use of lateral force modulation (a.k.a. X-modulation) to obtain information on the nanomechanical behaviour of PSA films (Moon and Foster, 2002; Moon et al., 2004). Only a few studies have attempted to relate the adhesion forces obtained by AFM force measurements to PSA macroscale properties (Raiteri et al., 1999; Phillips et al., 2007; Canetta et al., 2009).

To further investigate the effect of particle size and molecular weight distributions as well as the presence of bimodal populations of both of these two polymer characteristics, the present work focused on the acquisition of force curves on various samples with monomodal and bimodal distributions of molecular weight or particle size. The objective of this study was to evaluate the dependence of adhesion forces obtained by AFM on the MWD and PSD. Additionally, we wanted to find if there was a correlation between the adhesive properties experienced at the nanoscale (i.e., at the film surface) and those at the macroscale (e.g., tack and peel strength). PSA films of poly(2-ethyl hexylacrylate/methyl methacrylate/acrylic acid) were analyzed and the adhesion force and energy of such films cast from latexes with bimodal MWD or bimodal PSD was investigated as part of an exploratory study.

7.2 EXPERIMENTAL DETAILS

7.2.1 Materials and Preparation

The latexes used in this study were prepared according to methods previously reported (refer to Chapter 6) using 2-ethyl hexyl acrylate (EHA), methyl methacrylate (MMA) and acrylic acid (AA) via miniemulsion polymerization. All of the latexes prepared have a copolymer composition of 63/35/2 wt.-% of EHA/MMA/AA in order to keep the glass transition (T_g) equal in all of the samples. Two series of samples were investigated in the current study. Table 7.1 presents details on the particle sizes, molecular weights and mixture ratios for all of the samples. The first set of samples (sample set A) had equal particle diameters (D_p) of 170 nm and varying MWDs including two monomodal MWDs and

three 'in-situ bimodal' MWDs prepared using a one-pot two-step approach previously described (refer to Chapter 6). The second set of samples (sample set B) had an equal weight-average M_w of 275,000 g/mol and varying PSDs with two monomodal PSDs and three 'in-situ bimodal' PSDs. The five latexes in each set of experiments are labelled HL (high/low M_w) for sample set A and LS (large/small D_p) for sample set B. The latexes with monomodal distributions are considered the extremes and are labelled with the numbers 1 and 5 for both sets. The latexes with bimodal distributions are numbered 2, 3 and 4 depending on the formulation.

Table 7.1. Latexes for the monomodal and in-situ bimodal distributions

	Sample	Type	M_{w1} [g mol^{-1}][a]	M_{w2} [g mol^{-1}]	Mass % M_{w1}	Mass % M_{w2}
Sample set A	HL1	Monomodal	750,000		100	0
	HL2	Bimodal	770,000	91,000	75	25
	HL3	Bimodal	775,000	85,000	50	50
	HL4	Bimodal	776,000	97,000	25	75
	HL5	Monomodal		97,000	0	100
	Sample	Type	D_{p1} [nm]	D_{p2} [nm]	Mass % D_{p1}	Mass % D_{p2}
Sample set B	LS1	Monomodal	167	---	100	0
	LS2	Bimodal	70	310	27	73
	LS3	Bimodal	69	311	11	89
	LS4	Bimodal	70	315	4	96
	LS5	Monomodal	---	310	0	100

[a] The M_w's reported correspond to the molecular weight at the peak of the distribution in order to compare the peaks of monomodal and bimodal MWDs.

7.2.2 AFM analysis and calibration

AFM measurements were performed using a Multimode Scanning Probe Microscope (Veeco Instruments) with a NanoScope V controller in tapping mode. The latexes were filtered to remove any large particulates and 10 μL of a diluted latex solution (0.03 wt.-%) were deposited on microscope glass slides. The microscope glass slides had been previously cleaned with a 37% HCl solution for 24 h. The samples were left to dry at ambient

temperature in a particulate-free clean room and analyzed within 5 h after preparation. The relative humidity (RH) in the room where the samples were dried was consistently kept below 40%. Silicon AFM cantilevers (Vistaprobes by NanoScience Instruments) with a pyramidal geometry and tip radius of < 10 nm were used in this study. The cantilevers had a resonant frequency of 300 kHz with a spring constant of 40 N/m. Height and phase images were taken at ambient temperature using large values of drive amplitude so that the tip was able to move in and out of the surface. The scanned area was kept constant at 5 μm x 5 μm with a scan rate between 0.6 and 0.9 Hz. Two types of calibrations were performed. First, the deflection of each cantilever used was measured on a glass surface to determine the sensitivity, which refers to a measurement of the cantilever deflection in nanometres equivalent to a specific movement of the detection laser in the photodetector in Volts. Table 7.2 provides the calculated sensitivities for each of the samples. In the second type of calibration, the cantilever spring constant was estimated using the thermal noise method to convert the deflection of the cantilever into force units (in Newtons) (Hutter and Bechhoefer, 1993). Both types of calibrations were performed using the software provided by the instrument manufacturer (Veeco Instruments). The calculated spring constants are also shown in Table 7.2. These two types of calibrations were performed to convert the voltage signal of the photodetector into distance units and into force values. The calibrations were repeated whenever the cantilever was re-mounted into the instrument. Figure 7.2 shows a diagram of the laser deflection in AFM experiments.

7.2.3 PSA testing

Tack, peel and shear strength were measured according to the Pressure Sensitive Tape Council standards PSTC-6, PSTC-1 and PSTC-7, respectively (Pressure Sensitive Tape Council, 2004). The complete methodology has been previously described (refer to Chapter 2). The latex was filtered using glass wool and cast onto a 50 um Mylar® sheet. The cast film was dried at room temperature and conditioned for 24 h at standard conditions of temperature and humidity (23 ± 2°C and 50% ± 2 Relative Humidity).

Table 7.2. Sensitivity and spring constants of AFM cantilevers

Samples	Deflection sensitivity [nm/V]	Spring constant [N/m]
LS1, LS2, LS3, LS4, LS5	41.03	34.27
HL1, HL2	34.11	69.15
HL3, HL4, HL5	37.05	38.20

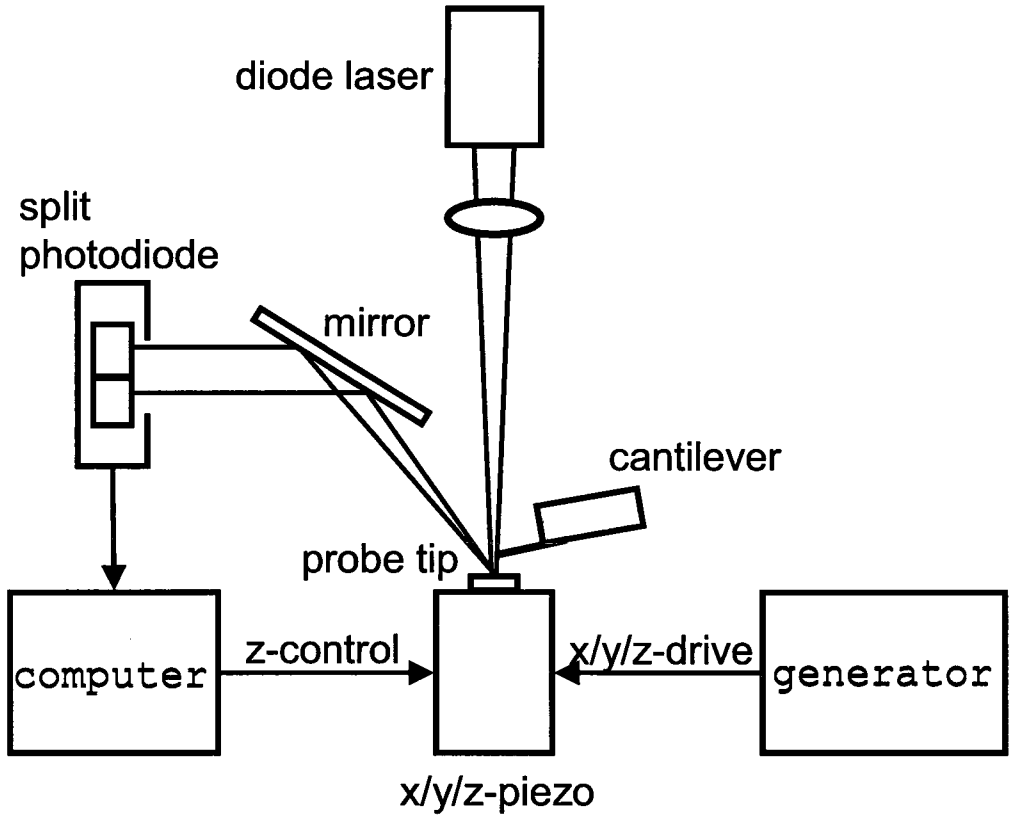

Figure 7.2. Block diagram of a laser deflection contact AFM

7.3 RESULTS AND DISCUSSION

In addition to imaging the surface of samples, AFM is able to acquire force-displacement curves that offer information on the surface properties. This technique has been considered particularly suited for the study of polymer systems precisely due to its ability to characterize the surface (Ho and Khew, 2002). In the case of the PSA films studied here, it offered information on the adhesion forces at the nanoscale. Table 7.3 presents the results of

the adhesion forces as well as the adhesion energy, which will be discussed in further detail throughout this paper. Let us point out that the adhesion energy is the energy required to deform the material at the surface and detach the tip and is calculated from the area under the force curve.

Table 7.3. Adhesion force and adhesion energy for sample sets A and B

	Sample	Adhesion force (nN)	Adhesion energy ($x10^{14}$ J)
Sample set A	HL1	99.583	3.144
	HL2	92.037	3.005
	HL3	68.936	3.281
	HL4	38.810	0.706
	HL5	203.962	6.916
	Sample	Adhesion force (nN)	Adhesion energy ($x10^{14}$ J)
Sample set B	LS1	71.045	1.884
	LS2	96.509	2.512
	LS3	60.544	1.266
	LS4	38.431	0.768
	LS5	71.364	2.547

The measurement of snap-off forces at the nanoscale with AFM also involves other types of forces. In reality, the adhesion force measured will be a combination of electrostatic, van der Waals and capillary forces. Capillary forces are especially important since they are caused by the presence of capillary condensation between the tip and the substrate (Maghsoudy-Louyeh and Tittman, 2008). As the AFM tip approaches a substrate, the capillary force on the tip is initially near zero until the tip contacts the surface of the water film. When contact is made, water wicks up around the tip to form a meniscus bridge between the tip and the substrate. The behaviour of the force curve will depend directly on the height of the water film adsorbed on the substrate (if present). Capillary condensation is a result of the relative humidity of the environment. However, the contribution of capillary forces to the total force will increase only above a certain critical humidity level (Ata et al., 2002). The measurements carried out in this study were performed at ambient conditions

with a relative humidity lower than 40%. It was expected that under these conditions, the influence of the capillary forces was minimal. It is acknowledged that a setup with a flow of inert gas or in liquid (i.e., measurement of force curves in a liquid solution) would perhaps have been better adapted and would have offered forces resulting purely from the contribution of the sample in question; however, we did not have access to this setup during the course of this study. Nevertheless, it is important to stress that under dry conditions (such as those used in this work), the formation of the meniscus bridge could be circumvented.

7.3.1 Influence of molecular weight distributions (MWD) on nanoscale adhesion measurements

This section illustrates the results obtained in the analysis of the PSA films with varying MWDs. Samples HL1 and HL5 were prepared using batch miniemulsion polymerization while samples HL2, HL3 and HL4 were prepared using a one-pot two-step miniemulsion polymerization approach to produce bimodal MWDs with peaks that would correspond to those of the monomodal MWDs of samples HL1 and HL5. Figure 7.3 shows the MWD of the samples analyzed in this part of the study.

It was expected that the polymer samples with bimodal MWDs would contain particles with high M_w (i.e., 750 000 g/mol) and with low M_w (97 000 g/mol) homogeneously distributed so that the two types of particles would present adequate adhesive strength while at the same time offering the inherent cohesive strength of high molecular weight polymers. Before analyzing the bimodal MWD samples, the monomodal MWD samples were characterized to establish a baseline with which to compare the bimodal MWD samples. Figure 7.4a shows the force-displacement curves obtained from the two very different polymers. The different curves and deformations encountered clearly demonstrate that the two samples have different adhesive behaviours. On the one hand, HL1 displayed a much lower snap-off force, accordingly to its stiffer nature while sample HL5 displayed a higher snap-off force as a result of the a larger more plastic deformation. However, "softer" polymers could give rise to a larger contact area under the same load and that would lead to perceived larger adhesion forces. As mentioned earlier, the adhesion force can be calculated

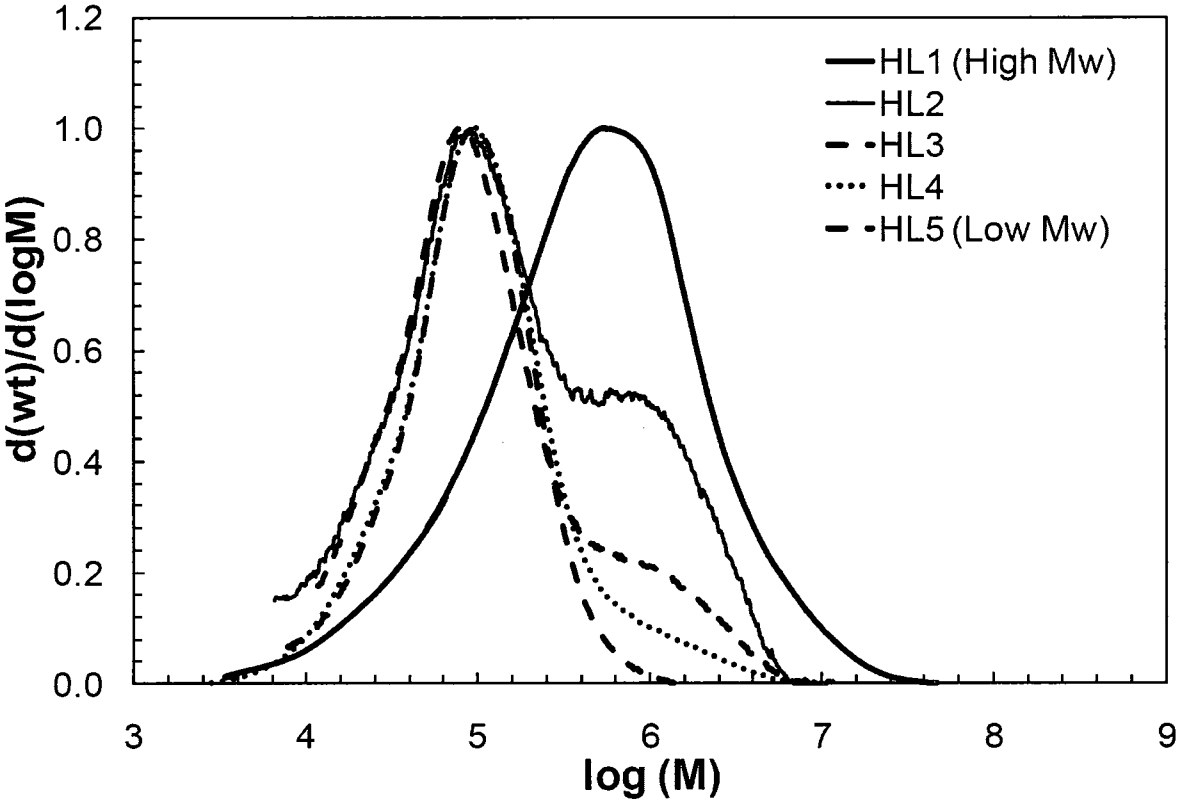

Figure 7.3. Molecular weight distributions of sample HL1 to HL5

based on the difference between the zero-line (cf. Figure 7.1) and the maximum force required to detach the tip from the PSA film surface. According to the measurements undertaken in this study, the adhesion force of sample HL1 was equal to 99.5 nN and that for sample HL5 was equal to 204 nN. Both of these polymers had the same composition of 65/35 wt.-% EHA/MMA and thus, the same T_g; however, the latter value is consistent with a more flexible soft material. This effect can also be appreciated in the histograms of the snap-off forces shown in Figure 7.4b. It can be observed that the snap-off force decreased dramatically when the M_w increased. This was certainly due to the fact that sample HL1 was a stiffer material with higher cohesive strength. The snap-off force histogram of sample HL5 was much broader than that for sample HL1, spreading over a range of 180 nN to 240 nN as opposed to a range of 85 nN to 120 nN.

The nanoscale results were compared to the macroscale PSA properties (see Figure 7.4c). The results showed that loop tack did not increase significantly (from 144.36 N/m to

167.32 N/m) with the decrease of M_w and with a considerable increase in the adhesion force obtained in the force-displacement curve (cf. Figures 7.4a and b). On the other hand, peel strength presented an almost 5-fold increase from 45.28 N/m to 216.54 N/m. The results in Table 7.3 show that the adhesion energy doubled from 3.144 x 10^{-14} J in sample HL1 to 6.916 x 10^{-14} J in sample HL5. Therefore, it is apparent that the adhesion force and energy can be related to peel strength due to the fact that this property involves large energy dissipation as was likely the case for the nanoscale measurements.

The AFM height images of samples HL1 and HL5 are shown in Figures 7.5a and e. As can be observed, the particles can be clearly distinguished in sample HL1 while in sample HL5, the particles coalesced, making it difficult to observe the individual particles.

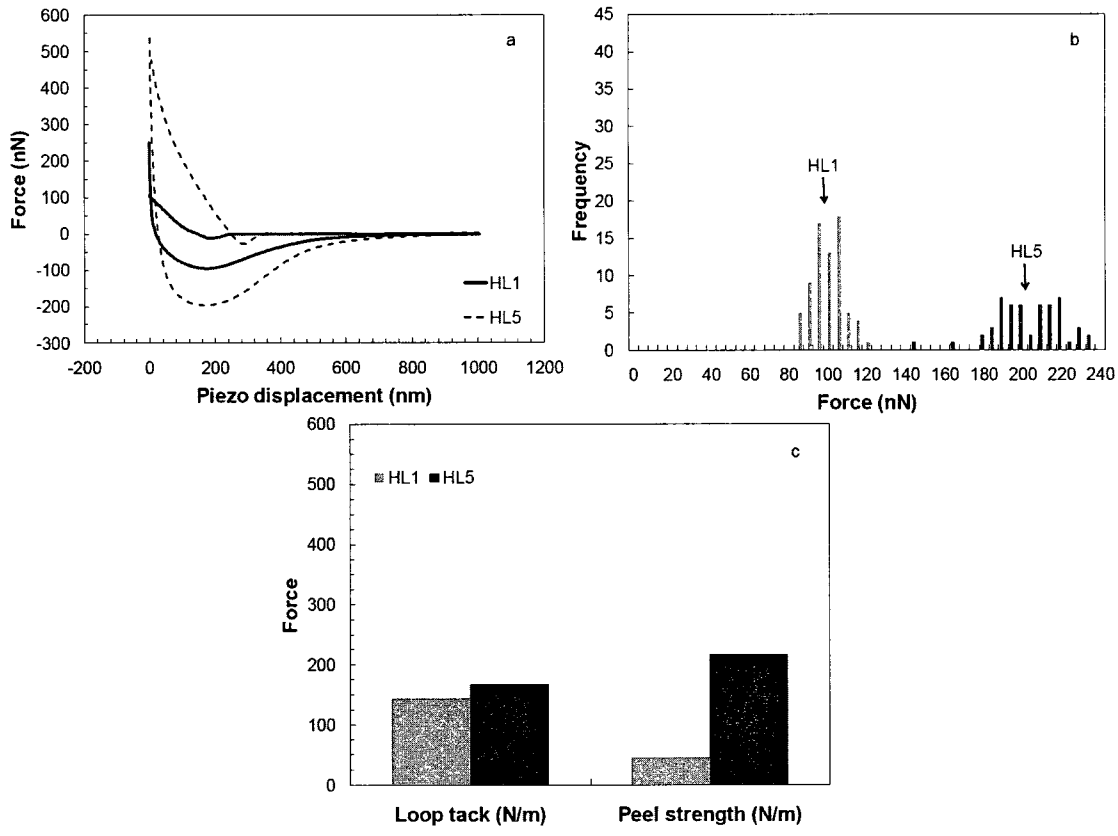

Figure 7.4. a) Force-distance curves; b) Histograms of snap-off forces and c) Loop tack and peel strength values for monomodal MWD miniemulsion-based samples HL1and HL5

Once the behaviour of the samples with monomodal MWDs was established, the three samples with bimodal MWDs were analyzed. Figures 7.6a and b show the force-

displacement curves and the snap-off force histograms obtained for the bimodal MWDs. Surprisingly, the adhesion force of sample HL4 (i.e., the sample with the highest fraction of low M_w) had the lowest adhesion force and energy. This was unexpected since the particles with low M_w had exhibited a large adhesion force when tested in the monomodal MWD sample (i.e., sample HL5). However, in the case of the bimodal MWD samples, the low M_w particles presented a different behaviour, i.e., a lower adhesion force. Bimodal MWD sample HL2 offered the largest adhesion force as observed in Figure 7.6b varying from 70 nN to 120 nN. Interestingly, the values obtained in sample HL1 (i.e., 80 nN to 120 nN) were close to the range obtained for sample HL2. The results also show that the force histograms do not present two separate peaks for the two types of particles, which suggests that the particles were well distributed and likely, had coalesced forming a homogeneous film.

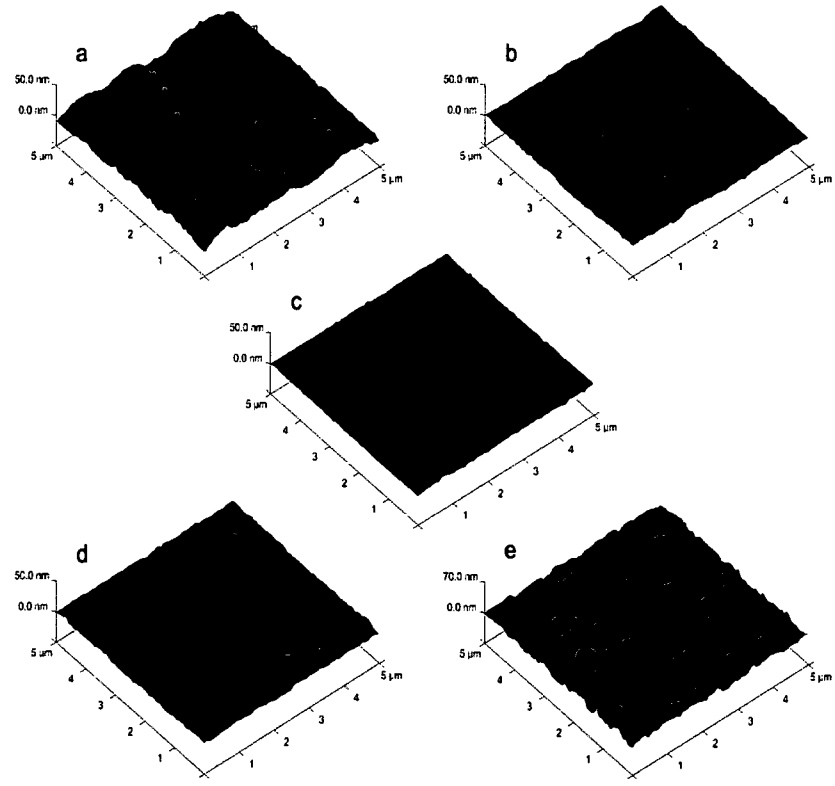

Figure 7.5. AFM three-dimensional images of sample set B. a) sample HL1 (monomodal MWD with a M_w = 750,000 g/mol); b) sample HL2; c) sample HL3; d) sample HL4; e) sample HL5 (monomodal MWD with a M_w = 97,000 g/mol)

Comparing these results against PSA properties in Figure 7.6c, one can see that the loop tack values increased with adhesion force as opposed to the decrease observed in peel

strength. Admittedly, the trends are opposed to those one would intuitively expect based on the results obtained in the monomodal MWD samples. One possible explanation is that in the case of the samples with bimodal MWDs, the low M_w particles acted merely as plasticizers, thus decreasing the adhesion force, which in turn, increased loop tack and decreased peel strength.

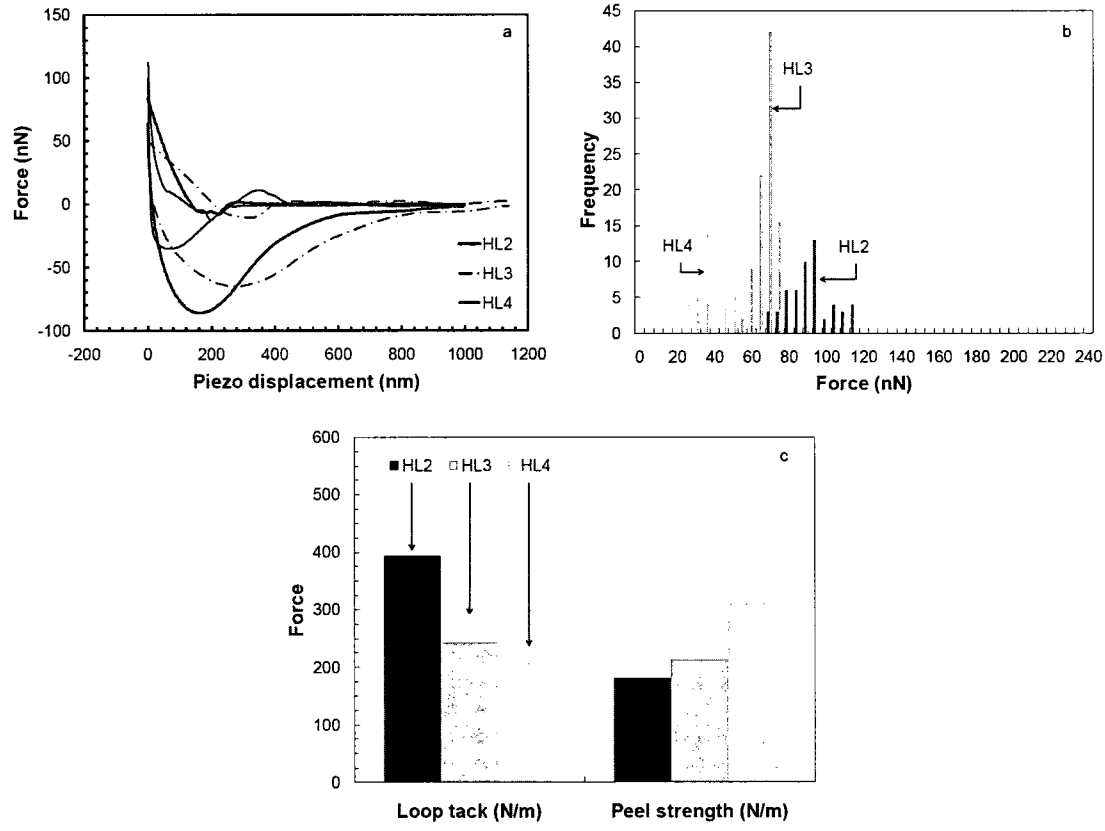

Figure 7.6. a) Force-distance curves; b) Histograms of snap-off forces and c) Loop tack and peel strength values for bimodal MWD miniemulsion-based samples HL2, HL3 and HL4

7.3.2 Influence of particle size distributions (PSD) on nanoscale adhesion measurements

Figure 7.7a and b show force–displacement curves for the monomodal PSD samples. These two samples had the same overall copolymer composition of 65/35 wt.-% with a T_g of

-45°C. Similarly, they both had a weight-average M_w of 275,000 g mol^{-1}. The difference between these two samples lied in the PSD. Sample LS1 had an average D_p of 167 nm and sample LS5 had an average D_p of 310 nm. As can be observed in Figures 7.7a and b (average force values shown in Table 7.3), there was not a significant difference in the adhesion forces, which was around 71 nN in both cases spanning a range from 50 nN to 90 nN.

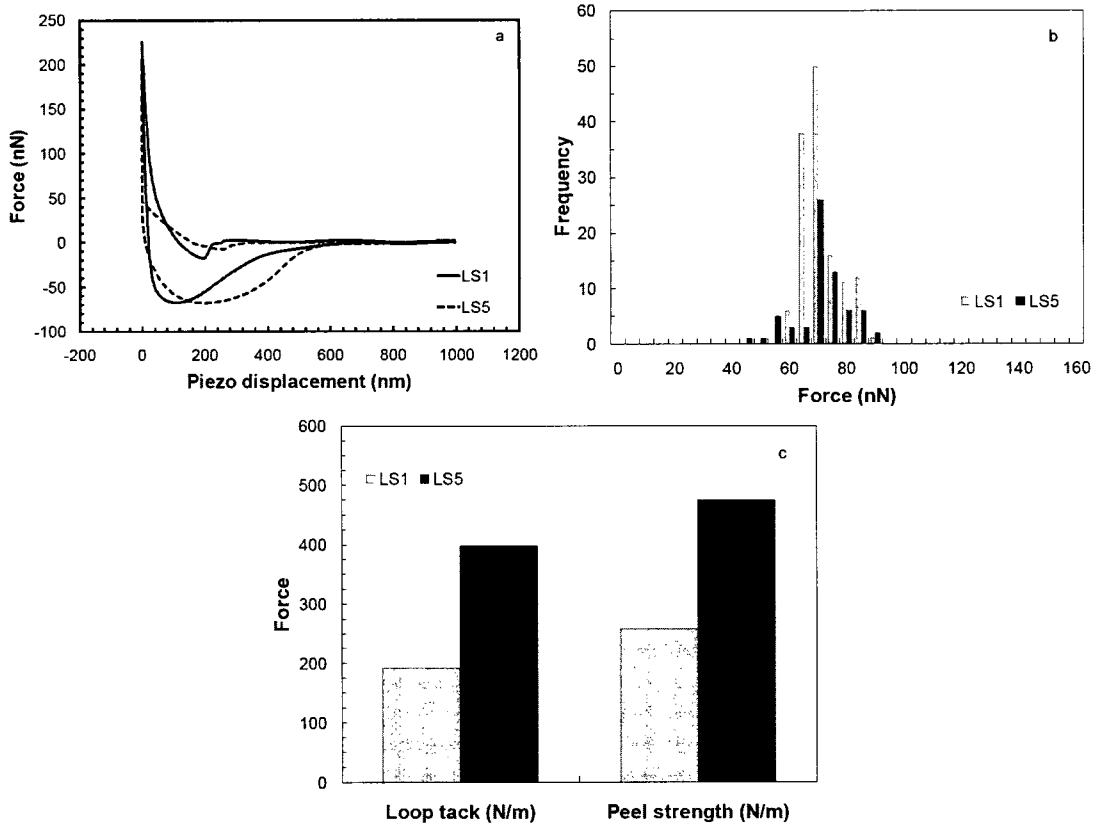

Figure 7.7. a) Force-distance curves; b) Histograms of snap-off forces and c) Loop tack and peel strength values for monomodal PSD miniemulsion-based samples LS1and LS5

Previously, the viscoelastic behaviour of the samples in this set was analyzed and no significant differences were found (refer to Chapter 6). However, the PSA properties did display a large increase in the values of loop tack and peel strength (cf. Figure 7.7c). It was also observed in Figure 7.7a that the force curve of sample LS5 displayed a larger area compared to that of sample LS1. In fact, this area represents the value of adhesion energy, which in the case of sample LS5 was equal to 2.54 x 10^{14} J. This value is 35% larger than the

adhesion energy of 1.88 x 10^{14} J obtained in sample LS1. It was also shown that, all things being equal (T_g and MWD), the adhesion energy was greatest for larger particles in the measurements carried out in this work.

It is known that differences in film formation pathways could lead to different surface assemblies that would result in changes to the PSA properties (Jovanovic and Dubé, 2004). While there is no consensus on this dependence (Eckersley and Rudin, 1996; DuChesne et al., 1999), it is reasonable to expect that particle size plays a role in film formation since larger particles would require a longer time to deform than smaller particles. Figure 7.8 shows the AFM height images of the samples with monomodal and bimodal PSDs. Specifically, Figure 7.8a and e display the surface topology of PSA samples with monomodal PSDs. As can be observed, the PSA film prepared with smaller particles formed a close-packed array (Figure 7.8a) when compared to the film prepared with larger particles, wherein the particles did not seem to be homogenously distributed. As a matter of fact, Figure 7.8e shows relatively large voids between polymer particles where as in Figure 7.8a, the particles are more likely arranged in a typical polyhedral formation (Jovanovic and Dubé, 2004).

It was also noticed that the slope of the approach curve (i.e., line C-D in Figure 7.1) was different for samples LS1 and LS5: sample LS1 had a steeper slope than sample LS5. The slope of this type of curves had been related to the elastic modulus of the material: the higher the modulus of the material, the less the deformation and the steeper the slope (Burnham et al., 1993), which suggests that the particles in sample LS1 were stiffer than those in sample LS5.

The particles of sample LS1 were produced using a batch miniemulsion polymerization process while the particles of sample LS5 were produced using a batch miniemulsion/semi-batch emulsion polymerization process in order to achieve large diameters. Even though, the conditions were carefully selected to produce the same MWD and T_g, it is possible that the surface of the larger particles had a more homogeneous copolymer composition in comparison to their core and to the smaller particles.

Finally, Figure 7.9a and b shows the force – displacement curves and histograms of the samples with bimodal PSDs. As can be observed, it is clear that the adhesion force

decreased with the fraction of large particles from an average value of 95.01 nN with a mass fraction of 0.73 (sample LS2) to an average value of 38.05 nN with a mass fraction of 0.96 (sample LS4). Sample LS4 contains a low mass fraction of the small particles (i.e., 0.04) and it was expected to behave similar to sample LS5 (monomodal PSD with an average D_p of 310 nm); however, sample LS5 had a larger adhesion force, as mentioned earlier. The value was about twice the value encountered for sample LS4. It is clear that the samples with bimodal PSDs behaved differently than their monomodal PSD counterparts. It seems that a small fraction of small particles was enough to disrupt the particle packing. Figure 7.8b, c and d show the AFM height images of the bimodal PSD samples. The images show a transition from Figure 7.8b where the surface topology contains small and large particles to Figure 7.8d, where one cannot distinguish the presence of small particle, likely due to their low mass fraction in the sample.

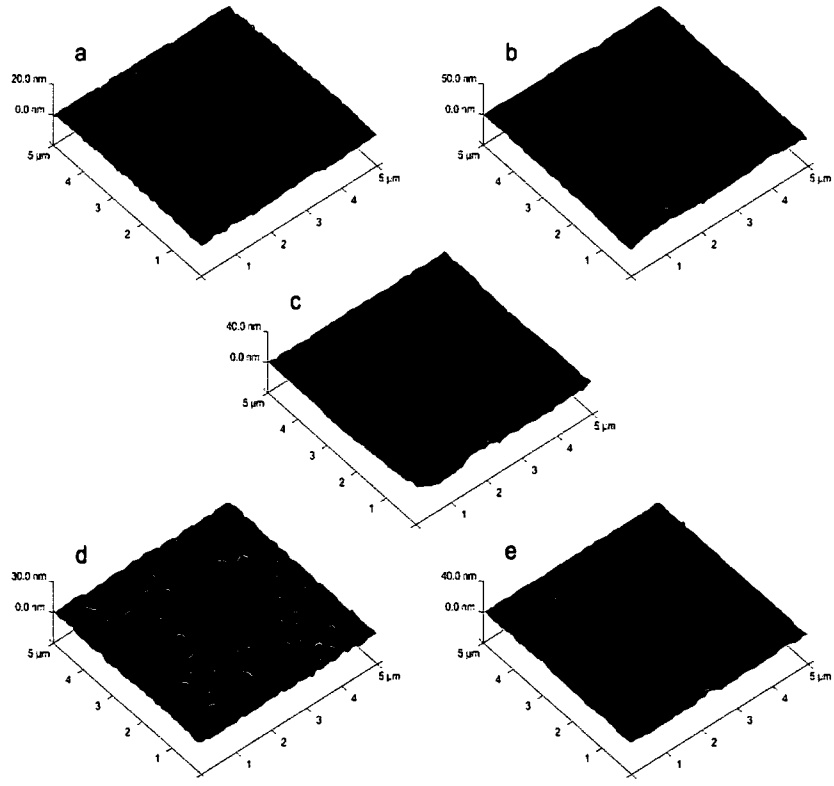

Figure 7.8. AFM three-dimensional images of sample set A. a) sample LS1 (monomodal PSD with a D_p of 167 nm); b) sample LS2; c) sample LS3; d) sample LS4; e) sample LS5 (monomodal PSD with a D_p of 310 nm)

Figure 7.9c shows the PSA properties of the samples with bimodal PSDs. In this sample set, the values of loop tack and peel strength were inversely proportional to the adhesion force. For example, loop tack went from a value of 290 N/m to 480 N/m when the adhesion force decreased from 96 nN to 38 nN. This trend was similarly observed in the results of peel strength. The question that arises is how the adhesion force is related to the PSA properties. However, further studies are required to clarify this dependence.

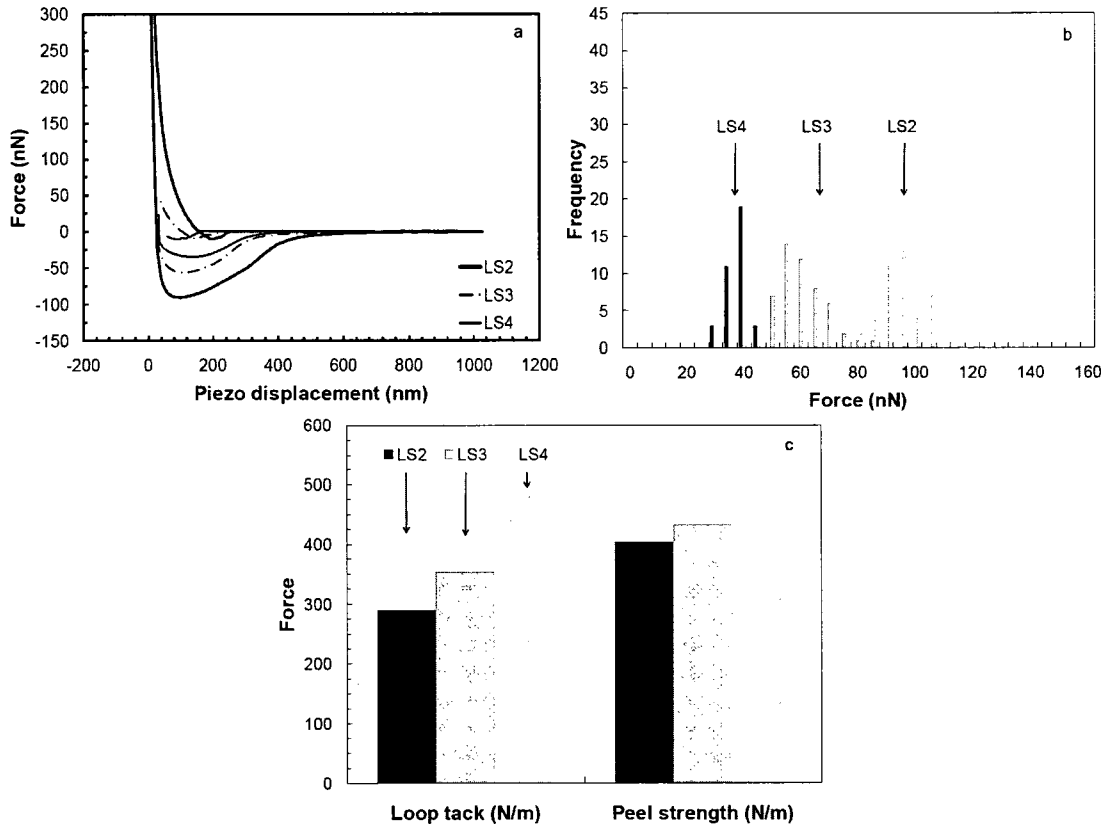

Figure 7.9. a) Force-distance curves; b) Histograms of snap-off forces and c) Loop tack and peel strength values for bimodal MWD miniemulsion-based samples HL2, HL3 and HL4

7.4 CONCLUSIONS

The adhesion forces estimated in this study depended on whether one was dealing with monomodal or bimodal distributions of molecular weight or particle size. The results showed that the samples with bimodal distributions were behaving differently than their monomodal counterparts. Sample set A contained an array of monomodal and bimodal MWD samples in order to evaluate the dependence of the adhesion on molecular weight. It

was observed that for the samples with monomodal MWDs, the adhesion force showed a large difference between the sample with a molecular weight of 97,000 g mol^{-1} and the sample with 750,000 g mol^{-1}, where the latter exhibited a large plastic deformation. The PSA properties were also analyzed and it was found that while loop tack did not increase significantly, peel strength exhibited an almost 5-fold increase, which can be correlated with the adhesion force results. On the other hand, the force curves of the bimodal MWD samples showed the film with the highest fraction of low M_w (i.e., sample HL4) had the lowest adhesion force. It is possible that in the case of the samples with bimodal distributions, the samples with more "soft" particles had acted as plasticizers and thus, decreasing adhesion force. It was also observed that the force histograms did not show the presence of two peaks corresponding to the two types of particles, which led us to conclude that the film had a homogeneous nature.

The second sample set included two samples with monomodal PSDs and three samples with bimodal PSDs. It was found that in the case of samples LS1 and LS5 (monomodal distributions with small and large diameters, respectively), there was no significant difference in the adhesion force while the results of adhesion energy displayed larger values for the larger D_p, which was consistent with the PSA properties results. Finally, the results of the bimodal PSD samples showed that the adhesion force and energy increased with the fraction of small particles where in a small fraction of these particles is enough to disrupt the particle packing and increase the adhesion forces. These results showed that, on one hand, the force curves obtained in AFM were able to detect differences in molecular weight and particle size. It was also corroborated that particle size did have an influence on adhesion force and on the PSA properties. Nevertheless, the relationship between adhesion forces at the nanoscale and the macroscale PSA properties is not clear yet.

7.5 ACKNOWLEDGEMENTS

The authors gratefully acknowledge the financial support of the Natural Science and Engineering Research Council (NSERC) of Canada and valuable discussions with Dr. Hugh Horton (Queen's University, Kingston, Canada). G.E.F. thanks the National Council of Science and Technology (CONACYT) of Mexico for the doctoral scholarship provided.

7.6 REFERENCES

Asua, J.M., 2002. Miniemulsion polymerization. Progress in Polymer Science 27, 1283-1346.

Ata, A., Rabinovich, Y.I., Singh, R.K., 2002. Role of surface roughness in capillary adhesion. Journal of Adhesion Science and Technology 16, 337-346.

Aymonier, A., Papon, E., Castelein, G., Brogly, A., Tordjeman, P., 2003. Influence of surface and bulk structures of acrylic PSA films onto their tack properties. Journal of Colloid and Interface Science 268, 341-347.

Bouzid, D., Gaboriaud, F., McKenna, T.F., 2005. Atomic force microscopy as a tool to study the distribution of rubber in high impact poly(propylene) particles. Macromolecular Materials and Engineering 290, 565-572.

Burnham, N.A., Colton, R.J., Pollock, H.M., 1993. Interpretation of force curves in force microscopy. Nanotechnology 4, 64-80.

Canetta, E., Marchal, J., Lei, C.H., Deplace, F., Konig, A.M., Créton, C., Ouzineb, K., Keddie, J.L., 2009. A Comparison of Tackified, Miniemulsion Core-Shell Acrylic Latex Films with Corresponding Particle-Blend Films: Structure-Property Relationships. Langmuir 25, 11021-11031.

Cappella, B., Sturm, H., Schulz, E., 2002. Stiffness and adhesion characterization of nanolithographed poly(methyl methacrylate) by means of force-displacement curves. Journal of Adhesion Science and Technology 16, 921-933.

Drelich, J., Mittal, K.L., 2005. Atomic Force Microscopy in Adhesion Studies, 1st edition ed. Brill Academic, Leiden, The Netherlands.

DuChesne, A., Bojkova, A., Rottstegge, J., Glasser, G., Neher, D., Krieger, S., 1999. Film formation of heterogeneous latex systems - a comparative study by mechanical testing, electron microscopy, interferometry and solid state NMR. Physical Chemistry Chemical Physics 1, 3871-3878.

Eaton, P.J., Graham, P., Smith, J.R., Smart, J.D., Nevell, T.G., Tsibouklis, J., 2000. Mapping the surface heterogeneity of a polymer blend: An adhesion-force-distribution study using the atomic force microscope. Langmuir 16, 7887-7890.

Eckersley, S.T., Rudin, A., 1996. Film formation of acrylic copolymer latices: A model of stage II film formation. Film Formation in Waterborne Coatings 648, 2-21.

Geurts, J.M., Lammers, M., German, A.L., 1996. The effect of bimodality of the particle size distribution on film formation of latices. Colloids and Surfaces A: Physicochemical and Engineering Aspects 108, 295-303.

Ho, C.C., Khew, M.C., 2002. Morphology and Adhesive Force of Natural Rubber Latex Films by Atomic Force Microscopy, in: Daniels, E.S., Sudol, E.D., El-Aasser, M.S. (Eds.), Polymer Colloids. Science and Technology of Latex Systems. American Chemical Society, Oxford, pp. 239-259.

Hutter, J.L., Bechhoefer, J., 1993. Calibration of atomic-force microscope tips. Review of Scientific Instruments 64, 1868-1873.

Jovanovic, R., Dubé, M.A., 2004. Emulsion-based pressure-sensitive adhesives: A review. Journal of Macromolecular Science: Polymer Reviews C44, 1-51.

Lam, S., Hellgren, A.C., Sjoberg, M., Holmberg, K., Schoonbrood, H.A.S., Unzue, M.J., Asua, J.M., Tauer, K., Sherrington, D.C., Goni, A.M., 1997. Surfactants in heterophase polymerization: A study of film formation using atomic force microscopy. Journal of Applied Polymer Science 66, 187-198.

Lei, C.H., Ouzineb, K., Dupont, O., Keddie, J.L., 2007. Probing particle structure in waterborne pressure-sensitive adhesives with atomic force microscopy. Journal of Colloid and Interface Science 307, 56-63.

Leite, F.L., Herrmann, P.S.P., 2005. Application of Atomic Force Spectroscopy (AFS) to Studies of Adhesion Phenomena: a Review, in: Drelich, J., Mittal, K.L. (Eds.), Atomic Force Microscopy in Adhesion Studies. Ridderprint, Leiden, The Netherlands, pp. 3-44.

Maghsoudy-Louyeh, S., Tittman, B.R., 2008. Assessment of hydrous affinity of selected material. Colloids and Surfaces A: Physicochemical and Engineering Aspects 331, 268-274.

Mallégol, J., Dupont, O., Keddie, J.L., 2001. Obtaining and interpreting images of waterborne acrylic pressure-sensitive adhesives by tapping-mode atomic force microscopy. Langmuir 17, 7022-7031.

Mallégol, J., Dupont, O., Keddie, J.L., 2003. Morphology and elasticity of waterborne acrylic pressure-sensitive adhesives investigated, with atomic force microscopy. Journal of Adhesion Science and Technology 17, 243-259.

Mallégol, J., Gorce, J.P., Dupont, O., Jeynes, C., McDonald, P.J., Keddie, J.L., 2002. Origins and effects of a surfactant excess near the surface of waterborne acrylic pressure-sensitive adhesives. Langmuir 18, 4478-4487.

Moon, S.H., Foster, M.D., 2002. Influence of humidity on surface behavior of pressure sensitive adhesives studied using scanning probe microscopy. Langmuir 18, 8108-8115.

Moon, S.H., Swearingen, S., Foster, M.D., 2004. Scanning probe microscopy study of dynamic adhesion behavior of polymer adhesive blends. Polymer 45, 5951-5959.

Paiva, A., Foster, M.D., 2001. Aging of model pressure sensitive adhesives studied with scanning probe microscopy. Journal of Adhesion 75, 145-+.

Paiva, A., Sheller, N., Foster, M.D., Crosby, A.J., Shull, K.R., 2000. Study of the surface adhesion of pressure-sensitive adhesives by atomic force microscopy and spherical indenter tests. Macromolecules 33, 1878-1881.

Paiva, A., Sheller, N., Foster, M.D., Crosby, A.J., Shull, K.R., 2001. Microindentation and nanoindentation studies of aging in pressure-sensitive adhesives. Macromolecules 34, 2269-2276.

Phillips, J.P., Deng, X., Stephen, R.R., Fortenberry, E.L., Todd, M.L., McClusky, D.M., Stevenson, S., Misra, R., Morgan, S., Long, T.E., 2007. Nano- and bulk-tack adhesive properties of stimuli-responsive, fullerene-polymer blends, containing polystyrene-block-polybutadiene-block-polystyrene and polystyrene-block-polyisoprene-block-polystyrene rubber-based adhesives. Polymer 48, 6773-6781.

Portigliatti, M., Hervet, H., Leger, L., 2000a. Nanotack test: adhesive behavior of single latex particles. Comptes Rendus De l Academie Des Sciences Serie Iv Physique Astrophysique 1, 1187-1196.

Portigliatti, M., Koutsos, V., Hervet, H., Leger, L., 2000b. Adhesion and deformation of a single latex particle. Langmuir 16, 6374-6376.

Pressure Sensitive Tape Council, 2004. Test Methods for Pressure Sensitive Adhesive Tapes, 14th ed. ed. Pressure Sensitive Tape Council, Northbrook, Illinois.

Raiteri, R., Butt, H.J., Beyer, D., Jonas, S., 1999. Heterogeneous polymer-containing films: a comparison of macroscopic properties with microscopic properties determined by atomic force microscopy. Physical Chemistry Chemical Physics 1, 4881-4887.

Schantz, S., Carlsson, H.T., Andersson, T., Erkselius, S., Larsson, A., Karlsson, O.J., 2007. Poly(methyl methacrylate-co-ethyl acrylate) latex particles with poly(ethylene glycol) grafts: Structure and film formation. Langmuir 23, 3590-3602.

Sommer, F., Duc, T.M., Pirri, R., Meunier, G., Quet, C., 1995. Surface-Morphology of Poly(Butyl Acrylate) Poly(Methyl Methacrylate) Core-Shell Latex by Atomic-Force Microscopy. Langmuir 11, 440-448.

Steward, P.A., Hearn, J., Wilkinson, M.C., 2000. An overview of polymer latex film formation and properties. Advances in Colloid and Interface Science 86, 195-267.

Tobing, S.D., Klein, A., 2000. Mechanistic studies in tackified acrylic emulsion pressure sensitive adhesives. Journal of Applied Polymer Science 76, 1965-1976.

Tzitzinou, A., Keddie, J.L., Geurts, J.M., Peters, A.C.I.A., Satguru, R., 2000. Film formation of latex blends with bimodal particle size distributions: Consideration of particle deformability and continuity of the dispersed phase. Macromolecules 33, 2695-2708.

Vorobyova, O., Winnik, M.A., 2001. Morphology of poly(2-ethylhexyl methacrylate): poly(butyl methacrylate) latex blend films. Macromolecules 34, 2298-2314.

Wang, T., Canetta, E., Weerakkody, T.G., Keddie, J.L., 2009. pH Dependence of the Properties of Waterborne Pressure-Sensitive Adhesives Containing Acrylic Acid. ACS Applied Materials & Interfaces 1, 631-639.

Xu, G.Z.H., Dong, J.P., Zhang, J.G., Severtson, S.J., Houtman, C.J., Gwin, L.E., 2008. Characterizing the distribution of nonylphenol ethoxylate surfactants in water-based pressure-sensitive adhesive films using atomic-force and confocal Raman microscopy. Journal of Physical Chemistry B 112, 11907-11914.

CHAPTER 8

GENERAL DISCUSSION AND CONCLUSIONS

The significant momentum generated by our society and by many governments towards the greening of consumer products has given researchers the opportunity and the environmental stewardship to create products that have a lower impact on the planet. Emulsion polymerization was a step forward in the use of technologies for the production of pressure-sensitive adhesives (PSA) with low volatile organic compounds content (Jovanovic and Dubé, 2004). Nevertheless, the performance of emulsion-based PSAs must still be better than those produced by traditional technologies such as solution polymerization (Tobing and Klein, 2000).

One alternative is miniemulsion polymerization, which has gained much attention due to its droplet nucleation mechanism. More than 1,000 scientific articles and around 150 patents concerning miniemulsion polymerization have been published during the last two decades (Asua, 2002; Schork et al., 2005; Landfester, 2009). One of the benefits of miniemulsion that was exploited in this thesis was the specific particle growth mechanism of miniemulsion polymerization, which enables the encapsulation of any compound that can be regarded as hydrophobic, e.g., oligomers, monomers and inorganic particles (Antonietti and Landfester, 2002). The present project had the intention of contributing to the improvement of PSA performance by using miniemulsion polymerization to create bimodal distributions of molecular weight or bimodal distributions of particle size.

The first part of this study was devoted to finding an adequate copolymer system that could be commercially used as a PSA and serve as our proof of concept for the creation of bimodal distributions. The first copolymer studied was poly(2-ethyl hexyl acrylate/vinyl acetate/methacrylic acid (EHA/VAc/MAA). The next step was to find a stabilization mixture that would ensure that polymerization would proceed primarily under droplet nucleation conditions (required for a "true" miniemulsion). A screening of surfactants was carried out including an anionic surfactant: sodium dodecyl sulfate (SDS), and two non-ionic surfactants: Triton X-405 and Disponil A3065. The difference between the two surfactants

used in this study is their chemical nature, which leads to differences in their colloidal behaviour. Triton X-405 is an octyl phenol ethoxylated surfactant with a high hydrophile/lipophile balance (HLB) of 17.6 and a critical micelle concentration (CMC) of 3.38 g/L. On the other hand, Disponil A3065 is a mixture of ethoxylated linear fatty alcohols with a lower HLB of 16.5 and a much lower CMC of 0.14 g/L (see Appendix A). The results found that when using the stabilization system SDS/Triton X-405, only part of the original monomer droplets nucleated while the rest likely served as monomer reservoirs. When only SDS was used in the preparation of the miniemulsion, it resulted in at least a 2-fold increase in the number of polymer particles with respect to the initial number of droplets. Conversely, the EHA/VAc/MAA miniemulsions prepared using the stabilization system SDS/Disponil gave remarkably stable miniemulsions with solids contents up to 43 wt.-% and their droplet size distributions did not changed significantly until day 9 after preparation (cf. Figure 8.1). Nevertheless, difficulties arising from the low reactivity of VAc led to incomplete conversions, resulting in poor PSA performance. This was because most of the particles were comprised of EHA, thus leading to T_g values outside of the recommended range for PSA applications.

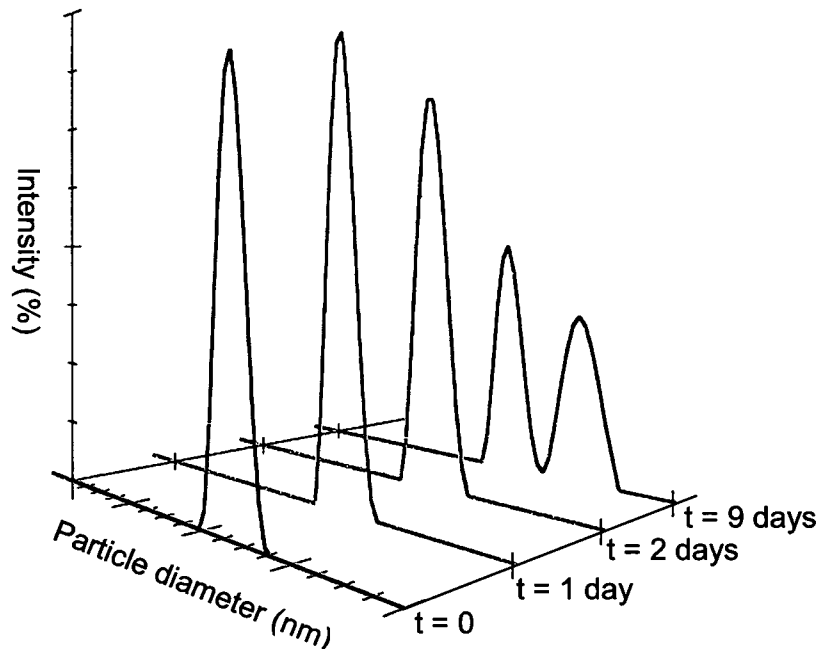

Figure 8.1 Droplet size distribution of an EHA/MMA/AA miniemulsion stabilized with a surfactant mixture of SDS/Disponil A3065

The VAc in the copolymer was substituted with methyl methacrylate (MMA), which has a higher hydrophobicity and is a more reactive monomer compared to VAc. It was found that the surfactant mixture SDS/Disponil A3065 in a 7/93 mol. % stabilized the miniemulsion adequately. The study also found that in order to obtain a relatively stable EHA/MMA miniemulsion, the amount of surfactant would have to be kept at concentrations that would result in polymer particle surface coverage of no more than 38%.

The next step in our research was devoted to a systematic comparison between PSAs produced by miniemulsion and conventional emulsion polymerization and how three important factors (chain transfer agent, surfactant and comonomer composition) affected the latex, polymer and PSA properties. Two 2^3 factorial designs were carried out, one for miniemulsion and another for conventional emulsion polymerization. Various differences were highlighted. For instance, the surfactant concentration did not present as significant an influence on the R_p of miniemulsion polymerization as it had in the case of conventional emulsion polymerization. Another difference found during the statistical analysis was related to the monomer composition, which had no influence on R_p in conventional emulsion polymerization. However, higher amounts of EHA (and lower MMA) led to higher conversions in miniemulsion polymerization, which was attributed to the fact that the propagation rate coefficient for EHA is an order of magnitude higher than it is for MMA.

Regarding polymer properties such as the M_w, it was found that conventional emulsion polymerization consistently led to higher weight-average M_w's. Nevertheless, it was observed that a batch miniemulsion polymerization was able to produce coagulum-free latexes of high M_w while latexes produced by batch conventional emulsion polymerization presented large amounts of coagulum (more than 50 wt.-% of the initial mass). In terms of the molecular weight between entanglements (M_e), it was observed that conventional emulsion and miniemulsion polymerization produced different values of this polymer property. In one of the runs, miniemulsion polymerization produced a polymer with a M_e that was half the value found in the conventional emulsion-based polymer. This is, even though conventional emulsion polymerization consistently produced polymers with higher weight-average M_w, it was possible to produce polymers with tighter networks using miniemulsion polymerization – under certain conditions. This was likely due to the fact that emulsion and miniemulsion polymerization follow different particle nucleation mechanisms, which

resulted in a different particle microstructure. In other words, polymer particles produced by miniemulsion polymerizations start with high concentrations of monomer in the droplets while those produced by conventional emulsion polymerization start with lower monomer concentrations (Schork and Lu, 2009). It is expected that in miniemulsion polymerization, lower M_w are caused by higher chain transfer to monomer by the propagating radicals. Another key difference between the two techniques lies in the fact that miniemulsion polymerization produced larger particle diameters resulting in a lower number of particles and this likely had an effect on the average number of radicals per particle. While the lower M_w had been already reported (Mouran et al., 1996), there was no report on entanglement densities. An additional chain transfer agent level (concentration of 0.1 wt.-% with respect to monomer) subsequently added to the factorial design in order to expand the range of properties attained, showed that miniemulsion polymerization was able to produce coagulum-free latexes with entanglement densities (M_w/M_e) up to ~11 with M_e as low as 26,000 g mol^{-1} in a single batch reaction. Figure 8.2 shows the viscoelastic behaviour of three miniemulsion-based samples with increasing values of M_w/M_e, which were prepared in a single batch reaction.

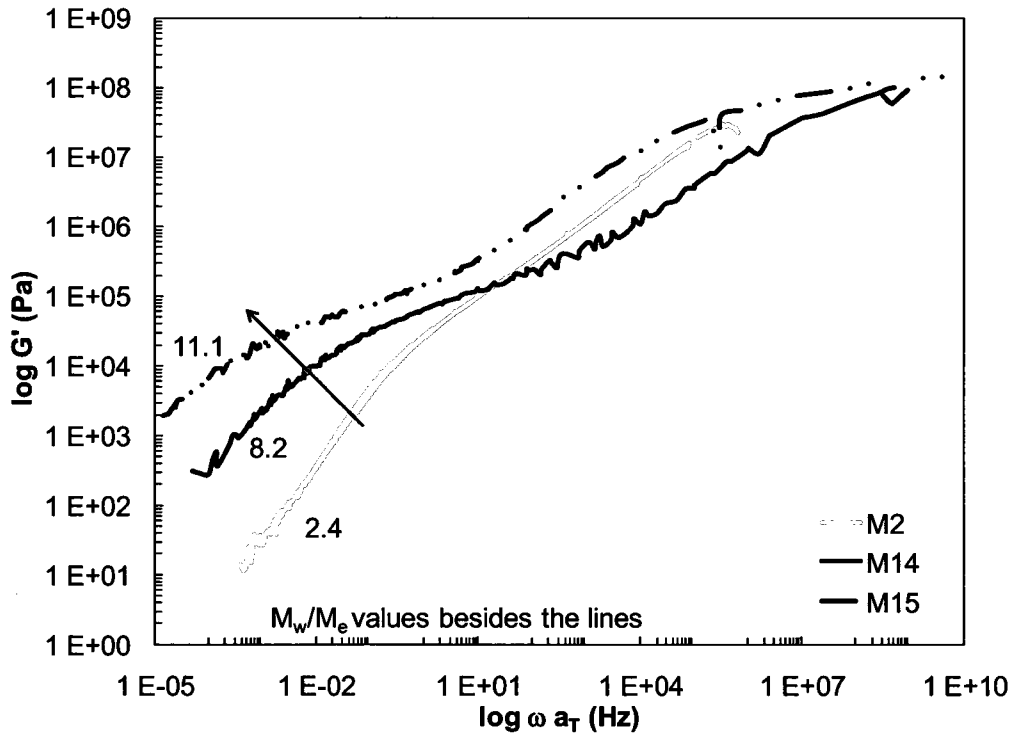

Figure 8.2 Storage and loss modulus of selected miniemulsion-based PSA samples

As to the PSA properties obtained, the analysis showed that for miniemulsion polymerization, the chain transfer agent concentration was the main factor affecting loop tack followed by the monomer composition and surprisingly, the surfactant concentration had very little effect. Additionally, it was observed that loop tack was directly proportional to the entanglement density (M_w/M_e) up to a maximum value of 7.5, at which point loop tack decreases. The same trend was observed for peel strength with fairly similar maxima. As to shear strength, it was found that higher entanglement densities led to higher values of this property.

Subsequent work was focused on the creation of bimodal distributions. A one-pot two-step miniemulsion polymerization strategy was engineered for the production of well-defined latexes with bimodal molecular weight (see Figure 8.3) or bimodal particle size distributions (see Figure 8.4). The latexes produced by this approach were termed "in-situ bimodal" and their viscoelastic and PSA properties were compared to the properties of monomodal distributions as well as bimodal distributions produced by standard post-polymerization blending. Regarding the bimodal MWD latexes, it was found that gel fractions of in-situ bimodal MWD latexes were higher than those obtained by post-polymerization blending, suggesting that additional intermolecular chain transfer reactions occurred during the miniemulsion polymerization. The viscoelastic analysis of the sample showed that increasing the fraction of particles with low M_w modified the microstructure from a crosslinked structure (as noted in the rubbery plateau region) to a lightly crosslinked structure (as noted in the terminal region). PSA performance analysis demonstrated that loop tack and peel strength exhibited higher values when the latexes were prepared "in-situ" as opposed to post-polymerization blending. They also displayed higher values compared to the monomodal MWDs.

Bimodal PSD latexes were also successfully created using the proposed approach. In contrast to bimodal MWD latexes, the samples with bimodal PSDs did not present any significant differences in the viscoelastic behaviour when comparing the different in-situ bimodal PSD latexes (i.e., different ratios of large-to-small particles) or when compared to the monomodal PSD samples. In terms of their PSA performance, it was observed that loop tack and shear strength were significantly different – depending on the ratio of large-to-small particles used – and in most cases, they displayed values larger than their corresponding

monomodal PSD latexes. On the other hand, PSA films cast from latexes with different ratios of large-to-small particles did not exhibit differences between the measured values of peel strength. It was only observed that various films with bimodal PSDs took on a peel strength value similar to that obtained from films cast from a monomodal PSD latex with large particles.

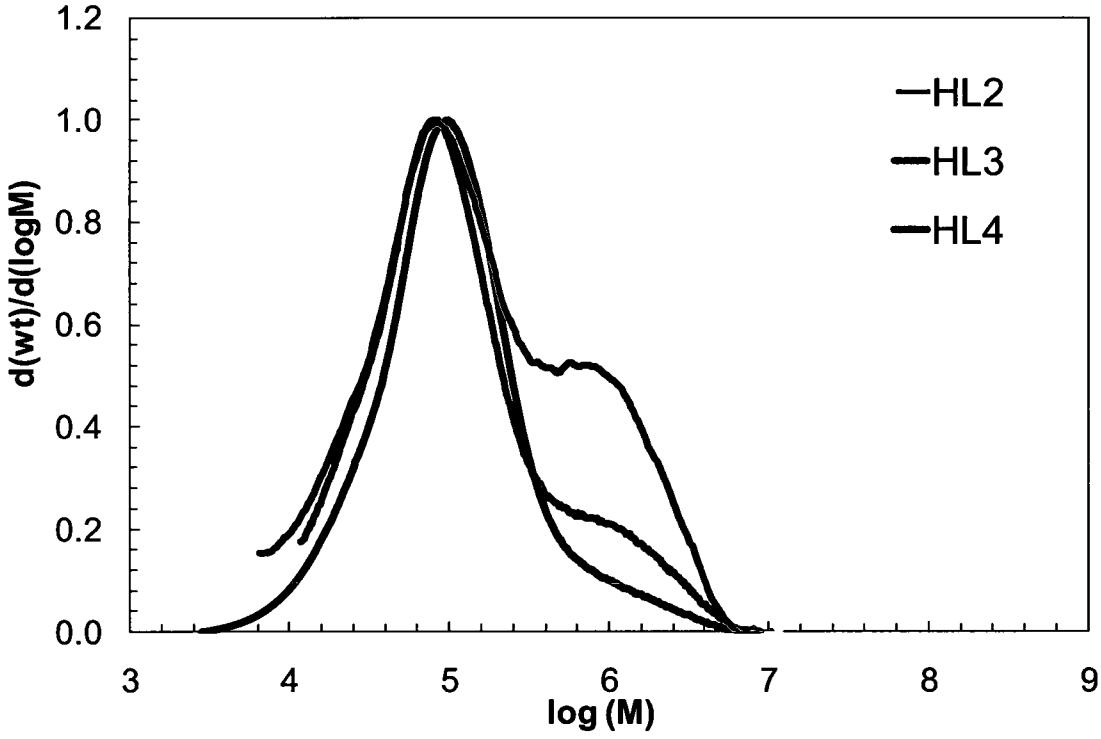

Figure 8.3 Bimodal molecular weight distributions

The final part of the research was devoted to an exploratory study of the use of Atomic Force Microscopy (AFM) to shed light on the influence of having a bimodal MWD or bimodal PSD in nanoscale measurements of adhesion force and energy. For the samples with monomodal MWDs, the adhesion force showed a large difference between the sample with a molecular weight of 97,000 g mol^{-1} and the sample with 750,000 g mol^{-1}. It was also observed that the histograms of the adhesion force did not show the presence of two peaks (corresponding to the two types of particles), which led us to conclude that the film had a homogeneous nature and the particles were intermixed, creating a single adhesion value. The

results of the bimodal PSD samples showed that the adhesion force and energy increased with the fraction of smallest particle diameter wherein a small fraction of these particles was enough to disrupt the particle packing and increase adhesion forces. The relationship between macroscale PSA properties and those at the nanoscale is still unclear. Studies have reported a linear relationship between the adhesion energy and tack (Raiteri et al., 1999); however, this trend was not found in the current project.

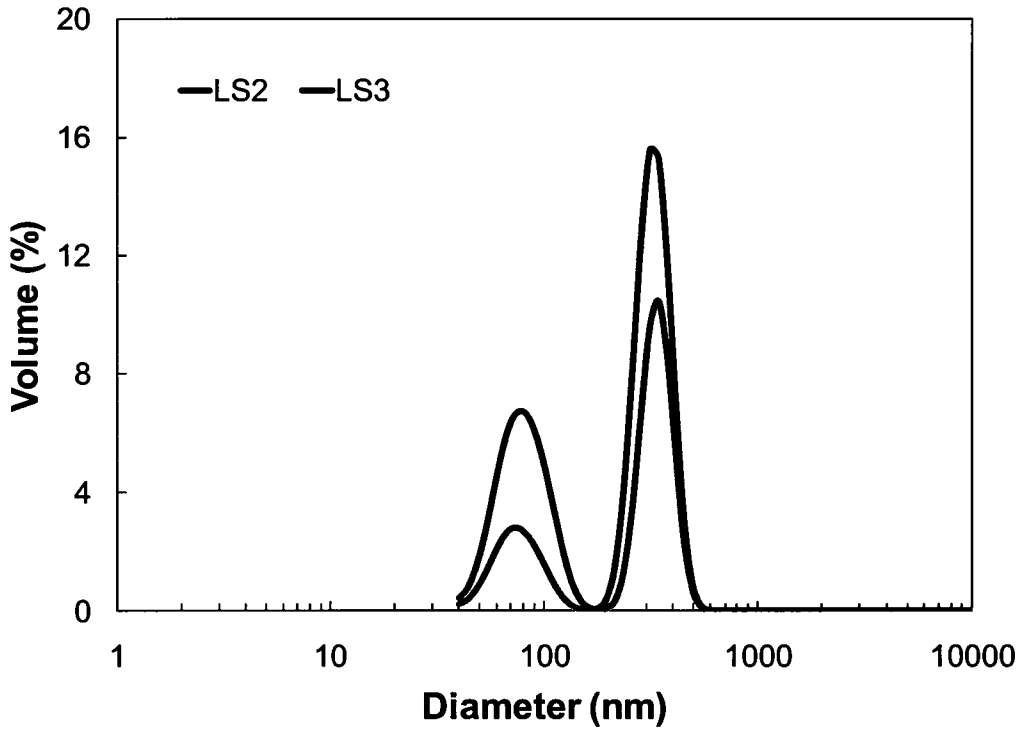

Figure 8.4 Bimodal particle size distributions

8.1 MAIN CONTRIBUTIONS AND FINDINGS

The contributions of this thesis are briefly detailed below, with an assessment of the objectives of the research project.

8.1.1. Stabilization of poly(EHA/VAc/MAA) and poly(EHA/MMA/AA) miniemulsion with intermediate solids content

The initial screening study of the two copolymers considered in this project led to satisfactory formulation conditions to create colloidally stable miniemulsion-based latexes with intermediate to high solids contents: 43 wt.-% for poly (EHA/VAc/MAA) and 54 wt.-% for poly (EHA/MMA/AA) (Chapters 3 and 4). The latexes produced using octadecyl acrylate as the hydrophobic compound (to boost the droplets' osmotic pressure) and a surfactant mixture of an anionic surfactant (sodium dodecyl sulfate) with a non-ionic surfactant (ethoxylate linear fatty alcohol) stabilized the miniemulsion against coalescence and diffusional degradation (Ostwald ripening). The results showed that a 7/93 wt.-% of anionic/non-ionic surfactant produces a miniemulsion with a narrow polydispersity that is stable for a period long enough to be polymerized. More importantly, it was shown that if the miniemulsion is adequately stabilized covering a specific monomer droplet surface area, the number of droplets can be kept constant and produce an equal number of particles.

8.1.2. Microstructural differences between miniemulsion-based and emulsion-based PSA films

The systematic comparison of miniemulsion- and emulsion-based latex polymers revealed that the weight-average molecular weight and the entanglement molecular weight of emulsion-based polymers are larger than that of miniemulsion-based polymers under certain conditions (Chapter 6). Miniemulsion polymerization produced more compact microstructures compared to conventional emulsion polymerization when MMA concentrations in the monomer droplets was the highest within the range studied in the present project (i.e., 65 wt.-%) and when chain transfer agent concentration was sufficiently low to produce a M_w above 80,000 g mol^{-1}. Lower concentrations of the chain transfer agent

evidently led to higher M_w and even more compact microstructures. The results showed that in a single step, batch miniemulsion polymerization was able to produce entanglement densities (ratio of weight-average molecular weight by the entanglement molecular weight) with values up to 11. The entanglement densities could also be tailored by changing the chain transfer agent concentration or the copolymer composition directly impacting the gel fraction and viscoelastic behaviour, which in turn affected PSA performance.

8.1.3. Creation of bimodal distributions of molecular weight and particle size with a one-pot two-step approach

If properly stabilized, a miniemulsion population will have a minimal interaction with other miniemulsion populations present in the reactor, as long as the first population has reacted enough to ensure that the monomer droplets have become polymer particles. The approach successfully created well-defined, and most importantly, predictable bimodal distributions of molecular weight and particle size. The benefit of the approach lies in its simplicity and flexibility. The factorial design carried out in a previous stage uncovered the range of initial reaction conditions needed to attain a specific adhesive property and thus, the multiple populations can be prepared as if they were to be polymerized individually and sequentially added to a single reactor. This approach represents a straightforward method to prepare bimodal distributions.

8.1.4. PSA performance

The factorial design highlighted the differences between the PSA films produced by the two techniques (conventional emulsion and miniemulsion polymerization) and confirmed that different particle nucleation mechanisms have an impact on the PSA performance. The factorial design established a range of polymer and adhesive properties obtainable under certain initial reaction conditions, which served to identify optimum conditions for the production of PSA with customized properties.

The one-pot two-step approach developed in this research project showed that the miniemulsion polymerization of multiple populations in one reactor produced higher gel

fractions in the "in-situ" bimodal polymer samples compared to conventional blends, which was mainly due to additional intraparticle crosslinking. This phenomenon contributed to an improvement of the PSA properties when compared to the latexes with monomodal distributions (be it of molecular weight or particle size) or those post-polymerization blended bimodal distributions latexes.

8.1.5. Measurement of nano-adhesive properties by Atomic Force Microscopy (AFM)

A series of PSA samples were prepared and analyzed using AFM to measure force-displacement curves. The samples were prepared from latexes with bimodal molecular weight distribution or with bimodal particle size distribution. The resulting force-displacement curves were used to estimate adhesion forces at the surface of the PSA films. Results showed that (i) the adhesion force decreased as the fraction of particles with low M_w increased in the sample and (ii) the adhesion force increased with higher fractions of particles with small D_p.

8.1.6. Publications

This research project contributed five peer-reviewed publications, where three of them have already been accepted and the remaining two will be submitted shortly. They comprise the manuscripts presented herein. An additional review paper on sensors for monitoring polymerization was prepared and published; however, it is not included in this thesis since it was not directly related to the main goal. A brief description of the review follows:

Critical overview of sensors for monitoring polymerizations
G.E. Fonseca, M.A. Dubé, A. Penlidis; Macromolecular Reaction Engineering, 3, 327-373, 2009.

- During the research project, a review of the available on-line and in-line sensor technologies specifically developed for polymerization reactors from 1990 up to the present day was compiled and published. It presents the state-of-the-art in the field including about 600 references of the sensor technology area in the last two decades. It includes sensors for

operational parameters in polymer reactors (i.e., temperature, pressure, level and flow) and, more importantly, sensors for polymer property monitoring (i.e., calorimetry, chromatography, and spectroscopy, among others). It also discusses other complementary topics such as state estimation, multivariate statistical methods, fault diagnosis techniques and optimal sensor selection and location.

8.2. RECOMMENDATIONS FOR FUTURE RESEARCH

The improvement of the performance of environmentally sound alternatives to the currently used solution-based PSAs is an ongoing area of research. The following list offers various recommendations for future research:

a) Simultaneous bimodal distributions of molecular weight and particle size

The polymer particles of the bimodal distributions produced in this study had the same copolymer composition but the approach presented in this thesis could also be used to create PSAs (or latexes) with different copolymer compositions (i.e., different T_g's) or using different monomers in various miniemulsion populations. The approach can also be used to create PSAs (or latexes) with multimodal MWD and PSD simultaneously, i.e., with two or more molecular weights and two or more particle sizes to be able to achieve different properties. A systematic study of the range of properties available with multimodal distributions (be it molecular weight, particle size or copolymer compositions) has the potential to satisfy a large number of applications.

b) Functionalization of the surface of the polymer particles to create continuous networks with higher values of shear strength

An interesting possibility is the preparation of various miniemulsions containing functional groups at the particle surface with the idea of inducing chemical bonding between particles. The reaction of those functional groups could form continuous networks between polymer particles that would potentially improve the cohesion of miniemulsion-based PSAs.

c) Miniemulsion polymerization with hydrophilic monomers

The applications of miniemulsion-based polymers could be diversified with the use of other types of reactants, such as hydrophilic monomers. An interesting area of research, for example, is the inverse miniemulsion of biocompatible and biodegradable polymers that can be used in the polymer matrix of PSAs used for drug-delivery applications.

d) Study of adhesion forces by AFM under liquid conditions

The measurement of adhesion forces at the nanoscale carried out in the present project was performed in air, which means that under certain conditions of relative humidity, capillary condensation on the surface of the PSA films may influence the results. A recommended approach is to perform the measurement of adhesion forces in solution. Such a study would require screening of appropriate testing conditions, particularly, the ionic strength of the solution. The benefit of this type of study is that it eliminates the contributions of capillary forces.

e) Systematic study of adhesion forces using AFM

A broader picture of the influence of molecular weight and particle size on the nanoscale adhesion forces can be obtained using a statistical approach to systematically measure a wider variety of polymer particle populations, in order to highlight other main contributions than those observed in the present study. The study of adhesion forces at the nanoscale would contribute to a better understanding of fundamental adhesion phenomena that could highlight the link between macroscale and nanoscale properties with the aim of developing mechanistic models.

8.3. FINAL REMARKS

The present thesis is a step towards the improvement of the performance of latex-based PSAs. The main objective was to be able to produce multimodal distributions of molecular weights and particle sizes in an attempt to fine-tune the PSA properties depending

on the desired application. A second objective of the thesis was to produce PSAs with the potential to compete with those produced by solution polymerization. These objectives were accomplished by i) using a combination of an anionic and a non-ionic surfactant that allowed us to adequately stabilize a miniemulsion comprised of a low T_g monomer (EHA), a high T_g monomer (MMA) and a carboxylated monomer (AA), which constituted a potential PSA system; ii) polymerizing the two miniemulsion populations sequentially in a one-pot two-step approach that created bimodal molecular weight or bimodal particle size distributions; and iii) preparing PSA films from the aforementioned approach that gave values of PSA properties that could be able to compete in the removable PSA market. While our objectives were fulfilled, as our recommendations outline, in order to take advantage of the full the potential that miniemulsion polymerization offers, more research is needed.

This study shows that miniemulsion polymerization is a versatile technique that could be used to create a wide variety of structured polymeric nanoparticles. While the main contributions of the present research were focused on PSA applications, it was also intended to provide the basis for a competitive polymerization technology.

8.4. REFERENCES

Antonietti, M., Landfester, K., 2002. Polyreactions in miniemulsions. Progress in Polymer Science 27, 689-757.

Asua, J.M., 2002. Miniemulsion polymerization. Progress in Polymer Science 27, 1283-1346.

Jovanovic, R., Dubé, M.A., 2004. Emulsion-based pressure-sensitive adhesives: A review. Journal of Macromolecular Science: Polymer Reviews C44, 1-51.

Landfester, K., 2009. Miniemulsion Polymerization and the Structure of Polymer and Hybrid Nanoparticles. Angewandte Chemie-International Edition 48, 4488-4507.

Mouran, D., Reimers, J., Schork, F.J., 1996. Miniemulsion polymerization of methyl methacrylate with dodecyl mercaptan as cosurfactant. Journal of Polymer Science Part A-Polymer Chemistry 34, 1073-1081.

Raiteri, R., Butt, H.J., Beyer, D., Jonas, S., 1999. Heterogeneous polymer-containing films: a comparison of macroscopic properties with microscopic properties determined by atomic force microscopy. Physical Chemistry Chemical Physics 1, 4881-4887.

Schork, F.J., Lu, F., 2009. Relative rates of branching in emulsion and miniemulsion polymerization. Macromolecular Reaction Engineering 3, 539-542.

Schork, F.J., Luo, Y., Smulders, W., Russum, J.P., Butte, A., Fontenot, K., 2005. Miniemulsion Polymerization. Advances in Polymer Science 175, 129-255.

Tobing, S.D., Klein, A., 2000. Mechanistic studies in tackified acrylic emulsion pressure sensitive adhesives. Journal of Applied Polymer Science 76, 1965-1976.

APPENDIX A

ADDITIONAL FIGURES

A.1. Determination of critical micelle concentration and area per surfactant molecule

A.1.1. Disponil A3065

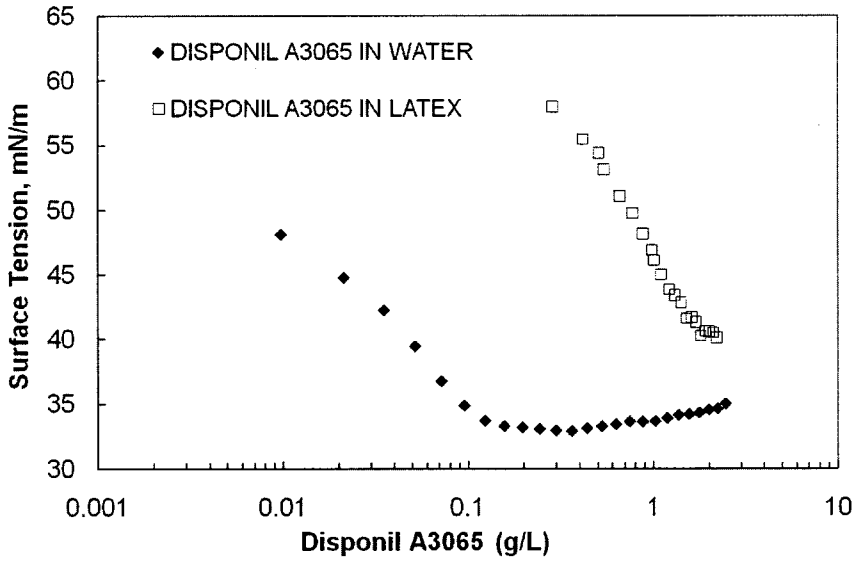

Figure B.1. Determination of the Critical Micelle Concentration of Disponil A3065 in distilled deionized water and surfactant-free 2EHA/MMA latex

A.1.2. Sodium Dodecyl Sulfate

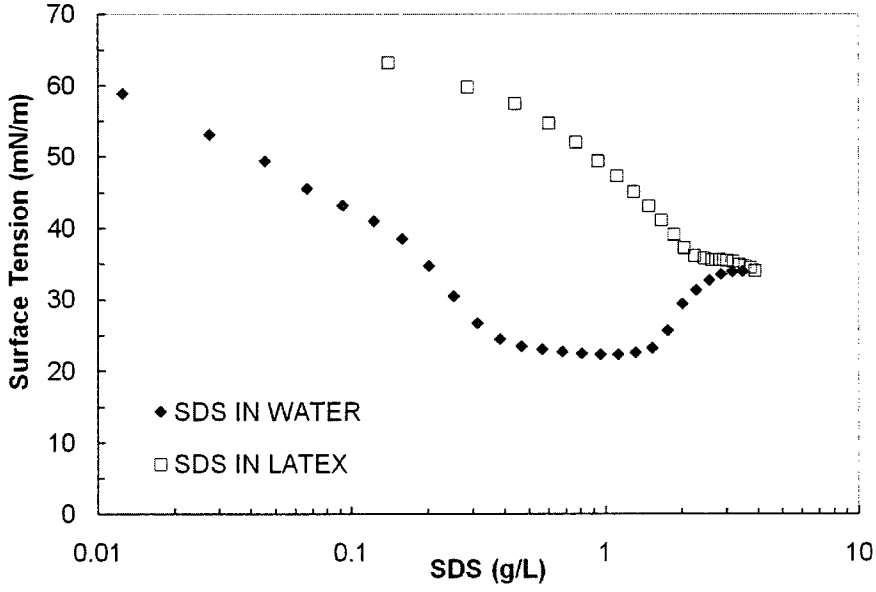

Figure B.2. Determination of the Critical Micelle Concentration of Sodium Dodecyl Sulfate in distilled deionized water and surfactant-free 2EHA/MMA latex

A.1.3. Triton X405

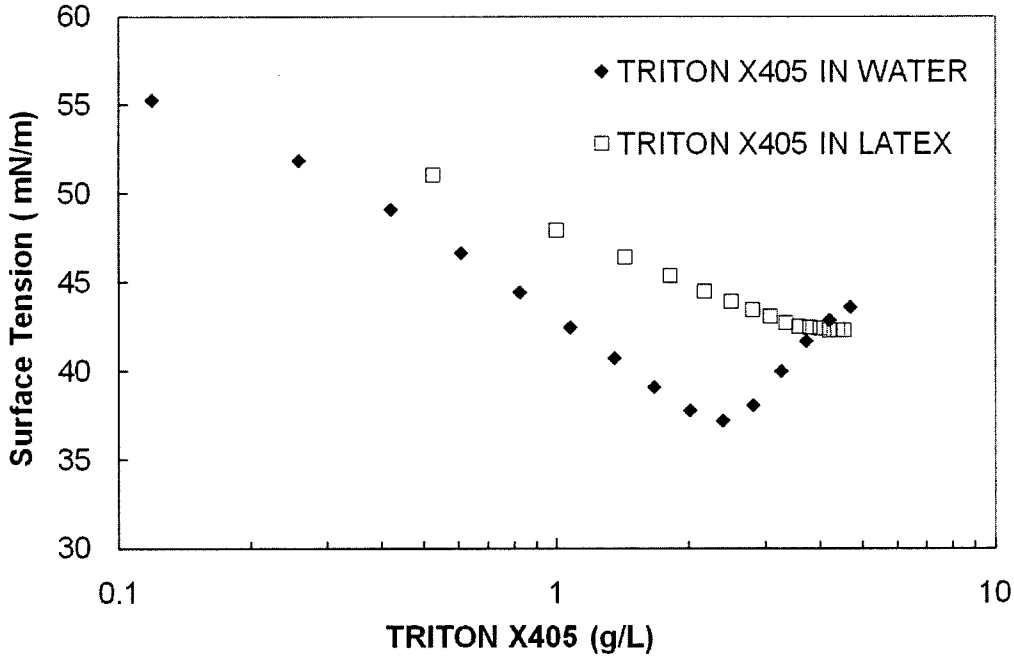

Figure B.2. Determination of the Critical Micelle Concentration of Triton X405 in distilled deionized water and surfactant-free 2EHA/MMA latex

A.1.4. Surfactant mixtures of SDS with Disponil A3065

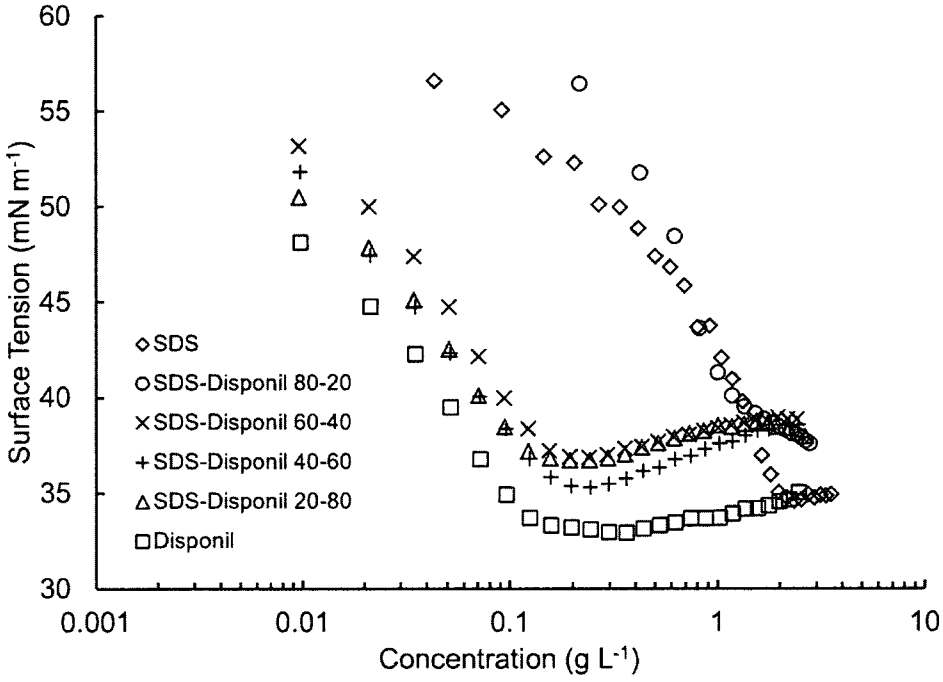

Figure B.3. Determination of the Critical Micelle Concentration in surfactant mixtures of SDS and Disponil A3065

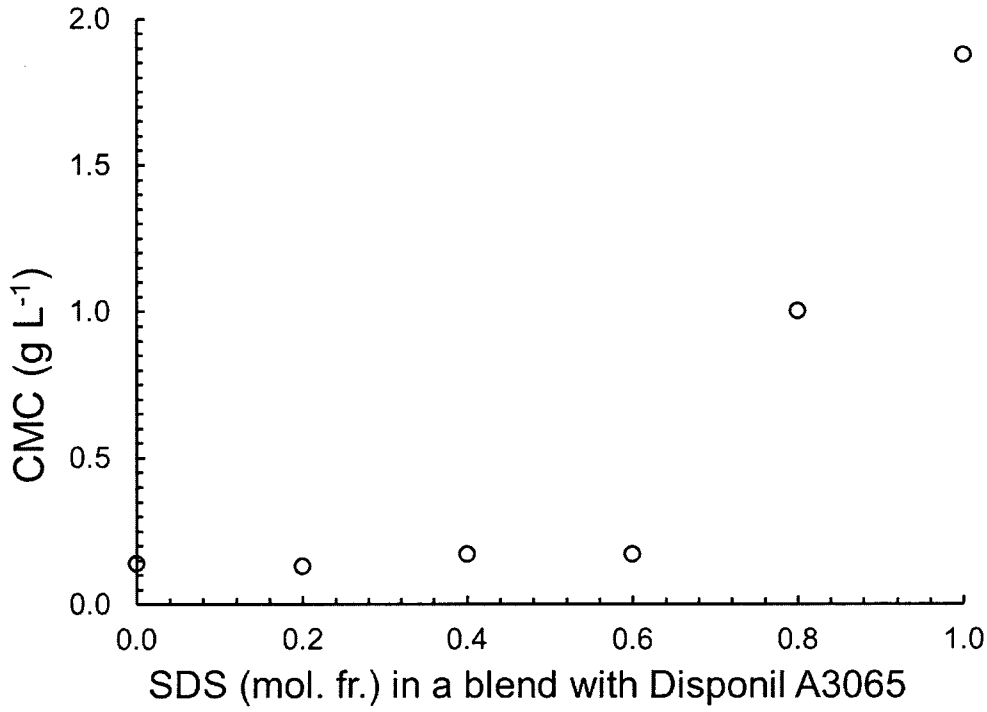

Figure B.4. Critical Micelle Concentration as a function of the mole fraction of SDS in a mixture with Disponil A3065

A.2. Additional Figures of Chapters 3 to 7

Conversion versus time plots of chapter 4

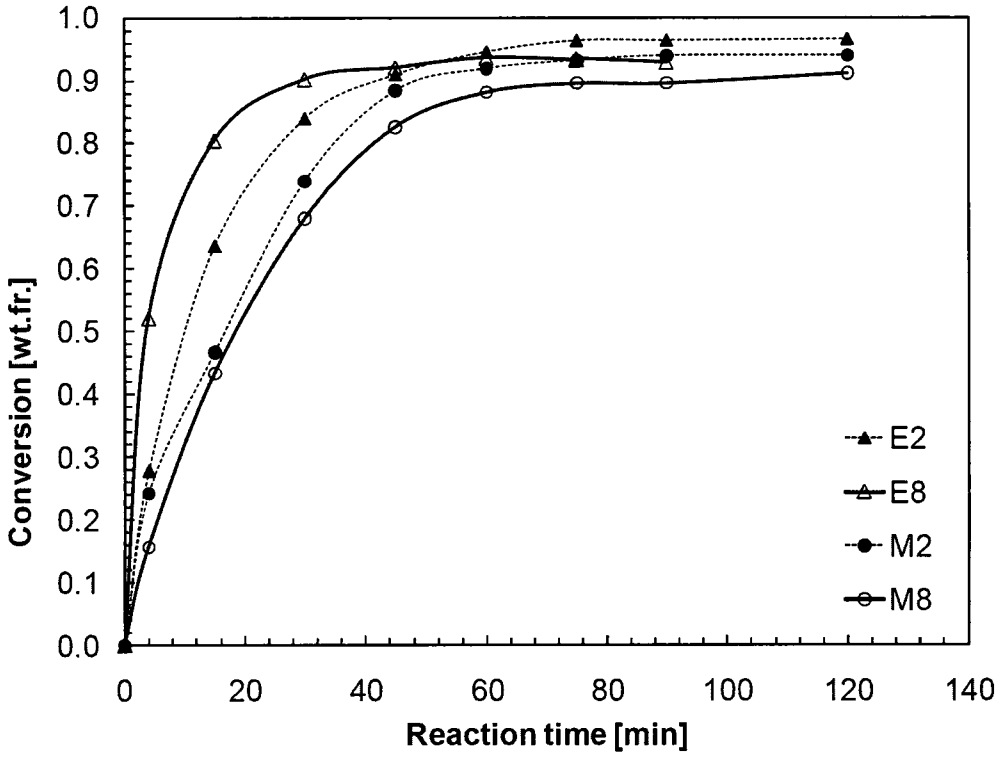

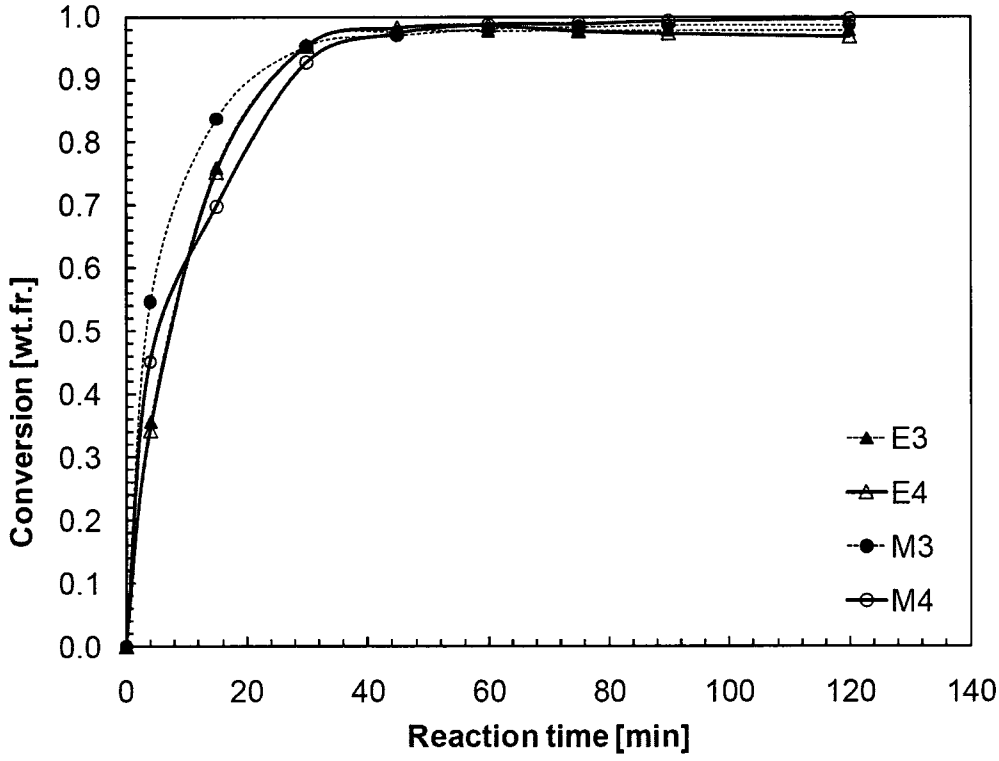

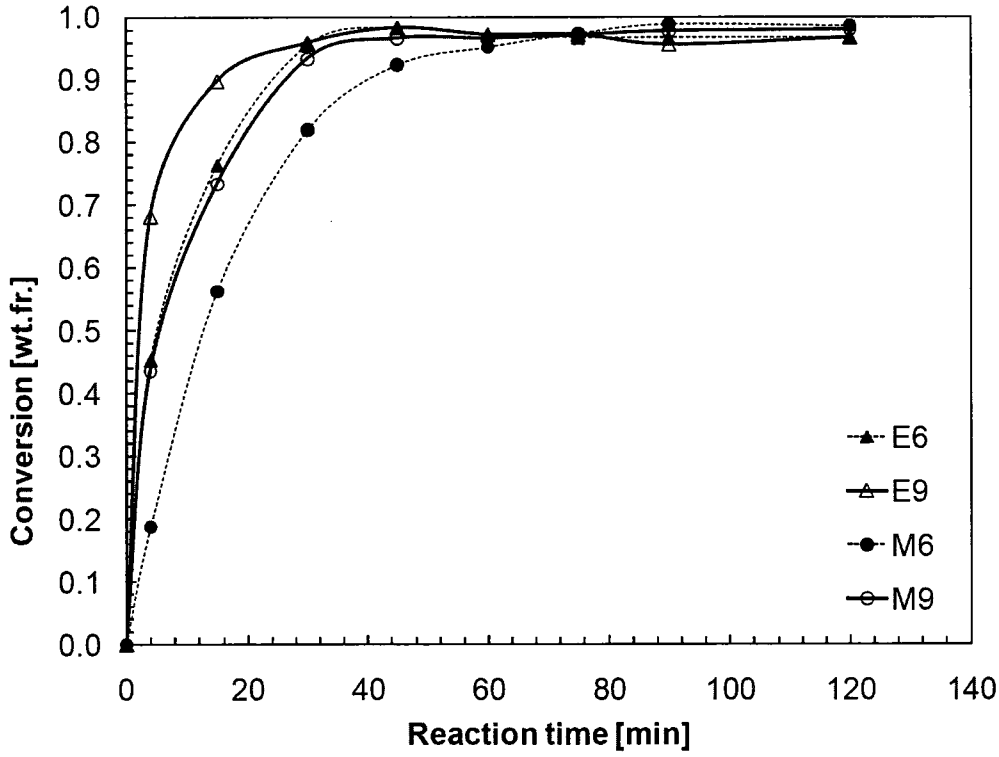
1.0
0.9
0.8
0.7
0.6
0.5
0.4
0.3
0.2
0.1
0.0
Conversion [wt.fr.]
0
20
40
60
80
100
120
140
Reaction time [min]
E6
E9
M6
M9

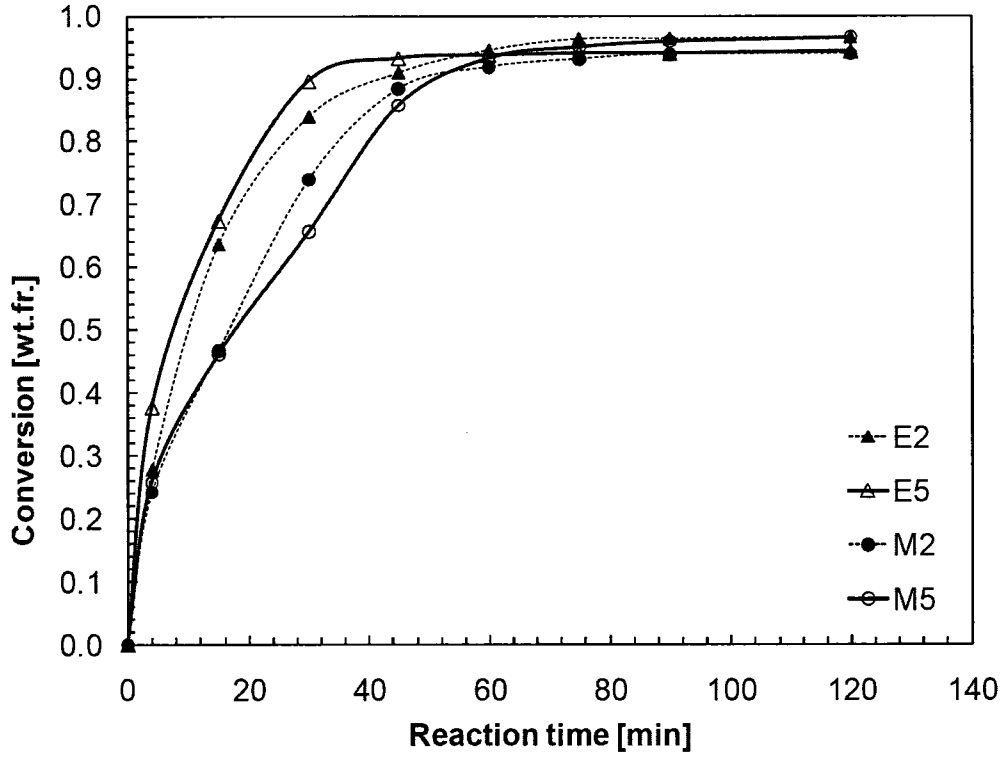
1.0
0.9
0.8
0.7
0.6
0.5
0.4
0.3
0.2
0.1
0.0
Conversion [wt.fr.]
0
20
40
60
80
100
120
140
Reaction time [min]
E2
E5
M2
M5

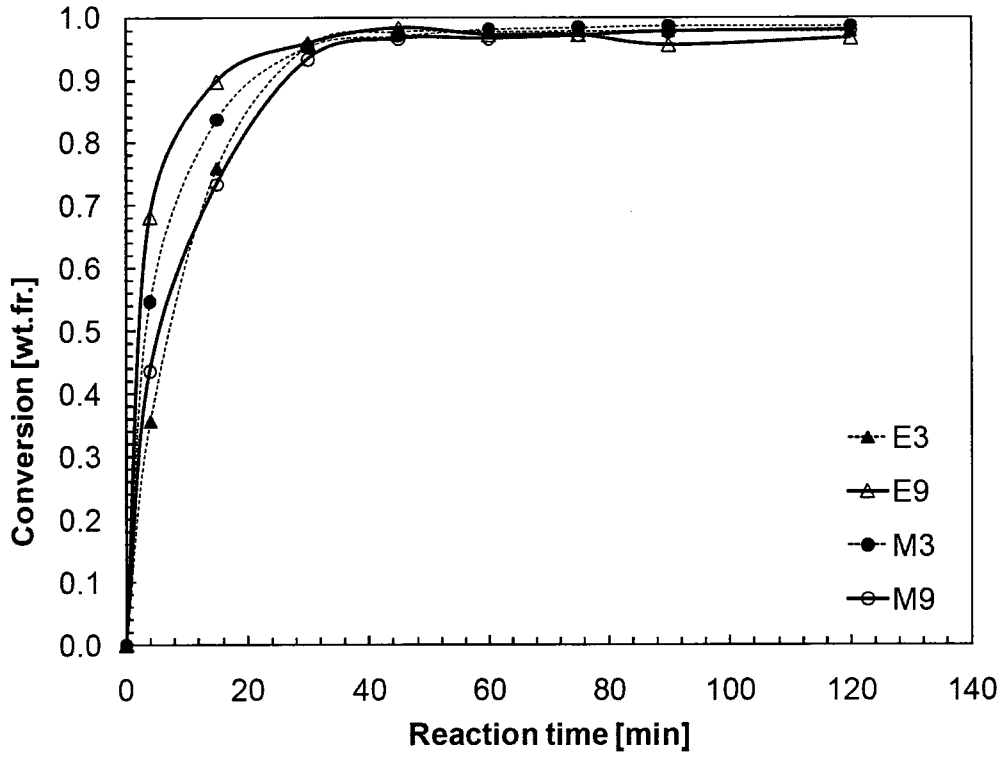
1.0
0.9
0.8
0.7
0.6
0.5
0.4
0.3
0.2
0.1
0.0
Conversion [wt.fr.]
0
20
40
60
80
100
120
140
Reaction time [min]
E3
E9
M3
M9

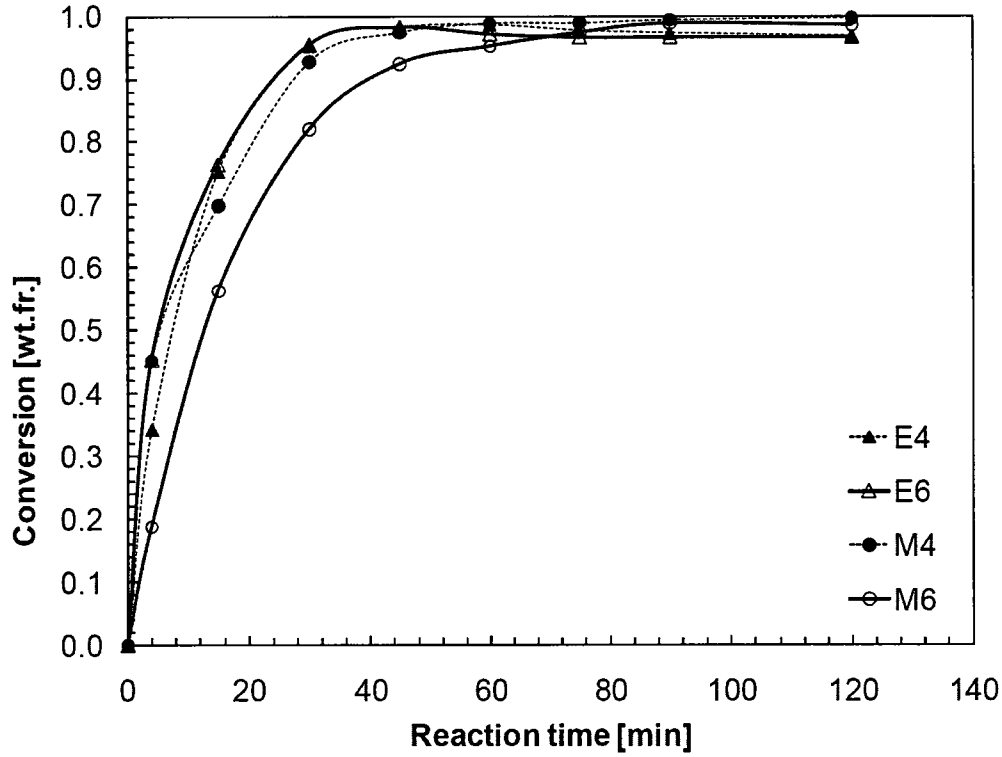
1.0
0.9
0.8
0.7
0.6
0.5
0.4
0.3
0.2
0.1
0.0
Conversion [wt.fr.]
0
20
40
60
80
100
120
140
Reaction time [min]
E4
E6
M4
M6

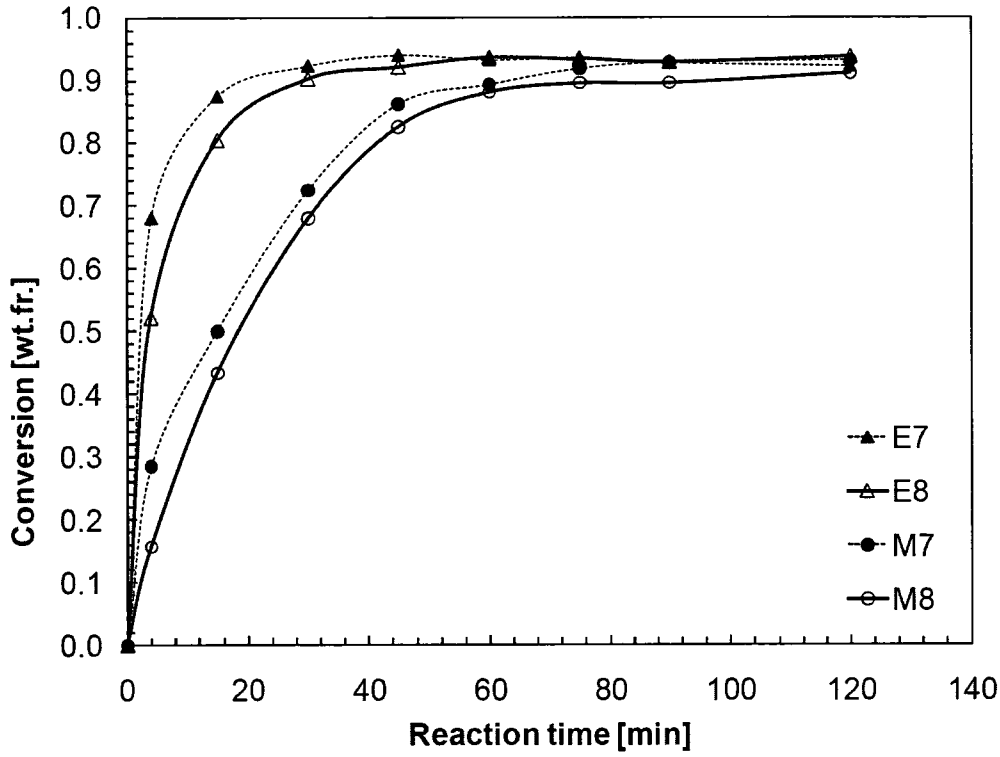
1.0
0.9
0.8
0.7
0.6
0.5
0.4
0.3
0.2
0.1
0.0
Conversion [wt.fr.]
0
20
40
60
80
100
120
140
Reaction time [min]
E7
E8
M7
M8

Differential Scanning Calorimetry analysis of Disponil A3065 (Chapter 5)

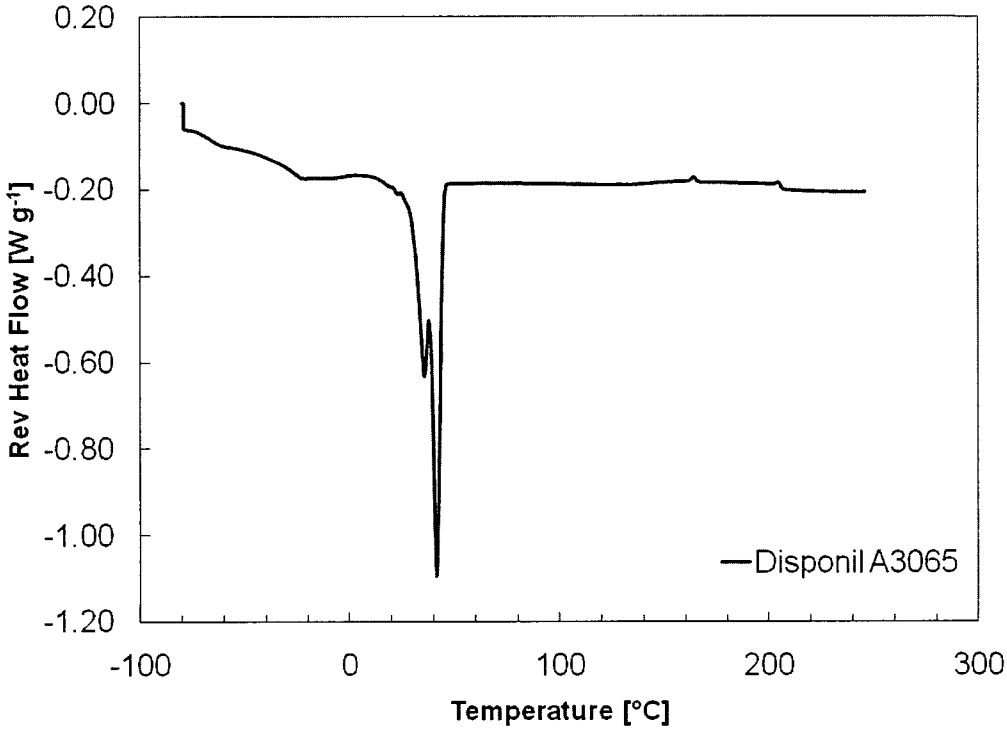

Droplet size and particle size distributions of sample HL2 (Chapter 6)